



The effect of NX-AS-401 on methicillin-resistant *Staphylococcus aureus*

Phillip Butterick

January 2020

**Submitted to Swansea University in fulfilment of the requirements for
the degree of Doctor of Philosophy**

Swansea University Medical School

Singleton Park Campus,

Sketty, Swansea, SA2 8PP

I. Declarations and Statements

DECLARATION

This work has not previously been accepted in substance for any degree and is not being concurrently submitted in candidature for any degree.

Signed  (candidate)

Date: 07/12/2021

STATEMENT 1

This thesis is the result of my own investigations, except where otherwise stated.

Where correction services have been used, the extent and nature of the correction is clearly marked in a footnote(s).

Other sources are acknowledged by footnotes giving explicit references. A bibliography is appended.

Signed  (candidate)

Date: 07/12/2021

STATEMENT 2

I hereby give consent for my thesis, if accepted, to be available for photocopying and for inter-library loans after expiry of a bar on access approved by the Swansea University.

Signed  (candidate)

Date: 07/12/2021

II. Acknowledgements

I would first like to thank Dr Rowena Jenkins, for giving me the opportunity to pursue this project, as well as all the support and advice throughout. You have supported me immensely both professionally and personally throughout these 3 years. (Especially the early morning drives to Swansea).

I would also like to give thanks to the MID group at Swansea, both past and current members, for all the help, and guidance throughout my time at Swansea University. Especially Dr Tom Wilkinson for all the encouragement and feedback throughout the project.

Thank you to all at Neem Biotech for their help over these years, for providing feedback and having to deal with all the paperwork/conference applications I have sent over the years. Without you this project would not have been possible. Special mention to project supervisor Dr Gareth Evans for all help and apologies for having to deal with the mountain of paperwork generated over these years.

I would also like to thank Dr Aled Roberts, for helping me over these few years, advising me on opportunities outside of the PhD and being supportive while we both complained about experiments gone wrong and numerous optimisations

Thanks also to current/previous supervisors, Dr Michael Graz, Dr Rose Cooper, Dr Almero Barnard, Dr Daniel Neef.

A finally last but by no means least, the biggest thank you to my wife Tes. You have made all of this possible, and I am sorry for probably spending the last 3 years talking about this project and then the last year stressed about writing it. You have made this all worthwhile and I could not have asked for a better partner throughout this.

III. Abstract

Antimicrobial resistance is a global health concern, with once treatable infections becoming resistant to current standard of care antimicrobials. The search for new antimicrobials has led Neem Biotech Ltd. to manufacture NX-AS-401 an ajoene containing compound derived from *Allium sativuum*, commonly known as garlic. The research contained within this thesis aimed to identify the effects of NX-AS-401 on Methicillin Resistant *Staphylococcus aureus* (MRSA), one of the most well documented and commonly isolated antimicrobial resistant bacterial pathogens. A multi-stage approach was utilised, identifying how NX-AS-401 affects planktonic growth, biofilm development and virulence factor production.

In Chapters 3 and 4 initial comparison between different NX-AS-401 formulations was performed in determined that ajoene content did not alter the antimicrobial effect of NX-AS-401. EUCAST broth microdilution compared NX-AS-401 to current standard of care antibiotic and determined effective inhibitory and bactericidal concentrations as 128 µg/ml and 2048 µg/ml respectively. When NX-AS-401 was used in combination with various antibiotic classes a synergistic effect was identified and the inhibitory concentrations of both agents were reduced.

The primary focus on Chapter 5 was how NX-AS-401 affected *S. aureus* biofilm formation. NX-AS-401 concentrations of 32 µg/ml inhibited biofilm formation and a concentration of 512 µg/ml caused disruption of pre-established biofilms. These effects were confirmed using scanning electron microscopy and confocal microscopy with live/dead staining. In gene expression studies it was determined that the effects of NX-AS-401 on *S. aureus* biofilms were strain dependent and a target gene was not identified.

Chapter 6 demonstrated that NX-AS-401 did not alter the production of *Staphylococcus aureus* exo-enzyme production *in vitro* during phenotypic studies. In *Galleria mellonella* low NX-AS-401 concentrations assisted in the recovery from *S. aureus* in a strain dependent manner, however, high concentrations caused increased *Galleria mellonella* fatality. NX-AS-401 altered the ability of *S. aureus* cells to invade human epithelial cells but did not prevent adhesion of *S. aureus* to the cells.

NX-AS-401 has multiple effects on *S. aureus* with the ability to affect both planktonic cells and biofilm structure showing promise as an antimicrobial. Its main effects are growth inhibition and biofilm disruption rather than causing bacterial cell death. These attributes and the synergistic effects between NX-AS-401 and multiple antibiotic classes, indicate NX-AS-401 has potential as a strong antimicrobial adjuvant.

IV. Table of Contents

I. Declarations and Statements.....	1
II. Acknowledgements.....	2
III. Abstract	3
IV. Table of Contents	5
V. List of figures	13
VI. List of tables.....	17
VII. List of Abbreviations.....	19
1.0 Introduction:	22
1.1 Wounds	22
1.2 <i>Staphylococcus aureus</i> (<i>S. aureus</i>)	27
1.2.1 Background	27
1.2.2 Virulence	28
1.2.2.1 Regulatory genes that control the expression of virulence factors.....	31
1.2.2.2 Changes in virulence factor expression during growth phases.	34
1.2.3 Biofilm formation.	36
1.2.3.1 Extracellular Matrix (ECM)	37
1.2.4 Biofilm management.....	40
1.3 Antibiotics and antibiotic resistance.....	42
1.3.1 Broad Classification	42
1.3.2 Mode and mechanism of action	44
1.3.3 Antibiotic resistance in <i>S. aureus</i>	49
1.3.4 Resistance mechanism acquisition	53
1.4 The problems with antibiotic development.	55
1.4.1 Antibiotics derived from ‘natural’ sources	61
1.4.2 <i>Allium sativum</i> (Garlic)	65

1.4.2.1 Allicin	67
1.4.2.2 Ajoene	68
1.4.2.3 NX-AS-401	69
1.5 Aims and Objectives.....	70
2.0 Materials and Methods	72
2.1 Materials	72
2.1.1 Manufacturers kits used.	75
2.1.2 Preparation of reagents	76
2.1.2.1 Media	76
2.1.2.2 NX-AS-401	78
2.1.2.3 Preparation of antibiotic solutions	79
2.1.2.4 Additional Reagents	80
2.2 Bacterial Strains.....	82
2.3 Methods	83
2.3.1 Preparation of a standardised bacterial inoculum (based on EUCAST guidelines; EUCAST 2017 Version 6.0 ⁽²⁴⁶⁾)	83
2.3.2 Technical and Biological Replicas.....	84
2.3.3 Antimicrobial Sensitivity Testing (AST)	84
2.3.3.1 EUCAST Disc Diffusion	84
2.3.3.2 EUCAST Minimum Inhibitory Concentration (MIC)	84
2.3.3.1 Minimum Bactericidal Concentration (MBC).....	85
2.3.4 Total Viable Cell (TVC) Counts.....	86
2.3.5 Growth Curves	87
2.3.6 Minimum Biofilm Inhibition/Eradication Concentration (MBIC/MBEC).....	87
2.3.6.1 Crystal violet.....	87
2.3.6.2 CellTiter-Blue Assay.....	88
2.3.7 Minimum Biofilm Eradication Concentration (MBEC)	88

2.3.8 Calculating the biofilm optical density cut off (OD ^{cut}) value of each <i>S. aureus</i> strain	89
2.3.9 Identification of biofilm phenotype based on composition.	89
2.3.10 Antibiotic Checkerboards.....	90
2.3.11 Antibiotic Interactions on <i>S. aureus</i> biofilms.	91
2.3.12 Scanning Electron Microscopy (SEM) Biofilm Sample Preparation.	92
2.3.13 Confocal Microscopy.....	93
2.3.14 Resistance Training	94
2.3.15 DNA Extraction	95
2.3.16 DNA Sequencing.....	95
2.3.17 Genome sequence analysis.....	95
2.3.18 Phenotypic Virulence Studies	96
2.3.19 Reverse Transcription - Quantitative Polymerase Chain Reaction (RT-qPCR)	97
2.3.20 <i>Galleria mellonella</i>	101
2.4 Cell Culture	103
2.4.1 Routine maintenance and sub-culture	103
2.4.2 Cytotoxicity Studies.....	104
2.4.3 Adhesion and Invasion Assays in HaCaT cells.	105
2.5 Statistical Analysis	106
3.0 Chapter 3: Optimisation of models to determine the effective concentrations of NX-AS-401 using early formulation NBR 26-6A	107
3.1 Introduction	107
3.1.1 The fight against antibiotic resistance.	107
3.2 Aims.....	109
3.3 Materials and Methods.....	110
3.3.1 Bacterial Strains	110

3.4 Results	111
3.4.1 Minimum Inhibitory\Bactericidal Concentration	111
3.4.1.1 Additional:	112
3.4.2 Time/Kill Curves	113
3.4.3 Minimum Biofilm Inhibition Concentration	114
3.4.4 Minimum Biofilm Eradication Concentrations on preformed <i>S. aureus</i> biofilms.....	115
3.4.5 Minimum Biofilm Eradication Concentrations on 48 hour preformed biofilms	116
3.4.5.1 Additional:.....	117
3.5 Discussion.....	118
3.5.1 The susceptibility of <i>S. aureus</i> NCTC 13142 to NBR 26-6A.	118
3.5.2 The effects of NBR 26-6A on the formation of <i>S. aureus</i> NCTC 13142 biofilm and disruption of pre-established biofilms.....	121
3.6 Conclusions.	125
4.0 Chapter 4: Identifying the mode of action of NX-AS-401 on planktonic <i>S.</i> <i>aureus</i> cells.....	127
4.1 Introduction	127
4.1.1 The active molecules of NX-AS-401	127
4.2 Aims.....	129
4.3 Materials and Methods.....	130
4.4 Results	131
4.4.1 Strain Characterisation.....	131
4.4.2 Vehicle Control.....	133
4.4.3 Minimum Inhibitory/Bactericidal Concentrations	135
4.4.4 Time/Kill Curves	137
4.4.4.1 Additional.....	138

4.4.5 Growth Curves	139
4.4.6 Resistance Evolution	141
4.4.7 Gene Sequencing	144
4.4.7.1 Phylogenetic Tree.....	144
4.4.7.2 Gene analysis of resistance mechanisms.....	146
4.4.7.3 Genotype and Phenotype discrepancies.	149
4.4.7.4 Single nucleotide polymorphism analysis.....	150
4.4.8 Antibiotic Interactions.....	153
4.5 Discussion.....	156
4.5.1 Antibiotic susceptibilities of <i>S. aureus</i> strains.....	156
4.5.2 NX-AS-401 effects on <i>S. aureus</i> growth	159
4.5.3 NX-AS-401 Tolerance and Resistance	164
4.5.4 Gene Sequencing and analysis.....	169
4.5.5 Antibiotic Interactions.....	176
4.6 Conclusions	181
5.0 Chapter 5: Identifying the mode of action of NX-AS-401 on <i>S. aureus</i> biofilms.	183
5.1 Introduction	183
5.1.1 Anti-Biofilm Targeting Antibiotics.....	183
5.1.2 The potential of NX-AS-401 as an anti-biofilm drug.	188
5.2 Aims.....	190
5.3 Materials and Methods.....	191
5.4 Results	192
5.4.1 Biofilm Characterisation.....	192
5.4.2 Effects of NX-AS-401 on <i>S. aureus</i> biofilm formation.	193
5.4.3 Effects of NX-AS-401 on pre-established <i>S. aureus</i> biofilms.....	196
5.4.4 Antibiotic Interactions.....	200

5.4.5 Scanning Electron Microscopy (SEM) and Confocal Laser Scanning Microscopy (CLSM).....	202
5.4.6 Reverse Transcription - quantitative Polymerase Chain Reaction (RT-qPCR)	220
5.5 Discussion.....	227
5.5.1 <i>S. aureus</i> biofilm characterisation	227
5.5.2 The effects of NX-AS-401 on biofilm formation and disruption.....	228
5.5.3 Antibiotic Interactions.....	233
5.5.4 Scanning Electron Microscopy (SEM) and Confocal Laser Scanning Microscopy (CLSM) Imaging.....	235
5.5.5 Reverse transcription - quantitative polymerase chain reaction (RT-qPCR) of biofilm associated <i>S. aureus</i> genes.	240
5.5.5.1 Gene expression changes in <i>S. aureus</i> biofilms treated with NX-AS-401 for two and four hours.	243
5.5.5.2 Gene expression changes in <i>S. aureus</i> biofilms treated with NX-AS-401 for 24 hours.	248
5.5.5.3 RT-qPCR Overview and implication in wounds.....	250
5.5.6 NX-AS-401 as an anti-biofilm agent	253
5.6 Conclusion	255
6.0 Chapter 6: NX-AS-401 as a potential anti-virulence agent.....	257
6.1 Introduction:	257
6.1.1 <i>S. aureus</i> virulence factors as therapeutic targets.....	257
6.1.2 Colonising Factors	260
6.1.3 Adhesins and Invasins	261
6.1.4 Lipases	262
6.1.5 Haemolysins and Leukocidins:	263
6.1.6 Deoxyribonuclease (DNase)	265
6.1.7 Protease	266

6.1.8 NX-AS-401 Anti-virulence.....	266
6.2 Aims.....	268
6.3 Methods.....	269
6.4 Results.....	270
6.4.1 NX-AS-401 Supplementation in solid media.....	270
6.4.2 Phenotypic Virulence.....	271
6.4.2.1 The effects of NX-AS-401 on beta (β) and gamma (γ) haemolysin produced by <i>S. aureus</i>	272
6.4.2.2 The effects of NX-AS-401 on the production and activity of <i>S. aureus</i> lipase.....	273
6.4.2.3 The effects of NX-AS-401 on the production and activity of <i>S. aureus</i> DNase.....	274
6.4.2.4 The effects of NX-AS-401 on the production and activity of <i>S. aureus</i> protease.....	275
6.4.3 <i>In vivo</i> virulence modulation of <i>S. aureus</i> by NX-AS-401 in <i>Galleria mellonella</i> (<i>G. mellonella</i>).....	277
6.4.3.1 NX-AS-401 toxicity.....	277
6.4.3.3 Optimisation of the lethal dose of <i>S. aureus</i>	278
6.4.3.4 The effects of NX-AS-401 on <i>S. aureus</i> lethality in <i>G. mellonella</i>	280
6.4.4 <i>In vitro</i> virulence in human skin epithelial cells.....	282
6.4.4.1 Cytotoxicity.....	282
6.4.4.2 Adhesion/Invasion.....	283
6.5 Discussion.....	285
6.5.1 Impact of NX-AS-401 on <i>S. aureus</i> virulence factor production <i>in vitro</i>	285
6.5.2 The effects of NX-AS-401 on <i>G. mellonella</i> and larvae infected with <i>S. aureus</i>	288
6.5.3 The ability of NX-AS-401 to modify adherence and invasion of <i>S. aureus</i> to human skin cells.....	292

6.5.4 NX-AS-401 as an anti-virulence agent.....	295
6.7 Conclusion	298
7.0 General Discussion:	300
7.1 NX-AS-401 and garlic derived molecules.	300
7.2 NX-AS-401 inhibits growth of <i>S. aureus</i>	Error! Bookmark not defined.
7.3 Antibiotic synergy with NX-AS-401	Error! Bookmark not defined.
7.4 The anti-biofilm effects of NX-AS-401.....	Error! Bookmark not defined.
7.5 Future perspectives.....	305
7.6 Other components of NX-AS-401.....	307
7.7 Further work:	308
8.0 References	311
1.0 Appendix.....	343
1.1 Antibiotic Sensitivities of Resistance Trained Isolates.....	343
1.2 Minimum Biofilm Eradication Concentration (MBEC) of antibiotics against <i>S. aureus</i> biofilms.	344
1.3 Nanodrop reading for cDNA samples	345
1.4 Calculated Primer Efficiencies.....	347
1.5 Single Nucleotide Polymorphisms (SNPs) identified from <i>S. aureus</i> isolates.....	348
1.6 QCAST report of assembled <i>S. aureus</i> isolates.....	378

V. List of figures

Figure 1.1 The four stages of wound healing ⁽⁶⁾	22
Figure 1.2 <i>Staphylococcus aureus</i> colonies on Mueller-Hinton agar (MHA) and an image of staphylococcal cells taken via scanning electron microscopy (SEM) by Phillip Butterick.....	27
Figure 1.3 Virulence factors produced by <i>S. aureus</i>	29
Figure 1.4 The relationship between <i>agrABCD</i> , <i>RNAIII</i> and virulence factor production.	33
Figure 1.5 Biofilm formation process and the composition of the extracellular matrix, image obtained from Ahmad <i>et al</i> (2019) ⁽⁷⁸⁾	36
Figure 1.6 Ajoene Z-Isomer (A) and Sulphonamide functional group (B).	46
Figure 1.7 Antibiotics and their specific targets.....	48
Figure 1.8 Timeline showing the development of AMR after antibiotic discovery	50
Figure 1.9 How bacteria develop antibiotic resistance mechanisms through mutation and horizontal gene transfer. Image obtained from Prof. D Karlsson ⁽¹⁶⁶⁾	54
Figure 1.10 Representative image of the application an antibiotic selective pressure.	55
Figure 1.11 <i>Allium Sativum</i> (Garlic).	65
Figure 2.1 Selection of colonies on an agar plate.	83
Figure 2.2 Example of Broth Microdilution plate layout	85
Figure 2.3 Example of TVC counts after incubation at 37 °C on MHA.....	86
Figure 2.4 Example of an antibiotic checkerboard plate layout:.....	90
Figure 2.5 <i>Galleria mellonella</i> testing conditions:.....	102
Figure 3.1 The MIC of NBR 26-6A against <i>S. aureus</i> NCTC 13142 via EUCAST broth microdilution.	111
Figure 3.2 Time/Kill Curve of NBR 26-6A against <i>S. aureus</i> NCTC 13142 over 48 hours:	113
Figure 3.3 <i>S. aureus</i> NCTC 13142 Biofilm inhibition by NBR 26-6A:	114
Figure 3.4 The effects of NBR 26-6A on pre-established 24-hour biofilms:.....	115
Figure 3.5 The effects of NBR 26-6A on pre-established 48-hour biofilms	116
Figure 4.1 Identifying the effects of DMSO on <i>S. aureus</i> growth.....	133

Figure 4.2 Results of EUCAST Broth Microdilution with NX-AS-401 against eight <i>S. aureus</i> strains.	135
Figure 4.3 Time/Kill Curves of NX-AS-401 against <i>S. aureus</i>	137
Figure 4.4 Difference in colony size of NX-AS-401 treated and untreated cells.	138
Figure 4.5 Growth Curves of NX-AS-401 against <i>S. aureus</i>	139
Figure 4.6 Repeated exposure of <i>S. aureus</i> to NX-AS-401 and gentamicin over 14 days.	142
Figure 4.7 Unrooted Neighbour-Joining phylogenetic tree of sequenced isolates created on FastTree.....	144
Figure 4.8 SNPs found in isolates under different experimental conditions.	151
Figure 4.9 Image from Levin <i>et al</i> , 2005 shows a disc diffusion D phenomenon ⁽³⁰²⁾	158
Figure 5.1 Image showing how antibiotic treatment can leave behind residual biofilm matrix and persister cells ⁽¹⁰⁷⁾	187
Figure 5.2 Changes in biomass caused by exposing <i>S. aureus</i> to NX-AS-401.....	193
Figure 5.3 Changes in biofilm metabolism caused by exposing <i>S. aureus</i> to NX-AS-401.	194
Figure 5.4 Changes in cell number caused by exposing <i>S. aureus</i> to NX-AS-401.....	195
Figure 5.5 Changes in the biomass of pre-established 48-hour <i>S. aureus</i> biofilms caused by NX-AS-401.....	196
Figure 5.6 NX-AS-401 mediated changes in resazurin metabolism of <i>S. aureus</i> biofilms pre-established over 48 hours.	197
Figure 5.7 NX-AS-401 mediated changes in biofilm cell number.	198
Figure 5.8 Representative SEM (Left) and CLSM (Right) images of NCTC 13142 biofilms treated with NX-AS-401.	204
Figure 5.9 Representative SEM (Left) and CLSM (Right) images of NCTC 12973 biofilms treated with NX-AS-401. Dashed circles highlight examples of <i>S. aureus</i> cells with unusual morphology in comparison to untreated cells.....	206
Figure 5.10 Representative SEM (Left) and CLSM (Right) images of UHW 3 biofilms treated with NX-AS-401:	208
Figure 5.11 Representative SEM (Left) and CLSM (Right) images of UHW 8 biofilms treated with NX-AS-401:	210

Figure 5.12 Representative SEM (Left) and CLSM (Right) images of UHW 15 biofilms treated with NX-AS-401:	212
Figure 5.13 Representative SEM (Left) and CLSM (Right) images of UHW 18 biofilms treated with NX-AS-401:	214
Figure 5.14 Representative SEM (Left) and CLSM (Right) images of UHW 19 biofilms treated with NX-AS-401:	216
Figure 5.15 Representative SEM (Left) and CLSM (Right) images of CRI 2 biofilms treated with NX-AS-401:	218
Figure 5.16 Gene expression changes in pre-established 48 hours <i>S. aureus</i> biofilms after exposure to 128 or 256 µg/ml NX-AS-401 for two hours.	221
Figure 5.17 Gene expression changes in pre-established 48 hours <i>S. aureus</i> biofilms after exposure to 128 or 256 µg/ml NX-AS-401 for four hours.	223
Figure 5.18 Gene expression changes in pre-established 48 hours <i>S. aureus</i> biofilms after exposure to 128 or 256 µg/ml NX-AS-401 for four hours.	225
Figure 5.19 The components in an extracellular biofilm matrix and potential biofilm matrix disruptors. Image obtained from Koo <i>et al</i> 2017 ⁽⁸⁹⁾	239
Figure 5.20 Transcription regulation of <i>S. aureus</i> virulence genes during normal cell function.	242
Figure 6.1 The role of membrane bound proteins on the internalisation of <i>S. aureus</i> into human epithelial cells, image obtained from Josse <i>et al</i> , 2017 ⁽⁶¹⁾	262
Figure 6.2 The activity of <i>S. aureus</i> haemolysin after exposure to NX-AS-401 on sheep blood agar.	272
Figure 6.3 <i>S. aureus</i> lipase activity on cells with and without exposure to NX-AS-401.	273
Figure 6.4 <i>S. aureus</i> DNase activity on cells with and without exposure to NX-AS-401.	274
Figure 6.5 <i>S. aureus</i> Protease activity on cells with and without exposure to NX-AS-401.	275
Figure 6.6 The toxic effects of NX-AS-401 on <i>G. mellonella</i> larvae over 5 days.	277
Figure 6.7 The effects of <i>S. aureus</i> cell density on the survival of <i>G. mellonella</i>	278
Figure 6.8 The effects of NX-AS-401 on infected <i>G. mellonella</i> survival.	280
Figure 6.9 The effects NX-AS-401 on HaCaT cell viability.	282

Figure 6.10 Alterations in the ability of <i>S. aureus</i> to adhere and invade HaCaT cells.	283
.....	
Figure 7.1 The molecular structure of Allicin and both ajoene E-Z isomers.	301
Figure 7.2 The S-thiolation of cysteine thiols by disulphide bonds in cancer cells.	
Image created based on data Kaschula <i>et al</i> 2015 ⁽²⁴⁰⁾	302
Figure 7.3 The effects of NX-AS-401 against methicillin resistant <i>Staphylococcus aureus</i> (MRSA).	310

Images obtained from sources under the creative commons license or with permission from the author by asking directly.

VI. List of tables

Table 1.1 <i>S. aureus</i> virulence factor regulatory systems, their role and function <i>in vivo</i> adapted from Jenul and Horswill (2019) ⁽⁴⁹⁾	32
Table 1.2 MSCRAMMS, binding mechanism and proposed function, Table adapted from Foster <i>et al</i> 2014 ⁽⁶⁹⁾	39
Table 1.3 Antibiotic classes and examples categorised into bacteriostatic and bactericidal.	42
Table 1.4 Antibiotic classes and their mode and mechanism of action.....	45
Table 1.5 Antibiotics and associated resistance mechanism type in <i>S. aureus</i>	52
Table 1.6 Drug discovery platforms, origins and current standard of care antibiotics.	58
Table 1.7 Plants and associated compounds which have demonstrated antibacterial activity, Table adapted from Prof. M Cowan 1999 ⁽¹⁹²⁾	62
Table 2.1 Reagent List	72
Table 2.2 Kit List:	75
Table 2.3 List and composition of media used to monitor changes <i>S. aureus</i> growth and phenotypic virulence:.....	76
Table 2.4 Antibiotics and diluents.	79
Table 2.5 Bacterial isolates used.....	82
Table 2.6 Cycle setting for conversion of RNA to cDNA using Promega GoScript™ Reverse Transcription Mix.	98
Table 2.7 RT-qPCR conditions	98
Table 3.1 WHO priority pathogens ^(146, 273)	107
Table 4.1 Antibiotic sensitivity of <i>S. aureus</i> strains.	131
Table 4.2 Resistance mechanism genes identified in all sequenced isolates.	146
Table 4.3 Zones of inhibition by disc diffusion on NX-AS-401 supplemented and un-supplemented media.	153
Table 4.4 Interactions between NX-AS-401 and antibiotics in antibiotic checkerboards identified using fractional inhibitory concentration indices (FICI) calculation.	154
Table 4.5 Interactions between NX-AS-401 and antibiotics in antibiotic checkerboards identified using the Bliss Model.	155
Table 5.1 Potential new anti-biofilm drugs.....	185

Table 6.1 Virulence factors and targeted in-development drugs provided by Kane <i>et al</i>, 2018 ⁽³⁹⁰⁾.	259
Table 6.2 Average TVC counts from agar plates containing different concentrations of NX-AS-401.	270
Table 6.3 Summary of virulence factors produced by each <i>S. aureus</i> strain:	276
Table 7.1 Methods for identifying changes in protein in bacteria.	306

VII. List of Abbreviations

16S	16S ribosomal RNA, RNA component of 30S subunit
3D	Three dimensional
µg/ml	Microgram per millilitre
µl	Microlitre
ABS	Absorbance
AIP	Autoinducing Peptide
AMP	Antimicrobial Peptide
AMR	Antimicrobial Resistant
ANOVA	Analysis of Variance
AST	Antibiotic Sensitivity Testing
BLAST	Basic Local Alignment Search Tool
CARD	The Comprehensive Antibiotic Resistance Database
CFU	Colony Forming Unit
CLSM	Confocal Laser Scanning Microscopy
CRI	Cardiff Royal Infirmary
DH₂O	Deionized Water
DMEM	Dulbecco's Modified Eagle Media
DMSO	Dimethyl Sulphoxide
DNA	Deoxyribonucleic Acid
ECM	Extracellular Matrix
eDNA	Extracellular Deoxyribonucleic Acid
EPS	Extracellular Polymeric Substance
ESBL	Extended Spectrum Beta-Lactamase
<i>E.coli</i>	<i>Escherichia coli</i>
EUCAST	European Committee on Antimicrobial Susceptibility Testing
FCS	Foetal Calf Serum
FICI	Fractional Inhibitory Concentration Indices
g/mol	Grams per mole - Molar Mass
HCA	Hierarchal cluster analysis

HCl	Hydrochloric Acid
HMDS	Hexamethyldisilane
MATE	Multi-drug And Toxin Extrusion
MBC	Minimum Bactericidal Concentration
MBEC	Minimum Biofilm Eradication Concentration
MBIC	Minimum Biofilm Inhibitory Concentration
MDR	Multi-Drug Resistant
MHA	Mueller-Hinton Broth
MHC	Major Histocompatibility Complex
MIC	Minimum Inhibitory Concentration
ml	Millilitre
MRSA	Methicillin Resistant <i>Staphylococcus aureus</i>
MSCRAMM	Microbial Surface Components Recognizing Adhesive Matrix Molecules
MSSA	Methicillin Sensitive <i>Staphylococcus aureus</i>
NBR 26-6A	First batch of NX-AS-401, batch number NBR 150026-6A
NCTC	National Collection of Typed Cultures
NHS	National Health Service
OD	Optical Density
PAGE	Polyacrylamide Gel Electrophoresis
PBS	Phosphate Buffered Saline
PC	Positive Control
PCR	Polymerase Chain Reaction
PHE	Public Health England
PHW	Public Health Wales
PI	Propidium Iodide
PIA	Polysaccharide intracellular adhesin
PSM	Phenol Soluble Modulins
PVL	Panton-Valentine Leukocidin
RNA	Ribonucleic Acid
RT-qPCR	Reverse Transcription - Quantitative Polymerase Chain Reaction

SDS	Sodium dodecyl sulphate
SEM	Scanning Electron Microscopy
SNP	Single Nucleotide Polymorphism
<i>Spp.</i>	Species
TB	Mycobacterium Tuberculosis
TEM	Transmission Electron Microscopy
TSS(T)	Toxic Shock Syndrome (Toxin)
TVC	Total Viable Cell
UHW	University Hospital of Wales
UK	United Kingdom
UV	Ultraviolet
VRSA/VISA	Vancomycin (Resistant/Intermediate) <i>Staphylococcus aureus</i>
WHO	World Health Organisation

1.0 Introduction:

1.1 Wounds

The treatment of wounds and their associated infections causes a large financial burden on the current NHS, costing approximately 5 % of the NHS' budget every year ⁽¹⁾. A wound is defined as physical disruption of skin or soft tissues usually via trauma ⁽¹⁻⁵⁾. They are split into the broad categories of acute wounds such as epidermal abrasions, burns and surgical sites or severe trauma such as crushing, breakages and chronic wounds such as pressure and venous ulcers ⁽¹⁻⁵⁾. The broad classification of wounds and their common occurrence makes it one of the largest areas to be covered by the NHS and requires a large budget to effectively treat and manage. In 2013/14 it was estimated that £4.5 – 5.1 billion was spent on wounds and associated co-morbidities ⁽¹⁾. Approximately 2.2 million patients were admitted with wounds during 2013/2014 and while a majority were acute wounds that healed within the normal time frame an estimated 575,000 of these patients suffered from chronic wounds, such as pressure and diabetic ulcers⁽⁴⁾ that are more difficult to treat and more costly to the NHS. Normal wound healing occurs in four phases (**Figure 1.1**). The stages can overlap during the healing process and overall healing can vary between days and months dependent on the severity and type of wound ⁽⁶⁾.

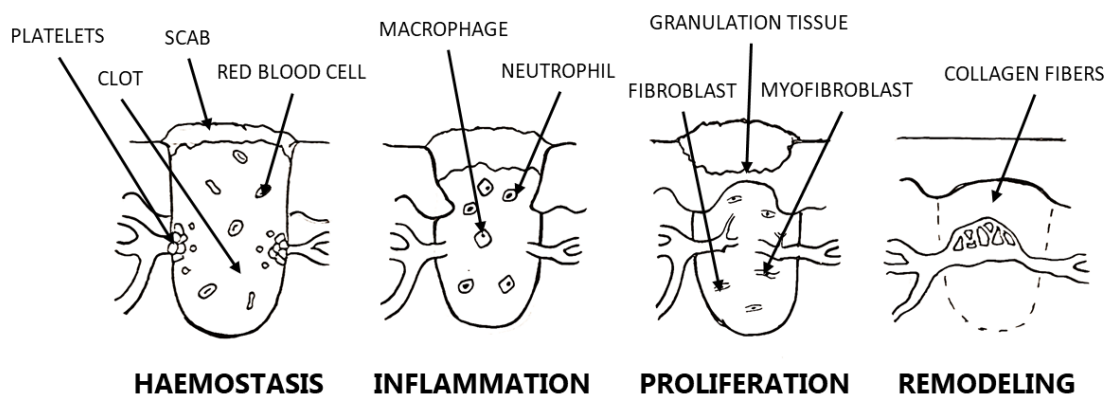


Figure 1.1 The four stages of wound healing ⁽⁶⁾.

The four phases of wound healing include, the haemostasis phase, this is the first and quickest stage often starting minutes after a wound has formed ^(6, 7). During the haemostasis phase platelets are activated and fibrin is gathered to form a clot slowing/preventing the loss of blood and entry of potentially harmful substances, bacteria and viruses ^(6, 7).

The second phase is the inflammation stage and involves the recruitment of immune components to the wound site. The immune components assist in the clearance of debris and any bacteria and viruses that may have entered through the creation of the wound ^(6, 7).

The third phase is the proliferation phase and is the most time variable phase based on the depth and type of wound ^(6, 7). The proliferation phase is the process of replacing damaged cells and tissues through regeneration of the dermis through a process called re-epithelisation (the creation of new skin cells), angiogenesis (the production of new blood vessels) before collagen synthesis and extracellular matrix formation is used to create a scaffold for the cells to begin restructuring ^(6, 7).

The fourth and final phase is remodelling which is the rearrangement of the cells according to a collagen framework and the restructuring of the blood vessels to a pre-wound condition ^(6, 7).

This process occurs in most wounds and should allow the wound to heal without complication. Wounds that occur suddenly and heal in the expected timeframe are referred to as acute wounds ⁽⁸⁾. Delayed wound healing can occur systemically based on factors such as age, gender, nutrition and medication, as well as underlying medical conditions such as diabetes, ischemia and cancer ⁽⁷⁾. Local factors that prevent wound healing include the presence of foreign bodies, poor oxygenation, and bacterial infection ⁽⁷⁾. Complications in wound healing or the development of bacterial infections that can inhibit the wound healing process leads to the development of chronic wounds ⁽⁷⁾.

Bacterial infection of wounds can cause major complications and increases the cost associated with treating patients with chronic wounds. Trauma results in the exposure of vulnerable soft tissues and mucous membranes that can be colonised by potential pathogens ^(9, 10). Colonisation can occur with bacteria that originate from a variety of

sources, such as the cause of the trauma in the cases of bites, cuts and post-surgical infections or from disruption/movement of host commensal microflora that harbours opportunistic pathogens ⁽⁹⁻¹¹⁾. Change of environment or over-proliferation of bacteria in a new site can cause changes in bacterial gene expression that allow organisms to secrete different products in the forms of proteases, lipases and toxins usually classified as virulence factors. Production of virulence factors can contribute to delayed healing of the wound and can lead to more serious clinical manifestations ⁽¹²⁾. Failure to identify the correct cause of a local infection can allow development into more serious systemic conditions such as sepsis ⁽⁹⁻¹¹⁾. Inadequate treatment of wounds with antiseptics or antibiotics can also allow for the formation of a bacterial biofilm that is difficult to remove with antibiotics and often requires more invasive treatment ^(13, 14).

Due to these complications, it has become increasingly important to identify the correct causative agent of wound infections as well as their antibiotic susceptibilities to allow appropriate and timely treatment. Current treatment guidelines vary as each health board often has their own best practice guidelines and treatment is highly variable based on the type of wound. For example, National Institute for Health and Care Excellence (NICE) provide guidelines for the treatment of surgical site infections (SSIs) ⁽¹⁵⁾. These guidelines cover pre-operative care such as the decolonisation of MRSA-carrying patients with topical antibiotic agents, such as a nasal mupirocin cream and chlorhexidine body wash ⁽¹⁵⁾. Guidelines also cover Intra-operative infection prevention through the use of alcohol or chlorhexidine topical antiseptics during surgery and finally advice on how to care for an infected wound post-surgery ⁽¹⁵⁾. Post-surgical antibiotic guidance is then based around laboratory identification of bacteria and antibiotic sensitivity testing (AST) ⁽¹⁵⁾. Further guidance is provided in separate NICE guidelines for specific wound infections such as cellulitis ⁽¹⁶⁾ and external guidance is provided for chronic wounds such as pressure ulcers ⁽¹⁷⁾.

These guidelines ^(15, 16, 18) cover a majority of wound types and provide guidance on how to treat both acute and chronic infections. These guidelines are essential for patient treatment but also provide details on antimicrobial stewardship that is designed to prevent the spread of antimicrobial resistant (AMR) bacteria ⁽¹⁹⁾. Guidance for AMR bacteria in wound care by both NICE and Wounds UK involves the

identification of the causative organism and determining the antibiotic sensitivity. It also states that antibiotics should only be given for a maximum of 14 days ^(8, 19). As well as the AMR guidance for each wound type, NICE have produced separate guidance for antimicrobial stewardship that provides additional information as well as sources of further information ⁽¹⁹⁾. Limiting the spread of AMR bacteria is important for both current and future wound care, as the more ubiquitous AMR bacteria become, the harder it becomes to treat the associated infections ^(8, 19).

The NICE guidance for infections includes the recommended doses and antibiotics for specific acute infections types, but also provides guidance for chronic wound infections such as diabetic foot ulcers. ⁽¹⁸⁾ Chronic wounds do not heal in an orderly or timely manner due to bacterial infection ^(20, 21), therefore NICE guidelines offer multiple recommendations. These include initial antibiotics, specific antibiotics for AMR bacteria, combination therapies for multi-species infections and finally more invasive treatments such as tissue debridement ⁽¹⁸⁾.

The best approach to wound infection management is the identification of the causative pathogen and its respective antibiotic sensitivity. This allows for a more targeted antimicrobial therapy and can reduce the spread of antimicrobial resistance ^(8, 22). However, there can be a discrepancy between the laboratory obtained antibiotic resistance profile determined *in vitro* and the efficacy of the antibiotic *in vivo* ⁽²³⁾. This is most commonly caused by the presence of an antibiotic resistant sub-population ⁽²³⁾, it can also be due to the vast differences between *in vitro* tests and the *in vivo* environment ⁽²⁴⁾. Different environments can modify bacterial cell gene expression and lead to increased efflux pump activity, or in some cases allows for the expression of unidentified resistance elements ^(21, 24). This can occur in places such as bacterial biofilms which demonstrate an increased tolerance to antibiotics. Increased tolerance can be caused by multiple factors, including overwhelming bacterial cell numbers, reduction in bacterial cell metabolism or secretion of an extracellular matrix that prevents the antibiotics reaching their target site ⁽²⁵⁾.

Another explanation for increased antibiotic tolerance is hetero-resistance. This occurs when a bacteria carries one copy of the resistance mechanism gene that is only expressed under certain circumstance such as antibiotic exposure ⁽²⁶⁾. Unfortunately

standard clinical laboratories procedures do not look for the presence of heterogenous resistance mechanisms ⁽²⁶⁾.

Pathogenic bacteria can often be isolated and identified via standard operating procedures employed in NHS pathology laboratories ⁽²⁷⁾. The procedures cover the detection and/or isolation of the most common pathogenic bacteria such as *Escherichia coli* (*E. coli*) and *Staphylococcus* species (spp.) to rarer pathogens such as *Vibrio* spp. and *Brucella* spp. ⁽²⁷⁾. Due to the carriage of *Staphylococcus* species as part of the commensal skin microbiome it is one of the most commonly isolated causes of bacterial infection ⁽²⁸⁾.

1.2 *Staphylococcus aureus* (*S. aureus*)

1.2.1 Background

Staphylococcus species are Gram positive coccus shaped bacteria, usually found in clusters of four (tetrads) and are the most commonly isolated bacterial pathogen (**Figure 1.2**)⁽²⁷⁻³⁰⁾. The genus contains multiple species, including *Staphylococcus epidermidis*, *Staphylococcus pseudintermedius*, *Staphylococcus capitis* and *S. aureus*⁽²⁸⁾. Most staphylococci are often found as part of the commensal human skin flora and are only deemed pathogenic if they are found in sites around the body where bacteria are not usually isolated, such as blood, cerebrospinal fluid and synovial fluid^(28, 31, 32).

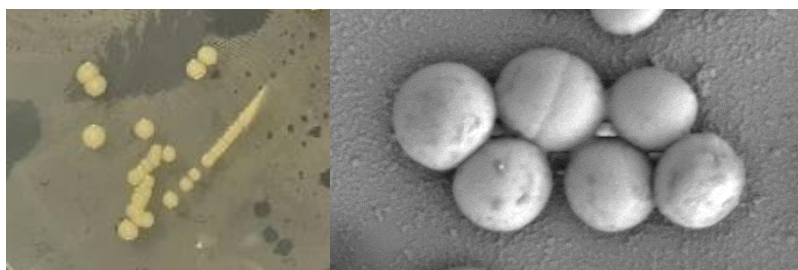


Figure 1.2 *Staphylococcus aureus* colonies on Mueller-Hinton agar (MHA) and an image of staphylococcal cells taken via scanning electron microscopy (SEM) by Phillip Butterick

S. aureus' name is due to the yellow/gold colour of its colonies (auris, Latin for gold) though colony colour varies due to the production of the pigment, staphyloxanthin (**Figure 1.2**)⁽²⁸⁾. Unlike the other members of the staphylococcal genus *S. aureus* is classified as a human pathogen, though it exists in approximately 30 % of the population as a commensal non-harmful skin bacterium and part of the human microbiome^(28-30, 33). Although *S. aureus* is very similar to other staphylococcal species it can produce different and specific virulence factors including exfoliative and enteric toxins that are not often seen in other staphylococcal species. Originally, the production of enzymes such as coagulase and DNase was used for laboratory identification, however this method is no longer reliable as non-*aureus* staphylococcal strains have also shown the ability to produce coagulase and DNase^(28-30, 33).

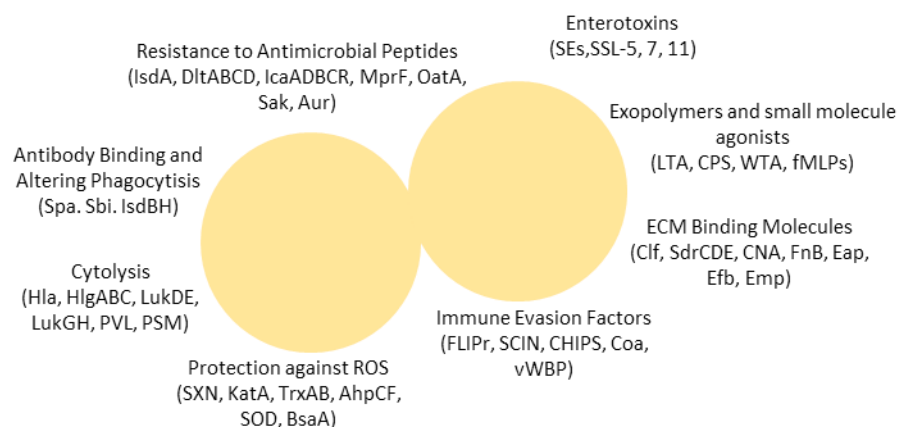
Therefore, identification has become more specific, requiring the use of MALDI-TOF or genetic identification using the *S. aureus* 16S gene.

1.2.2 Virulence

S. aureus can produce a myriad of virulence factors (**Figure 1.3**), the general function of these virulence factors is control on the environment for bacterial survival and growth. Virulence factors include enzymes and toxins that break down host tissues and cells allowing for nutrient acquisition ^(34, 35). Virulence factors also include antimicrobial peptides, and other toxins that remove competitive organisms and allow host immune system evasion preventing their eradication and causing persistent infection ^(34, 36, 37). The production of some virulence factors is linked to infection severity, an increase in either the variety or amount of virulence factors produced by a bacterial strain results in a more damaging infection ⁽³⁵⁾.

Unique virulence factor production changes the behaviour of *S. aureus* in comparison to other *Staphylococcus* spp. as it allows *S. aureus* to cause infection without prior changes in the environment or breakdown in the physical barriers of the immune system (for example skin and mucous membranes) ^(28-30, 33). An example of a toxin unique to *S. aureus* that allows for direct infection is Panton-Valentine leukocidin (PVL) that specifically targets host immune cells. Strains that produce this toxin are often pathogenic causing infection immediately rather than due to a changes in environment caused by a wound ⁽³⁸⁻⁴⁰⁾.

Some of the factors associated with pathogenicity for *S. aureus* (**Figure 1.3**) are often grouped into different classifications such haemolysins, enterotoxins, exfoliative toxins, and other enzymes that degrade proteins, lipids and DNA ^(34, 35).



AhpCF	Alkyl hydroperoxide reductase subunits C and F	Luk	Leukocidin
Aur	Aureolysin	MprF	Multiple peptide resistance factor
BsaA	Glutathione peroxidase	OatA	O-acetyltransferase A
CHIPS	Chemotaxis inhibitory protein of staphylococcus	PSM	Phenol-soluble modulins
Clf	Clumping factor	PVL	Panton-Valentine leukocidin
CNA	Collagen adhesin	ROS	Reactive oxygen species
Coa	Coagulase	Sak	Staphylokinase
CPS	Capsule	Sbi	Staphylococcal IgG-binding protein
Eap	Extracellular adherence protein	SCIN	Staphylococcal complement inhibitor
Efb	Extracellular fibrinogen binding protein	SdrCDE	Ser-Asp rich fibrinogen/bone sialoprotein-binding protein subunits C, D, and E
FLIPr	Formyl peptide receptor-like 1 inhibitory protein	SE	Staphylococcal enterotoxin
fMLP	N-formyl-methionyl-leucyl-phenylalanine	SOD	Superoxide dismutase
FnBPAB	Fibronectin binding protein A and B	Spa	Staphylococcal protein A
Hla	α -hemolysin	SSL	Staphylococcal superantigen-like protein
HlgABC	gamma-hemolysin subunits A, B, and C	SXN	Staphyloxanthin
IcaADBCR	Intercellular adhesin subunits A, D, B, C, and R	TrxAB	Thioredoxin (TrxA) and thioredoxin reductase (TrxB)
Isd	Iron-regulated surface determinant	vWbp	Von Willebrand factor binding protein
KatA	Catalase	WTA	Wall teichoic acid
LTA	Lipoteichoic acid		

Figure 1.3 Virulence factors produced by *S. aureus*.

Image created from information obtained from Kobayashi *et al* ⁽⁴¹⁾

There are many different virulence factors produced by *S. aureus* but the presence of virulence factor genes, and whether they are produced or not is strain specific ^(42, 43). Therefore, pathogenicity fluctuates between *S. aureus* strains with some capable of causing more harm than others. This is another example of where *S. aureus* differs from other staphylococci as while *S. aureus* can be commensal, all strains have been identified as pathogenic ^(42, 43).

The presence of virulence factors in a single strain can also be altered through the acquisition of genetic material. Accessory genetic elements can code for additional resistance genes and virulence factors and for example, pathogenicity islands, and provide the code for multiple virulence factors, primarily superantigens such as the enterotoxins and toxic shock syndrome toxin (TSST) ⁽⁴⁴⁾. If strains acquire multiple copies of the same virulence gene it can allow for increased activity as additional copies of virulence genes or promoter sequences and increase expression and production of toxins/enzymes ⁽⁴⁵⁾. Accessory gene elements can also include gene sequences that prevent virulence factor production, as seen with bacteriophages ϕ Sa3 and Sa6int that contain genetic material that integrates with the genes for haemolysin beta and lipase preventing their production ⁽⁴⁶⁾.

The variability between virulence factor production between *S. aureus* strains has shown that not only are they responsible for localised infections with broad symptoms (such as those seen in wounds) but they can also cause specific disease states if the infectious strain is known to produce a specific virulence factor. For example *S. aureus* is the most common cause for soft tissue skin infections, causing boils, furuncles, impetigo, folliculitis and cellulitis ⁽³⁴⁾ which is linked to *S. aureus* producing either PVL or high levels of haemolysin alpha ⁽³⁴⁾. In contrast, specific disease states such as staphylococcal scalded skin syndrome in new-borns and toxic shock syndrome are directly associated with exfoliative toxins A and B ^(47, 48).

1.2.2.1 Regulatory genes that control the expression of virulence factors

Regulation of the expression of virulence genes is required for virulence factor production. *S. aureus* contains complex multiple gene regulatory systems (**Table 1.1**), which can both suppress and increase expression of both virulence regulators and virulence factor genes directly.

Table 1.1 *S. aureus* virulence factor regulatory systems, their role and function *in vivo* adapted from Jenul and Horswill (2019) ⁽⁴⁹⁾

Regulator	Role	<i>In vivo</i>
Accessory gene regulator (<i>agr</i>)	Cell-to-cell communication (quorum sensing) with auto-inducing peptides as signal; <i>agr</i> activation leads to expression of toxins and exo-enzymes	Required for virulence in animal models of skin infection, pneumonia, and endocarditis
Two component system (<i>SaeRS</i>)	Induction of exo-protein production, including many virulence factors	Required for virulence in animal models of skin infection and pneumonia
Two component system (<i>SrrAB</i>)	Oxygen-responsive TCS; induction of <i>plc</i> and <i>ica</i> expression; repression of <i>agr</i> , TSST-1 and <i>spa</i>	Required for defence against neutrophils
Two component system (<i>ArlRS</i>)	Autolysis and cell surface TCS; induction of MgrA expression and repression of <i>agr</i> and autolysis	Required for virulence in animal models of skin infection and endocarditis
Staphylococcal accessory regulator (<i>SarA</i>)	Cytoplasmic regulator; induction of exo-proteins and repression of <i>spa</i>	Required for virulence in animal models of biofilm infection
Repressor of Toxins (<i>Rot</i>)	Cytoplasmic regulator of toxins and extracellular proteases; <i>agr</i> activation prevents Rot translation	Mutation of <i>rot</i> restores virulence in <i>agr</i> -null background in rabbit endocarditis model
Global Regulator (<i>MgrA</i>)	Cytoplasmic regulator; Induction of efflux pumps and capsule expression; repression of surface proteins	Required for virulence in animal models of skin infection and endocarditis
Sigma Factor B (<i>SigB</i>)	Stationary phase sigma factor; inhibits <i>agr</i> activity	Important for the establishment of chronic infection in rat lung model

The most well studied *S. aureus* virulence regulator is the *agr* system which has multiple roles in the function of *S. aureus* (Figure 1.4) (42, 49, 50). In terms of pathogenicity *agr* exists as a self-regulating complex of *agr A-D*, it is directly responsible for the expression of an autoinducing peptide of phenol-soluble modulins (51, 52), small proteins that can be cytolytic .

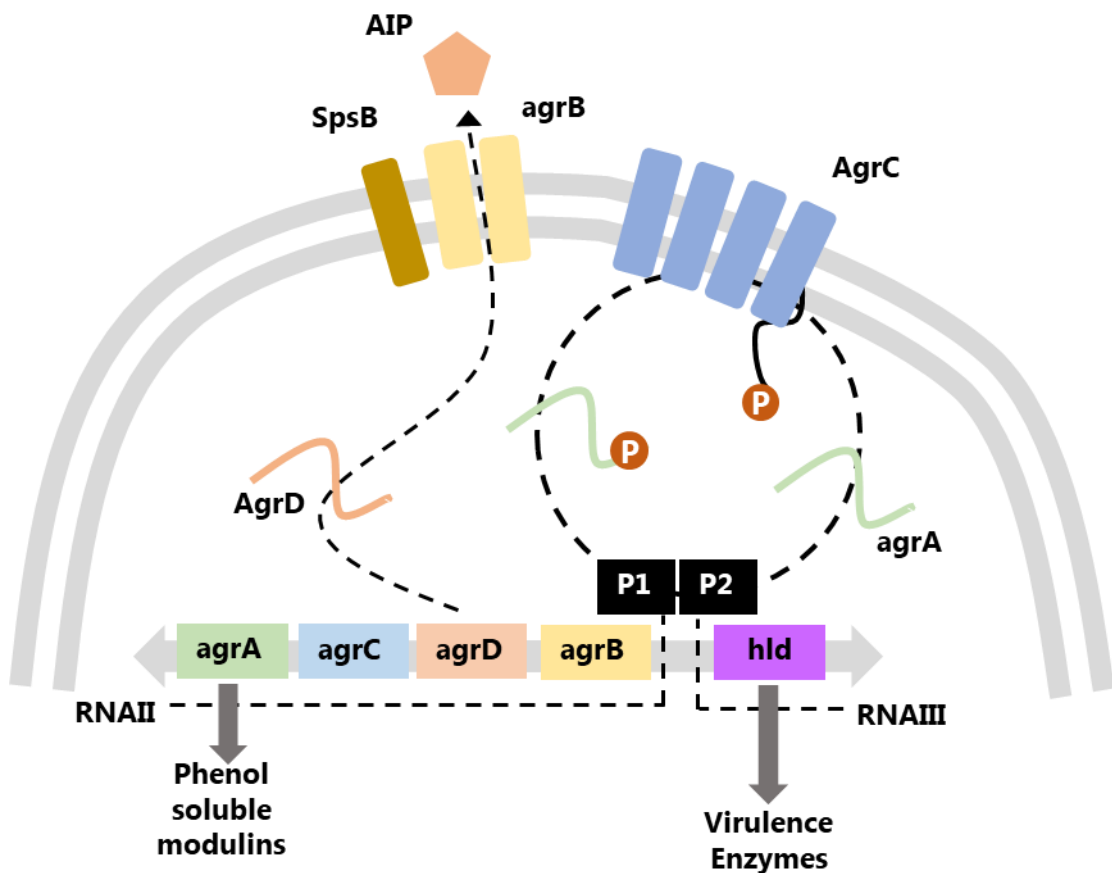


Figure 1.4 The relationship between *agrABCD*, *RNAIII* and virulence factor production.

Figure created from data obtained from Kong *et al* 2016 (53).

However, one of the main functions of *agr* is virulence modulation through controlling expression of RNAIII. The RNAIII operon is unusual as it also codes for haemolysin delta, however its other function is the upregulation of multiple virulence genes that code for toxins, leukocidins and proteases (42, 49, 50).

The two component systems *saeRS*, *srrAB* and *arlRS* all regulate virulence based on response to environmental conditions (49). For example, *saeRS* increases virulence in

response to human neutrophils, *srrAB* can modulate virulence in low oxygen conditions, while *arIRS* assists in the clumping of *S. aureus* in the presence of fibrinogen ⁽⁴⁹⁾.

The two-component system *arIRS* has been researched more than the other systems and has been shown to also reduce *agr* expression to limit bacterial autolysis while also regulating the expression of *mgrA* that control bacterial cell clumping ⁽⁴⁹⁾.

Similar, to *arIRS* the function of regulators *sarA*, *sigB*, and *rot* is also to modulate virulence factor expression by modifying the regulatory genes. The global regulator *sarA* increases *agr* expression while *sigB* and *rot* repress *agr* expression resulting in reduced virulence factor production ^(54, 55).

The global genetic regulators of *S. aureus* are governed by external factors and change production of virulence factors dependent on the environment ^(42, 43, 49, 56). Examples of this change *in vitro* is how the production of enzymes and toxins is media dependent, with changes in the production of factors such as RNA III, haemolysins and coagulase varying between growth in tryptic soy broth, speciality media and serum ^(51, 56).

1.2.2.2 Changes in virulence factor expression during growth phases.

In the development of an infection the production of virulence factors is also dependent on the *S. aureus* growth cycle, as different resources are required for each stage ^(49, 51). During the initial colonisation / lag phase, *S. aureus* expresses adhesins to allow for attachment of bacterial cells to the new surface, in wounds this would be the wound bed that is usually composed of damaged epithelial tissue ^(33, 57). The adhesins and invasins produced include clumping factors, fibronectin binding proteins, and microbial surface components recognizing adhesive matrix molecules (MSCRAMMS) ^(33, 57-59). These components are important to the binding of *S. aureus* cells to host cells and allow for immune system evasion. Immune evasion is a complex multi-factorial process, the adhesion and invasion through into host cells is one method. Other immune evasion processes include the recruitment of host immune components such as fibrin that can form a scaffold around *S. aureus* cells preventing the phagocytic activity of the host white cells ^(60, 61).

During log phase growth stage, *S. aureus* virulence factor production is reduced as the focus shifts to bacterial multiplication and cell division, however expression of *ica* and haemolysin gamma increase during late log phase growth ^(54, 62). Studies have shown global changes in the gene regulation of *S. aureus* during growth, however few studies have specifically targeted virulence factor production during each phase. However, it has been seen that global virulence regulator RNA III expression is reduced during log phase growth, meaning repressors of toxins are continually expressed and exotoxin production is decreased ^(50, 63-65).

Upon entry into the stationary phase RNA III expression increases and *S. aureus* begins to produce more exo-toxins and exo-enzymes ^(62, 66, 67). This allows for acquisition of nutrition to allow for further bacterial growth ⁽⁶²⁾ while toxin production also assists in defending *S. aureus* from the host immune system preventing its eradication to allow persistence ^(62, 66, 67). During the stationary phase there is also increased production of *S. aureus* bacteriocins, small peptides that act as antibacterial agents eliminating any competition from bacteria at the colonisation site ⁽⁶⁸⁾.

If infection persists *S. aureus* also begins to produce some of the colonisation factors produced during the lag phase of the growth cycle and stationary phase, however for a different role other than surface colonisation ⁽⁶⁹⁾. Virulence factors such as clumping factor, fibronectin binding protein and the MSCRAMM group can assist in the development of *S. aureus* colonisation/infection into a more robust and persistent structure of biofilm ⁽⁶⁹⁻⁷¹⁾.

1.2.3 Biofilm formation.

A bacterial biofilm is the development of a structure from singular cells to a three dimensional (3D) structure. The 3D structure can either be bound to a surface or as a form a free floating aggregate (**Figure 1.5**)⁽⁷²⁻⁷⁴⁾. A bacterial biofilm can be comprised of single or multiple bacterial strains and can also often include different species^(73, 74). The structure is comprised of both living and dead cells, the living cells have varying degrees of activity with different processes and different levels of metabolism^(73, 74). The bacterial cells within the biofilm can communicate through a system called quorum sensing, where cells modulate their virulence factors production, metabolism and their growth/death⁽⁷⁵⁻⁷⁷⁾.

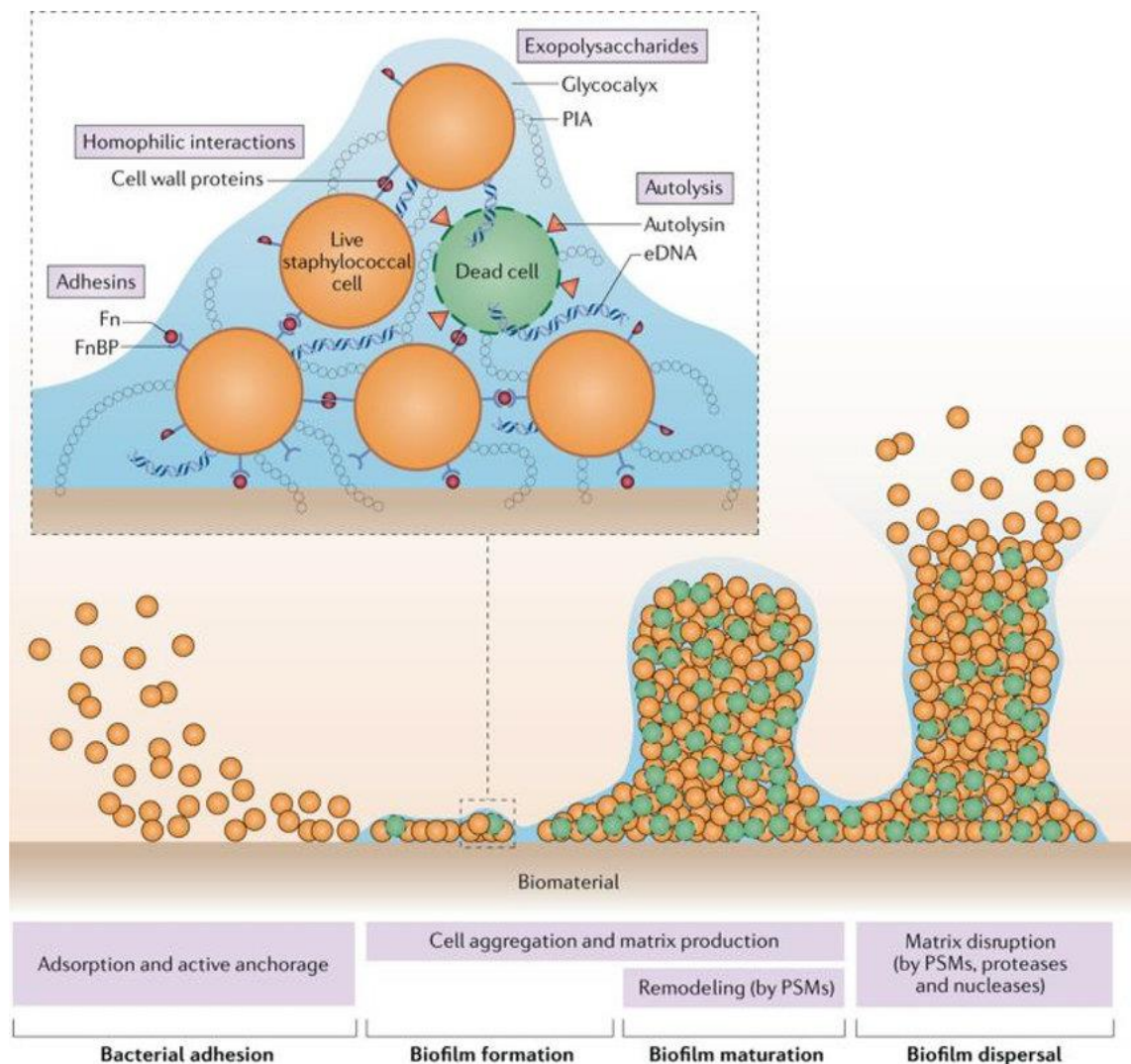


Figure 1.5 Biofilm formation process and the composition of the extracellular matrix, image obtained from Ahmad *et al* (2019)⁽⁷⁸⁾.

During biofilm formation (**Figure 1.5**), single cells irreversibly bind to a surface, then once they anchor the bacterial cells begin to divide and adhere to each other ⁽⁷⁹⁻⁸²⁾. However, the “mushroom” type of biofilm (**Figure 1.5**) is often only seen *in vitro* due to biofilms forming on surfaces. In contrast *in vivo* biofilms often have different 3D structures due to the attachment of cells onto surfaces with different levels of hydrophobicity or surfaces that may already be colonised by other bacteria ^(83, 84). *In vivo* biofilms also tend to be thinner than their *in vitro* counterparts but a higher number of smaller aggregates form ⁽⁸⁴⁾. However, regardless of whether they are formed *in vitro*, or *in vivo*, biofilm formation is dependent on the production of an extracellular matrix (ECM) ⁽⁸⁵⁾.

1.2.3.1 Extracellular Matrix (ECM)

The ECM begins to form during lag phase growth, however it is the latter biofilm maturation stage where more ECM is produced and modulation via phenol soluble modulins and other exo-enzymes creates a robust structure ^(86, 87). The biofilm ECM is often created from multiple elements, this can include protein, polysaccharide, extracellular DNA (eDNA), amyloid scaffolding, and surface bound proteins. *S. aureus* biofilms also recruit host immune components such as fibrin and fibrinogen to provide a more robust scaffold and reduce the action of the human immune system ^(81, 86, 87).

The ECM connects all the cells together, and when mature *in vivo* the ECM contains “water” channels that allow for the flow of nutrients into the deeper layer of the biofilm while also allowing enzymes produced and molecules associated with quorum sensing to leave the biofilm or interact with other bacterial cells ⁽⁸⁸⁾.

The components of the ECM are often strain specific and matrix composition can include more protein, eDNA or polysaccharide depending on the strain ^(86, 89-92). This is due to the presence/absence of specific virulence regulators (**Table 1.1**) or due to the resources obtainable from the environment ⁽¹³⁾. For example, the *ica* locus is important in biofilm development and expression is linked to polysaccharide intracellular adhesin (PIA), while protein-based biofilms are controlled through *sigB*, *alt* and fibronectin binding protein production ^(13, 93). In cases where all mechanisms are present, biofilm phenotype is based around available resources, in high nutrient environments the

biofilm will contain mixed phenotypes ⁽⁹⁴⁾. Regardless of ECM phenotype biofilm formation is governed by global gene regulators *agr/sarA* that fluctuate throughout biofilm formation and maintenance as they are used to regulate the biofilm ^(50, 77). Regulation of *S. aureus* biofilms occur through the effects of *agr/sarA* on the *arlRS*, a system that promotes the agglutination and aggregation of bacterial cells ^(50, 77).

Bacterial biofilm formation and maintenance is controlled by the bacterial cell to cell communication system, quorum sensing ⁽⁹⁵⁾. Quorum relates to bacterial cell density, thus when a biofilm is formed the activity of the cells and biofilm as a total is governed through chemical signalling between cells ⁽⁹⁶⁾. In staphylococci the main regulatory mechanism for quorum sensing is the *agr* system ^(95, 96). Apart from control of virulence (**Section 1.2.2**) the *agr* system also controls biofilm formation through the production of an auto-inducing peptide (AIP) ^(95, 96). It is regulation of this peptide that allows for different stages of biofilm formation as AIP induces *agr* expression ⁽⁹⁶⁾. In early stages, *agr* expression is suppressed and so is exo-enzyme activity, this allows for the early formation of a biofilm matrix ^(95, 96). In latter stages of biofilm maturation *agr* expression is increased alongside toxin and enzyme production, the increased enzymes enable dispersal and dissemination of the biofilm, ensuring bacterial propagation ^(95, 97).

The role of the two component systems such as *lytRS* ⁽⁹⁸⁾ and *SrrAB* ⁽⁴⁹⁾ and regulatory system *sarA* is to regulate *agr* expression and therefore biofilm formation and maintenance, this is due to their direct effects on the expression of MSCRAMMS (**Table 1.2**) that are all vital for biofilm formation ⁽⁹⁹⁾.

Table 1.2 MSCRAMMS, binding mechanism and proposed function, Table adapted from Foster *et al* 2014 ⁽⁶⁹⁾.

Protein group	Ligand and binding mechanism	Function
Clumping factor A (ClfA)	Fibrinogen γ -chain carboxyl terminus; DLL Complement factor I	Adhesion to immobilized fibrinogen; immune evasion by binding soluble fibrinogen Immune evasion; degradation of C3b
Clumping factor B (ClfB)	Fibrinogen α -chain repeat 5, keratin 10 and loricrin; DLL	Adhesion to desquamated epithelial cells; nasal colonization
Serine–aspartate repeat protein C (SdrC)	β -neurexin; DLL	Unknown
	Desquamated epithelial cells	Nasal colonization?
SdrD	Desquamated epithelial cells	Nasal colonization?
SdrE	Complement factor H	Immune evasion; degradation of C3b
(isoform of SdrE)	Fibrinogen α -chain; DLL	Adhesion to ECM
Fibronectin-binding proteins A (FnBPA) and B (FnBPB)	FnBPA A domain binds the C terminus of fibrinogen γ -chain and elastin; DLL. FnBPB A domain also binds fibronectin but not by DLL	Adhesion to ECM
	Fibronectin (FnBPA and FnBPB C-terminal repeats, β -zipper)	Adhesion to ECM; invasion
Collagen adhesin (Cna)	Collagen triple helix; collagen hug Complement protein C1q	Adhesion to collagen-rich tissue Prevention of classical pathway of complement activation

Expression and production of the MSCRAMMS is modulated throughout biofilm formation by regulatory mechanisms such as *sarA*, *sigB* and *agr* ⁽⁶⁹⁾. The functions (**Table 1.2**) identify why each mechanism is required and also indicate that the lack of one MSCRAMM many not impede biofilm formation as several have similar functions ⁽⁶⁹⁾. This indicates an intrinsic redundancy in the system, in mutants where the function

of one MSCRAMMS has been removed or impaired another has taken over its role allowing for biofilm formation to continue ⁽⁶⁹⁾.

1.2.4 Biofilm management

Once fully formed bacterial biofilms are one of the potential causes of chronic wounds, as their development can prevent proper wound healing by inhibiting re-epithelisation and causing a low grade inflammatory response ⁽¹⁰⁰⁾. If left untreated local biofilms can lead to systemic infection ^(101, 102). Mature biofilms demonstrate increased *agr* expression leading to greater biofilm dispersal (**Figure 1.5**), this allows for dissemination of the bacteria to an additional site within the host and leading to systemic infection ⁽¹⁰²⁾.

Overall prophylactic treatment and preventing biofilm formation gives better patient outcomes as it is much easier to treat an infection prior to the development of a bacterial biofilm ^(21, 103, 104). Bacterial biofilms demonstrate the ability to adapt to new challenge such as antibiotics and host immune responses. This adaptability prevents complete bacterial eradication, preventing normal wound healing ^(21, 104, 105). These include the change in metabolic activity of bacterial cells, as some of the living cells can be metabolically inert, in this state antibiotics are often ineffective as they cannot penetrate through normal membrane channels ⁽¹⁰⁶⁻¹⁰⁸⁾. While bacterial cells remain dormant, growth is restricted or halted, therefore no additional cell wall is being created and this limits the effect of antibiotics that target cell walls, such as penicillins/beta-lactams ⁽¹⁰⁷⁾. The metabolically inert cells are called persister cells due to their ability to survive heavy antibiotic treatment ⁽¹⁰⁶⁻¹⁰⁸⁾. Once the antibiotic has been removed from the environment the persister cells can become more metabolically active and begin the infection process again ⁽¹⁰⁶⁻¹⁰⁸⁾.

Additional complications in the use of antibiotics in treatment of bacterial biofilms comes from the ECM that acts as a coating that protects the bacterial cells from the host immune system ^(86, 89, 91, 92). The small channels of the ECM allow nutrient flow into the interior of the biofilm and also prevents the movement of larger immune components and molecules ^(86, 89, 91, 92). The ECMs small channels and ionic charge grants the ability to sequester and restrict molecule movement and prevent the

activity of antibiotics ^(86, 89, 91, 109). The increased tolerance to antibiotics can cause treatment failure, however, unlike antibiotic resistance this tolerance is transient and once a biofilm is dispersed normal antibiotic sensitivity returns ^(91, 104).

Both persister cells and the ECM cause problems for bacterial biofilm clearance and therefore stronger treatment options are required; this can include antibiotic combination therapies, where two or more antibiotics are used, or more invasive measures such as host tissue removal in a process called debridement ^(91, 104, 110, 111).

Another cause of biofilm treatment failure is the acquisition of antimicrobial resistance (AMR). *In vivo* biofilms tend to be polymicrobial in nature where there is a constant exchange of mobile genetic elements between species and therefore a greater chance of acquiring AMR genes ^(81, 112, 113). The ability of bacterial organisms to become resistant to a specific antibiotic or whole antibiotic classes, render the antibiotic ineffective against the target organism causing treatment failure and continuous infection ^(45, 109, 112, 114-117).

1.3 Antibiotics and antibiotic resistance

1.3.1 Broad Classification

Antibiotics are classified by various criteria including their molecular structure, source of origin and activity ^(118, 119). In both research and clinical laboratories antibiotics are commonly divided into two broad categories based on their activity, bacteriostatic and bactericidal ^(120, 121). Table 1.3 outlines how each of the antibiotic classes are categorised according to *in vitro* tests.

Table 1.3 Antibiotic classes and examples categorised into bacteriostatic and bactericidal.

The antibiotics classes are split into two broad categories, these categories can assist in clinical situations and help to decide which antibiotic would be the best treatment option.

Bacteriostatic	Bactericidal
Glycyclines	Aminoglycosides
Example: Tetracycline	Example: Gentamicin
Lincosamides	β -lactams
Example: Clindamycin	Example: Penicillin
Macrolides	Fluoroquinolones
Example: Erythromycin	Example: Ciprofloxacin
Oxazolidinones	Glycopeptides
Example: Linezolid	Example: Vancomycin
Streptogramins	Lipopeptides
Example: Dalphopristin	Example: Daptomycin
Sulphonamides	Nitrofurans
Example: Sulphamethoxazole	Example: Nitrofurantoin

The definitions for whether antibiotics are classified as bacteriostatic and/or bactericidal differs depending on whether they are employed for research, *in vitro* or

in clinical, *in vivo* situations ^(120, 122). The definition of a bacteriostatic antibiotic *in vitro* is one that can inhibit bacterial growth by >90 % ^(120, 123) and the *in vitro* definition of a bactericidal antibiotic is when bacterial cells cannot be recovered at a concentration less than four times the MIC ^(120, 122).

In vivo determination is less easily defined as antibiotics can act as either a bacteriostatic or bactericidal agent dependent on the organism it is utilised against and is dependent on what concentrations can be achieved in the host. For example chloramphenicol is bactericidal against *Streptococcus* species but bacteriostatic against *S. aureus* when given at the same concentration, this means that clinically chloramphenicol fits into both bacteriostatic and bactericidal categories ⁽¹²⁰⁾. The different classifications are also used to guide infection treatment, with bactericidal antibiotics used to directly eradicate bacterial cells that are difficult for the host to eradicate due to either a compromised immune system or infections in host sites where immune function is limited (such as cerebrospinal fluid) ^(120, 123). Bacteriostatic drugs are often employed against infections where host immune factors can also assist in clearance of the infection, this is predominately beneficial when treatment with bactericidal antibiotics can cause eradication of commensal bacteria, and allow for secondary infection by opportunistic pathogens, such as yeast infections that occur after antibiotic treatment ⁽¹²⁰⁾.

Historically it was thought to be inadvisable to mix antibiotics from the two categories in Table 1.3 as they could act in a manner which was antagonistic to one another ^(121, 124, 125). This is thought to be caused by bactericidal drugs taking effect during cell division or cell growth that is inhibited by bacteriostatic drugs rendering the bactericidal drugs less effective ⁽¹²¹⁾.

However, it has been shown this is not always the case and what can be seen as antagonism *in vitro* is not reproduced *in vivo*, ⁽¹²⁴⁾ with bacteriostatic and bactericidal antibiotics proving capable of clearing infections in areas where host immune function is limited, such as heart valves in endocarditis ⁽¹²⁰⁾. The difference between *in vitro* and *in vivo* performance is likely due to secondary effects antibiotics have on the host immune system that are difficult to identify *in vitro*. For example bacteriostatic macrolides gather near macrophages in the host and assist in bacterial eradication ⁽¹²⁰⁾. Antibiotics such as linezolid can reduce the damage of prolonged inflammation during

infection by suppressing cytokine synthesis, an effect that has been seen in a variety of animal models with different bacterial infections ranging from rat paw wounds to pneumonia and sepsis in mice ⁽¹²⁶⁾.

Unfortunately, interactions between antibiotics and host components can also be negative with the action of bactericidal antibiotics such as the beta-lactam oxacillin reduced *in vivo* due to an affinity of binding to host plasma proteins (primarily albumin) ⁽¹²⁷⁾. Protein binding differs between antibiotic class with beta-lactam drugs displaying high protein binding between 60-94 % ⁽¹²⁷⁾ while other drugs such as gentamicin have a lower protein binding of 0-30 % ⁽¹²⁸⁾.

While the classification of bacteriostatic/bactericidal shown in Table 1.3 is useful to support clinical decisions, the classifications remain broad. For novel antibiotics further investigation is needed to understand the mode and mechanism of action against bacteria.

1.3.2 Mode and mechanism of action

Mode of action indicates the functional or anatomical effects an antibiotic has on a bacterial cell and is used to describe changes in growth kinetics, cell structure and cell morphology ⁽¹²⁹⁾. The mode of action can be determined by identifying an antibiotic's effect on growth kinetics via time/kill curves or growth curves while alterations to cell morphology can be visualized using different microscopy techniques such as electron microscopy, confocal microscopy and atomic force microscopy ^(130, 131).

Mode of action identifies the method by which an antibiotic elicits an antimicrobial effect in general terminology ⁽¹²⁰⁾ whereas mechanism of action is more specific and often includes identifying alterations to specific metabolic pathways, protein synthesis, DNA replication or cell wall formation as shown in Table 1.4 ⁽¹²⁰⁾. Uncovering an antimicrobial mechanism of action begins with determining the mode of action, then elucidating how that effect is created. Determining a compound's effects on growth, cell morphology and virulence factor production is essential information when uncovering new antimicrobial agents ⁽¹³²⁾.

Table 1.4 Antibiotic classes and their mode and mechanism of action.

Descriptions provided by Kapoor *et al*, 2017 ⁽¹¹⁸⁾ that specify the mechanisms and mode of action in a selection of different antibiotic classes. The ones in this table are the six antibiotics that were utilised throughout this project and the additional sulphonamide class of antibiotics that is structurally similar to NX-AS-401.

Antibiotic Class	Agent Name	Mode of Action	Mechanism of Action
Aminoglycoside	Gentamicin	Prevent Protein Synthesis	Binding of 30S subunit causing premature termination of mRNA
Tetracycline	Tetracycline	Inhibit DNA translation	Binding of 30S ribosomal subunit to prevent t-RNA binding
Macrolide	Erythromycin	Prevents protein biosynthesis	Binds to the 50s subunit of the bacterial rRNA complex
Lincosamide	Clindamycin	Prevents protein biosynthesis	Binds to the 50s subunit (specifically 23s) of the bacterial rRNA complex
Beta-Lactam	Cefoxitin	Prevents cell wall formation	Inhibits crosslinking of peptidoglycan
Fluoroquinolone	Ciprofloxacin	Prevents cell division	Inhibition of DNA gyrase, type II topoisomerase and topoisomerase IV
Sulphonamide	Sulphamethoxazole	Prevent Folic acid synthesis	Inhibits dihydropteroate synthase preventing the formation of dihydroptericoic acid

While there are many different antibiotic classes, Table 1.4 shows that the modes of action are broadly similar, many prevent the synthesis of proteins or translation of DNA by binding to molecular subunits ⁽¹¹⁸⁾. There are also antibiotic classes with different mechanisms of action, such as the sulphonamides ⁽¹³³⁾. Once a widely used antibacterial agent, sulphonamide use has been greatly reduced due to increased

resistance and increased cases of adverse reactions ^(133, 134). Sulphonamide's mechanism of action is disruption of folic acid synthesis and subsequent DNA/RNA synthesis and they are classified as a bacteriostatic drug ⁽¹³⁴⁾. Sulphonamide and the garlic-derived compounds allicin and ajoene share similar functional groups, e.g. S-carbonyl sulphoxides and S-S disulfide bonds. ⁽¹³³⁻¹³⁵⁾. Even though they contain sulphur containing elements (**Figure 1.6**), sulphonamide bonds act as competitive inhibitors to dihydropteroate synthase whereas disulphide bonds react with thiolates, this indicates a different mechanism of action ^(133, 134, 136).

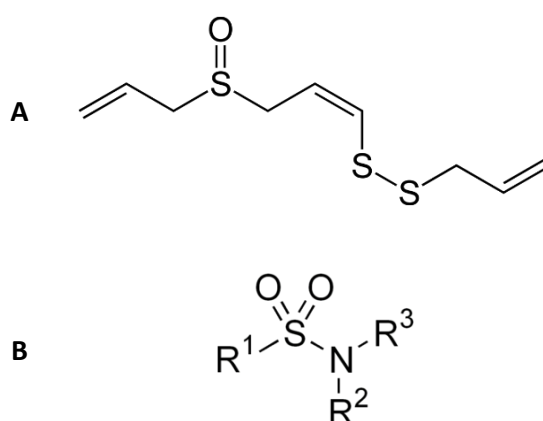


Figure 1.6 Ajoene Z-Isomer (A) and Sulphonamide functional group (B).

While there are different elements, the functional groups of ajoene and the sulphonamide are similar with the presence of a sulphonamide bond in sulphonamides and a disulphide bond found in ajoene.

Identifying the mechanism of action is important in the development of new antibiotics as they help predict how the molecules may interact with other components, such as host factors that can inhibit drug function *in vivo* ⁽¹³¹⁾. It also aids in the development of compounds with similar mechanisms that have greater antibacterial activity or those that are adapted/reformulated to overcome resistance mechanisms ⁽¹³¹⁾.

Another purpose for identifying the mechanism of action is to better understand how an antibiotic should be used and its effects in specific infections. For example, the drug mupirocin which is only used as a topical ointment has a unique mechanism of action,

targeting the t-RNA synthetase of *Staphylococcus* and *Streptococcus* species ⁽¹²⁸⁾. However, while effective topically it is rapidly metabolised if it enters systemic circulation and excreted via the renal system ⁽¹²⁸⁾. Without understanding the mechanism and its reaction with the host *in vivo* systemic studies may have indicated that mupirocin was an ineffective antibiotic, and it may not have been used as an effective topical treatment.

The antibiotics in Table 1.4 are classified as broad-spectrum antibiotics as demonstrated in Figure 1.7, these antibiotics are able to target a large range of bacteria ⁽¹³⁷⁾. These are often used where bacterial infection is indicated but the target organism and its respective antibiotic susceptibilities have yet to be confirmed ⁽¹³⁷⁾. For example, in wounds where inflammation and pus are present or would healing is delayed, yet a causative organism has yet to be determined ⁽¹⁰³⁾. In these cases, the causative bacterial organism and its antibiotic sensitivities have yet to be identified, therefore a broader treatment regimen is better for patient prognosis, and can be changed to a narrower spectrum antibiotic upon identification and AST ⁽¹⁰³⁾.

Antibiotics are often selective for bacteria based on their Gram stain results as shown in Figure 1.6 ⁽¹³⁸⁾. For example, penicillins prevent cross linking of peptidoglycan found in the cell wall of all bacteria but are mainly utilised against Gram-positive bacteria. This is because penicillins are unable to enter Gram-negative cells due to the lipopolysaccharide and protein layers not present in Gram-positives ^(118, 139). Antibiotics that are Gram-negative specific include colistin and polymyxins that specifically target the outer lipid and cytoplasmic membranes ⁽¹⁴⁰⁾.

Broad Spectrum Antibiotics

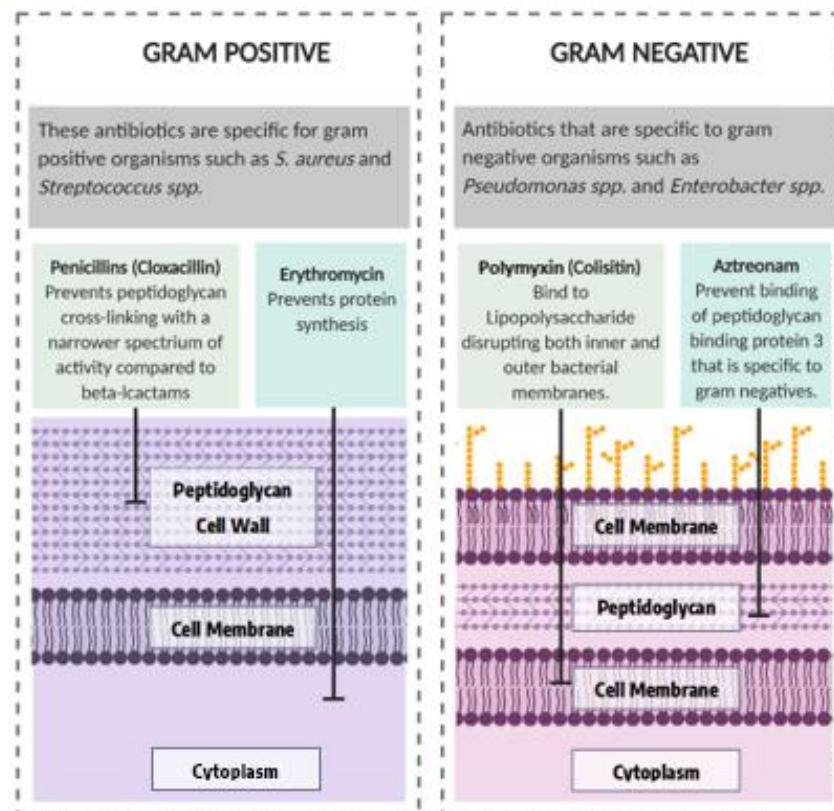
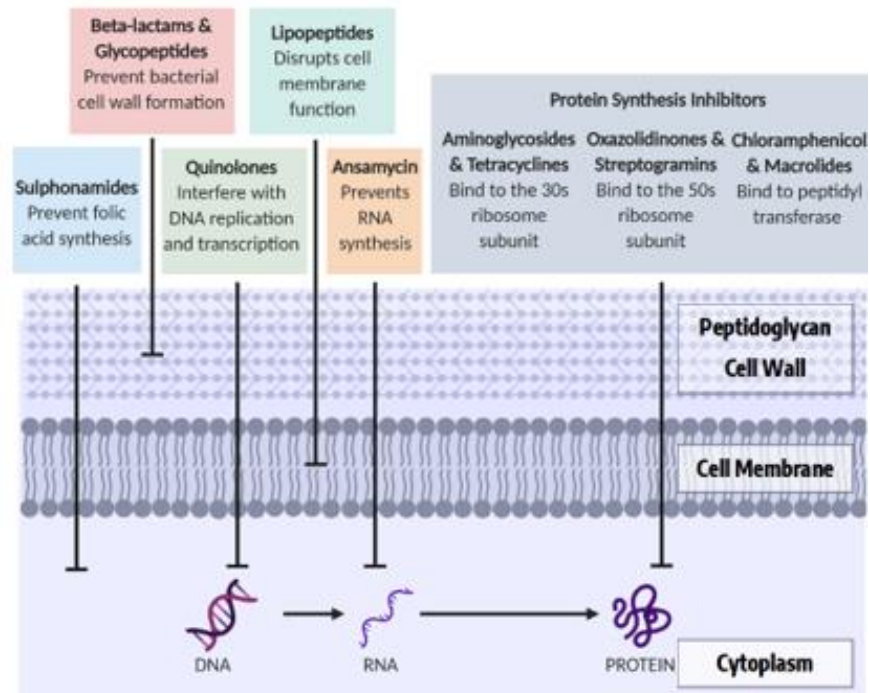


Figure 1.7 Antibiotics and their specific targets.

This Figure shows the different antibiotic classes, and the black bars indicate where in the bacterial cell they elicit their mechanism of action. This covers antibiotics that can act on all antibiotics and those that target bacteria based on their Gram result.

Broad spectrum antibiotics can be effective on both Gram positive and negative organisms, however, efficacy can vary, for example cephalosporins are an extended spectrum beta-lactamases that target peptidoglycan cross-linking ⁽¹⁴¹⁾. Cephalosporins are also sub-divided into antibiotic generations, with each generation having different targets. The first, second and fifth generations are more effective against Gram-positives organisms including MRSA, while third and fourth generations are more active against Gram-negatives due to an increased ability to penetrate through the bacterial cell membrane ⁽¹⁴¹⁾.

There are many antibiotic classes, each with their own mechanism of action (**Table 1.4**) providing multiple treatment options for bacterial infections ⁽¹¹⁸⁾. However, the evolution of antimicrobial resistance and the development of multi-drug resistance organisms is reducing the efficacy of antibiotics worldwide.

1.3.3 Antibiotic resistance in *S. aureus*

Antimicrobial resistance is one of the largest concerns in global healthcare systems ^(118, 142-145). The evolution of once treatable organisms to become resistant to the activity of specific antibiotics requires immediate action ^(132, 146). While some actions have been taken, such as antibiotic stewardship that limits the use of antibiotics, this does not solve the issue, as while information has been disseminated, antibiotic usage has continued to rise ^(19, 147). The most recent annual report into AMR by Public Health England has shown that the percentage of antibiotic-resistant infections has increased over the past five years, however it is dependent on antibiotic class with increases between 0.5 – 10 % ⁽¹⁴⁸⁾. One of the most significant changes is a 2.3 % decrease in the number of methicillin-resistant *Staphylococcus aureus* (MRSA) associated infections ⁽¹⁴⁸⁾.

S. aureus has become an example of how an organism can adapt to many antibiotic classes, with different strains showing resistance to beta-lactams, aminoglycosides, fusidic acid, mupirocin, rifampicin and tetracyclines ^(142, 144, 145) indicating resistance to most antibiotic classes used in their treatment. The percentage of isolates resistant to other antibiotics, such as erythromycin was also higher (>70 %) if the *S. aureus* isolate

was methicillin resistant when compared to methicillin sensitive *S. aureus* isolates (<15 %) (145).

The development of methicillin resistance in *S. aureus* is one of the most well documented and researched areas of antibiotic resistance (29, 109, 149, 150). In this case the resistance mechanism was thought to primarily occur in hospitals, however community cases also started to increase (30, 151). One of the most common resistance mechanisms that confers methicillin resistance in *S. aureus* is the *sccMEC* cassette (152). In general, hospital acquired MRSA infections contains *sccMEC* types I, II and III, while community strains carry *sccMEC* types IV and V (152). The rapid spread of the MRSA “superbug” meant that the first choice and widely used beta-lactam class were suddenly unviable as antibiotic treatments (29, 109, 149, 150).

Methicillin resistance was thought to be discovered shortly after methicillin discovery and many years later that it became prominent in isolates obtained from infection (29). However, it has also been shown that methicillin resistance was first seen 14 years prior to the discovery of methicillin (153). This indicates that methicillin was not a driving factor behind the development of resistance, and the increased use of beta-lactam based antibiotics may be the cause for increased presence of MRSA in the population (153). As shown in Figure 1.8 as quickly as antibiotics have been discovered, resistance mechanisms are also identified. In some cases just a few years after discovery widespread antibiotic resistance occurs (24, 114, 132).

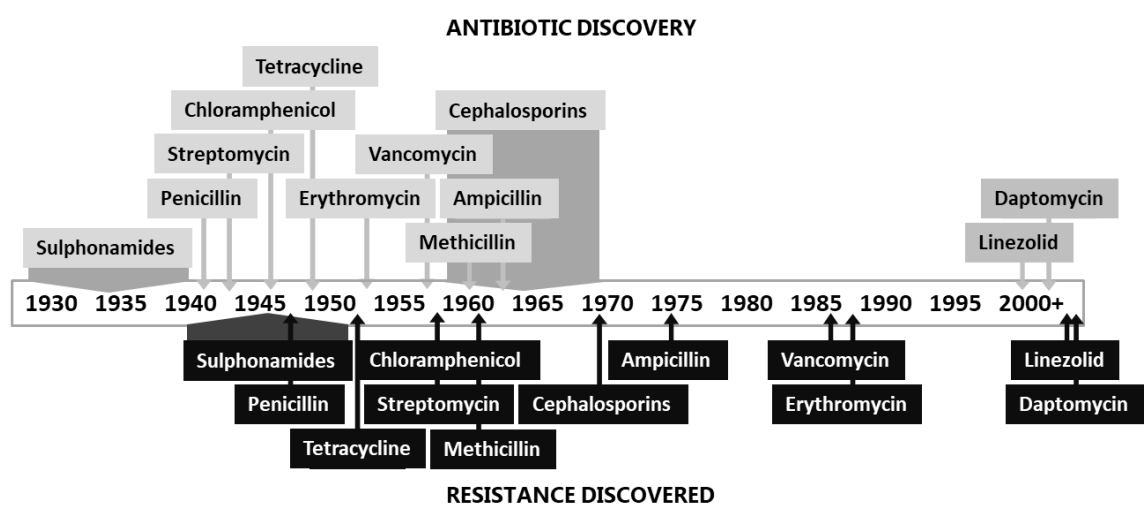


Figure 1.8 Timeline showing the development of AMR after antibiotic discovery

Resistance to many of the antibiotic treatment options is already widespread, therefore it is a bigger concern that bacteria will become resistant to last line antibiotics ⁽¹⁴⁴⁾. This has already occurred with a class of bacteria called carbapenemase producing Enterobacteriaceae that are resistant to most or all antibiotic classes ⁽²⁴⁾. In the treatment of all types of *S. aureus* infections (wounds, bacteraemia etc.) the last antibiotic options are the glycopeptides and resistance has already been seen to these antibiotics ^(154, 155).

The development of vancomycin-resistant *Staphylococcus aureus* (VRSA) is not a future concern for the treatment of *S. aureus* associated infections, as it is already present ^(154, 155). While VRSA incidence remains low, there is an increase in the amount of vancomycin intermediate *S. aureus* (VISA) ⁽¹⁵⁴⁾. VISA is defined differently as the vancomycin resistance mechanisms identified so far are either transient or unsustainable, due to instability of the plasmid carrying the *vanA* gene that confers vancomycin resistance ⁽¹⁵⁶⁾. The *vanA* gene also causes a fitness cost that reduces *S. aureus* growth and renders the bacterium more susceptible to other hostile factors like host immune components and other bacteria ^(154, 156, 157).

Identification of antibiotic resistance mechanisms can aid in the development of new antibiotics and other drugs that can either negate/overcome resistance mechanisms.^(158, 159) However, antibiotic resistance can occur for many different reasons, this can include mutations in the target binding site, the production of a slightly different target that prevent antibiotic action ^(118, 144, 160-162). It can also include the production of antibiotic targeting enzymes, or efflux pumps that specifically target an antibiotic class ^(118, 144, 160-162). Table 1.5 demonstrates the many different resistance mechanism of *S. aureus* and how multiple mechanisms are employed to generate resistance to each antibiotic class.

Table 1.5 Antibiotics and associated resistance mechanism type in *S. aureus*.Table adapted from by Dr. W Reygaert 2018 ⁽¹⁶³⁾.

Antimicrobial Agents	Resistance Mechanism
Glycopeptides	Limiting Drug Uptake
β -lactams	Modification of Drug Target
Glycopeptides	
Lipopeptides	
Aminoglycosides	
Tetracyclines	
Macrolides	
Lincosamides	
Oxazolidinones	
Streptogramins	
Fluoroquinolones	
Metabolic Pathway Inhibitors	Inactivation of Drug
β -lactams	
Chloramphenicol	Active Drug Efflux
Tetracyclines	
Fluoroquinolones	

The mechanisms of antibiotic resistance are often specific for each antibiotic class, by interfering with the ability of an antibiotic to interact with the target site ⁽¹⁶³⁾. The first method described here is the limitation of drug uptake, this is one of the mechanisms of action for cell wall targeting antibiotics and is often employed by multiple bacterial species against many different antibiotic classes, including cephalosporins and carbapenems ^(118, 163). This method requires the reduction of porins within the bacterial cell wall or membrane ^(114, 118, 144, 162, 163). Porins are structures within the wall or membrane that allow for both entrance of molecules from the environment, while also allowing the exit of enzymes and toxins.

Modification of the drug target is the most common mechanism seen in AMR infections, these are specific to the antibiotic class's mechanism of action ^(114, 118, 144, 162, 163). They can occur due to genetic mutation or methylation that changes the final protein structure, or through creation of alternative versions of the target molecules, such as the alternative penicillin binding protein in staphylococci that prevent the action of beta-lactams. ^(118, 163). Either of these two methods can then create a new final product that prevents the action of an antimicrobial ^(118, 163).

Antibiotic inactivation is often through the employment of specific enzymes that cleave the drug and prevent its action ^(118, 163). The most common example is the production of beta-lactamases, produced by bacteria such as *E. coli* and *Klebsiella spp.* The final mechanism involving drug efflux can be utilised by pre-existing efflux pumps or the development of specific transporter such as those that target tetracyclines ^(118, 163, 164). This is a method used by bacteria for the elimination of hazardous environmental components such as immune components and toxic chemicals as well as antibiotics ^(118, 163-165).

1.3.4 Resistance mechanism acquisition

Although resistance mechanisms can develop through spontaneous mutation or methylation of DNA, the most common acquisition of resistance mechanisms is through the process of horizontal gene transfer ^(45, 142, 166-168). Figure 1.9 shows the three mechanisms of horizontal gene transfer transformation, conjugation and transduction along with their associated vectors ⁽¹⁶⁶⁾.

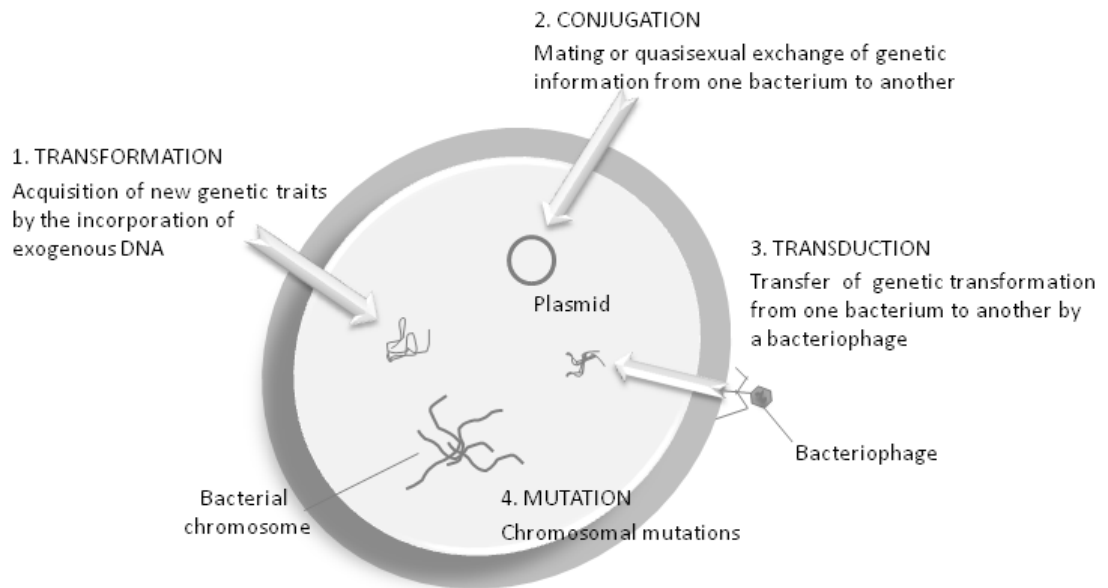


Figure 1.9 How bacteria develop antibiotic resistance mechanisms through mutation and horizontal gene transfer. Image obtained from Prof. D Karlsson ⁽¹⁶⁶⁾

Acquired genetic elements can be non-species-specific allowing for the antibiotic sensitive organisms to gain resistance mechanisms from intrinsically resistant organisms ^(167, 169). This is one of the major concerns in VRSA development as *S. aureus* may acquire the resistance elements from vancomycin resistant *Enterococci*, another Gram-positive organism which already displays wide-spread vancomycin resistance ⁽¹⁵⁵⁾.

Horizontal gene transfer is a common process, but the transfer of genetic material can be increased due to the application of a selective pressure, such as antibiotic treatment of a wound ^(170, 171). In addition, areas where bacteria are competing for resources (soil, sand water sources) or in locations with molecules toxic to bacteria/low antibiotic concentrations (sewage, hospital waste and inadequate antibiotic therapy) ^(170, 171) will favour the process.

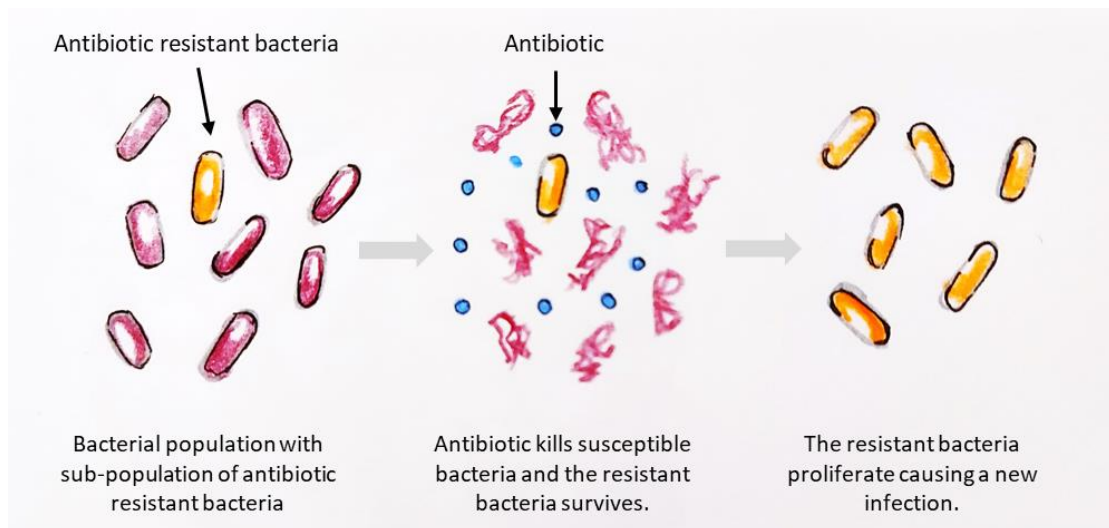


Figure 1.10 Representative image of the application an antibiotic selective pressure.
Image created from information provided in Mulvey and Simor 2009 ⁽¹⁷⁰⁾

Inadequate treatment and overuse of antibiotics is a well-known contributor to the spread of AMR. The use of antibiotics can apply a selective pressure (**Figure 1.10**), eliminating antibiotic susceptible bacteria while leaving the resistant strains alive ^(170, 171). These selective pressures ensure the propagation of resistant species and when a single bacterial stain acquires multiple resistance mechanisms the resulting multi-drug resistant (MDR) bacteria become difficult to treat. To overcome the spread of MDR bacteria new treatment options and antibiotic are required.

1.4 The problems with antibiotic development.

The multitude of resistance mechanisms and the speed of which they become common has led to a stagnation in the development of antibiotics ^(119, 158, 172). There has been little investment by the pharmaceutical industries for development of antibiotics due to the costs associated with developing a drug that may not work *in vivo* or that may become obsolete after a short time of use in the clinic ⁽¹⁵⁹⁾. It is only recently due to the increasing percentage of AMR infections and the development resistance to last line antibiotics that research has once again turned to antibiotic development ⁽¹⁵⁹⁾. Recent development has seen pharmaceutical companies join together to create a fund that can assist antibiotic development ⁽¹⁷³⁾. This joins current

existing organisations, such as antibiotic discovery accelerators/incubators, that have also been previously established to both develop antibiotics and promote awareness of AMR ^(174, 175).

Previously, new antibiotics have been developed from an existing antibiotic class, with even the most recent “new” antibiotic classes being derived from existing antibiotics ^(159, 176). The last discovered clinically employed antibiotic class was the lipoglycopeptide telavancin in 2009, a synthetic modification of vancomycin ⁽¹⁷⁶⁾. While the previous two new classes glycycline (tigecycline) in 2005 and ketolides (telithromycin) in 2001 derived from tetracyclines and erythromycin, respectively ⁽¹⁷⁷⁾. The last novel antibiotic was the oxazolidinone classification that included linezolid and prior to that the latest antibiotic was in 1987 ⁽¹⁷⁷⁾. Resistance to these antibiotics has been seen due to prior resistance of the antibiotic they were derived from or due to overuse causing the antibiotic selective pressure ^(119, 132, 158, 159).

The focus has shifted to the development of completely new antibiotic classes, that may not just inhibit growth or kill bacteria, but demonstrate different primary or secondary effects ^(119, 132, 158, 159). This has included the use of anti-biofilm (**Chapter 5**) and anti-virulence targeting drugs (**Chapter 6**) to prevent the establishment of chronic infection and reduce infection severity, respectively ^(110, 158, 159, 178-180).

While other treatment options have focussed on combination therapies or the inclusion of drugs that can overcome/disable the known resistance mechanism ⁽¹⁸¹⁾, the most effective of these latter options have often included a beta-lactam based antibiotic and a beta-lactamase inhibitor, such as amoxicillin/clavulanic acid or piperacillin and tazobactam ⁽¹⁸¹⁾.

In the search for new antibiotics, multiple sources have been examined, these have varied from bacterial selective viruses (bacteriophages), the products of other microbes, such as bacteria and fungi, and finally natural sources such as plants, animals and historical remedies ^(158, 159).

Along with many potential bacterial targets for treatment options there are also multiple options for the development of treatments. These can be dependent on the treatment type, for example antibiotics, vaccination and anti-virulence drugs or they can be dependent on the source of the new treatment ^(119, 132). With so many possible

avenues for treatments of antibiotic resistant bacteria, standardised methods, models, and development cascades are essential for stream-lining research, productivity and helping reduce overall costs. Table 1.6 identifies some of the known antibiotic development platforms that have been and are still used for antibiotic development and which agents have already been developed through them ⁽¹¹⁹⁾.

Table 1.6 Drug discovery platforms, origins and current standard of care antibiotics.

Table created from information found in Gadjács, Mario 2019 ⁽¹¹⁹⁾ and Lewis 2013 ⁽¹⁵⁸⁾. Drug discovery has been divided into platforms based on the origins of current standard of care antibiotics as well as providing details on novel drug types and their intended function ^(119, 158, 159). These platforms provide insight into our most commonly used antimicrobials, and it also helps to identify potential sources of antibiotic molecules ^(119, 158, 159).

Platform	Brief Description of Pros and Cons	Compounds in Practice discovered by platform.
Waksmann-platform/Natural products-platform ^(119, 158, 159)	<ul style="list-style-type: none"> • Screening for secondary metabolites in soil microorganisms (<i>Streptomyces</i>) with antibacterial activity • Background of known compounds during screening presents a major issue • Focusing on uncultured microorganisms and compound de-replication are promising approaches • Screening for antibacterial compounds from plant and marine origins represents an untapped resource of potential drugs 	Penicillin (First antibiotic discovered) Streptomycin (First drug active against tuberculosis (TB)) Daptomycin (MDR Gram-positives)
Domagk-platform/In situ screening-platform ^(119, 158, 159, 182)	<ul style="list-style-type: none"> • Screening the efficacy of antimicrobial compounds at the site of infection with the use of infection models; e.g., in an <i>in situ</i> mouse model or in a <i>Caenorhabditis elegans</i> worm model • Detects prodrug compounds that would be missed by high-throughput 	Sulphonamides (sulphamidochrysoidine)

	<p>screening and validation approaches</p> <ul style="list-style-type: none"> • Ethical considerations (related to the use of animal models) 	
<p>Species-selective platform (119, 158, 159)</p>	<ul style="list-style-type: none"> • Screening against a specific bacteria, resulting in compounds that act selectively against that pathogen • Requires a target that is innate and specific to microorganism • Lower probability of toxicity in the human host • New compounds will not affect commensals in the gut 	<p>Bedaquiline F₁F₀-ATPase-inhibitor in <i>Mycobacterium tuberculosis</i></p>
<p>High-throughput screening, Combinatorial chemistry (119, 158, 159)</p>	<ul style="list-style-type: none"> • Screening of public/commercially available libraries of compounds against bacterial strains and/or defined prokaryotic targets (ligand–target binding assay, specificity tests) 	<p>Oxazolidinones</p>
<p>Resistance reversing compounds (119, 158, 159)</p>	<ul style="list-style-type: none"> • Compounds affecting a defined mechanism of bacterial resistance, e.g., antibiotic-degrading enzymes, efflux pumps • Strains that are resistant to specific antibiotics may be sensitized, maintaining the efficacy of current drug pool 	<p>Beta-lactamase inhibitors (clavulanic acid, sulbactam, tazobactam, avibactam etc.) No efflux pump inhibitor has been approved yet for clinical use</p>
<p>Antimicrobial peptides (AMPs) (119, 158, 159)</p>	<ul style="list-style-type: none"> • Use of small-sized, positively charged, amphipathic molecules synthesized by plants, animals, or other bacteria • They play an important role in innate immunity in humans 	<p>No AMP has been approved yet for clinical use, however, some have been utilised in clinical trials⁽¹⁸³⁾.</p>

	<ul style="list-style-type: none"> • Structurally, they may be α-helices, β-sheets, or extended coils, all with different mechanisms of action • Toxicity in humans in higher concentrations • Difficulties in formulation 	
<p>Virulence modulation ^(119, 158, 159)</p>	<ul style="list-style-type: none"> • Compounds targeting expression and/or activity of bacterial virulence factors (capsule, toxins, fimbriae, biofilm) essential in their pathogenesis • Various small-molecule compounds and monoclonal antibodies have been described • Selective pressure to develop resistance is not present • The clinical relevance of virulence modulators is hard to determine <i>in vitro</i> 	<p>No virulence modulator has been approved yet for clinical use, however, some been utilised in clinical trials ⁽¹⁸⁴⁾.</p>

The use of a specific platform and standardised methods as shown in Table 1.6 could greatly reduce the time required to develop new antibiotics ⁽¹¹⁹⁾. These platforms each have unique requirements and challenges to assist in antibiotic development and as research and technology has progressed some have become more favourable than others.

For example, the Waksman platform was responsible for the discovery of many still in-use antibiotic classes but was abandoned by pharmaceutical companies due to overuse and the belief that no further antibiotics could be gained from soil samples ^(119, 158). However, improvements in genetic analysis have uncovered that potentially 99 % of bacteria found in soil are unculturable in laboratory environments and could provide new sources of antibiotics ⁽¹⁸⁵⁾. These bacteria and their products as well the addition of screening natural products such as plant and marine sources has also seen an increased adoption of this research platform for antimicrobial discovery ^(158, 186).

This platform specifically applies to NX-AS-401 which contains ajoene a naturally occurring molecules found in the *Allium sativum* or garlic plant. While originally the molecule was identified from garlic, only small amounts are created through crushing of garlic bulbs ⁽¹⁸⁷⁾. Therefore further development was required to allow the creation of ajoene via thermal rearrangement of the less stable-allyl sulfide molecule ⁽¹⁸⁷⁾.

1.4.1 Antibiotics derived from 'natural' sources

Most of the antibiotics in current use are derived from natural sources as they originate from micro-organisms. A newer approach to antibiotics is to look at other natural sources, including marine life, insects, plants and their associated by-products ^(158, 186, 188-190). This makes natural sources one of the largest areas for antimicrobial research, in both recent and historic use including a variety of different remedies have been tried to treat bacterial infections ^(158, 159, 186, 189-191). Development of an antibacterial compound from a natural source requires a multidisciplinary approach, years of research and comes with a high financial cost ^(188, 190). The initial process is the identification of antibacterial activity, however with an almost inexhaustible number of compounds to choose from this is a difficult task ^(186, 189-191). This has been shown in Table 1.7 which provides a list of known antibiotic properties of plants.

Table 1.7 Plants and associated compounds which have demonstrated antibacterial activity, Table adapted from Prof. M Cowan 1999 ⁽¹⁹²⁾

Common name	Compound	Class	Activity
Allspice	Eugenol	Essential oil	General
Aloe	Latex	Complex mixture	<i>Corynebacterium, Salmonella, Streptococcus, S. aureus</i>
Apple	Phloretin	Flavonoid derivative	General
Basil	Essential oils	Terpenoids	<i>Salmonella</i> , bacteria
Bay	Essential oils	Terpenoids	Bacteria, fungi
Black pepper	Piperine	Alkaloid	Fungi, <i>Lactobacillus, Micrococcus, E. coli, E. faecalis</i>
Blueberry	Fructose	Monosaccharide	<i>E. coli</i>
Buttercup	Protoanemonin	Lactone	General
Chamomile	Anthemic acid	Phenolic acid, Coumarins	<i>M. tuberculosis, S. typhimurium, S. aureus</i> , helminths, Viruses
Clove	Eugenol	Terpenoid	General
Cranberry	Fructose, Other	Monosaccharide	Bacteria
Dill	Essential oil	Terpenoid	Bacteria
Eucalyptus	Tannin	Polyphenol, Terpenoid	Bacteria, viruses
Green tea	Catechin	Flavonoid	General
Hops	Lupulone, humulone	Phenolic acids, (Hemi)terpenoids	General
Lemon balm	Essential oil	Terpenoid	<i>Ascaris</i>
Lemon verbena	Glabrol	Phenolic alcohol	<i>S. aureus, M. tuberculosis</i>
Licorice	?		<i>Plasmodium</i>
Oak	Quercetin (available commercially), Hexanal	Flavonoid, Aldehyde	General
Olive oil	Allicin	Sulphoxide	Bacteria, <i>Candida</i>
Onion	?	Terpenoid	Fungi
Peppermint	Reserpine	Alkaloid	General
Rosemary	Tannins	Polyphenols	Ruminal bacteria
Sainfoin	?		Helminths
Sassafras	Carvacrol	Terpenoid	General
Savory	Rhein	Anthraquinone	<i>S. aureus</i>
Senna	?		General

St. John's wort	?		Enteric bacteria
Tarragon	Caffeic acid	Polyphenols, Terpenoid	Viruses, bacteria, fungi
Thyme	Thymol, Tannins, Tatarol	Polyphenols, Flavones, Flavonol	<i>P. acnes</i> , other Gram-positive bacteria
Turmeric	Turmeric oil, Essential oil	Terpenoid	General
Valerian	Salicin	Phenolic glucoside	
Willow	Tannins, Essential oil	Polyphenols, Terpenoid	General
Yarrow	?		<i>E. coli</i> , <i>Salmonella</i> , <i>Staphylococcus</i>

The plethora of options listed in Table 1.7 are only some of the options, as this does not include animal products and many still have unknown mechanisms of action. The development pipeline from source of origin to licensed antibacterial is a long and expensive process, therefore only promising products are taken forward ^(119, 132).

During analysis of these compounds individual molecules also require analysis to identify their effects, not only for antibacterial purposes but also to identify potentially harmful effects such as direct toxicity, interactions with other medications or neutralisation by host components ⁽¹⁹³⁾. Identification of which molecules have antibacterial activity and fractionation of the compound may identify more active components or indicate a synergistic relationship between them ^(194, 195). Once antibacterial activity has been determined further work is required, testing the potential antibiotic against many different bacterial species and many strains ^(194, 195).

Two examples of natural compounds that have been studied extensively include honey ⁽¹⁹⁶⁻¹⁹⁹⁾ and ginger ^(200, 201). While the former is often used in whole preparations, products such as ginger are often turned into various extracts or essential oils for ease of use.

Honey represents the challenge of "natural" antimicrobial products as while it has proven antibacterial effect its activity varies based on initial composition and that in turn is based on geographical region and season ⁽¹⁹⁶⁻¹⁹⁹⁾. The composition can vary, with levels of sugar, water, hydrogen peroxide (H₂O₂) and protein concentrations varying between sources and batches ^(196, 197). Since honey can be composed of >100

molecules, it is difficult to ascertain its complete mechanism of action ^(196, 197). Studies have shown that components of honey have different antibacterial effects, for example the percentage of H₂O₂ is directly linked with bacterial eradication in some honey ^(196, 197). However, in other cases the pH and water content are also antibacterial by altering enzyme function and eliciting osmotic pressure damage to the bacterial cells, respectively ^(196, 197). These are some of the actions linked to multiple honey types, before further in-depth investigation into the action of specific honey molecules such as phenolic acids, flavonoids and methylglyoxal which all have antibacterial activity ^(196, 197).

Meanwhile plant-based remedies such as ginger are comparative to the garlic based antimicrobial as it shows how plants contain multiple molecules with similar functional groups that have antimicrobial activity ^(200, 201). Ginger have been extensively researched for antibacterial effects, as well as other health benefits ^(200, 201). This has included antifungal, antiviral, anti-cancer and anti-inflammatory effects ^(200, 201). Research has utilised aqueous and alcoholic extracts, powders and the root itself ^(200, 201). Fractionation of ginger has proven that these activities are not limited to a single molecule but many found within the organism, primarily a group of molecules called gingerol but others such as paradols, and zingerone have also been identified ^(200, 201).

Overall, there are many sources for potential new antibiotics, many require further work, refinement, and greater understanding of their mechanism of action. One such source is the plant *Allium sativum* commonly known as garlic. This plant has been used historically as a treatment for infection and has once again become a topic of interest in the search for new antibiotics.

1.4.2 *Allium sativum* (Garlic)

Garlic (**Figure 1.11**) itself has been studied extensively for its proposed health benefits, in various forms from oils, aqueous and alcoholic extracts, single molecules and in historic salves and ointments ^(135, 202-212).



Figure 1.11 *Allium Sativum* (Garlic).

The beneficial health effects have been well documented overall, with evidence supporting that garlic can provide anti-inflammatory ^(202, 209) and anti-cancer effects ^(207, 208), as well as can improve cardiovascular health ^(203, 213) and can also acts as both antibacterial and anti-fungal ^(135, 194, 204, 206, 210, 212, 214-220). These effects have all been seen historically but the use of garlic for health reasons waned as other products such as penicillins and standardised medications became more widely available ^(204, 211).

The necessity for new antimicrobial agents has brought garlic back to the forefront of research. The health benefits of whole garlic preparations have been studied extensively, with multiple authors reporting how aqueous garlic extracts and garlic oils can produce antibacterial effects against a wide variety of species ^(221, 222). Historic solutions containing garlic such as Bald's eyesalve have recently been studied to understand their mechanisms and determine if they can combat MDR bacterial infections ^(205, 223). Bald's eyesalve contains a mixture of onion, garlic, wine, and bile salts, however, removal of the garlic component severely compromised the antibacterial effects ⁽²²³⁾. Garlic aqueous and alcohol extracts have shown that the solutions elicit an antibacterial effect on a wide arrange of organisms, including Gram-

negatives, Gram-positive, anaerobes and mycobacterium (194, 204, 210, 214-217, 219, 221, 222). The concentrations required for bacterial eradication are dependent on organism and preparation and the underlying mechanism of action has yet to be determined (194, 204, 210, 214-217, 219, 221, 222). Garlic has also demonstrated anti-biofilm activity (194, 206, 215, 218, 219), however in the one study Furner-Pardoe *et al* (223) their finding was that garlic had no anti-biofilm activity.

Homogenised garlic and extract are not costly to prepare but their use is limited and there is the potential for greater antibiotic efficacy if the active molecules could be determined. Identification of the active molecules could lead to understanding their mechanism of action against bacteria and assist in optimising the extracts and preparations for improved efficacy as well as means to upscale production (224). Several molecules have been identified from garlic fractionation (**Figure 1.12**).

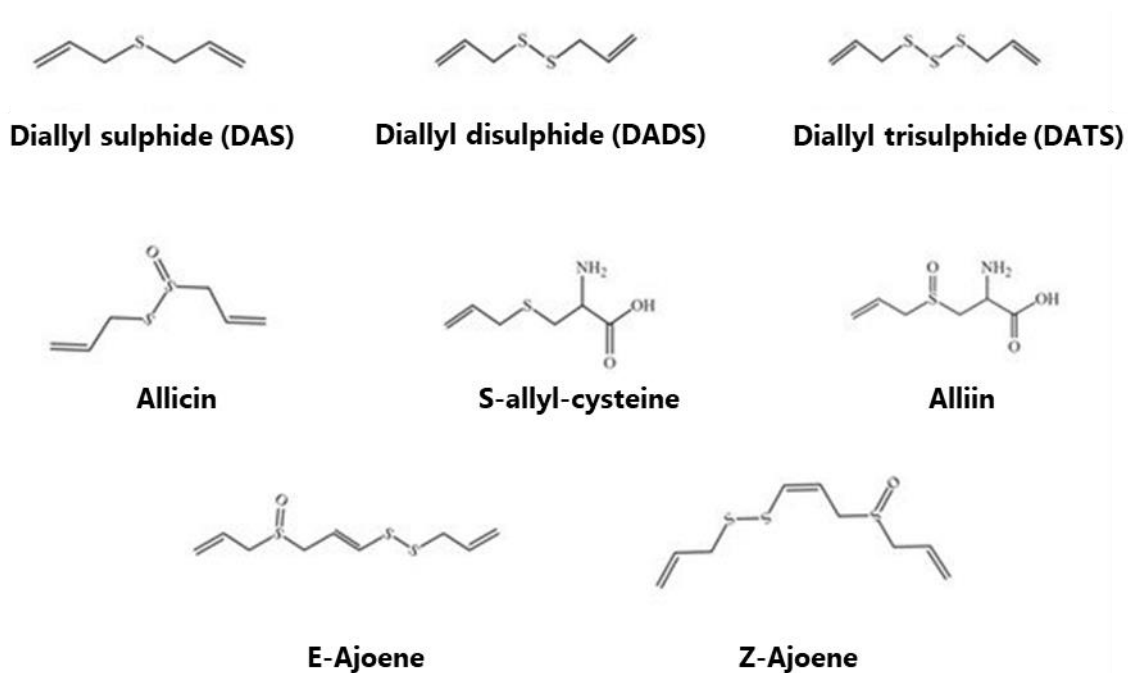


Figure 1.12 The bioactive molecules found within garlic.

Image created from information in Shang *et al* 2019 (212)

The most common trait of the molecules above (**Figure 1.12**) is the presence of a sulphur bond, this may be a single sulphur bond (sulphide) or more (disulphide and trisulphide) (203, 212). This bond is seen throughout nature but in the garlic derived molecules it may be responsible for the medicinal effects of garlic. The diallyl

tri/di/sulphide group has demonstrated antibacterial activity in previous studies ^(135, 214, 216) and has also been studied for its medicinal effects, however it is a skin irritant and one of the causative agents for garlic allergy and therefore makes it difficult to support its use *in vivo* ^(135, 214, 225).

As shown in Figure 1.12 alliin and S-diallyl-cysteine are similar molecules, only separated by a double sulphoxide bond. There has been little research into the health benefits of these two compounds as alliin is enzymatically degraded by alliinase to allicin when garlic is chopped or crushed. This means homogenisation and extracts contain very little alliin ^(135, 204, 212, 214). Therefore, the focus of individual garlic derived molecules has focused extensively on the effects of allicin.

1.4.2.1 Allicin

Much like whole garlic extracts, the proposed medicinal benefits of allicin are plentiful. The molecule itself is claimed to be anti-cancer, anti-fungal, anti-viral, anti-bacterial and can promote cardiovascular health ^(66, 135, 180, 205, 212, 214, 215, 226-232).

In terms of antibacterial activity allicin has demonstrated effects on a wide range of organisms including both Gram-positive, Gram-negative and MDR pathogens ^(66, 135, 180, 212, 214, 215, 226, 228-230, 232). As well as being able to inhibit bacterial growth and kill bacteria, a secondary anti-biofilm effect has been identified that may make allicin potentially effective in the treatment of chronic wounds ^(135, 180, 215, 226, 229).

Despite all of these claims, the complete function of allicin on the human body or bacteria has yet to be determined. Current research has identified that it is readily absorbed across cell membranes, but does not cause cell leakage ⁽²²⁷⁾. It is also well documented that molecules of this type are known to act upon cysteine based residues and in studies where cysteine has been added alongside allicin the antimicrobial activity was severely impaired ⁽²³¹⁾. However, this is a broad identification of its mechanism and the specific activity has yet to be determined. As an anti-fungal agent there is evidence that shows allicin reacts with the thiol group on glutathione an important molecule in cysteine metabolism and stress reactions ^(233, 234). Alteration of

this vital component is thought to lead to cell apoptosis, but whether this mechanism is the same for bacterial glutathione is unknown ⁽²³⁴⁾.

While allicin has demonstrated a variety of health benefits, the issue arises on its stability. The molecule itself is unstable, degrading over 20 hours at 20 °C and within minutes at temperature over 80 °C into the diallyl polysulphides ⁽²³⁵⁾. In Bald's eyesalve the antibacterial properties of the garlic component were thought to be due to the actions of allicin ^(205, 223). However, this was not confirmed as allicin was not detected via chromatography ^(205, 223). Therefore, the presence of allicin can be disputed as the mixture is created by leaving it in the dark for nine days ^(205, 223) and allicin is known to have a short half-life <2.5 days ⁽²³⁵⁾. Therefore indicating that there are other active garlic components.

1.4.2.2 Ajoene

The lack of stability of allicin makes it less desirable as a potential antibiotic, and since there may be other garlic-based molecules with antibacterial activity further research is required. Thermal rearrangement of allicin molecules can result in the creation of a more stable molecule, ajoene ⁽¹⁸⁷⁾. When garlic is macerated in oil only small amounts of ajoene are produced ⁽²³⁶⁾. Therefore, the development of a semi-synthetic molecule via thermal rearrangement allows for upscaled production.

The ajoene molecule is larger than allicin (**Figure 1.12**), and two isomers are often formed. The molecule is more stable than allicin with stability at 37 °C over 24 hours ⁽¹⁹⁴⁾, however it is still quickly degraded in whole blood with a half-life < one minute ⁽²³⁷⁾.

Much like allicin, there have been many health benefits attributed to the action of ajoene. Studies have once again focused on anti-viral, anti-fungal anti-cancer, cardiovascular, and antibacterial properties ^(135, 179, 187, 194, 207-209, 213, 216, 217, 220, 236, 238-243). However, there is substantially less research into the effects of ajoene compared to allicin and garlic.

The limited antibacterial data ^(135, 194, 217, 241, 244) comprises of a few studies that primarily focus on anti-Gram-negative activity and not its ability to inhibit or kills cells, but rather the ability of ajoene to inhibit and disrupt the formation of bacterial biofilms, specifically *Pseudomonas aeruginosa* (*P. aeruginosa*) ^(194, 241, 244). These studies have provided some information into the activity of ajoene, specifically the different functions of the E and Z isomers, proving that the Z isomer is much more effective at eliciting an effect in Gram-negatives, but not for killing ^(194, 217). While much like allicin, the mechanism of action for ajoene has yet to be determined. The little research has shown that it may differ from that of allicin. For example, as an anti-fungal ajoene does not target the glutathione but rather the synthesis of phosphatidylcholine biosynthesis a component of biological membranes ⁽²⁴³⁾. However, phosphatidylcholine is rarely found in pathogenic bacterial membranes, giving no hints to the anti-bacterial mechanism for ajoene ⁽²⁴⁵⁾.

1.4.2.3 NX-AS-401

NX-AS-401 is a garlic derived formulation that contains >90 % ajoene in a 50:50 E and Z isomer mix, and other unidentified garlic derived molecules. The compound has not been thoroughly researched for its effects on bacteria. Limited NX-AS-401 studies have primarily focused on its effect on *P. aeruginosa* where it has demonstrated the ability to inhibit quorum sensing and prevent biofilm formation ⁽¹⁹⁴⁾.

The main component of NX-AS-401 is ajoene, however the remaining constituents contain small molecules that have yet to be identified. Determining whether the percentage of ajoene present alters antimicrobial activity is important as this may lead to the identification of small garlic derived molecules that are also active against bacteria.

1.5 Aims and Objectives.

Since the primary component of NX-AS-401 is ajoene, the initial studies focused on the potential mechanism of antimicrobial action that ajoene has on bacteria. These include exchange reactions between the disulphide bond of ajoene and other disulphide bonds predominantly those found in cysteine residues that prevents protein prenylation. This is similar to the known mechanism of allicin (**Section 1.3.2.1**). An additional hypotheses for the mechanism of action for NX-AS-401 involves the ability to interact with specific pathogen associated proteins, such as the MSCRAMM group in *S. aureus* and therefore preventing biofilm formation/cell attachment as seen in other species such as *Pseudomonas* ^(194, 241). The final hypothesis is that garlic based compounds can alter cell permeability by disrupting the cytoskeleton framework similar to protein disruption ⁽²⁰⁸⁾.

This thesis aimed to identify the mechanisms of action of NX-AS-401, it focused on identifying the effects on the commonly isolated pathogen *Staphylococcus aureus* to determine the spectrum of activity against Gram-positive organisms.

A multi-stage approach was used to gain an overall understanding of the effects of NX-AS-401 on *S. aureus*, this included:

- Identifying whether the percentage of known garlic component and antimicrobial, ajoene, affected the efficacy of NX-AS-401. This was carried out by comparing two NX-AS-401 batches containing 70% and 90% ajoene respectively. This section also provided the opportunity to optimise standard methods.
- Comparing the potential role of NX-AS-401 with current standard of care antibiotics. Here the concentration that provided an antimicrobial effect was measured by identifying its minimum inhibitory/bactericidal concentrations in comparison with EUCAST clinical breakpoints using EUCAST methodologies for *S. aureus*. Further studies focused on determining when NX-AS-401 exposure affected *S. aureus* growth and whether repeated exposure caused increased tolerance, development of resistance or resulted in specific gene mutations.

- Determining whether NX-AS-401 had the potential to assist in chronic wound healing by identifying the effects NX-AS-401 had on *S. aureus* biofilm formation and the ability to disrupt pre-established biofilms. This section aimed to identify if NX-AS-401 could permeate pre-formed biofilms and cause bacterial cell death or if it caused dissemination of the bacteria potentially leading to systemic infection. This employed adapted EUCAST methods and biofilms were measured via mass, metabolism, and viable cell number. Confocal microscopy with live/dead staining and scanning electron microscopy used to confirm NX-AS-401 mediated changes in biofilm. RT-qPCR was performed to determine if NX-AS-401 affected a specific gene target.
- Identifying whether sub-MIC NX-AS-401 treatment modulated *S. aureus* virulence or infection progression. This aimed to ascertain if low doses of NX-AS-401 remained an effective treatment or whether these concentrations may exacerbate injury. This included directly monitoring exo-enzyme function through phenotypic media tests. A systemic approach to virulence modulation utilised *Galleria mellonella* (*G. mellonella*) to determine whether NX-AS-401 alters *S. aureus* virulence *in vivo* and also identify its effects on the innate immune system. *In vitro* cell culture was used to understand the role of NX-AS-401 as a topical agent for wounds and associated infections. Immortalised human keratinocyte cell line HaCaT was exposed to NX-AS-401 to identify any cytotoxic properties. HaCaT cell were also infected with *S. aureus* and treated with NX-AS-401 to determine if NX-AS-401 altered the ability of *S. aureus* to adhere and invade host cells.

2.0 Materials and Methods

2.1 Materials

A list of all the reagents, suppliers and product numbers that were used throughout this thesis.

Table 2.1 Reagent List

Reagent	Supplier	Product Number
0.4 % Trypan Blue Solution	Gibco	15250061
10,000 U/ml Penicillin / Streptomycin	Gibco	15140122
10µg Gentamicin Discs	Oxoid	CT0024B
100 % Foetal Calf Serum (Qualified)	Gibco	11550356
15µg Erythromycin Discs	Oxoid	CT0020B
1M Tris-HCL Buffer	Fisher Scientific	10031793
2µg Clindamycin Discs	Oxoid	CT0064B
30µg Cefoxitin Discs	Oxoid	CT0119B
30µg Tetracycline Discs	Oxoid	CT0054B
5µg Ciprofloxacin Discs	Oxoid	CT0425B
Agar Silver Paint	Agar Scientific	AGG3790
Alamar Blue Reagent	Thermo-Fisher	DAL1025
Cefoxitin Sodium Salt	Oxoid	C4786-250MG
Celltiter-Blue Assay	Promega	G8081
Cellulase from <i>Aspergillus niger</i>	Merck	C1184
Ciprofloxacin Powder	Oxoid	17850-25G-F
Clindamycin Hydrochloride Powder	Oxoid	C5269-10MG

Columbia Blood Agar (Sheep)	Thermo-Fisher	PB0123
Crystal Violet Solution	Merck	C0775
Defibrinated Horse Blood	Oxoid	11974152
Deionised H ₂ O (DH ₂ O)	Swansea University	
Dimethyl Sulphoxide (DMSO)	Sigma-Aldrich	276855-250ML
DNase Agar	Oxoid	PO0128
Dulbecco's Modified Eagle Media [+ pyruvate]	Gibco	41965039
Egg yolk solution	Oxoid	SR0047
Erythromycin Powder	Oxoid	E5389-5G
Ethanol	Fisher Scientific	10610813
FilmTracer Live/Dead	Thermo-fisher	L10316
Gentamicin Solution	Gibco	15750060
Gentamicin Sulphate Salt	Merck	G3632-5G
Glacial Acetic Acid	Fisher Scientific	10384970
Glutaraldehyde (25 %)	Merck	G5882-100ML
Glyceryl tributyrat	Merck	T8626-100ML
Hexamethyldisilazane (HMDS)	Merck	440191-100ML
Hydrochloric Acid (HCl) 1M	Fisher Scientific	10467640
Immersion Oil	Merck	56822-250ML
L-Glutamine 200nM (100X)	Gibco	25030081
Lysostaphin (500 units/ml)	Merck	L7386-5MG
Lysozyme	Merck	L6876-5G
Methanol	Fisher Scientific	10675112
Mueller Hinton Agar	Oxoid	CM0337

Mueller Hinton Broth	Oxoid	CM0405B
NaCl	Fisher Sci	BP358212
NaOH tablets	Merck	S8045
NX-AS-401	Neem Biotech	N/A
Osmium Tetroxide (OsO4)	Agar Scientific	AGR1015
Phosphate Buffered Saline for Tissue Culture	Gibco	10010023
Phosphate Buffered Saline (PBS)	Sigma-Aldrich	79382
PIPES Buffer	Merck	P6757-100G
PowerUP SYBR Green Master Mix	Thermo Scientific	A25777
Proteinase K	Promega	V3021
Resazurin powder	Fisher Sci	10269990
RNA Later	Thermo-fisher	AM7021
Skim Milk Powder	Oxoid	LP0031B
Sodium Acetate	Merck	1062681000
Sodium Metaperiodate	Merck	S1878-100G
Tetracycline Powder	Oxoid	T8032-10MG
Triton X-100	Merck	T8787-100ML
TrypLE Express (No Phenol Red)	Gibco	12604021
Tween 20	Merck	P9416-100ML

2.1.1 Manufacturers kits used.

A list of all kits, their catalogue numbers and contents that were used throughout this thesis.

Table 2.2 Kit List:

Name	Provider	Catalogue Number	Contents
QIAamp DNA mini	Qiagen	51204	QIAamp mini spin columns, Proteinase K, Buffer AL, Buffer ATL, Buffer AW1, Buffer AW2, Buffer AE 2ml Collection tubes
Maxwell RSC simplyRNA Cells	Promega	AS1390	1-Thioglycerol, Maxwell RSC Cartridge, Elution Tubes, Blue Dye, Lysis Buffer, Nuclease-Free Water, Homogenization Solution, DNase I (lyophilized) Maxwell RSC Plungers
GoScript™ Reverse Transcriptase	Promega	A2801	Reverse Transcriptase Mix Random Primers
FilmTracer Live/Dead	Thermo-fisher	L10316	SYTO 9 Propidium Iodide

2.1.2 Preparation of reagents

2.1.2.1 Media

Mueller-Hinton Agar (MHA; Oxoid, Hampshire, UK) and Mueller-Hinton Broth (MHB; Oxoid, Hampshire, UK) were made according to the manufacturer's instructions at 38 g/L and 21 g/L, respectively. Phosphate Buffered Saline (PBS) (Oxoid, UK) was made according to manufacturer's instructions by dissolving one tablet in 200 ml of deionized H₂O (DH₂O) obtained through the laboratory deionization equipment. All media was sterilised via autoclave at 121°C for 15 minutes.

Additional media types were prepared to monitor changes *S. aureus* growth and for phenotypic virulence tests (**Section 2.1.18**) as listed in Table 2.3.

Table 2.3 List and composition of media used to monitor changes *S. aureus* growth and phenotypic virulence:

Media Type:	Media Composition
NX-AS-401	0 – 12.5 ml of NX-AS-401 added to 100ml of MHA to create agar plates containing 0 – 128 µg/ml NX-AS-401.
DNase	OXOID, created to manufacturer's instructions.
Blood	5ml of Defibrinated Horse Blood per 100ml MHA
Lipid	2.5ml of Tributyrin and 2.5 of Tween 80 per 100ml of MHA
Milk	100ml of Skim Milk per 100ml of Double Strength MHA

In studies involving MHA supplemented with NX-AS-401, once MHA had been autoclaved and cooled to 60 °C, NX-AS-401 was added to produce the desired concentration. For example, to create the highest concentration of 128 µg/ml, 1.25 ml of 10240 µg/ml NX-AS-401 stock solution was added to 100 ml of MHA.

Stocks of defibrinated horse blood, Tributyrin and Tween 80 were aliquoted previously to prevent contamination of the whole stock. Aliquots were aseptically added to previously autoclaved media after cooling to 50°C to prevent lysis/degradation. NX-AS-

401 supplementation was added to 50°C media using filter sterilisation (0.22 µm). If any supplemented media presented with contamination plate were discarded and fresh media produced.

2.1.2.2 NX-AS-401

NX-AS-401 was provided by Neem Biotech Limited (Abertillery, UK). Two formulations were used in this study.

NBR160026-6A (referred to as NBR 26-6A) used in chapter 3 and NX-AS-401 used in Chapter 4 onwards were both provided by Neem Biotech. The difference between the compounds was the percentage of ajoene in the solution. NBR 26-6A contained approximately 70 % mixed E and Z isomers of ajoene whereas the latter formulation referred to as NX-AS-401 (Chapter 4 onwards) contained >90 %.

Preparation of both NBR 26-6A and NX-AS-401 was the same. The compound was weighed at 102.4 mg and diluted in 5 ml of 80 % Dimethyl Sulphoxide (DMSO; Merck, Southampton, UK) and a further 5 ml of required media (MHB, PBS or DH₂O) to create a stock solution of 10.24 mg/ml. Stocks were then divided into 1 ml aliquots to prevent loss of integrity via multiple freeze/thaw cycles and stored frozen at -20°C. For use, aliquots of 1 ml were removed and allowed to defrost completely before further dilution to a working concentration in the required media.

Since DMSO has proven antibacterial activity against *S. aureus* (**Section 4.4.2**) 1 ml NX-AS-401 stock solutions were always dissolved in 10 or greater ml of diluent. This was to ensure that DMSO concentration remained <4 % during all experiment to ensure that any growth inhibition was caused by NX-AS-401 and not the DMSO solvent.

2.1.2.3 Preparation of antibiotic solutions

All antibiotic powders were purchased from Oxoid Hampshire, UK. Further information in Table 2.4 which provides each antibiotic and diluent utilised. Antibiotic stock solutions were divided into 1ml aliquots and stored at -20 oC. The aliquots were thawed completely and vortexed before further dilution. To create working stock solutions, antibiotics were filter sterilised via 0.22 µm filter and diluted in the required media (MHB, PBS or DH₂O). All stock solutions contained 50 mg of powder dissolved in their respective diluent to create stock solutions of 5 mg/ml.

Table 2.4 Antibiotics and diluents.

Antibiotic	Diluent
Gentamicin	10 ml of deionised H ₂ O (DH ₂ O) / MHB
Tetracycline	1 ml of 100 % ethanol diluted in 9 ml DH ₂ O / MHB
Ciprofloxacin	1 ml of 0.1 M hydrochloric acid (HCL) diluted in 9 ml DH ₂ O / MHB
Clindamycin	10 ml of DH ₂ O / MHB
Erythromycin	1 ml of 95 % ethanol diluted further in 9 ml DH ₂ O / MHB
Cefoxitin	10 ml of DH ₂ O / MHB

2.1.2.4 Additional Reagents

Crystal violet powder (Merck, Southampton, UK) was weighed (10 g/L) and dissolved in sterile H₂O to produce a 1 % crystal violet solution.

Resazurin solutions (0.15 mg/ml) were prepared by dissolving 15 mg of resazurin powder (Fisher Scientific, UK) in 100 mL of sterile PBS, all solutions were filter sterilised (0.22 µm) freshly made prior to testing to prevent degradation of resazurin to resofurin by UV light.

Lysostaphin (Merck, Southampton, UK) was made as a 200 units/ml solution by dissolving 10 mg in 1 ml of sterile DH₂O and filter sterilised (0.22 µm). Solutions were freshly made for each extraction and created solutions were never frozen to prevent enzyme degradation.

Lysozyme (Merck, Southampton, UK) was made up to a 2.115x10⁶ units/ml solution by dissolving 528.75 mg in 10 ml of sterile DH₂O and filter sterilised (0.22 µm). Solutions of lysozyme were stored for a maximum of 48 hours at 1-5 °C.

Cellulase from *Aspergillus niger* was (Merck, Southampton, UK) made up to 0.5 units/ml by dissolving 16.6 mg in 10 ml of sterile DH₂O and filter sterilised (0.22 µm).. Solutions of cellulase were stored for a maximum of 48 hours at 1-5°C.

0.1 M PIPES solution was prepared by dissolving 12 mg of powder in 100 ml of sterile deionised water, pH was adjusted to 6.8 or 7.4 using NaOH tablets and filter sterilised (0.22 µm)..

Sodium acetate buffer was prepared by adding 1.84 ml of glacial acetic acid (Fisher Scientific, UK) and 1.48 g of sodium acetate (Merck, Southampton, UK) to 350 ml of DH₂O. pH was then adjusted with either glacial acetic acid or 1N NaOH to a final pH of 5.5 and filter sterilised (0.22 µm)..

Sodium metaperiodate solution was prepared by adding 856 mg of sodium metaperiodate (Merck, Southampton, UK) to 100 mL of 50 mM sodium acetate buffer and filter sterilised (0.22 µm)..

20 mM Tris-HCL buffer was prepared by dilution of 2 mL 1 M Tris-HCL (Fisher Scientific, UK) in 8 mL of sterile DH₂O, pH was monitored and adjusted with 1 M HCL if required and filter sterilised (0.22 µm)..

0.1 mg/ml Proteinase K was prepared by adding 1 mg of proteinase K to 10 ml of 20 mM Tris-HCL buffer pH 7.5 and filter sterilised (0.22 µm)..

2.2 Bacterial Strains

Table 2.5 Bacterial isolates used

Name	Species Name	Source	Original source stock:	Originally obtained from:
NCTC 13142	<i>Staphylococcus aureus</i>	Reference isolate	Cryobeads	National Collection of Typed Cultures
NCTC 12973	<i>Staphylococcus aureus</i>	Reference isolate	Cryobeads	National Collection of Typed Cultures
UHW 3	<i>Staphylococcus aureus</i>	Clinical isolate	Cryobeads	University Hospital of Wales (Chronic Wound)
UHW 8	<i>Staphylococcus aureus</i>	Clinical isolate	Cryobeads	University Hospital of Wales (Chronic Wound)
UHW 15	<i>Staphylococcus aureus</i>	Clinical isolate	Cryobeads	University Hospital of Wales (Chronic Wound)
UHW 18	<i>Staphylococcus aureus</i>	Clinical isolate	Cryobeads	University Hospital of Wales (Chronic Wound)
UHW 19	<i>Staphylococcus aureus</i>	Clinical isolate	Cryobeads	University Hospital of Wales (Chronic Wound)
CRI 2	<i>Staphylococcus aureus</i>	Clinical isolate	Cryobeads	University Hospital of Wales (Chronic Wound)
1457	<i>Staphylococcus epidermidis</i>	Clinical Isolate	Glycerol	Dr. Llinos Harris
5179-R1	<i>Staphylococcus epidermidis</i>	Clinical Isolate	Glycerol	Dr. Llinos Harris

All strains were stored at -80 °C on Cryobeads™ (Pro-Lab, Cheshire, UK) containing a proprietary preservation media and 10% glycerol and were cultured onto un-supplemented Mueller Hinton Agar plates or into Mueller Hinton Broth when required.

2.3 Methods

2.3.1 Preparation of a standardised bacterial inoculum (based on EUCAST guidelines; EUCAST 2017 Version 6.0 ⁽²⁴⁶⁾)

A single Cryobead™ was removed from -80 °C stock and streaked onto a fresh MHA plate and incubated at 37 °C overnight. The next day the plate was used to prepare inoculum (**Figure 2.1**). Unless otherwise stated, inocula were standardised according to the following protocol:

EUCAST methodologies⁽²⁴⁶⁾ required a standardised inoculum of 10^6 CFU/ml, therefore a sweep of bacteria was selected using a sterile plastic loop and suspended in the required liquid media (PBS, MHB). The optical density of the suspension was measured at 625 nm using a Jenway Spectrophotometer (Fisher Scientific, Leicestershire, UK). EUCAST ⁽²⁴⁶⁾ guidelines state that an absorbance reading between 0.08 and 0.1 absorbance units (a.u.) at 600-625 nm is equivalent to 10^8 CFU/ml. This is equal to a 0.5 McFarland Standard.

Then total viable cell (TVC) counts (**Section 2.3.4**) were performed on bacterial standards to ensure a standardised number of cells were used in each experiment. Once a standard equal to 10^8 CFU/ml was created this was diluted 1:100 in the relevant media (PBS, MHA etc.) to a final cell density of 10^6 CFU/ml.



Figure 2.1 Selection of colonies on an agar plate.

A sweep was taken from the areas highlighted by the white box to create a standardised inoculum.

2.3.2 Technical and Biological Replicas

All experiments were performed in triplicates for biological replicates. Each biological replicate consisted of three technical replicates providing an n=9 unless otherwise stated.

2.3.3 Antimicrobial Sensitivity Testing (AST)

2.3.3.1 EUCAST Disc Diffusion

Antibiotic disc diffusion was performed on MHA and utilised Kirby-Bauer discs (Oxoid, Hampshire, UK) following the EUCAST disc diffusion protocol ⁽²⁴⁶⁾. A 10⁶ CFU/ml inoculum was created according to Section 2.3.1, the inoculum was spread onto an MHA plate using a sterile cotton swab ensuring the entire plate surface was covered. Discs were then applied within 15 minutes using sterile forceps, the plates were inverted before incubation at 37 °C for 18-20 hours.

Then zones of inhibition were measured using digital callipers (Powerfix, UK), the measurements were compared against the EUCAST clinical breakpoints version 9.0 ⁽²⁴⁷⁾ to determine antibiotic resistance / sensitivity profiles.

2.3.3.2 EUCAST Minimum Inhibitory Concentration (MIC)

MICs for both NX-AS-401 and antibiotics were determined following the EUCAST broth microdilution methodology ⁽²⁴⁸⁾. All experiments tested antibiotics against bacteria at a starting density of 5 x 10⁵ CFU/ml against a concentration gradient of NX-AS-401 or relevant antibiotic in accordance with a defined template (**Figure 2.2**). Broth microdilution was performed in 96 well plates, read at 625 nm in a BMG Fluostar spectrophotometer (BMG Labtech, Aylesbury, UK), and incubated at 37 °C for 18-20 hours. Then, plates were read again, and the MIC calculated as the lowest concentration that prevented growth by 90 % according to absorbance. Antibiotics MICs were compared to the EUCAST clinical breakpoints version 9.0 document to identify antibiotic susceptibility / resistance profiles ⁽²⁴⁷⁾.

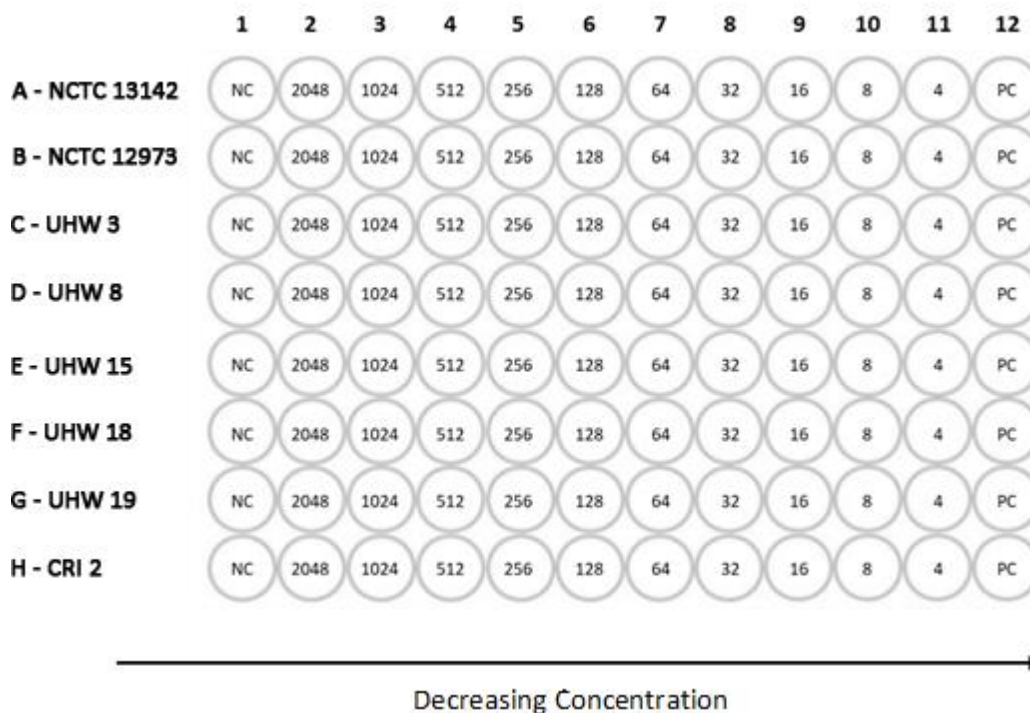


Figure 2.2 Example of Broth Microdilution plate layout

An antibiotic concentration gradient was created via serial dilution with 100 µl of stock NX-AS-401/antibiotic and 100 µl and sterile MHB. Each column contained a different antibiotic concentration, and a different bacterial strain was inoculated into each row. A negative control (NC) containing only MHB was placed into column 1. Column 12 contained a positive control (PC) that only contained 5×10^5 CFU/ml.

In Chapter 3 treatment of *S. aureus* NCTC 13142 with NBR 26-6A was extended to 48 hours in these experiments to identify a timepoint and concentration that could eradicate all bacteria.

2.3.3.1 Minimum Bactericidal Concentration (MBC)

Minimum bactericidal concentrations were determined by spreading the 200 µl contents of treated wells where growth was inhibited above 90 % onto MHA plates. Then, plates were incubated for 20-24 hours at 37 °C before visual inspection. Plates where growth was absent were identified as the bactericidal concentrations, and the MBC identified as the lowest concentration able to prevent growth on agar.

2.3.4 Total Viable Cell (TVC) Counts

TVC counts were performed on a minimum of five separate occasions during this study according to the Miles and Misra methodology ⁽²⁴⁹⁾. NX-AS-401 concentrations between 0 - 2048 µg/ml were tested in the initial Time/Kill curve experiments. TVC counts were performed on standardised bacterial inoculums created according to section 2.3.1 in a greater volume of 50 ml. These standardised inoculums were either diluted 1:2 with sterile MHB or MHB containing the required NX-AS-401 concentration (4 - 2048 µg/ml). Samples were taken at predetermined intervals, hourly for the first 12 hours and then every six hours until 48 hours. The samples were serially diluted 1:10 using sterile PBS. Then, 10 µl of each dilution was placed onto MHA plates and the 10 µl droplets were allowed to dry before plates were inverted and incubated at 37 °C for 24 hours (**Figure 2.3**). Then, colonies were counted and multiplied by the dilution factor to determine the TVC (CFU/ml) as shown in the calculation below.

Calculation used to determine CFU/ml:

$$\text{CFU/ml} = (\text{Number of colonies} \times \text{dilution factor}) / \text{volume}$$
$$1,000,000,000 \text{ or } 10 \times 10^9 = (10 \times 10^6) / 0.01$$



Figure 2.3 Example of TVC counts after incubation at 37 °C on MHA

Bacterial suspensions were serially diluted 1:10 and plated. After incubation bacterial colonies were counted allowing for numeration and quantification.

2.3.5 Growth Curves

Growth curves were performed by following the methods stated in Section 2.3.3.2, however, the 96 well plate was covered with a gas permeable plate seal and incubated at 37 °C in a Fluostar BMG (BMG Labtech, Aylesbury, UK) plate reader at 37 °C for 24 hours and optical density was read hourly at 625 nm.

2.3.6 Minimum Biofilm Inhibition/Eradication Concentration (MBIC/MBEC)

The effects on biofilm formation and disruption cannot be performed via standard optical density measurements. Biofilm density restricts the efficacy of optical density readings, therefore, additional methodologies were required, as detailed below.

The ability of antimicrobial agents to inhibit biofilm formation was monitored after MIC testing (**Section 2.3.3.2**). The planktonic cells and residual media/inhibitor/antimicrobial agent were carefully removed via pipetting. Remaining biofilm was measured via TVC counts (**Section 2.3.4**) with mass and metabolism measured using the following methods respectively:

2.3.6.1 Crystal violet

Quantification of biofilm biomass was performed using the crystal violet method described by O'Toole ⁽⁸²⁾.

After the removal of the planktonic phase, biofilms were washed twice with sterile PBS to remove any loosely attached cells. The remaining biofilm was fixed with 100 % methanol for 15 minutes (Fisher Scientific, Loughborough, UK) prior to staining with 0.1 % crystal violet for 30 minutes (Merck, UK). The excess crystal violet stain was removed via pipette and the biofilms were washed twice with PBS to remove residual stain. Finally, 7 % glacial acetic acid (Fisher Scientific, UK) was added to release the colour from the cells. The plate was read in a spectrophotometer BMG Fluostar (BMG Labtech, Aylesbury, UK) set to 570-590 nm.

2.3.6.2 CellTiter-Blue Assay

Biofilm metabolism was measured using resazurin reagents ⁽²⁵⁰⁾. The conversion of resazurin to resofurin can be measured via both colour change and fluorescence. Resazurin assays were performed in accordance with the Promega Cell-Titre blue assay guide ⁽²⁵⁰⁾. After the removal of the planktonic phase, biofilms were washed twice with sterile PBS to remove any remaining planktonic cells. Then, 20 µl of Resazurin and 180 µl of PBS were added to each well, the plate was wrapped in foil prior to incubation in the dark at 37 °C for four hours. Then, upon removal, plates were read for fluorescence using the Fluostar BMG set to 550 nm^{EX} / 590 nm^{EM}.

2.3.7 Minimum Biofilm Eradication Concentration (MBEC)

S. aureus biofilm was grown in a 96 well plate by inoculating with 100 µl of standardised bacterial inoculum and 100 µl of sterile MHB. The plates were incubated for 24 or 48 hours at 37 °C to allow biofilm development. Planktonic cells and additional media were carefully removed using a pipette and the established biofilms were then treated with a concentration gradient of NX-AS-401 used for MIC determination (**Section 2.3.3.2**). Then plates were incubated for a further 20 hours at 37 °C. Post-treatment biofilm disruption was monitored using TVC counts (**Section 2.3.4**) and the two methods described above (**Section 2.3.6.1-2**)

2.3.8 Calculating the biofilm optical density cut off (OD^{cut}) value of each *S. aureus* strain

OD^{cut} is a value that represents the ability of each strain to form a biofilm.

The biofilm forming potential of a strain was determined after crystal violet staining (**Section 2.3.6.1**) via the following calculation provided by Stepanovic *et al*, 2000⁽²⁵¹⁾ ⁽²⁵²⁾:

NC = Negative Control OD = Optical Density

$$\text{OD}^{\text{cut}} = \frac{\text{Sample OD}}{(\text{Average OD values of NC} + 3 \times \text{Standard deviation of the NC})}$$

The OD^{cut} value was then compared to the original sample OD to determine biofilm forming potential. In accordance with the method created by Stepanovic *et al*, 2000⁽²⁵¹⁾ ⁽²⁵²⁾ OD^{cut} values measure the ability of a strain to form a biofilm. Values identify a strain as a (0-2) weak, (2-4) moderate or (4+) strong biofilm former.

2.3.9 Identification of biofilm phenotype based on composition.

Biofilms were generated over 48 hours (**Section 2.3.6.**) The biofilms were then treated with either 200 µl of 40 mM Sodium metaperiodate solution or 200 µl of 0.1 mg/ml proteinase K (**Section 2.3.2.4**) and incubated at 37 °C for two hours according to the method described by McCarthy *et al*, 2015⁽¹⁰⁹⁾. Once incubation was complete the plate was stained with crystal violet (**Section 2.3.6.1**) and compared to untreated biofilm controls. Two *Staphylococcus epidermidis* strains, 1457 and 5179-R1 were provided by Dr Llinos Harris and have been previously identified as polysaccharide and protein biofilm formers respectively ⁽²⁵³⁾. Both *S. epidermidis* strains were used as controls to ensure the activity of sodium metaperiodate on polysaccharide-based biofilms and proteinase K on protein-based biofilms.

2.3.10 Antibiotic Checkerboards

Antibiotic checkerboards were set up in a 96 well plate, in a similar layout used for EUCAST broth microdilution (Section 2.3.3.2). Two gradients were created (Figure 2.4), horizontally and vertically using two antimicrobial agents. Then 100 µL of standardised bacterial inoculum (5×10^5 CFU/mL) was added to each well. The plate was then read in the spectrophotometer Fluostar BMG (BMG Labtech, Aylesbury, UK) at 625 nm. The plate was incubated at 37°C for 18-20 hours and read again using the Fluostar BMG. Antibiotic interactions were determined via Fractional Inhibitory Concentrations Indices (FICI) values⁽²⁵⁴⁾ and using the Bliss independence model^(255, 256) in the MacSynergy II software⁽²⁵⁶⁾.

FICI Calculation obtained from Wind et al⁽²⁵⁴⁾:

$$\text{FICI} = (\text{MIC}_A^{\text{combi}}/\text{MIC}_A^{\text{alone}}) + (\text{MIC}_B^{\text{combi}}/\text{MIC}_B^{\text{alone}})$$

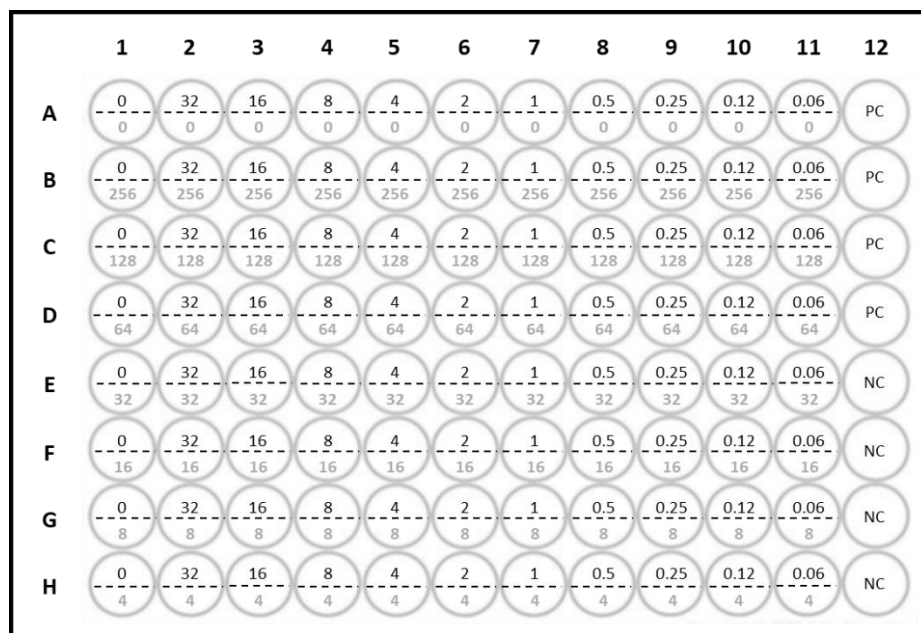


Figure 2.4 Example of an antibiotic checkerboard plate layout:

An antibiotic concentration gradient was created via serial dilution with 100 µL of working stock NX-AS-401 + antibiotic and 100 µL and sterile MHB. NX-AS-401 concentration gradients were performed vertically (Concentrations in grey) and antibiotic gradients were performed horizontally (concentrations in black)

2.3.11 Antibiotic Interactions on *S. aureus* biofilms.

Pre-established biofilms could not be measured using absorbance and problems arose with crystal violet and metabolic assays (**Further discussed in Chapter 5**). Instead antibiotic interactions were identified via TVC counts (**Section 2.3.4**).

Sensitivity of *S. aureus* biofilms was tested with a fixed antibiotic and NX-AS-401 concentration. Biofilms were established over 48-hours (**Section 2.3.6**) and once incubation was complete the growth media was removed. The biofilms were then treated with 200 µl of NX-AS-401, gentamicin, ceftiofur (all at 1024 µg/mL) or tetracycline (512 µg/ml) alone. Combination treatments included NX-AS-401 (1024 µg/ml) and gentamicin (1024 µg/ml), ceftiofur or tetracycline (512 µg/ml). Plates were incubated at 37 °C for 18-20 hours before the supernatant was removed, and the cell number determined via TVC count (**Section 2.3.4**).

The biofilm quantification methods outlined in Section 2.3.6 were used to measure the interactions between NX-AS-401 and antibiotics against bacterial biofilm. Crystal violet assays (**Section 2.3.6.1**) and resazurin assays (**Section 2.3.6.2**) failed to provide accurate data, discussed further in Section 5.5. Therefore, TVC counts (**Section 2.3.4**) were the only reliable method showing reproducible results.

2.3.12 Scanning Electron Microscopy (SEM) Biofilm Sample Preparation.

S. aureus biofilms were prepared by placing a glass cover slip in the bottom of the wells of a 24 well plate (Corning Costar Untreated, UK). The wells were inoculated with 0.5 ml of standardised bacterial inoculum (5×10^5 CFU/mL) and 0.5 ml of sterile MHB. The plates were incubated for 48 hours at 37 °C, before the spent media and planktonic cells were removed. The established biofilms were then treated with increasing concentrations of NX-AS-401 (0 - 1024 µg/ml) and incubated for 18-20 hours. After incubation, the planktonic cells and remaining media was removed carefully via pipette. After ensuring all excess media was removed, the samples underwent fixation/dehydration steps according to the protocol provided by Richards *et al* ⁽²⁵⁷⁾. Glass coverslips were rinsed carefully with 0.5 mL of 0.4 M PIPES, pH 7.4 for two minutes prior to fixation with 0.5 mL of 2.5 % glutaraldehyde in 0.4 M PIPES, pH 7.4 for five minutes. The glutaraldehyde was removed, and samples were washed with 0.4 M PIPES, pH 7.4 for two minutes, repeated three times. Further fixation was performed with 0.5 mL of 1 % OsO₄ in 0.4 M PIPES, pH 6.8 and incubated for 60 minutes at room temperature. The additional liquid was removed, and samples were rinsed with distilled water three times for two minutes each. Dehydration was performed through successive five minute immersions in a 0.5 ml ethanol series consisting of 50 %, 70 %, 96 % 100 % followed by an additional series of 0.5 ml ethanol and hexamethyldisilazane (HMDS) consisting of 2:1, 1:1, 1:2 ratios. A final dehydration step of 0.5 mL of 100 % HMDS was applied for five minutes twice before transfer of the coverslip to paper where they were left to air dry. Finally, the coverslips were mounted onto stubs (Agar Scientific Ltd, Essex, UK) and sealed with silver agar paint (Thermofisher, UK) around the edge of the coverslip. The glass coverslip was then sputtered with chromium at a thickness of 10 nm (Quorum Technologies Q150TE Coater, Sussex, UK).

In total three images were taken of each prepared sample that best represented the biofilms and the effects of NX-AS-401.

2.3.13 Confocal Microscopy

S. aureus biofilms were prepared by placing a glass cover slip in the bottom of the wells of a 24 well plate (Corning Costar Untreated, UK). The wells were inoculated with 0.5 ml of standardised bacterial inoculum (5×10^5 CFU/ml) and 0.5 ml of sterile MHB. The plates were incubated for 48 hours at 37 °C, before spent media and planktonic cells were removed. The established biofilms were then treated with increasing concentrations of NX-AS-401 (0 - 1024 µg/ml) and incubated for 18-20 hours. Coverslips were stained in accordance with the manufacturers protocol by submerging them in 2 ml filter-sterilised water with 6 µl of both SYTO 9 (3.34 mM in DMSO) and propidium iodide (20 mM in DMSO) from the FilmTracer LIVE/DEAD Biofilm Viability Kit (Invitrogen, UK). The glass coverslips were submerged for 20-30 minutes at room temperature and covered to protect them from UV bleaching. Glass coverslips were then removed and washed twice in PBS before mounting onto glass slides and sealed with clear nail varnish around the edge of slide. Mounted and prepared slides were imaged immediately to prevent degradation of the stain by UV light. Visualisation was performed on the Confocal microscope using a 63X Oil Immersion Lens (Merck, Southampton, UK).

In total nine images were taken of each isolate and testing condition. The CLSM biofilm images were then analysed via Comstat 2.1 software (comstat.dk) ^(258, 259) and the results averaged. This allowed for biofilm quantification and comparison between live (SYTO 9) and dead (propidium iodide) cells.

2.3.14 Resistance Training

Resistance training of *S. aureus* isolates was performed over 14 days to mimic modern healthcare practices where antibiotic therapies and dressing types are changed after 14 days to combat antibiotic resistance ⁽⁸⁾.

The experiment was carried out in a broth microdilution plate according to EUCAST guidelines (**Section 2.3.3.2**) using both NX-AS-401, gentamicin and *S. aureus* as described previously. However, following the initial 20-hour incubation period, the MIC was determined, and a fresh 10⁶ CFU/ml inoculum was prepared using the *S. aureus* cells exposed to ½ or ¼ MIC. This inoculum was used to create a new EUCAST broth microdilution plate (**Section 2.3.3.2**). The experiment was repeated daily, over 14 days. Then, on day 14 the isolates were streaked onto MHA and incubated at 37 °C for 20-24 hours. These isolates were stored on Cryobeads™ at -80°C for further AST and genetic sequencing.

Furthermore, on day 14 a “wash-out” period began where the *S. aureus* cells were grown overnight in NX-AS-401/antibiotic free MHB. A new 10⁶ CFU/ml inoculum created from the overnight culture (**Section 2.3.1**) and both another antibiotic free culture was prepared, and a further MIC broth microdilution plate performed (**Section 2.3.3.2**). This experiment continued for 14 days (day 14-day 28) or until the MIC of the antibiotic free culture returned to the original day zero MIC indicating a change in tolerance to NX-AS-401 or gentamicin.

Concentration ranges used in the experiment were dependent on changes in MIC over the experiment. Resistance training to gentamicin was used as a control to monitor development of tolerance/resistance in a ‘standard of care’ antibiotic.

After resistance training stored isolates underwent disc diffusion AST (**Section 2.3.3.1**) to identify any changes in resistance/susceptibility patterns.

2.3.15 DNA Extraction

The frozen stocks of resistance trained *S. aureus* isolates were grown overnight at 37°C in MHB containing $\frac{1}{4}$ or $\frac{1}{2}$ MIC NX-AS-401 or gentamicin (0.25 µg/mL) to maintain selective pressure. The next day samples were incubated for 30 minutes at 37 °C in 200 µl of lysostaphin before genomic DNA extraction was performed with the QIAamp DNA Mini Kit (Qiagen, UK) according to manufacturer's instructions.

2.3.16 DNA Sequencing

Illumina sequencing, *de novo* genome assembly, alignment and annotation was provided by and performed at Swansea University by Dr. Matthew Hitchings at the Swansea Genome Centre. A condensed QCAST report on the assembled genomes is provided in Appendix 1.6

2.3.17 Genome sequence analysis

Further Genome sequence analysis was performed using:

Snippy was used ⁽²⁶⁰⁾ to develop a core phylogeny and compare the number of single nucleotide polymorphisms (SNPs) that occurred in treated and untreated strains.

FastTree ⁽²⁶¹⁾ was used to develop a unrooted neighbour-joining phylogenetic tree from assembled genomes (further information on assembled genomes is in **Appendix 1.6**)

The comprehensive antibiotic resistance database (CARD) resistance gene identifier software ⁽²⁶²⁾ and the centre for genomic epidemiology Resfinder 3.2 software ⁽²⁶³⁾ were used to identify resistance genes in each strain.

2.3.18 Phenotypic Virulence Studies

To identify the effects of NX-AS-401 on *S. aureus* virulence, isolates were grown on different media types, including DNase, blood, lipid, and milk (**Section 2.1.2.1, Table 2.3**) with or without NX-AS-401 supplementation. Duplicate inoculums were prepared according to Section 2.3.1 with one MHB culture containing sub-inhibitory concentration (4 µg/ml) of NX-AS-401. A 1 µl loop was then coated with each inoculum and stabbed into the agar surface. Plates were then incubated at 37 °C for 24 hours. The zones of lytic activity were measured using electronic callipers (Powerfix, UK).

Visualisation of DNase plates required the addition of 0.1 M of HCL to cover the agar surface. This was left to incubate at room temperature for five minutes before removal and measurement with electronic callipers (Powerfix, UK).

NX-AS-401 demonstrated different effective concentrations and activity in solid MHA in comparison to liquid MHB. Optimisation tests were performed using MHA plates supplemented with 128, 64, 32, 16, 12 and 8 µg/ml of NX-AS-401 were created (**Section 2.1.2.1**) and TVC counts (**Section 2.3.3**) were performed on them to determine the sub-inhibitory concentrations. To maintain the selective pressure and prevent virulence factor production reverting to normal, one batch of each media was additionally supplemented with a sub-inhibitory NX-AS-401 concentration to identify whether NX-AS-401 caused changes in virulence factor expression when growth was not inhibited.

2.3.19 Reverse Transcription - Quantitative Polymerase Chain Reaction (RT-qPCR)

RT-qPCR was performed on *S. aureus* biofilms established for 48 hours prior to application of the NX-AS-401 treatment. In brief, biofilms were grown in 24 well plates with 1 ml of MHB prior to the addition of 1 ml of 10^6 CFU/ml bacterial suspension (**Section 2.3.1**). Plates were then incubated at 37 °C for 48 hours. The media was then removed from the pre-established biofilms and replaced with fresh media containing either 128 or 256 µg/ml NX-AS-401 for either: 2, 4 or 24 hours. An untreated control was also included where MHB was replaced at 48 hours.

Following treatment at the required time point the supernatant was removed and the biofilms carefully washed twice with PBS via pipette. Biofilms were removed from the wells by adding 1 ml of cellulase from *Aspergillus niger* (0.5 units/ml) (prepared according to section 2.1.2.4 and incubated at 37 °C for 30 minutes in a shaking incubator (VWR, Leicestershire, UK) at 200 rpm. This step was performed to remove any extracellular polymeric substances in the biofilm matrix and ensure that the exterior polysaccharides did not limit the effects of lysostaphin and lysozyme ⁽²⁶⁴⁾ . Once incubation was complete, the well contents were transferred into 1 ml sterile Eppendorfs. Samples were centrifuged at 5000 x G for 10 minutes to form a pellet and additional liquid was removed carefully. RNA was preserved by adding 1 ml of RNA Later to each sample the pellet resuspended via vortex. Samples were then frozen at -80 °C to until RNA extraction could be performed.

Frozen samples were allowed to thaw before extraction and then centrifuged at 5000 x G for 10 minutes to form a pellet. RNA later was removed, and extraction formed on the remaining pellet. RNA extraction was performed on biofilm samples by incubating the *S. aureus* biofilms in 30 µl of lysostaphin (200 units/ml) and 200 µl of lysozyme (2.115×10^6 units/ml) prepared according to section 2.1.2.4 for 30 minutes at 37°C. RNA extraction was performed via Maxwell RSC and utilising the Promega Maxwell simplyRNA Cells kit in accordance with the manufacturer's protocol.

After extraction, RNA was quantified via Nanodrop and all samples standardised to 50 µg/ml using nuclease free water. Then, RNA was converted to cDNA using the Promega GoScript™ Reverse Transcription Mix and random Primer kit following the manufacturers protocol and appropriate cycling conditions (**Table 2.6**).

Table 2.6 Cycle setting for conversion of RNA to cDNA using Promega GoScript™ Reverse Transcription Mix.

	Step	Temperature	Time	Number of Cycles
1	Anneal primer	25°C	5 minutes	1 cycle
2	Extension	60°C	60 minutes	1 cycle
3	Inactivation	70°C	15 minutes	1 cycle
4	Hold	4°C	∞	1 cycle

Once cDNA was obtained samples were stored at -20 °C to preserve cDNA until undergoing qPCR using Thermofisher PowerUp SYBR Green and utilising the QuantStudio 7 system (Thermofisher Scientific, UK). Once samples were prepared for qPCR cDNA was quantified via Nanodrop and sample diluted to make a 50 ng/μl concentration (**Nanodrop results and dilution factors are provided in Appendix 1.3**)

Then, qPCR was performed in the QuantStudio 7 system (Thermofisher Scientific, UK) under the defined PCR conditions (**Table 2.7**) .

Table 2.7 RT-qPCR conditions

Stage	Method 1:			Method 2 (Optimised):		
	Temp (°C)	Time (seconds)	Cycle No.	Temp (°C)	Time (seconds)	Cycle No.
Hold	50	120	1	50	120	1
	95	120	1	95	120	1
PCR	Denature	95	15	95	15	
	Annealing	60	60	60	30	40
	Extension	72	30	72	30	
Melt Curve		95	15	95	15	1
		60	60	60	60	1
		95	15	95	15	1

Primer efficiencies were determined against each strain ensuring an efficiency greater than 90 % was achieved (**Appendix 1.4**). A full list of the primers is provided in table

2.8. After DNA sequences were obtained primers underwent alignment via BLAST ⁽²⁶⁵⁾ against the control sequence to determine whether the primers would be effective.

Fold changes in gene expression observed in qPCR experiment were identified via the delta delta CT method in comparison to the 16S housekeeper gene ⁽²⁶⁶⁾.

Further analysis was performed using one way hierarchal clustering analysis (HCA) to determine trends in the RT-qPCR data. HCA was performed using SPSS, dendrograms were created using an agglomeration schedule, wards methods with measured Euclidean distance and Z-score transformed by strain ^(267, 268). One way HCA was performed to keep primers clustered based on their activity, such as virulence factor regulation/production, biofilm association or whether they were regulator of gene expression.

Table 2.8 Primer targets, sequences and efficiencies against each *S. aureus* strain.

Primer sequences were obtained from Kannappan et al ⁽²⁶⁹⁾, (1) Balamuguran et al ⁽⁷⁵⁾ (2), Tuchscher et al ⁽⁵⁵⁾(3) or designed by Neem Biotech (4).

Primer Name	Target	Forward (5' to 3')	Reverse (3' to 5')
<i>icaA</i> (1)	Intracellular Adhesion	ACACTTGCTGGCGCAGTCAA	TCTGGAACCAACATCCAACA
<i>sigB</i> (3)	Sigma Factor B	ATGTACGTTTATTGAAGGATTG	TAATTTCTAATTGCCGTTCTC
<i>clfA</i> (1)	Clumping Factor Alpha	ATTGGCGTGGCTTCAGTGCT	CGTTTCTCCGTAGTTGCATTTG
<i>agrA</i> (3)	Accessory Gene Regulator A	AACTGCACATACACGCTTACA	GGCAATGAGTCTGTGAGATT
<i>gyrB</i> (3)	Gyrase B	AATTGAAGCAGGCTATGTGT	ATAGACCATTTTGGTGTGG
<i>16s RNA</i> (1)	16s Ribosomal RNA	ACTCCTACGGGAGGCAGCAG	ATTACCGCGGCTGCTGG
<i>sarA</i> (2)	Staph. Accessory Gene Regulator	TCTTGTTAATGCACAACAACGTAA	TGTTTGCTTCAGTGATTCGTTT
<i>fnbA</i> (1)	Fibronectin binding protein B - precursor	ACAAGTTGAAGTGGCACAGCC	CCGCTACATCTGCTGATCTTGTC
<i>hla</i> (2)	Haemolysin Alpha	ACAATTTTAGAGAGCCCAACTGAT	TCCCAATTTTGATTCACCAT
<i>hld</i> (2)	Haemolysin Delta and RNA III	AAGAATTTTTATCTTAATTAAGGAAGGAGTG	TTAGTGAATTTGTTCACTGTGTCGA
<i>Rot</i> (4)	Repressor of Toxins	GTTTTGGGATTGTTGGGATG	GCATTGCTGTTGCTCTACTTGC
<i>splF</i> (4)	Serine Protease	CAACAAACAGCCGGATCCGAAAATACTGTAAAC	GTCTAAGCTCGTGTATTTATCTAAATTATC
<i>lytR</i> (4)	Sensory Transduction Protein	CCCGGATCCGACAAGAGGAG GAATAAATATG	CCCGAATCCGACCATTGCCCTACGTTTG
<i>atl</i> (4)	Bifunctional Autolysin Precursor	ATGGATACGAAGCGTTTAGC	CACTACATCTGCACCTTTCCG
<i>sle1</i> (4)	N-acetylmuramoyl-L-alanine amidase	GAGGGATCCGGTTAAAGATGGTGCTAAAGTTGTC	GAGGTCGACCTAATGATGATGATGATGATG GTGAATATATCTATAATTATTACTTGG

2.3.20 *Galleria mellonella*

The ability of NX-AS-401 to modulate the *in vivo* virulence of *S. aureus* was monitored using the *Galleria mellonella* (*G. mellonella*) model ⁽²⁷⁰⁾.

Larvae were obtained from Biosystems Technologies (TruLarv) to ensure appropriate weight, health and an antibiotic free environment ⁽²⁷¹⁾. Injection and handling of the *G. mellonella* was performed according to the Biosystems Technologies procedures ⁽²⁷⁰⁾. Determining NX-AS-401 toxicity through *G. mellonella* mortality was performed using the K. Ignasiak and A. Maxwell method ⁽²⁷²⁾.

Dose optimisation tests determined the bacterial cell densities required to kill all *G. mellonella* within five days. Cytotoxicity studies determined the optimum tolerated dose of NX-AS-401 by injecting larvae with 10 µl of NX-AS-401 (1.6 – 25.6 mg/kg) into the last proleg and incubated at 37 °C for five days to determine mortality.

Once optimised *G. mellonella* were inoculated with 10 µl of 10⁴ CFU/ml of each strain of *S. aureus*. Inoculums were prepared according to section 2.3.1. Larvae were injected with 10 µl of *S. aureus* inoculum and were injected with 10 µl of either 1.6 or 25.6 mg/kg NX-AS-401 immediately afterwards. *G. mellonella* were then incubated for five days at 37 °C and counted at the same time daily to monitor survival. At the end of five days the *G. mellonella* were frozen before disposal via autoclave. For each experiment, a control group of *G. mellonella* larvae inoculated with 10 µl of sterile PBS was administered to ensure that injection trauma was not responsible for death. A full description of each optimisation and experimental stage is described (**Figure 2.5**).

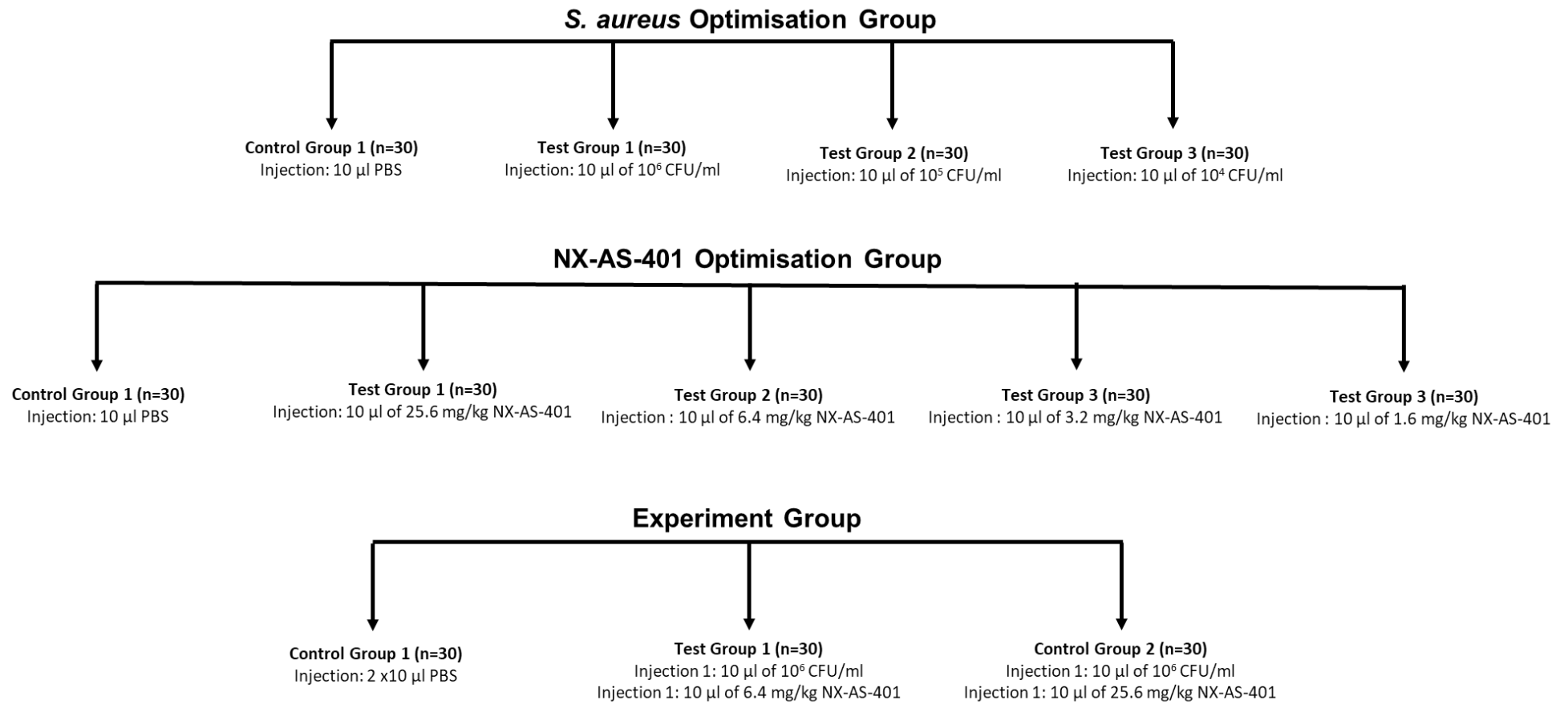


Figure 2.5 *Galleria mellonella* testing conditions:

Schematic diagram confirming the doses of antibiotic and *S. aureus* given in optimisation tests and experiments.

2.4 Cell Culture

2.4.1 Routine maintenance and sub-culture

Human keratinocyte cell line, HaCaT, 300493 (Cell Line Service, Eppelheim, Germany) were utilised to determine if NX-AS-401 could prevent the adherence and internalisation of *S. aureus*. Control experiments also determined the cytotoxic effects of NX-AS-401 to identify appropriate doses.

HaCaT cells were cultured from frozen stocks held in liquid nitrogen. The cells were grown at 37 °C 5 % CO₂ in Dulbecco's Modified Eagle Medium (DMEM) with additional pyruvate 110 mg/L. Additional supplements included 10 % foetal calf serum (FCS), 1 % 10,000 U/ml Penicillin/Streptomycin (Pen/Strep) and 1 % 200 mM L-Glutamine. Flasks were incubated at 37 °C 5 % CO₂ with DMEM change every two days until cells reached confluency before passage to allow for continued growth.

Cell passage was performed by removing the DMEM and washing the adhered cell monolayer twice with 10 ml of PBS. Any remaining PBS was removed carefully via pipette before the addition of 10 ml of TrypLE. The liquid was swilled around the flask before incubation at 37 °C for 10 minutes. After incubation cell detachment was confirmed via light microscopy, if cells were still adhered further incubation was performed for no longer than 30 minutes as >30 minutes of exposure to TrypLE caused cell lysis.

Once detachment was confirmed 10 ml of DMEM was added to neutralise the TrypLE. Cells were then centrifuged at 40,000 RPM for five minutes. After centrifugation, the cells TrypLE/DMEM media was removed and replaced with 10 ml of fresh DMEM with additional supplementation. This cells resuspended by vortex before enumeration in a class counting chamber using 15 µl of HaCaT cell suspension and 15 µl trypan blue.

The cell suspension was then diluted with the appropriate amount of DMEM for the desired cell density or to obtain confluency at a specific date based on flask size used.

2.4.2 Cytotoxicity Studies

Previously cultured HaCaT cells that had reached confluency in the 175 ml flask underwent the same protocol for passaging (**Section 2.4.1**). However, before inoculation of the second flask the cells were enumerated in a haemocytometer to standardise 10^5 cells per ml inoculum. Counted HaCaT cells were diluted in DMEM with additional supplements including 10 % FCS, 1 % Penicillin/Streptomycin (Pen/Strep) and 1 % L-Glutamine to prepare an inoculum of 10^5 HaCaT cells per ml/ 4000 cells per cm^2 . The standardised cell suspension was seeded into the 96 well plate and incubated over 18-20 hours at 37 °C, 5 % CO_2 . After incubation, the wells were inspected visually using inverted light microscopy and to ensure confluency. If cells failed to become confluent, they underwent an additional 18-20 hour incubation until a cell monolayer was established.

A cytotoxicity assay was performed on HaCaT cells in a pre-seeded 96 well plate (**Section 2.4.2**). Once the HaCaT cells had formed a confluent monolayer in the 96 well plate the media and unattached cells were removed via pipette.

DMEM with additional supplements included 5 % FCS, 0.5 % Penicillin/Streptomycin (Pen/Strep) and 0.5 % L-Glutamine was used to prepare a 200 μl NX-AS-401 concentration gradient as utilised during MIC testing (**Section 2.3.3.2**). The plate was incubated at 37 °C 5 % CO_2 for 4 hours with NX-AS-401 treatment.

After incubation the plate were removed from the incubator and each well was inoculated with 20 μL of Alamar Blue Reagent (A metabolic assay based on the resazurin used previously)⁽²⁷³⁾. The plates were incubated for two hours at 37 °C 5 % CO_2 in the dark to protect from UV light and allow for colour change. Plates were then measured in a BMG Fluostar spectrophotometer (BMG Labtech, Aylesbury, UK) at 560^{EX}/590^{EM}. Positive controls of untreated cells caused a colour change (blue to bright pink) with high levels of fluorescence, dead cells or those with low metabolism remained blue or a slight colour change occurred due to breakdown of resazurin via UV light.

2.4.3 Adhesion and Invasion Assays in HaCaT cells.

A 96 well plate was prepared in accordance with section 2.4.2 was used to monitor adhesion and invasion of treated and untreated *S. aureus* cells.

Adhesion and invasion assays were performed according to Kintarak *et al* ⁽²⁷⁴⁾. *S. aureus* cell suspensions (10^8 CFU/ml) (0.08-0.1 ABS at 625 nm) were prepared to generate a multiplicity of infection ratio of 200:1. Multiplicity of infection refers to the number of bacterial cells per HaCaT cells, and was selected based on the study by Kintarak *et al* ⁽²⁷⁴⁾.

Bacterial suspensions were prepared by growing in MHA over 24 hours, diluting to 0.08-0.1 ABS and harvested by centrifugation for five minutes at 13,000 g. Cells were then resuspended in the same volume of DMEM media without additional supplementation to a cell concentration of 10^8 CFU/ml and confirmed via TVC counts (**Section 2.3.4**). Three bacterial inoculums were prepared, a negative control and NX-AS-401 at 16 µg/ml or 32 µg/ml. These concentrations were chosen as they were sub-MIC and only reduced cell numbers after 24 hours according to TVC counts and were also non-toxic to HaCaT cells according the cytotoxicity tests (**Section 2.4.2**).

HaCaT cells were infected by applying a 200 µl aliquot of bacterial suspension to each well and the plates was incubated for four hours at 37 °C to allow for *S. aureus* adherence and invasion.

For adhesion assays the HaCaT cells were treated with 0.1 % Triton X-100 (Sigma-Aldrich, UK) for 10 minutes to lyse the HaCaT cells and preserve the *S. aureus* cells. (Optimisation tests confirmed that 0.1 % Triton X-100 was not harmful to *S. aureus* cells.) For invasion assays the HaCaT cells were treated with 200 µg/ml gentamicin for one hour to kill any adhered cells prior to lysis of the HaCaT cells via 0.1 % Triton X-100 for one minute.

After HaCaT cell lysis the well contents underwent TVC counts (**Section 2.3.4**) to determine the number of *S. aureus* cells present. The number of adherent bacteria was calculated by subtracting the number of internalized bacteria from the total number of cell-associated bacteria.

2.5 Statistical Analysis

Difference between controls and experimental condition were analysed using various statistical approaches, initially whether data was normally distributed was identified via D'Agostino-Pearson test. Statistical significance was determined by a p value ≤ 0.05 . Unless otherwise stated statistical analysis was performed using GraphPad Prism version 8.

Statistical analysis of disc diffusion and virulence zones of inhibition tests was determined via Mann-Whitney tests comparing treated and untreated samples.

Minimum inhibitory concentrations of NX-AS-401 were identified as being ≤ 10 % against the positive control. The statistical significance of broth microdilution tests against both planktonic *S. aureus* and pre-established biofilms was determined by Kruskal-Wallis tests (non-parametric) and post-hoc Dunn test comparing NX-AS-401 concentrations that reduced growth and biofilm formation by >90 % and reduced the biomass of pre-established biofilms by 50 % against the positive control. The non-parametric one-way ANOVA, Kruskal-Wallis test was chosen for this analysis due to the independent variable and for the experimental replicants.

Statistical significance in time/kill curves, growth curves and the invasion/adhesion of HaCaT cells was determined used the Holm-Sidak method (non-parametric). This tests allowed for multiple comparison, comparing treated data sets, with those of the untreated control. This test was chosen due to the increased power over the Bonferroni tests.

The significance between antibiotic interactions on biofilm cell viability were determined via Kruskal-Wallis tests and post-hoc Dunn test (non-parametric) due to the inability to perform FICI calculation or apply the MacSynergy II software ⁽²⁵⁶⁾. Testing was performed between biofilms treated with combinations and when antibiotics were applied alone.

Statistical significance in the survival curves for *Galleria mellonella* experiments were confirmed via Mantel-Cox and Gehan-Breslow-Wilcoxon tests, these are logrank tests used to compare two survival curves. These tests were used to compare NX-AS-401 treated to untreated *G. mellonella*.

3.0 Chapter 3: Optimisation of models to determine the effective concentrations of NX-AS-401 using early formulation NBR 26-6A

3.1 Introduction

3.1.1 The fight against antibiotic resistance.

Antibiotic-resistant bacterial infections have placed a large burden on healthcare systems throughout the world ^(1, 117). The development of resistance to multiple antibiotics classes or antibiotics that are considered the last line of defence, such as glycopeptides and carbapenems ⁽¹⁴⁶⁾ has made the development of new antibiotics a necessity. A list of the pathogens that require new treatment options immediately has been provided by the World Health Organisation (WHO) (**Table 3.1**).

Table 3.1 WHO priority pathogens ^(146, 275).

Table created from information in WHO news release “WHO publishes list of bacteria for which new antibiotics are urgently needed” ⁽¹⁴⁶⁾.

Priority 1: Critical	Priority 2: High	Priority 3: Medium
<i>Acinetobacter baumannii</i> , carbapenem-resistant	<i>Enterococcus faecium</i> , vancomycin-resistant	<i>Streptococcus pneumoniae</i> , penicillin-non-susceptible
<i>Pseudomonas aeruginosa</i> , carbapenem-resistant	<i>Staphylococcus aureus</i> , methicillin-resistant, vancomycin-intermediate, and resistant	<i>Haemophilus influenzae</i> , ampicillin-resistant
<i>Enterobacteriaceae</i> , carbapenem-resistant, ESBL producing	<i>Helicobacter pylori</i> , clarithromycin resistant	<i>Shigella</i> species, fluoroquinolone resistant
	<i>Campylobacter</i> species, fluoroquinolone resistant	
	<i>Salmonellae</i> , fluoroquinolone resistant	
	<i>Neisseria gonorrhoea</i> , cephalosporin-resistant, fluoroquinolone resistant	

However, while antibiotic resistance is already wide-spread and new treatment options are required, antibiotic development is a lengthy process ⁽²⁷⁶⁾. From discovery of a potential new antimicrobial to *in vivo* testing requires years of work and a large financial cost, currently estimated at \$1581 million per drug ⁽²⁷⁷⁾. This cost combined with the high failure rate of antibiotics during pre-clinical or clinical stages mean that businesses lack the motivation to invest, knowing that the financial loss is unlikely to be recouped ⁽²⁷⁶⁾. The cost and lack of financial incentive has caused a stagnation in drug development over the last 10 years ⁽²⁷⁶⁾. Therefore, the lists of priority pathogens provided by WHO (**Table 3.1**), are important for guiding research and investment towards essential targets ^(132, 275).

Novel compound NX-AS-401 is still in development and multiple formulations were created to identify the most effective anti-bacterial formulation. NX-AS-401 development has resulted in batches of the compound that contain different percentages and ratio of ajoene isomers. Batch NBR 26-6A contains approximately 70 % ajoene in a 1:1 ratio of E-Z isomers. Latter batches focused on increasing the ajoene content and potentially changing the ratio of isomers to identify the most active components.

3.2 Aims

- To optimise methods for testing NX-AS-401 against *S. aureus*, using NBR26-6A an early batch of NX-AS-401.
- To establish the minimum inhibitory and bactericidal concentrations of NBR 26-6A against *S. aureus* strain NCTC 13142.
- To identify the effects of NBR 26-6A on *S. aureus* strain NCTC 13142 growth kinetics and cell number over time.
- To identify the effects of NBR 26-6A on *S. aureus* strain NCTC 13142 biofilm formation and on pre-established biofilms formed over both 24 and 48 hours.

3.3 Materials and Methods

Materials and Methods are provided in Chapter 2. Deviations from the information provided in Chapter 2 are outlined below.

3.3.1 Bacterial Strains

During the initial testing of NX-AS-401 (Batch number: NBR160026-6A) only one bacterial strain was utilised, *S. aureus*, NCTC 13142 obtained from Public Health England Culture Collection.

3.4 Results

3.4.1 Minimum Inhibitory\Bactericidal Concentration

To determine the effective concentrations of NBR 26-6A and how it compares to standard of care antibiotics the MIC for NBR 26-6A against *S. aureus* NCTC 13142 was determined via EUCAST broth microdilution (**Figure 3.1**)

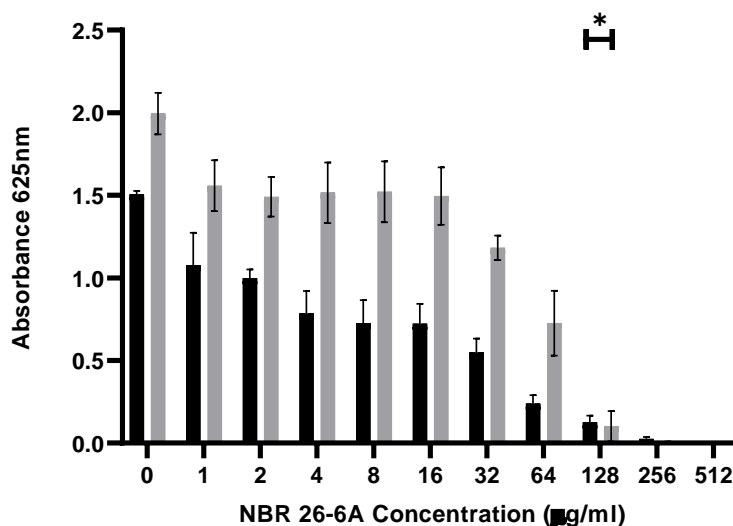


Figure 3.1 The MIC of NBR 26-6A against *S. aureus* NCTC 13142 via EUCAST broth microdilution.

Black bars show the results of *S. aureus* NCTC 13142 treated with NBR 26-6A for 20 hours as recommended in EUCAST guidelines. Grey bars display changes in absorbance when NBR 26-6A treatment was extended to 48 hours. Significant 90% ($p < 0.05$) reductions in growth compared to the positive control are marked with an asterisk (*) for both time points. Error bars represent standard error of the mean.

NX-AS-401 reduced growth at all concentrations in comparison to the untreated control for both 20 and 48 hour treatments. The MIC was determined by 90% growth inhibition compared to the positive control and was identified as 128 µg/ml after *S. aureus* NCTC 13142 was treated with NBR 26-6A for both 20 and 48 hours.

An MBC for NBR 26-6A against *S. aureus* NCTC 13142 for the 20 hour treatment was not identified as colonies formed at all concentrations when cultured onto MHA. After exposure was increased to 48 hours the MBC was identified at 512 µg/ml.

3.4.1.1 Additional:

In its current formulation NBR 26-6A was an oil like preparation and even with a prior dilution in DMSO NBR 26-6A would not readily solubilise into MHB at concentrations >512 µg/ml. Lack of solubility may be attributed to the different polarities of MHB and NBR 26-6A causing emulsification rather than dissolution ⁽²⁷⁸⁾. Solutions of NBR 26-6A at concentrations >512 µg/ml demonstrated increased turbidity; therefore NBR 26-6A concentrations were kept ≤512 µg/ml to prevent turbidity effecting absorption results obtained from the plate reader during broth microdilution.

3.4.2 Time/Kill Curves

The effects of NBR26-6A on *S. aureus* growth over time were determined via Time/Kill curves that were calculated from TVC counts (Figure 3.2).

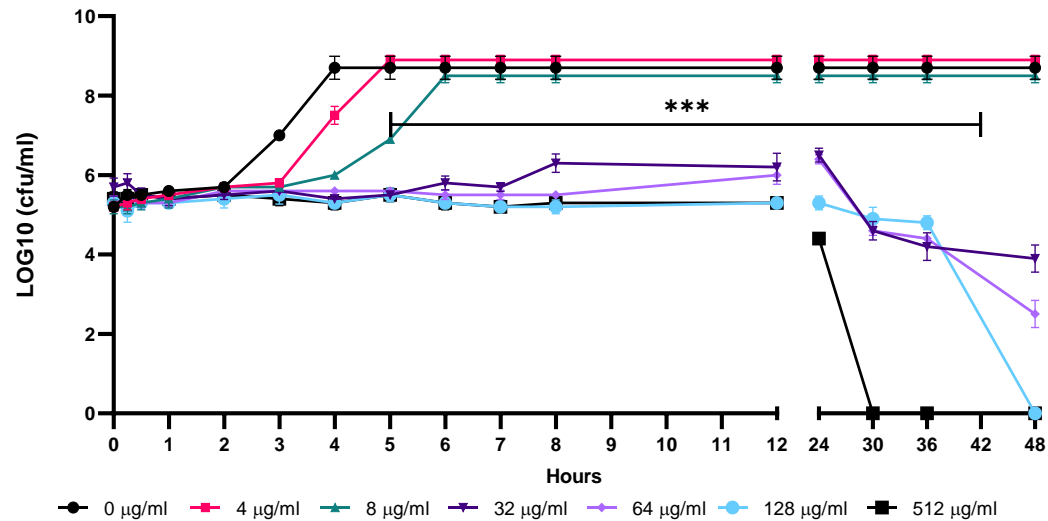


Figure 3.2 Time/Kill Curve of NBR 26-6A against *S. aureus* NCTC 13142 over 48 hours:

Significant ($p < 0.0001$) reductions in growth compared to the positive control are underneath bars with triple asterisks (***) . Error bars represent standard error of the mean.

TVC counts identified that NBR 26-6A concentrations of 32 µg/ml and above significantly inhibited the growth of *S. aureus* NCTC 13142 over 24 hours in comparison to the positive control. NBR 26-6A concentrations (4-8 µg/ml) delayed *S. aureus* growth for one and two hours respectively before cell numbers increased to the same as the positive control. Treatment extension to 48 hours demonstrated a significant ($p > 0.0001$) decline in *S. aureus* NCTC 13142 cell numbers when treated with NBR 26-6A concentrations of 32-128 µg/ml in comparison to the untreated control.

3.4.3 Minimum Biofilm Inhibition Concentration

The ability of *S. aureus* NCTC 13142 to form a biofilm in the presence of NBR 26-6A was monitored via three methods, crystal violet (mass), resazurin (metabolism) and TVC counts (cell number) (**Figure 3.3**).

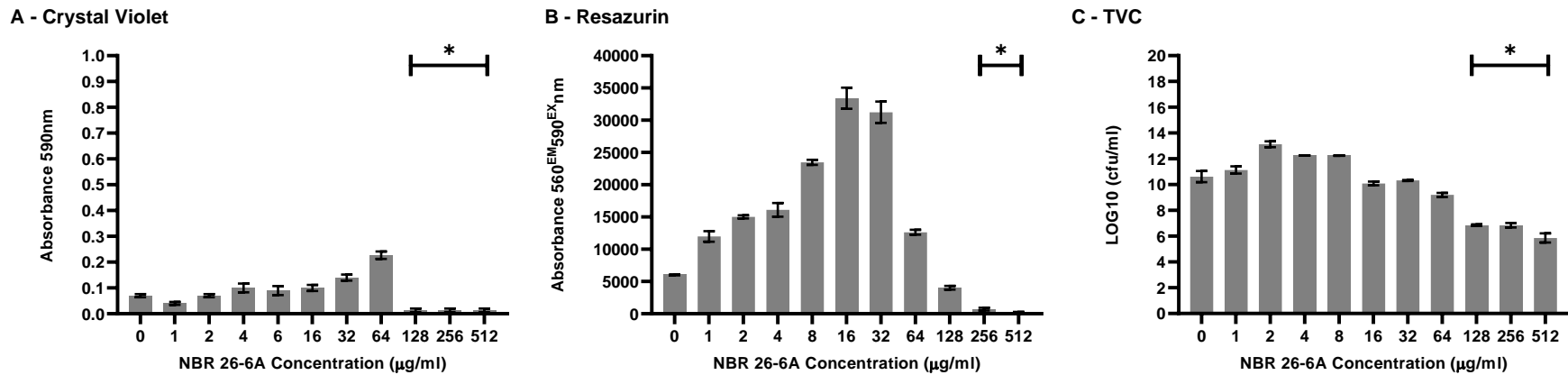


Figure 3.3 *S. aureus* NCTC 13142 Biofilm inhibition by NBR 26-6A:

A Crystal violet, **B** Resazurin metabolism **C** TVC counts for the presence of viable cells. Formation inhibition of >90 % when compared to the untreated control as indicated by an asterisk (*). Error bars represent standard error of the mean.

Sub-inhibitory NBR 26-6A concentrations of 64 µg/ml significantly ($p < 0.05$) increased biomass and NBR 26-6A concentrations of 1-64 µg/ml significantly increased ($p < 0.05$) metabolic activity of *S. aureus* NCTC 13142 in comparison to the positive control. All three methods identified that NBR 26-6A at concentrations ≥ 128 µg/ml significantly ($p < 0.05$) inhibited biofilm formation.

3.4.4 Minimum Biofilm Eradication Concentrations on preformed *S. aureus* biofilms

S. aureus NCTC 13142 Biofilms were established over 24 (**Figure 3.4**) and 48 (**Figure 3.5**) hours prior to the application of an NBR 26-6A concentration gradient.

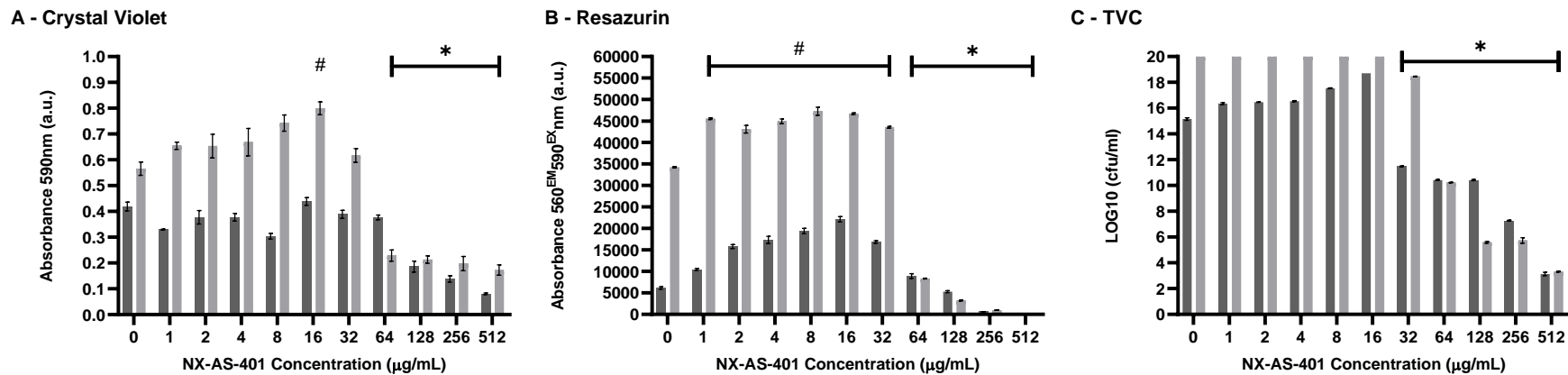


Figure 3.4 The effects of NBR 26-6A on pre-established 24-hour biofilms:

A Crystal violet, **B** Resazurin metabolism **C** TVC counts. Dark grey bars indicate 20 hour NBR 26-6A treatment, light grey bars indicate a 48 hour NBR 26-6A treatment. Statistically significant decreases ($p < 0.05$) are indicated by an asterisk (*) and significant increases ($p < 0.05$) are indicated by the hash symbol (#). Error bars represent standard error of the mean.

NBR 26-6A concentrations ≥ 128 µg/ml reduced biomass by 50 % according to crystal violet assay with no concentration able to reduce mass by >90 % (**Figure 3.4 A**). NBR 26-6A at ≥ 256 µg/ml reduced resazurin metabolism by 90 % for both 20 and 48 hour treatments (**Figure 3.4 B**) and cell counts were reduced at NBR 26-6A concentrations of ≥ 32 µg/ml and ≥ 64 µg/ml after 20 hours and 48-hour treatment, respectively (**Figure 3.4 C**).

3.4.5 Minimum Biofilm Eradication Concentrations on 48 hour preformed biofilms

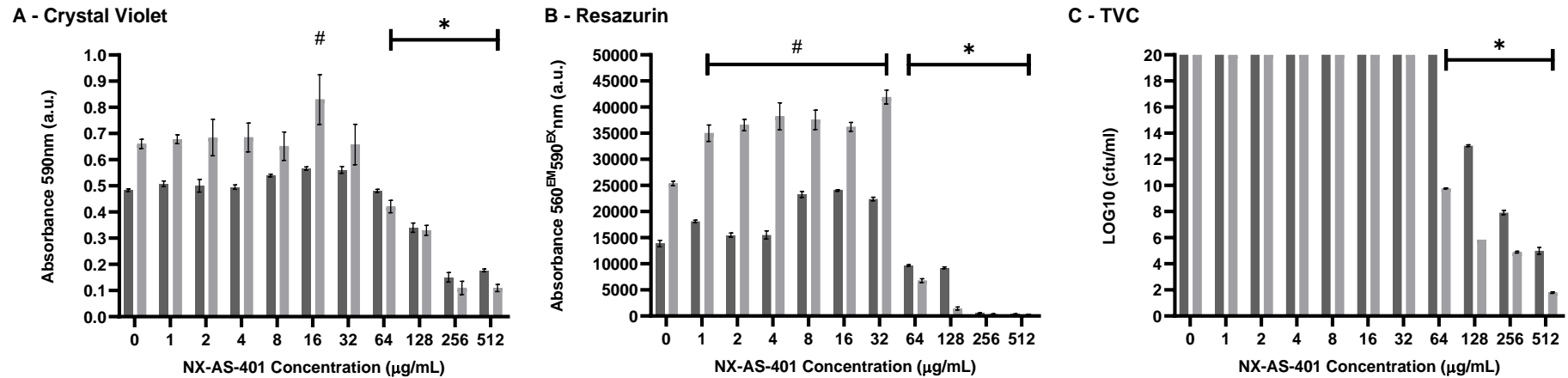


Figure 3.5 The effects of NBR 26-6A on pre-established 48-hour biofilms

A Crystal violet, **B** Resazurin metabolism **C** TVC counts. Dark grey bars indicate 20 hour treatment; light grey bars indicate 48-hour extended treatment. Statistically significant results ($p < 0.05$) where absorbance values and cell numbers $\leq 50\%$ of the positive control are indicated by an asterisk (*). Significant increases ($p < 0.05$) are indicated by the hash symbol (#). Error bars represent standard error of the mean.

NBR 26-6A demonstrated the ability to disrupt *S. aureus* NCTC 13142 biofilms established over 48 hours by $\geq 50\%$ over three different methodologies. (**Figure 3.5 A**) NBR 26-6A concentrations $\geq 256 \mu\text{g/ml}$ reduced biomass by 50% according to crystal violet assay with no concentration able to reduce mass by 90%. (**Figure 3.5 B**) $\geq 256 \mu\text{g/ml}$ was required to reduce resazurin metabolism by 90% for both 20 and 48 hour treatments. (**Figure 3.5 C**) Cell counts were reduced at concentrations of $\geq 128 \mu\text{g/ml}$ after 20 hours and $\geq 64 \mu\text{g/ml}$ after 48-hour treatment.

3.4.5.1 Additional:

S. aureus NCTC 13142 biofilms were formed over 24 and 48 hours. However, biofilms formed over 24 hours by *S. aureus* NCTC 13142 were unstable with the structures weakly attached to the cell culture treated plate wells and easily sheared mechanically via pipetting. Therefore, additional repeats were necessary to reduce error bars and identify trends with NBR 26-6A treatment.

3.5 Discussion

There are many challenges in combating the rise of antibiotic resistant infections, with novel approaches and new antibiotics desperately required ⁽¹⁵⁸⁾. Antibiotic development is a long process beginning with the identification of a novel antibacterial treatment and determining its effects against bacteria *in vitro*. While many potential agents have been identified few ever go through testing and clinical trial and make it into clinical use as shown in Section 1.4 (**Table 1.6**) ⁽¹¹⁹⁾.

NBR 26-6A is an early stage formulation consisting of the molecule ajoene as well as other unknown compounds. Ajoene does have known antibacterial activity, however research on the effects are limited and primarily focus on the effects against Gram-negative organisms ^(179, 217). To identify its potential as an antibiotic this chapter's aim was to identify what effects it has on *S. aureus* growth and development; this would also focus on the potential application of NX-AS-401 batch NBR 26-6A against both acute and chronic wound infections.

3.5.1 The susceptibility of *S. aureus* NCTC 13142 to NBR 26-6A.

The minimum inhibitory concentration, determined by growth inhibition by >90 %, was identified as 128 µg/ml (**Figure 3.1**). In comparison to other antibiotics the concentrations required for NBR 26-6A to inhibit growth of *S. aureus* NCTC 13142 is high, the EUCAST Guidelines for 2019 show that the MIC for most antibacterial agents against *S. aureus* are approximately 1 µg/ml with only few antibiotics such as Nitrofurantoin which require higher effective concentrations of 64 µg/ml ⁽²⁴⁶⁾. However, this may not indicate that NBR 26-6A is ineffective as an antibiotic as EUCAST clinical breakpoints are not solely based on the antibiotic concentrations that can inhibit growth or kill bacteria. EUCAST breakpoint also account for the pharmacological properties of an antibiotic, including potential side effects and absorption into host tissues when utilised *in vivo* ⁽²⁷⁹⁾.

Identifying whether NBR 26-6A could be effectively utilised in patients at a dose of 128 µg/mL required further investigation into its toxic effects by utilising *in vitro* human

cell lines or animal models. A comparison of current standard of care antibiotics shows that antibiotic toxicity varies per class.

The current toxicology for NBR 26-6A has yet to be determined so an MIC of 128 µg/ml may be high in comparison to other antibiotics. The insolubility of NBR 26-6A indicates that it may be problematic to achieve high concentration *in vivo*, however the MIC concentrations identified here may be achievable for the intended purpose of NX-AS-401 as a topical antibiotic for wounds. An example of this is the topical sodium-sulphacetamide lotion that contains 10 % of the sulphonamide antibiotic sulphacetamide ⁽²⁰⁾. The sulphonamide class of antibiotics which are structurally similar to NBR 26-6A and ajoene have seen reduced usage in current practise due to widespread resistance and the adverse effects caused by sulphonamides ⁽¹³³⁾. However, while most of the antibiotic class is no longer used clinically, one drug, sulphamethoxazole, is often used in combination with trimethoprim. When used alone the LD₅₀ is 2690 mg/kg when given to rats via intraperitoneal injection indicating a lower toxicity than more utilised antibiotics such as gentamicin and ciprofloxacin ^(128, 280).

Comparison of the MIC of NBR 26-6A and the previous study by Naganawa on ajoene against *S. aureus* identifies a large difference between the action of both compounds with the study by Naganawa identifying an MIC of 16 µg/ml ⁽²¹⁷⁾. This could be due to the differences in compound synthesis and/or the mixture of ajoene isomers and unknown molecules. The previous study by Naganawa 1996 utilised 80 % Z-form ajoene ⁽²¹⁷⁾ which has been identified as the more active isomer ⁽²⁴²⁾ in comparison to the 70 % ajoene in NBR 26-6A which was a 50:50 ratio of E and Z forms. The methods employed by Naganawa also differed from the EUCAST guidelines, with absorbance read at 660 nm and MICs performed in peptone-yeast extract medium ⁽²¹⁷⁾ rather than MHB. PYEM media is designed for the growth of yeasts not bacteria and 660 nm is the wavelength used to determine the growth of yeast in PYEM ⁽²⁸¹⁾. Currently the growth kinetics of *S. aureus* in PYEM have yet to be documented to see if they are similar to *S. aureus* grown in MHB.

While MIC does vary between the results of this chapter and the study by Naganawa they both demonstrate that ajoene has an effect on *S. aureus* and as demonstrated in Figure 3.1 concentrations below the MIC of 128 µg/ml to as low as 1 µg/ml can inhibit

the *S. aureus* NCTC 13142 from achieving the same turbidity as the positive control, indicating inhibition of growth. However, while NBR 26-6A was able to inhibit growth at concentrations as low as 1 µg/ml total eradication of *S. aureus* NCTC 13142 only occurred after cells had been exposed to a concentration 512 µg/ml for 48 hours. The results here do match the study by Jakobsen *et al* where ajoene was capable of producing a temporary bacteriostatic effect ⁽¹⁹⁴⁾.

Antibiotics are often broadly classified into two categories bacteriostatic (inhibits growth) or bactericidal (eradicates cells) based on their activity. Antibiotics are usually categorised as bacteriostatic when the bactericidal dose is greater than four times the MIC ⁽²⁸²⁾. This classifies NBR 26-6A as a bacteriostatic antibiotic with some bactericidal effects when the concentration is high enough, as the MIC is 128 µg/ml at 24 hours and the bactericidal effect occurs at 512 µg/ml after 48 hours. While bactericidal effects sound more desirable, both methods can be effective in the treatment of bacterial infections. Bactericidal agents are often used for infections where host immune components are reduced, for example joint infections where blood flow is limited ⁽¹²⁰⁾.

Figure 3.2 displays the effects of NBR 26-6A on cell viability over 48 hours. The result varies from those seen in the microbroth dilution (**Figure 3.1**) as a concentration of 32 µg/ml was enough to inhibit the growth of *S. aureus* NCTC 13142. This result was likely due to differences between the methods, primarily the upscale of the experiment size from 200 µl per well to a 50 ml culture. It has been well documented ^(246, 283) that inoculum size can alter the results of broth microdilution as documented in Lenhard & Bulman 2019 ⁽²⁸⁴⁾ these effects are exacerbated by the 250 times increase in volume utilised for this experiment.

Figure 3.2 also confirms the bacteriostatic effects of NBR 26-6A with concentrations between 32-128 µg/ml preventing growth of *S. aureus* NCTC 13142, but not reducing cell number until treatment had been applied for >24 hours. The decrease in cell numbers was an effect only seen during the time/kill curves and was not detected during broth microdilution. This could be due to the reliance of broth microdilution on absorbance spectroscopy, this method of analysis uses light passing through a cell suspension and obtaining an optical density reading based on scattering light off particles within the solution ⁽²⁸⁵⁾. This method did not discriminate between cells that

are alive, dead, extracellular material or if they have lysed, forming debris ⁽²⁸⁵⁾. The decrease in viable cells may occur between 24-48 hours but was not identified via broth microdilution could be due to this limitation.

3.5.2 The effects of NBR 26-6A on the formation of *S. aureus* NCTC 13142 biofilm and disruption of pre-established biofilms.

Changes in biofilms were monitored via three different methods to improve understanding of the effect of NBR 26-6A as each method measured a different aspect of the biofilm. Many studies have documented the limitations of the industry standard crystal violet method, this is due to the stain binding to any residues found in the well, including the extracellular matrix found coating biofilms ^(71, 82, 286). These limitations prevent determining the number of viable cells in the biofilm but allow for quantification of the biofilm mass (biomass) ⁽²⁸⁷⁾. This can assist in identifying whether a drug has an effect on bacterial cells or the extracellular matrix. ⁽²⁸⁷⁾

Inhibition and disruption of *S. aureus* biofilms by exposure to NBR 26-6A determined whether the compound was more effective as a preventative treatment or effective against pre-established infections. Although antibiotics can be used as a prophylactic measure to prevent post-surgical infections, the majority of infections seen in clinic are pre-established acute and chronic wound infections ⁽¹⁾. Acute infections are often easier to treat requiring only a short course of antibiotic or even a topical application ⁽⁸⁾. Chronic infections are more difficult to treat and often associated with biofilms where the tertiary structure increases antibiotic tolerance, reducing the efficacy of the chosen antibiotic and allowing for the infection to persevere ⁽⁸⁹⁾.

To identify the efficacy of NBR 26-6A against *S. aureus* NCTC 13142 biofilms dosing strategies were used that determined the concentration of NBR 26-6A that could inhibit biofilm formation and disrupt pre-established *S. aureus* NCTC 13142 biofilms.

The minimum biofilm inhibitory concentration (MBIC) is the lowest concentration that prevents biofilm formation and potentially prevent chronic infections associated with biofilms ⁽⁸⁶⁾. The MBIC of NBR 26-6A against *S. aureus* NCTC 13142 was identified via crystal violet, and resazurin TVC results as 128 µg/ml (**Figure 3.3 A-C**). Absorbance

readings for the crystal violet and resazurin assays were reduced by 90 % in comparison to the positive control and TVC counts demonstrated two-fold decrease, meaning a decrease in cell number >90 % at this concentration. However, this biofilm inhibition occurred at the same concentration as the MIC and is likely caused due to the arrested development of *S. aureus* NCTC 13142 rather than action on the biofilm formation itself. This could still mean that NBR 26-6As has the potential to prevent the development of chronic infections if applied to a wound shortly after it has occurred but further investigation via RNAseq, qPCR and proteomic studies would be required to identify whether NBR 26-6A acts upon biofilm associated gene regulation directly. This was tested with later batches of the NX-AS-401 compound via RT-qPCR (**Chapter 5**).

Although biofilm inhibition and prophylactic treatment would be the preferred treatment option, infections treated in clinic are often established prior to the patient visiting a clinician for treatment ⁽²⁾. Therefore, it is important to identify whether NBR 26-6A had the ability to disrupt pre-established biofilms. There are many variables in the ability of *S. aureus* to form a strong biofilm with biofilm forming potential varied per strain due to genetic diversity. *S. aureus* NCTC 13142 may also have formed a weak biofilm due to the use of un-supplemented MHB. Growth media composition is important in biofilm formation, with some *S. aureus* strains able to form stronger biofilms in the presence of salt and glucose or in more nutrient rich environments and *in vivo* ^(71, 86).

S. aureus NCTC 13142 biofilms formed over 48 hours performed better than those formed over 24 hours, biofilms were less prone to mechanical shearing via pipette. The biofilms established over 48 hours are also a better representative of biofilms found in chronic wounds, where biofilms often form over longer periods of time ⁽²⁸⁸⁾. However, *in vitro* studies are restricted in identifying the effects a potential antibiotic may have *in vivo* due to their limitation in replicating host factors such as the immune system, protein binding and tissue penetration ⁽²⁸⁹⁾.

In figures 3.3, 3.4 and 3.5 both mass (**A**) and metabolic activity (**B**) of *S. aureus* NCTC 13142 was increased at NBR 26-6A concentrations below the identified MBIC (128 µg/ml) and MBEC (256 µg/ml) when compared to the untreated control. Since cell number is not increased at these concentrations (**Figures 3.3-3.5 C**), it appears that the

increase in mass and metabolism is caused by changes in the production and regulation of *S. aureus* NCTC 13142 metabolism. It has already been shown that sub-optimal treatment of *S. aureus* biofilms with low antibiotic concentrations increases biofilm growth and development⁽²⁵⁾ with low levels of antibiotics such as clindamycin causing an increase in both volume and presence of eDNA in the extracellular matrix in *S. aureus* biofilms^(91, 290, 291).

While these effects are antibiotic specific a similar mechanism of action could occur with NBR 26-6A causing the increase in biomass seen at sub MBIC (128 µg/mL) and MBEC (256 µg/ml) concentrations. For example, the study by Song *et al* used reverse transcription quantitative polymerase chain reaction (RT-qPCR) to show that the presence of a sub-inhibitory antibiotic concentration in the environments causes upregulation of sigma factor B (*sigB*) a genetic regulator associated with environmental stress in *S. aureus*⁽⁹¹⁾. Upregulation of *sigB* leads to an increase in the transcription of biofilm associated genes alanine autolytic enzyme (*atl*), accessory gene regulator (*agrA*) and both fibronectin binding proteins (*fnb*)⁽⁹¹⁾. The upregulation in expression of global regulator such as *sigB* and changes to the cell state caused by low antibiotic concentrations can also lead to a upregulation in other metabolic processes, such as resazurin to resofurin⁽²⁹²⁾. This response can result in the additional protection for *S. aureus* as increases in fibronectin binding protein synthesis increasing the amount of extracellular matrix^(61, 293). The extracellular matrix confers protection from both antibiotic molecules and host immune cells by binding antibiotic molecules via electrostatic interaction and creating channels that limit the movement of host immune cells^(61, 91, 293).

In a clinical setting this implies that treatment of a biofilm with a sub-inhibitory dose of antibiotic or NBR 26-6A could potentially have the opposite effect to that intended and increase biomass and metabolism as seen in Figure 3.3 - 3.5 A and B. This effect is a stress response referred to as antibiotic pressure that is often caused by low antibiotic concentrations in the environment. While antibiotic or NBR 26-6A concentration is too low for complete eradication, the presence of it does elicit changes in growth patterns and potentially gene regulation, this requires confirmation by RT-qPCR⁽²⁹⁰⁾.

Stress responses for *S. aureus* are not uncommon due to the constant changes in their environment, and have been elucidated for the stress associated with lack of nutrition

(stringent stress), the presence of reactive oxygen species (oxidative stress), membrane damage (envelope stress) and changes in temperature (heat stress) ⁽²⁹⁴⁾.

However, while this is the most likely theory the effects of antibiotic pressure were not conclusively proven via these experiments alone. Determining whether NBR 26-6A can elicit an antibiotic pressure will require the use of quantitative PCR and metabolomic studies to identify global changes in gene expression and metabolism. Further investigations are also required to understand how NBR 26-6A effects *S. aureus* growth, and to understand its mechanism of action, this could allow for optimisation of NBR 26-6A and increase its efficacy for potential *in vivo* use.

3.6 Conclusions.

Aim: To establish the minimum inhibitory and bactericidal concentrations of NBR 26-6A against *S. aureus* NCTC 13142.

NBR 26-6A has a demonstrated MIC of 128 µg/ml against *S. aureus* strain NCTC 13142 growth of *S. aureus* NCTC 13142 in accordance with EUCAST guidelines, however cell numbers were not decreased at NBR 26-6A concentration of <32 µg/ml.

The MBC of NBR 26-6A against *S. aureus* NCTC 13142 could not be identified after 18-20 hour exposure. An MBC only occurred after 48 hours of treatment and *S. aureus* NCTC 13142 was only completely eradicated by NBR 26-6A at concentrations ≥512 µg/ml.

The MIC/MBC of NBR 26-6A is much greater than current standard of care antibiotics and further investigation is required to determine if these concentrations are obtainable with no adverse effects as a topical application.

Aim: To identify the effects of NBR 26-6A on *S. aureus* NCTC 13142 growth kinetics and cell number over time.

Time/kill curves indicated that NBR 26-6A concentrations >32 µg/ml prevented an increase in *S. aureus* NCTC 13142 cell number but did not cause a reduction in cells until after 24 hours. NBR 26-6A concentrations of 4 and 8 µg/ml caused temporary inhibition of growth for one and two hours respectively before cell numbers increased equal to the untreated control.

Aim: To identify the effects of NBR 26-6A on *S. aureus* NCTC 13142 biofilm formation and on pre-established biofilms formed over both 24 and 48 hours.

When NBR 26-6A was utilised against *S. aureus* NCTC 13142 biofilms it only showed the ability to inhibit biofilms at a concentration equal to the established MIC 128 µg/ml. However, it also demonstrated the ability to disrupt *S. aureus* NCTC 13142 biofilms pre-established over both 24 and 48 hours at concentration between 64-256 µg/ml dependent on biofilm aspect measured.

Although NBR 26-6A may be a potential treatment for *S. aureus* infections, there are limitations due to its formulation, with problems arising such as compound precipitation restricting the concentrations that could be used and potentially causing an inaccurate MIC result to be obtained from broth microdilution tests.

Having identified the rudimentary antimicrobial capabilities of NBR 26-6A the next challenges are determining whether ajoene content affects the efficacy of NX-AS-401, and whether resistance can develop as shown in chapter 4. Further identification of NX-AS-401s effect on *S. aureus* biofilms and attempts at establishing its mechanism of action is the main aim of Chapter 5. Chapter 6 focuses on additional effects of NX-AS-401 and whether it can alter *S. aureus* virulence and reduce the severity of an infection.

4.0 Chapter 4: Identifying the mode of action of NX-AS-401 on planktonic *S. aureus* cells

4.1 Introduction

4.1.1 The active molecules of NX-AS-401

Although the mechanism of action for NX-AS-401 is currently unknown, its composition does contain >90 % ajoene, this molecule contains a disulphide bridge which may be responsible for its antibacterial activity, though this is yet to be confirmed ⁽²¹⁷⁾. As previously stated (**Chapter 1, Section 1.3.2**) NX-AS-401 does contain components that are structurally similar to those found in the antibiotic class sulphonamides. However, the two types of bond present act differently with sulphonamide bonds reacting with dihydropteroate synthase to prevent folate synthesis and disulphide bonds reacting with thiol groups ⁽¹³⁴⁾.

Since NX-AS-401 contains various garlic derived components its antimicrobial properties may not just be caused by the activity of the main component ajoene. Antimicrobial activity may be mediated by the smaller unidentified compounds present in the formulation and these may contain other sulphur based bonds, including sulphonamide, disulphide and sulphoxide. These bonds are all different and react with different groups, this includes amines, thiols, cysteine residues and also utilised a solvents ^(133, 161, 182, 295).

The variety of sulphur bonds and their associated reactions indicate that they might not have the same mechanism of action as each other. Therefore, sulphonamide resistance mechanisms may have no effect on ajoene and ajoene may also not cause the same adverse reactions seen with sulphonamides due to differences in how the body metabolises ajoene.

The antibiotic clinical breakpoints provided by EUCAST do not include values for sulphonamide based drugs alone and only show values when in combination with trimethoprim. Therefore, determining whether the isolates used for this study were resistant or sensitive was not possible and comparison could not be drawn between sensitivity to NX-AS-401 and sulphonamide drugs.

Identifying whether ajoene content effects NX-AS-401 efficacy and whether resistance or increased tolerance to NX-AS-401 can be generated through repeated exposure will assist in identifying the potential of NX-AS-401 as a antimicrobial.

4.2 Aims

- Aim: To identify the MIC and MBC of NX-AS-401 against *S. aureus* in comparison to NBR 26-6A.
- To identify the mode of action (bacteriostatic/ bactericidal) of NX-AS-401 against *S. aureus*
- To identify potential resistance and tolerance to NX-AS-401
- To identify whether exposure of *S. aureus* to sub-inhibitory concentration of NX-AS-401 or gentamicin induces mutations in specific gene sites or increased the generation of single nucleotide polymorphisms (SNPs)
- To identify synergism /antagonism of NX-AS-401 with current standard of care antibiotics.

4.3 Materials and Methods

No changes have been made to the materials and methods provided in Chapter 2.

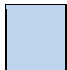


4.4 Results

4.4.1 Strain Characterisation

Antibiotic susceptibility for all *S. aureus* strains were identified via EUCAST disc diffusion (**Table 4.1 A**) and confirmed via EUCAST broth microdilution (**Table 4.1 B**).

Table 4.1 Antibiotic sensitivity of *S. aureus* strains.

A The susceptibility of *S. aureus* to standard of care antibiotics was identified via disc diffusion. Zone sizes were compared to the breakpoints provided by EUCAST Clinical Breakpoint Guideline Version 9.0 ⁽²⁴⁷⁾. **B** Antibiotic susceptibilities were confirmed via broth microdilution, and MIC was determined by comparison to the breakpoints provided by EUCAST Clinical Breakpoint Guideline Version 9.0 ⁽²⁴⁷⁾. An asterisk (*) denotes strains that displayed the “D phenomenon”, explained further in Section 4.5.1 indicating inducible clindamycin resistance when exposed to erythromycin.

Sensitive =  Intermediate =  Resistant = 

	Gentamicin		Clindamycin		Ciprofloxacin		Erythromycin		Tetracycline		Cefoxitin	
	Zone (mm)	Result	Zone (mm)	Result	Zone (mm)	Result	Zone (mm)	Result	Zone (mm)	Result	Zone (mm)	Result
NCTC 13142	24	S	26	S	27	S	29	S	30	S	0	R
NCTC 12973	21	S	26	S	25	S	23	S	28	S	30	S
UHW 3	18	S	0	R	0	R	0	R	27	S	13	R
UHW 8	19	S	20	S	25	S	17	I	23	S	30	S
UHW 15	19	S	22	S	25	S	24	S	27	S	30	S
UHW 18	19	S	23	S	25	S	24	S	27	S	30	S
UHW 19	20	S	23	S	24	S	17	I	12	R	30	S
CRI 2	19	S	0	R*	0	R	0	R	27	S	13	R

B	Gentamicin		Clindamycin		Ciprofloxacin		Erythromycin		Tetracycline		Cefoxitin	
	MIC	Result	MIC	Result	MIC	Result	MIC	Result	MIC	Result	MIC	Result
NCTC 13142	0.5	S	0.25	S	0.25	S	0.25	S	0.25	S	>4	R
NCTC 12973	0.25	S	0.25	S	0.25	S	0.5	S	0.25	S	<4	S
UHW 3	0.5	S	8	R	8	R	8	R	0.25	S	>4	R
UHW 8	1	S	0.25	S	0.25	S	0.25	S	0.25	S	<4	S
UHW 15	1	S	0.25	S	0.25	S	0.25	S	0.25	S	<4	S
UHW 18	1	S	0.25	S	0.25	S	0.25	S	0.25	S	<4	S
UHW 19	0.5	S	0.25	S	0.25	S	1	S	8	R	<4	S
CRI 2	0.5	S	0.25	R*	8	R	8	R	0.25	S	>4	R

Antibiotic susceptibility testing identified that all strains were susceptible to gentamicin. Strains UHW3 and UHW 8 were resistant to four out of the six antibiotics tested, while strains UHW 8, UHW 15, and UHW 18 demonstrated susceptibility to all antibiotic classes tested in this project. UHW 19 was the only strain with resistance to tetracycline. NCTC 13142, UHW 3 and CRI 2 were the only strains resistance to cefoxitin identifying them as MRSA. CRI 2 was the only strain that demonstrated the D phenomenon, an inducible clindamycin resistance when co-exposed to erythromycin via disc diffusion.

The same antibiotic susceptibility patterns were identified by both methods for all eight strains with the only difference between methods being an 'intermediate' erythromycin result for UHW 8 and UHW 19 in disc diffusion as opposed to 'susceptible' in broth microdilution.

4.4.2 Vehicle Control

NX-AS-401 required dilution in DMSO which has demonstrated antibacterial activity (295). Broth microdilution using DMSO was conducted to identify the MIC of DMSO against *S. aureus* to allow for a working DMSO concentration that did not affect growth to be selected for future work (Figure 4.1).

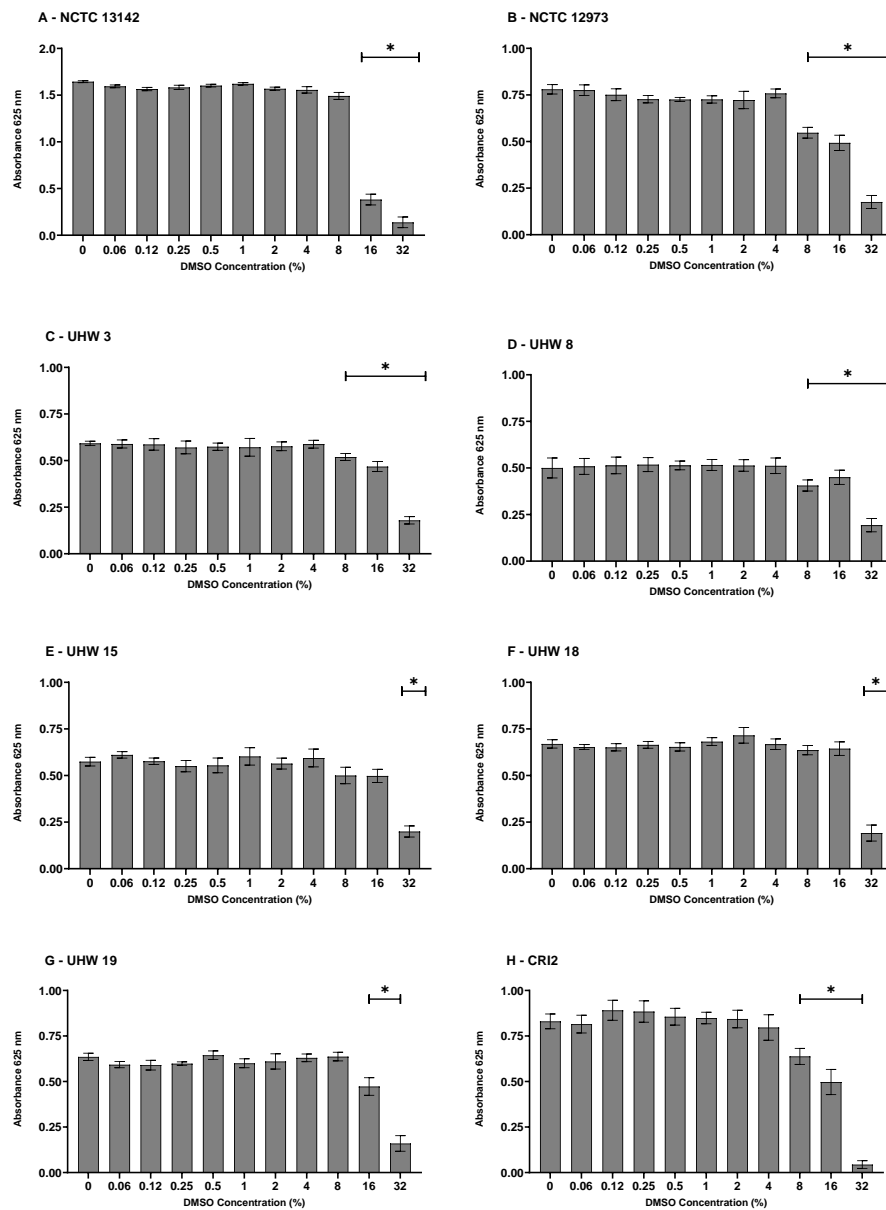


Figure 4.1 Identifying the effects of DMSO on *S. aureus* growth.

Concentrations of DMSO that significantly ($p < 0.05$) inhibited the growth of *S. aureus* in comparison to the untreated control are marked with an asterisk (*) Error bars represent standard error of the mean.

Susceptibility to DMSO was strain specific, however, concentrations of ≥ 8 % inhibited *S. aureus* cell growth in all eight strains. Therefore, DMSO concentrations ≤ 4 % were used in all further experiments.

4.4.3 Minimum Inhibitory/Bactericidal Concentrations

The MIC of NX-AS-401 was identified via adapted EUCAST Broth micro-dilution. MBC was identified by culturing the well contents containing NX-AS-401 concentrations that inhibited growth >90 % onto MHA (Figure 4.2).

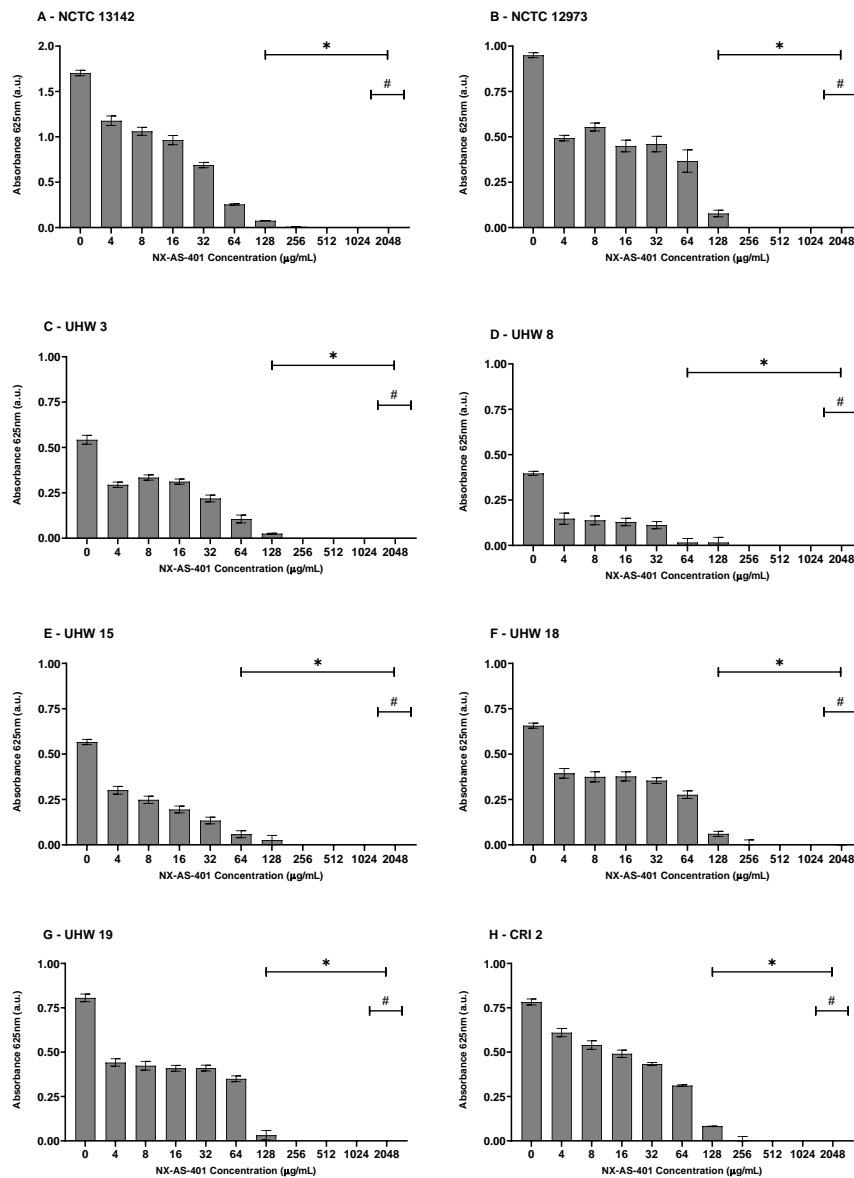


Figure 4.2 Results of EUCAST Broth Microdilution with NX-AS-401 against eight *S. aureus* strains.

Significant ($p < 0.05$) inhibition of *S. aureus* growth in comparison to the untreated control are marked with an asterisk (*). Error bars indicated standard error of the mean.

The lowest concentrations where growth was significantly ($p < 0.05$) inhibited by $>90\%$ was identified as the MIC. For strains NCTC 13142 (A), NCTC 12973 (B), UHW 3 (C), UHW 18 (F), UHW 19 (G) and CRI 2 (H) the MIC was identified as $128\ \mu\text{g/ml}$. UHW 8 (D) and UHW 15 (E) had greater susceptibility to NX-AS-401 with an MIC of $64\ \mu\text{g/ml}$. Concentrations of $2048\ \mu\text{g/ml}$ were identified as the MBC for eight *S. aureus* all strains, as after treatment no viable cells were recovered on MHA.

It was also noted that NCTC strains produced higher absorbance values after 20 hours in comparison to the clinical strains.

4.4.4 Time/Kill Curves

The effects of different concentrations of NX-AS-401 on the growth of *S. aureus* was monitored via TVC counts over 24 hours. Samples were taken at intervals to determine when NX-AS-401 affected *S. aureus* counts (**Figure 4.3**).

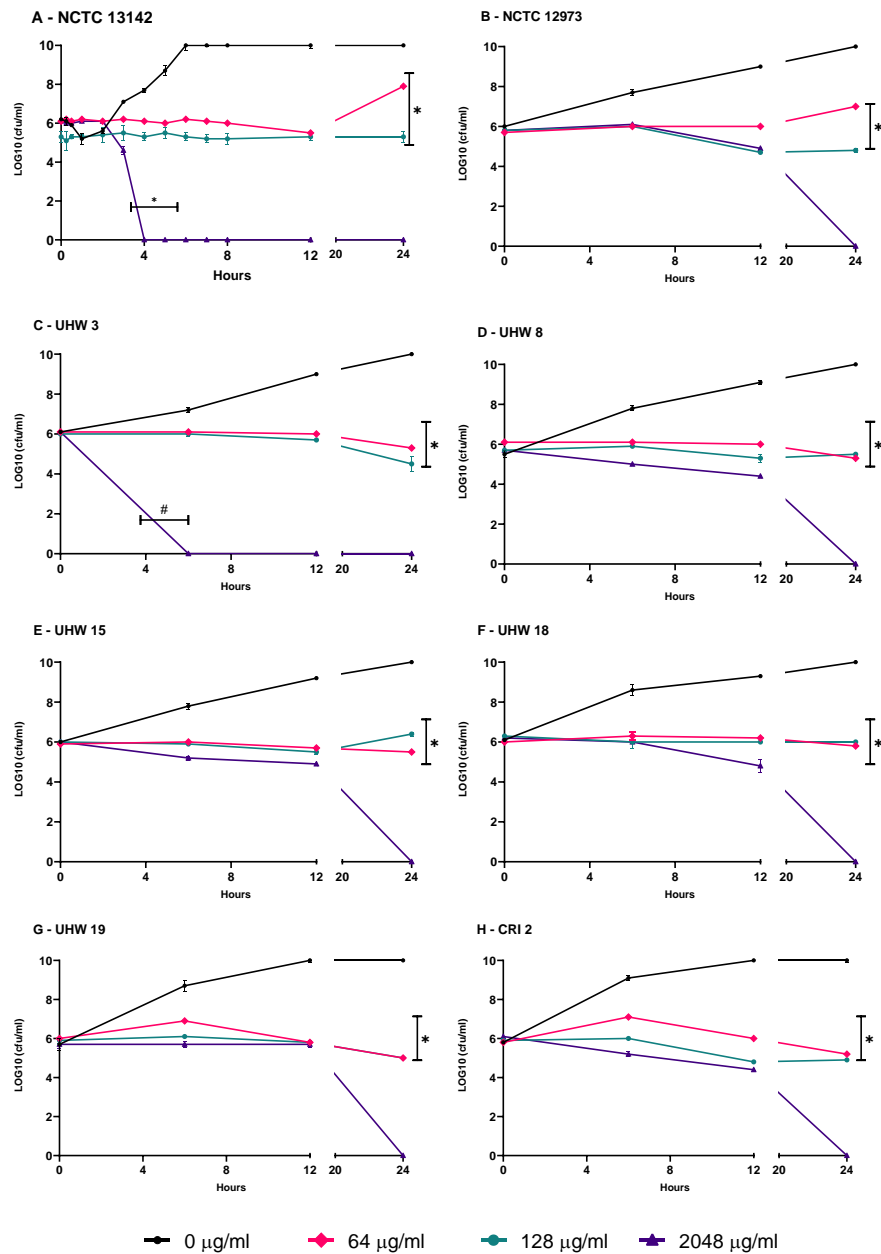


Figure 4.3 Time/Kill Curves of NX-AS-401 against *S. aureus*.

Statistically significant ($p < 0.0001$) differences between cell number in comparison to the positive control are indicated by lines underneath the triple asterisk bars (*). Error bars represent standard error of the mean.

NX-AS-401 concentrations of 64 and 128 $\mu\text{g/ml}$ were capable of significantly inhibiting *S. aureus* cell growth in all strains from six hours onwards. The NX-AS-401 MBC concentration of 2048 $\mu\text{g/ml}$ eradicated all *S. aureus* cells in all eight strains by 24 hours. However, strains 13142 (A) and UHW 3 (C) seemed more susceptible to the bactericidal effects of NX-AS-401 with bacterial cell eradicated between four and six hours.

4.4.4.1 Additional

An observation was made during TVC counts regarding colony size displayed in Figure 4.4. It was noticed that after treatment with NX-AS-401 *S. aureus* colony sizes were reduced in comparison to the untreated controls.

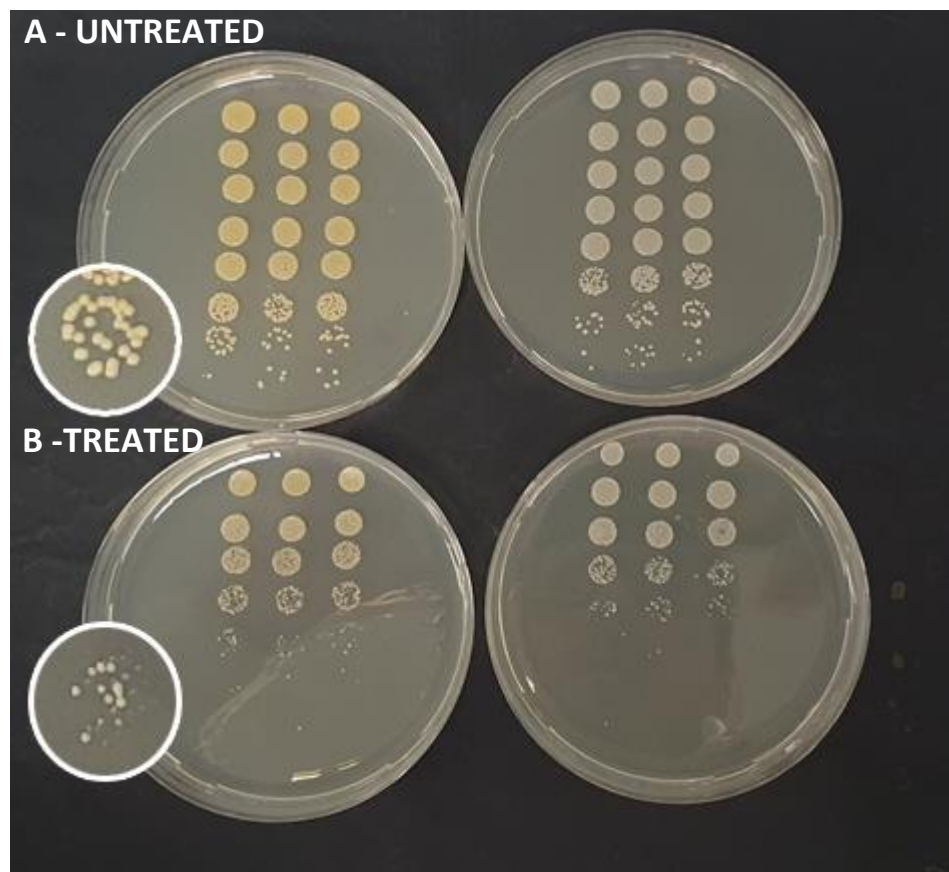


Figure 4.4 Difference in colony size of NX-AS-401 treated and untreated cells.

The image shows how treatment with NX-AS-401 impacted the size of colonies formed on solid agar. *S. aureus* cells treated with NX-AS-401 formed smaller pin-point colonies when compared to the untreated controls.

4.4.5 Growth Curves

Growth curves for *S. aureus* treated with a concentration gradient of NX-AS-401 were obtained by incubating a EUCAST broth microdilution plate in a spectrophotometer (BMG, Spectrostar Nano) and reading at 625 nm hourly (Figure 4.5).

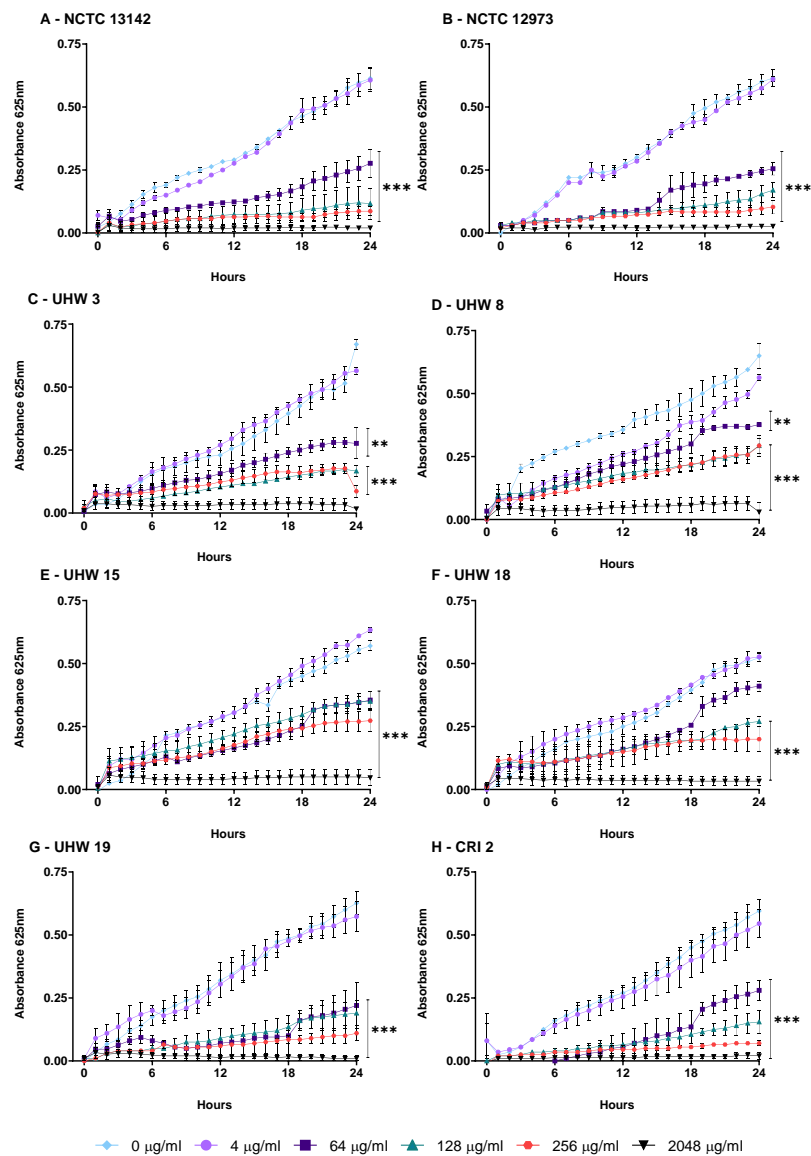


Figure 4.5 Growth Curves of NX-AS-401 against *S. aureus*.

Statistically significant absorbance values between NX-AS-401 concentrations in comparison to the positive control are indicated by the concentration marked with either double asterisk (***) where $p < 0.001$ or a triple asterisk (***) where $p < 0.0001$. Error bars represent standard error of the mean.

S. aureus growth was not inhibited at NX-AS-401 concentrations of 4 µg/ml compared to an untreated control, while concentrations of 64-2048 µg/ml inhibited growth in all strains up to 24 hours. The level of inhibition appears strain specific with strains UHW 8, 15 and 18 showing results that contrast with the EUCAST broth microdilution in Figure 4.2.

4.4.6 Resistance Evolution

NX-AS-401 or gentamicin broth microdilution was performed daily for 14 days to determine if repeated exposure to a sub-inhibitory concentration of NX-AS-401 or gentamicin increased tolerance. Inocula were created from the previous day's *S. aureus* cells that had been exposed to either sub-MIC gentamicin or NX-AS-401. Daily MICs were determined via optical density and MIC was taken as 90 % inhibition in comparison to the positive control (**Figure 4.6**).

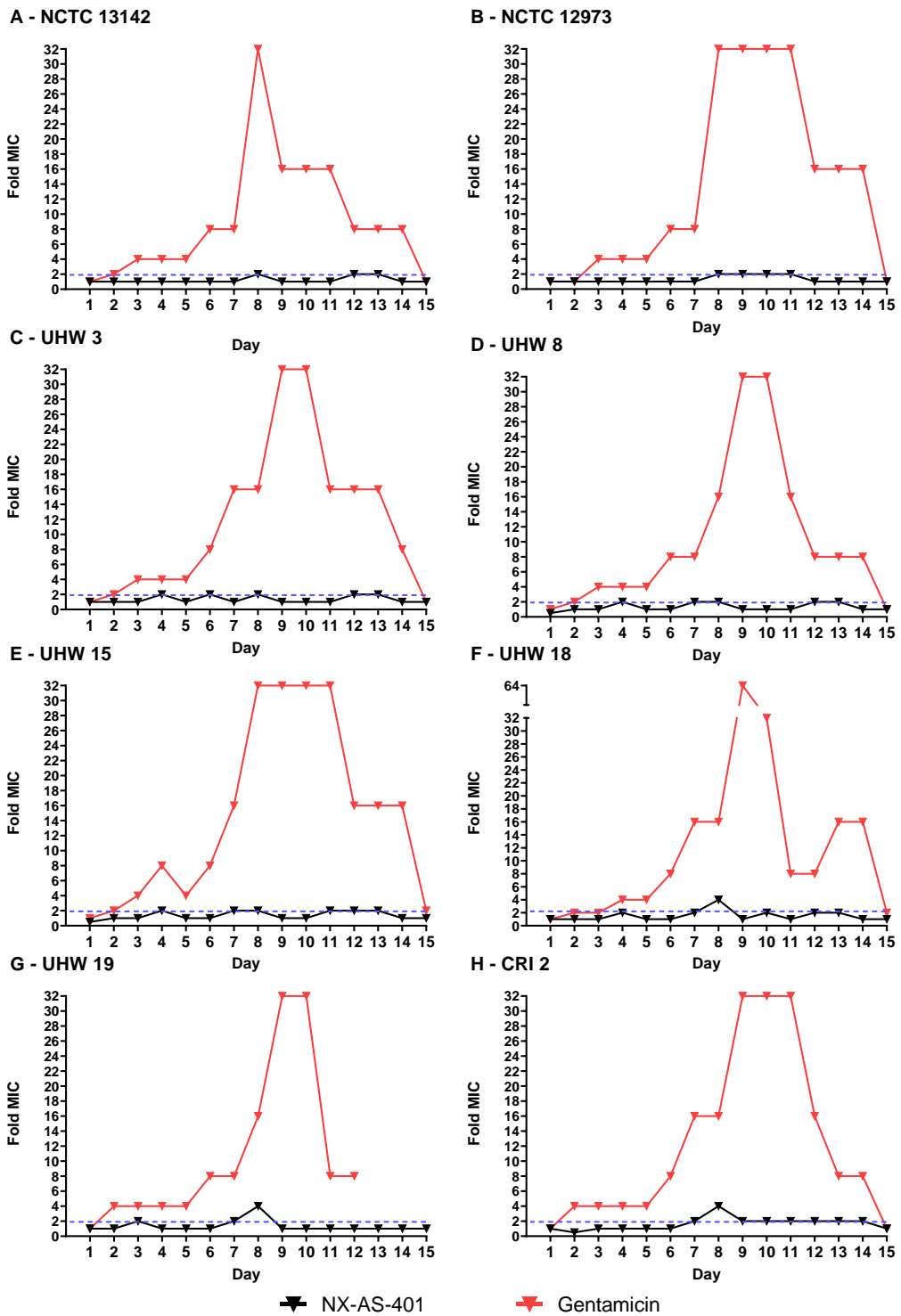


Figure 4.6 Repeated exposure of *S. aureus* to NX-AS-401 and gentamicin over 14 days.

Tolerance of *S. aureus* to NX-AS-401 is shown by black lines and gentamicin by red lines. The blue dotted line indicates a two-fold increase in the MIC, an increase above this line indicates the development of antibacterial tolerance and may result in treatment failure according to EUCAST ⁽²⁴⁷⁾.

S. aureus exposed to NX-AS-401 continued to have a sensitivity to NX-AS-401 at the original MIC or within the accepted 2-fold margin of error except for strains UHW 18, UHW 19 and CRI 2 where on day eight the MIC increased above the two-fold margin of error for one day before decreasing to equal or below the two-fold change. This is more indicative of an increase in tolerance rather than a consistent development of resistance.

Repeated gentamicin exposure caused a consistent increase in MIC above the two-fold margin of error that lasted for 11 to 13 days. Susceptibility to both NX-AS-401 and gentamicin returned after one day in antibiotic free media with growth being inhibited at the MIC determined on day one. UHW 19 performed differently from other strains as after 12 days of exposure cells were non-viable at all gentamicin concentrations.

Post resistance training isolates were also subjected to antibiotic susceptibility testing via EUCAST disc diffusion (**Appendix 1.1**) to determine if the resistance trained strains had lost resistance mechanisms or undergone mutations that conferred resistance to the additional antibiotics used throughout his project (ciprofloxacin, tetracycline, erythromycin, clindamycin and ceftiofur). The results showed that there was no change in the antibiotic susceptibility patterns in the strains exposed to sub-inhibitory NX-AS-401 and gentamicin or the isolate passage in antibiotic free media for 14 days. This indicates that if used clinically if NX-AS-401 failed to eradicate the infection in the allotted clinical time-frame of 14 days its use would not impact the efficacy of other antibiotic treatments.

However, further analysis of the bacterial genome was performed to identify whether repeated exposure of sub-inhibitory NX-AS-401, gentamicin or antibiotic free passage caused loss or acquisition of resistance genes.

4.4.7 Gene Sequencing

4.4.7.1 Phylogenetic Tree

Illumina sequencing (Section 2.3.16) was performed on 32 isolates, the original eight *S. aureus* isolates used in this study and the same strains after a 14 day passage in either antibiotic free media or concentration gradient of either NX-AS-401 or gentamicin as part of the resistance evolution experiment (Section 4.4.6). Isolate sequences were grouped in a phylogenetic tree (Figure 4.7) before identification of resistance mechanisms via CARD and Resfinder (Table 4.2). Finally, SNP analysis was performed via Snippy (Figure 4.8).

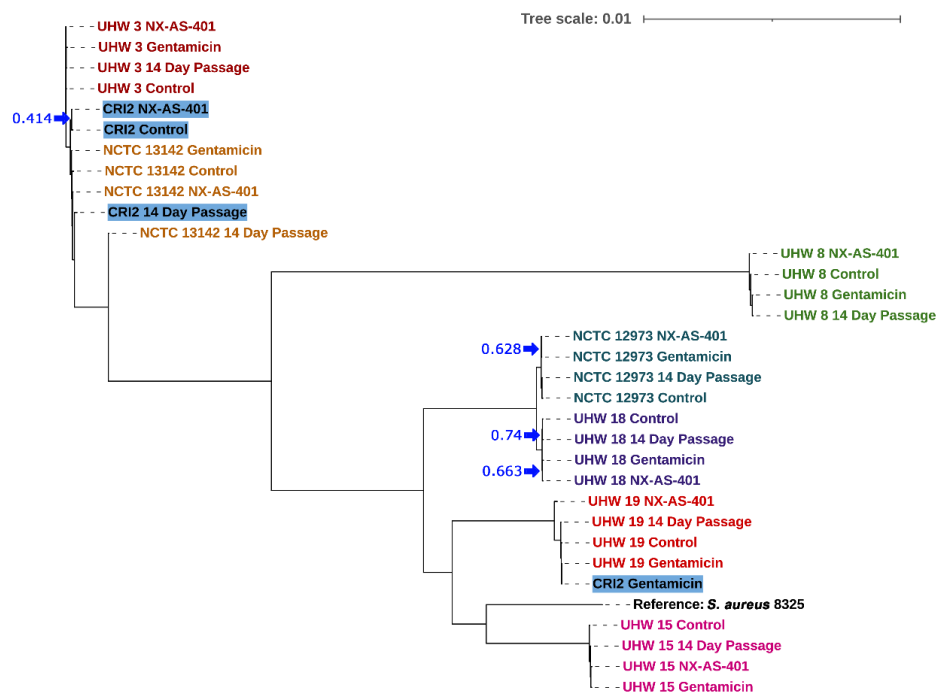


Figure 4.7 Unrooted Neighbour-Joining phylogenetic tree of sequenced isolates created on FastTree.

A neighbour joining tree was chosen to see how similar isolates were after the evolution experiment and not to determine evolutionary links that would be inferred from a maximum parsimony/likelihood tree. Details of the assembled genomes is provided in Appendix 1.6. Individual isolates are grouped based on colour, with isolate CRI 2 highlighted blue due to spread across the phylogenetic tree.

Local bootstrapping values were >0.99 on all nodes apart from were indicated above by the blue arrows and text.

Overall, seven of the eight isolates tested and sequenced remained similar after the resistance evolution experiment (**Section 4.4.6**).

Isolate CRI 2 NX-AS-401 sequenced poorly (**Appendix 1.6**), with a genome length of 64137. The reason for poor sequencing was not determined but likely due to contamination during post resistance evolution culture, DNA extraction or sequencing/library creation. The contamination and poor assembly that results is the likely cause for the low bootstrapping support score of 0.414. While other CRI 2 isolates sequenced well the CRI 2 Gentamicin isolate clustered with UHW 19, once again this seems to be due to contamination or mislabelled with a isolate UHW 19.

Isolate UHW 18 also demonstrated moderate bootstrapping support with values of 0.663 and 0.74. Finally, NCTC 12973 isolates showed moderate-low bootstrapping with a value of 0.628

The reference strain used to create this tree was *S. aureus* 8325 as the full annotated genome is available.

4.4.7.2 Gene analysis of resistance mechanisms.

Table 4.2 Resistance mechanism genes identified in all sequenced isolates.

Table A lists all the resistance genes and their targets found in the eight *S. aureus* strains utilised throughout his project. Data has been collated from the Comprehensive antibiotic resistance database (CARD) ⁽²⁶²⁾ and other sources ^(114, 169, 296).

Table B shows that while the strains utilised in this study had similar antibiotic susceptibility patterns, they had different antibiotic resistance mechanisms. Resistance gene were identified from sequences analysed via two methods (**Section 2.4.13**) CARD and Resfinder 3.2.

The presence of norA complex (further described in the discussion) without the *arIS* part of its two-component regulatory system is indicated by #.

Table A

Gene	Mechanism	Target Antibiotic
<i>norA</i> / <i>LmrS</i>	<u>This containing the follow resistance associated genes:</u>	
	Staphylococcus aureus <i>norA</i>, <i>arlS</i>, <i>arlR</i> and <i>mgrA</i> : <i>arlS</i> and <i>arlR</i> are promoters and <i>mgarA</i> is a regulator for <i>norA</i> expression. <i>Nor A</i> is an efflux pump targetting hydrophilic fluoroquinolones. Basal expression levels do not confer resistance	Flouroquinolones
	<i>mepR</i> : Efflux pump, common, does not cause resistance	All
	Staphylococccys aureus <i>LmrS</i> : Efflux pump	Linezolid, chloramphenicol and trimethoprim
<i>blaZ</i>	Beta-lactamase - an enzymatic inactivation of beta-lactam antibiotics	Beta-lactams
<i>mecA</i>	Encodes for PBP2a and different synthesis pathways for peptidoglycan that works in the presence of beta-lactams.	Beta-lactams
<i>fosb</i>	Enzyme that adds thiol groups onto fosfomycin rendering it inactive	Fosfomycin
<i>tet38</i>	Antibiotic efflux pump	Tetracyclines
<i>parC</i>	Point mutation that prevents binding of antibiotics to the <i>parC</i> subunit of topoisomerase IV	Flouroquinolones
<i>parE</i>	Point mutation that prevents binding of antibiotics to the <i>parE</i> subunit of topoisomerase IV.	Flouroquinolones
<i>fusA</i>	Mutation that prevents the binding of fusidic acid to the translation elongation factor, rendering fusidic acid ineffective.	Fusidic acid
<i>ermC</i>	Catalyses the methylation of the 23s ribosomal RNA. Can be induced by erythroymcin binding to the leader peptide and allowing <i>ermC</i> expression. The gene can also be found without the leader peptide, allowing for expression without the presence of erythromycin.	Streptogramins, lincosamides and macrolides
<i>gyrA</i>	Point mutation that prevent binding of antibiotics to topisomerase subunit <i>gyrA</i>	Flouroquinolones
<i>glpT</i>	Mutation to sugar importer <i>glpT</i> , preventing the uptake of phosphorylated sugar and preventing antibiotic uptake	Fosfomycin
<i>murA</i>	Alteration in <i>murA</i> a catalyst in the first part of peptidoglycan synthesis that is blocked by fosfomycin	Fosfomycin
<i>tetM</i>	Protein that binds to the 30s ribosomal subunit preventing the actions of tetracyclines.	Tetracyclines

Table B

Strain / Condition	Analysis method	Resistance Genes Identified													
		<i>norA</i> / <i>lmrS</i>	<i>blaZ</i>	<i>mecA</i>	<i>fosB</i>	<i>tet38</i>	<i>parC</i>	<i>parE</i>	<i>fusA</i>	<i>ermC</i>	<i>gyrA</i>	<i>glpT</i>	<i>murA</i>	<i>tetM</i>	
13142	Control (Day 0)	CARD RGI	✓		✓										
		Resfinder			✓										
	NX-AS-401 (14)	CARD RGI	✓	✓	✓										
		Resfinder		✓	✓										
	Gentamicin (14)	CARD RGI	✓		✓										
		Resfinder			✓										
Untreated (14)	CARD RGI	✓	✓	✓											
	Resfinder		✓	✓											
12973	Control (Day 0)	CARD RGI	✓	✓		✓									
		Resfinder		✓											
	NX-AS-401 (14)	CARD RGI	✓	✓		✓									
		Resfinder		✓											
	Gentamicin (14)	CARD RGI	✓	✓		✓									
		Resfinder		✓											
Untreated (14)	CARD RGI	✓	✓		✓	✓									
	Resfinder		✓												
UHW 3	Control (Day 0)	CARD RGI	✓ #	✓	✓			✓	✓	✓	✓				
		Resfinder			✓					✓	✓				
	NX-AS-401 (14)	CARD RGI	✓ #		✓			✓	✓	✓	✓	✓			
		Resfinder			✓						✓	✓			
	Gentamicin (14)	CARD RGI	✓ #	✓	✓			✓	✓	✓	✓	✓			
		Resfinder		✓	✓						✓	✓			
Untreated (14)	CARD RGI	✓ #		✓			✓	✓	✓	✓	✓				
	Resfinder			✓						✓	✓				
UHW 8	Control (Day 0)	CARD RGI	✓ #									✓	✓		
		Resfinder										✓	✓		
	NX-AS-401 (14)	CARD RGI	✓ #									✓	✓		
		Resfinder										✓	✓		
	Gentamicin (14)	CARD RGI	✓ #									✓	✓		
		Resfinder										✓	✓		
Untreated (14)	CARD RGI	✓ #									✓	✓			
	Resfinder										✓	✓			
UHW 15	Control (Day 0)	CARD RGI	✓ #	✓											
		Resfinder		✓											
	NX-AS-401 (14)	CARD RGI	✓ #	✓											
		Resfinder		✓											
	Gentamicin (14)	CARD RGI	✓ #	✓											
		Resfinder		✓											
Untreated (14)	CARD RGI	✓ #	✓												
	Resfinder		✓												
UHW 18	Control (Day 0)	CARD RGI	✓			✓									
		Resfinder													
	NX-AS-401 (14)	CARD RGI	✓			✓									
		Resfinder													
	Gentamicin (14)	CARD RGI	✓			✓									
		Resfinder													
Untreated (14)	CARD RGI	✓			✓										
	Resfinder														
UHW 19	Control (Day 0)	CARD RGI	✓			✓							✓		
		Resfinder											✓		
	NX-AS-401 (14)	CARD RGI	✓			✓							✓		
		Resfinder											✓		
	Gentamicin (14)	CARD RGI	✓			✓							✓		
		Resfinder											✓		
Untreated (14)	CARD RGI	✓			✓							✓			
	Resfinder											✓			
CRI 2	Control (Day 0)	CARD RGI	✓ #		✓			✓		✓	✓				
		Resfinder			✓					✓	✓				
	NX-AS-401 (14)	CARD RGI	Failed to sequence												
		Resfinder	Failed to sequence												
	Gentamicin (14)	CARD RGI	✓ #		✓	✓			✓		✓	✓			
		Resfinder			✓						✓	✓			
Untreated (14)	CARD RGI	✓ #		✓				✓		✓	✓				
	Resfinder			✓						✓	✓				

4.4.7.3 Genotype and Phenotype discrepancies.

Out of the 32 isolates sequenced six contained genes associated with resistance mechanisms that while present in the genome were not identified in the phenotype.

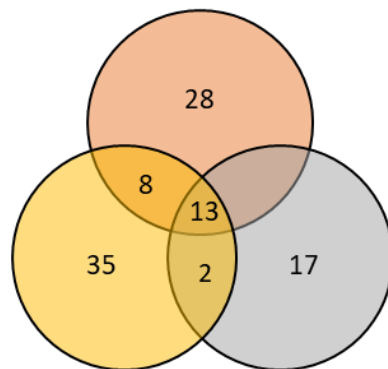
The only changes identified between the control and trained isolates were, NCTC 13142 acquired the *blaZ* gene in both NX-AS-401 and 14-day passage isolate while UHW 3 showed *blaZ* in both the control and gentamicin trained isolate . The 14-day passage isolate of NCTC 12973 showed acquisition of the *tet(38)* resistance gene. CRI 2 also acquired *fosb* resistance in gentamicin trained isolate.

4.4.7.4 Single nucleotide polymorphism analysis

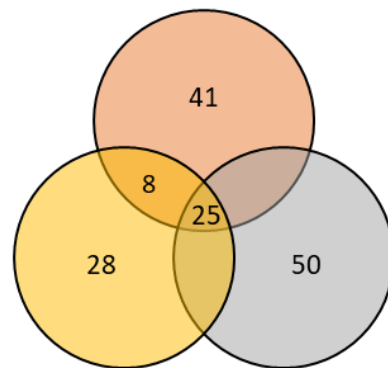
Venn diagrams have been used to show the number of SNPs that occurred in each *S. aureus* strain under each of the resistance training conditions in comparison to the day zero control. These were used to identify if antibiotic SNPs occurred in high-mutable regions of the genome and thus would occur during *S. aureus* growth, or whether they were specifically caused by gentamicin/NX-AS-401 exposure. A full list of the SNPs identified via Snippy is provided in Appendix 1.5.

NX-AS-401 SNPs =  Gentamicin SNPs =  14 Day Passage SNPs = 

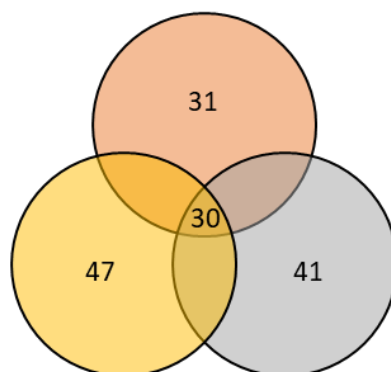
A – NCTC 13142



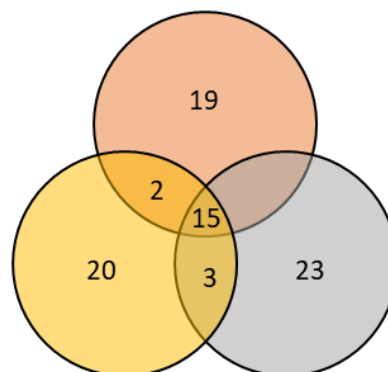
B – NCTC 12973



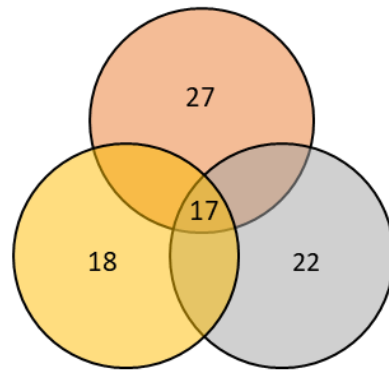
C – UHW 3



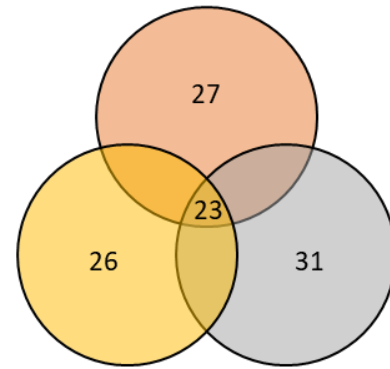
D -UHW 8



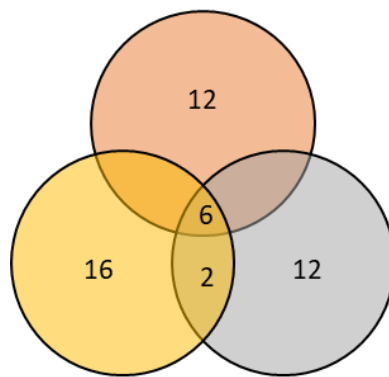
E – UHW 15



F – UHW 18



G – UHW 19



H – CRI 2

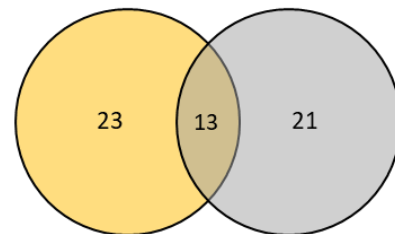


Figure 4.8 SNPs found in isolates under different experimental conditions.

Yellow circles indicate *S. aureus* isolates treated with sub-MIC NX-AS-401 for 14 days. Orange circles indicate *S. aureus* isolates treated with sub-MIC Gentamicin for 14 days. Grey circles indicate *S. aureus* isolates that were passaged in antibiotic free media for 14 days. Central number in the individual circles were the number of SNPs found in that isolate, numbers in the overlapping circles indicate the number of SNPs that occurred in the same genetic location in those overlapping experimental conditions. Unfortunately, the CRI 2 isolate treated with NX-AS-401 failed to sequence properly and the data is unable to identify the correct number of SNPs.

The number of SNP mutations generated varied per *S. aureus* strain with the largest numbers occurring in strains NCTC 12973 and UHW 3 and lowest number occurring in UHW 19. The percentage of the identical SNPs occurring under all three experimental conditions also varies with strains NCTC 13142 and CRI 2 having 37 % identical SNPs in all testing conditions and the highest being UHW 18 which had 74 % identical SNPs under all three testing conditions (NX-AS-401, gentamicin and untreated). The same SNPs (2-3) occurred in NCTC 13142, UHW 3 and UHW 19 for both gentamicin and 14-day passaged cells (**Appendix 1.5**). The same SNPs were also identified in strains NCTC 13142, NCTC 12973 and UHW 3 under the sub-MIC NX-AS-401 and gentamicin experimental conditions.

While some SNPs were found in all three testing conditions and similar ones were identified between gentamicin and 14 days passage or gentamicin and NX-AS-401 treatment, there were no SNPs that occurred in only the NX-AS-401 and 14 day (Number between orange and grey sections) passage treatment groups.

4.4.8 Antibiotic Interactions

NX-AS-401 and antibiotic interactions were monitored via disc diffusion performed on Mueller-Hinton agar with and without a sub-inhibitory (12 µg/ml) NX-AS-401 supplemented into the agar (**Table 4.3**). Interactions were confirmed via antibiotic checkerboards and analysed via FICI calculation and BLISS independence model (**Table 4.4 & 4.5**).

Table 4.3 Zones of inhibition by disc diffusion on NX-AS-401 supplemented and un-supplemented media.

Statistically significant ($p < 0.05$) increases in zones of inhibition are highlighted blue. Statistically significant increases were regarded as combinations with potential synergy between NX-AS-401 and the antibiotics.

Antibiotics	NCTC 13142			NCTC 12973			UHW 3			UHW 8		
	Zone size (mm)		P-VALUE	Zone size (mm)		P-VALUE	Zone size (mm)		P-VALUE	Zone size (mm)		P-VALUE
	Solo	Combination		Solo	Combination		Solo	Combination		Solo	Combination	
Erythromycin	30	30	N/A	21	27	0.03	0	0	N/A	17	36	0.00
Tetracycline	30	32	0.05	28	32	0.02	24	27	0.00	23	32	0.01
Ciprofloxacin	27	31	0.01	25	30	0.01	0	0	N/A	24	31	0.02
Gentamcin	24	27	0.04	20	24	0.00	18	25	0.01	19	27	0.03
Cefoxitin	0	0	N/A	30	30	N/A	0	0	N/A	30	33	0.10
Clindamycin	26	35	0.00	25	29	0.01	0	0	N/A	20	33	0.00
Antibiotics	UHW 15			UHW 18			UHW 19			CRI 2		
	Zone size (mm)		P-VALUE	Zone size (mm)		P-VALUE	Zone size (mm)		P-VALUE	Zone size (mm)		P-VALUE
	Solo	Combination		Solo	Combination		Solo	Combination		Solo	Combination	
Erythromycin	23	24	0.61	25	29	0.00	0	0	N/A	0	0	N/A
Tetracycline	25	30	0.30	26	32	0.24	0	0	N/A	27	32	0.01
Ciprofloxacin	24	33	0.01	25	27	0.47	24	29	0.02	0	0	N/A
Gentamcin	20	23	0.03	20	24	0.01	20	23	0.01	20	25	0.00
Cefoxitin	30	30	N/A	28	35	0.00	30	32	0.24	0	0	N/A
Clindamycin	23	28	0.00	0	0	N/A	23	31	0.00	0	0	N/A

Table 4.4 Interactions between NX-AS-401 and antibiotics in antibiotic checkerboards identified using fractional inhibitory concentration indices (FICI) calculation.

FICI values identify antibiotic interaction based on the calculation provided in section 2.3.10. Synergy is identified based on the calculated value, <0.5 = Synergy, $0.5 - 2.0$ = Indifference and >2.0 = Antagonism ⁽²⁹⁷⁾. The FICI calculation (**Section 2.3.10**) takes single point values from treatments alone and in combination.

Synergy =  Indifference = 

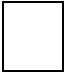



<i>S. aureus</i> Strain	Antibiotic					
	Gentamicin	Clindamycin	Ciprofloxacin	Erythromycin	Tetracycline	Cefoxitin
NCTC 13142	0.3	0.3	0.25	0.27	0.18	0.23^R
NCTC 12973	0.4	0.2	0.24	0.4	0.24	1.25
UHW 3	0.4	0.9 ^R	0.68 ^R	1.02 ^R	0.56	1.02 ^R
UHW 8	0.4	0.7 ^R	0.38	1.51 ⁱ	0.75	1.5
UHW 15	0.2	0.48	0.29	0.25	0.22	1.58 ^R
UHW 18	0.4	0.42	0.30	0.21	0.23	1
UHW 19	0.4	0.45	0.45	0.52 ^R	0.56 ^R	1.01
CRI 2	0.4	0.65 ^R	0.45^R	1.02 ^R	0.21	1 ^R

All strains displayed synergy between NX-AS-401 and gentamicin when used in combination. Strains that were intrinsically resistant to an antibiotic (^R) showed indifference when used in combination therapies. Only NCTC 13142 indicated synergy between cefoxitin and NX-AS-401 despite being resistant to cefoxitin. The remaining seven strains demonstrated indifference regardless of susceptibility to cefoxitin. Strains with intermediate (ⁱ) disc diffusion results displayed no synergy according to the FICI calculation.

Identification of antibiotic interactions were also performed using the Bliss model that defines synergy, indifference or antagonism across the whole antibiotic checkerboard plate, values of 0-2 indicates indifference, 2-5 indicates synergy with a low chance of replicating it *in vivo*, values of 5-9 indicates synergy with a moderate chance of it occurring *in vivo* and values >9 indicates major synergy that will likely be replicated *in vivo* ⁽²⁹⁸⁾

Table 4.5 Interactions between NX-AS-401 and antibiotics in antibiotic checkerboards identified using the Bliss Model.

Strains that are resistant (^R) or demonstrate intermediate susceptibility (ⁱ) remain indifferent during combination therapy. A colour gradient has been used to easily identify the strength of each antibiotic interaction as shown.

Indifference =  Low Synergy =  Moderate Synergy =  High Synergy = 

<i>S. aureus</i> Strain	Antibiotic					
	Gentamicin	Clindamycin	Ciprofloxacin	Erythromycin	Tetracycline	Cefoxitin
NCTC 13142	38.86	2.39	9.97	4.89	5.86	0 ^R
NCTC 12973	16.7	9.76	5.54	10.28	49.1	0
UHW 3	17.93	0 ^R	0 ^R	0 ^R	4.87	0 ^R
UHW 8	13.11	1.47 ^R	3.85	0 ⁱ	7.75	0
UHW 15	13.53	5.25	3.85	13.82	7.75	0 ^R
UHW 18	17.07	3.54	3.83	7.04	6.01	0
UHW 19	14.2	9.87	1.36	1.5 ^R	2.69 ^R	0
CRI 2	13.11	4.77 ^R	0 ^R	0 ^R	5.79	0 ^R

Two strains/antibiotic combinations, CRI 2 with clindamycin and UHW 19 with tetracycline demonstrated synergy despite the presence of a resistance mechanism. Cefoxitin was the only antibiotic to show indifferent antibiotic interactions across all strains according to the Bliss independence model.

4.5 Discussion

The results above are all indicative of NX-AS-401 affecting the growth of eight different *S. aureus* strains. The methodologies employed against planktonic *S. aureus* cells measured changes in growth and viability for both short-term (<12 hours) and longer exposure times that included >20 hours to up to 14 days. Investigations were also performed into the *S. aureus* strains themselves to ensure variety and provide an opportunity to identify the effects of NX-AS-401 against a range of different resistance mechanisms and phenotypes.

4.5.1 Antibiotic susceptibilities of *S. aureus* strains.

All *S. aureus* isolates underwent antibiotic sensitivity testing to identify their respective antibiotic susceptibilities. The antibiotics listed in Section 1.3.2 Table 1.4 (excluding sulphonamides) were used for AST against all eight strains, results are provided in Table 4.1 for both (A) disc diffusion and (B) broth microdilution.

Both antibiotic sensitivity testing methods provided the same susceptibility patterns with all strains except for UHW 8 and UHW 19 (which demonstrated intermediate sensitivity to erythromycin via disc diffusion) deemed sensitive via EUCAST broth microdilution tests. Intermediate results are not uncommon in disc diffusion testing and in the clinic would require repetition of disc diffusion or an additional broth microdilution test to identify if an organism is resistant or sensitive ⁽²⁴⁶⁾. Intermediate results and errors are more likely to occur with disc diffusion as although disc diffusion is the method of choice for clinical laboratories due to its high throughput, issues can arise as the test is more susceptible to error due to inoculum errors, incorrect creation of a lawn plate, misplacement of discs and composition of the agar medium ^(299, 300). In total four of the eight strains, NCTC 12973, UHW 8, UHW 15 and UHW 18 were susceptible to all six antibiotic agents.

Comparisons between the antibiotic susceptibility patterns (**Table 4.1**) and current data from Public Health Wales (PHW) showing spread of resistance to different antibiotics in *S. aureus* isolated from wound swabs between 2008-2017 ⁽¹⁴⁵⁾ which shows a similar spread of resistance in these isolates despite the low number used in

this project when compared to the thousand used in the PHW study. The PHW data states that <2 % were gentamicin resistant while ~6 % were resistant to tetracycline⁽¹⁴⁵⁾. This data is comparable with the isolates used in this study in which none (0 %) were resistant to gentamicin and one strain (UHW 19) is resistant to tetracycline (12 %).

Three (NCTC 13142, UHW 3 and CRI 2) of the eight *S. aureus* strains demonstrated ceftioxin resistance classifying them as MRSA. This indicates that 37.5 % of the strains used in this project were MRSA positive. The small number of *S. aureus* strains used in this project makes comparison to current MRSA epidemiology in wounds difficult as well as how MRSA strains differ between wound types (burns, surgical etc.)^(30, 151). It is currently indicated that MRSA incidence can vary from as low as 7 % in surgical sites to as high as 60 % in burn wounds⁽¹⁵¹⁾. The recent PHW data did not provide the percentage of MRSA isolated from wounds, therefore data from Public Health England was used for comparison and identified that the percentage of MRSA isolates from wounds has risen to 35.7 % in 2019⁽³⁰¹⁾. This indicates that the percentage of MRSA used in this study (37.5 %) is representative of the MRSA numbers isolated from wounds in NHS England (35.7 %).

Strains UHW 3 and CRI 2 demonstrated the same susceptibility patterns with resistance to ciprofloxacin, clindamycin, erythromycin and ceftioxin. Ciprofloxacin resistance has been identified in 40 % of MSSA isolates and 80 % of MRSA isolates, in this study two of the eight strains (25 %) demonstrated ciprofloxacin resistance, a lower presence than found from wound isolates in the UK according to PHE⁽¹⁴³⁾. However, both of the strains UHW 3 and CRI 2 are ceftioxin resistant indicating that of the three MRSA strains used throughout this project 66.6 % were resistant to ciprofloxacin which is closer to the current epidemiology of ciprofloxacin resistance in *S. aureus*⁽¹⁴³⁾.

The percentage of resistance to clindamycin and erythromycin (25 %) is also consistent with epidemiology studies, showing erythromycin resistance in *S. aureus* isolated from wounds between 16-18 %⁽¹⁴⁵⁾. Meanwhile clindamycin resistance in wound isolates has been identified in ~28.2 % of wound isolates⁽³⁰²⁾.

Clindamycin resistance can be difficult to identify as it is often an inducible resistance that is often only detected via disc diffusion testing ⁽³⁰³⁾. Inducible resistances occur via a shared resistance mechanism for two antibiotic classes. Clindamycin-induced resistance is confirmed by exposure to both clindamycin and erythromycin which results in the expression of the *ermC* resistance gene a ribosomal methylase that changes the 50S subunit binding site shared by both macrolides and lincosamides ⁽³⁰⁴⁾. These inducible resistances are detected through a method known as the D phenomenon (**Figure 4.9**).

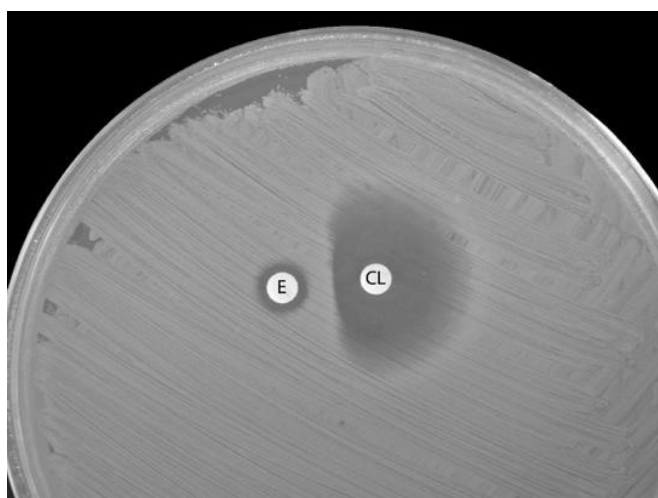


Figure 4.9 Image from Levin *et al*, 2005 shows a disc diffusion D phenomenon ⁽³⁰⁴⁾.

The D phenomenon occurs during disc diffusion on the side of the clindamycin disc closest to the erythromycin disc. The bacteria closest to erythromycin could grow closer to the clindamycin disc due to the induced resistance thus changing disc diffusion test results.

Detection of this is vital for successful clinical therapy with clindamycin. While the antibiotic resistance seems transient and detection can only occur via exposure to both agents, mutations can occur in the *ermC* promoter changing the resistance from inducible to constantly present ⁽³⁰⁴⁾. Since NX-AS-401 is a potential novel antibiotic it is unknown whether current resistance mechanisms can decrease its efficacy and whether these resistance mechanisms need to be induced by exposure to a secondary antibiotic in combination treatment. Antibiotic interactions in Sections 4.4.7 and 4.4.8 identified whether any of the identified resistance mechanisms could be induced to reduce NX-AS-401 efficacy.

Characterisation of the *S. aureus* strains indicated that the range of isolates used throughout this project had varying antibiotic susceptibility profiles that represented the levels of resistance seen in clinical isolates throughout the UK. Identification of antibiotic susceptibility patterns also allowed for appropriate antibiotic controls to be selected throughout the project and assisted in identifying concentration necessary for antibiotic interaction studies.

4.5.2 NX-AS-401 effects on *S. aureus* growth

Figure 4.2 shows that even though the bacterial strains possess different antibiotic sensitivity patterns, NX-AS-401 affects the growth of all *S. aureus* strains at concentrations ≥ 4 $\mu\text{g/ml}$. As seen with NBR 26-6A (**Chapter 3, Figure 3.1**) sub-MIC (<128 $\mu\text{g/ml}$) doses of both NBR 26-6A and NX-AS-401 were able to decrease *S. aureus* growth in relation to the positive control. Growth inhibition was dose dependent with concentrations of 128 $\mu\text{g/ml}$ inhibiting growth $\geq 90\%$ in all strains. Only strains UHW 8 and UHW 15 were more susceptible to the effects of NX-AS-401 with an MIC of 64 $\mu\text{g/ml}$. Overall this data shows that ajoene content does not alter the antimicrobial effects of NX-AS-401 as both formulations have the same MIC of 128 $\mu\text{g/ml}$.

Time/kill curves generated from TVC counts were used to identify the effects of different NX-AS-401 concentrations over time and where in the *S. aureus* growth cycle NX-AS-401 elicited an effect. Figure 4.3 showed that *S. aureus* growth was inhibited at concentration of 64 and 128 $\mu\text{g/ml}$ in all strains apart from NCTC 13142. Discrepancies between the MIC seen in broth microdilution and identified via TVC counts may be caused by the increased volume of the experiment with the increased inoculum size, 50 ml in TVCs as opposed to 200 μl in broth microdilution. Increases in starting inoculum can affect experiment outcomes due to the inoculum effect as discussed in Chapter 3, Section 3.5.1. However, unlike the NBR 26-6A formulation, NX-AS-401 did not precipitate out of MHB. Therefore, it did not affect the turbidity of the samples and allowed for more accurate absorbance readings. In comparison to formulation NBR26-6A the results are very similar with growth inhibited at concentrations of 128 $\mu\text{g/ml}$ and lower, since NX-AS-401 could be utilised at higher concentrations than NBR 26-6A the cell eradication that occurs at high concentrations occurred 4-6 hours after

exposure when treated with 2048 µg/ml as opposed to requiring >24 hours for an NBR 26-6A concentration of 512 µg/ml.

The change in colony size shown in Figure 4.4 is likely due to antibiotic/environmental pressure caused by the presence of NX-AS-401 forcing a phenotypic change in the bacterial cells ^(106, 291). This selective pressure has been seen with other antibiotics when used at intermediate levels ^(305, 306). For example a study by Lee *et al* ⁽³⁰⁵⁾ shows that increasing sub-inhibitory antibiotic concentration causes a decrease in colony size.

This could also be caused by phase variation which involves a sudden change in gene expression ^(307, 308). Phase variation is often seen in bacteria in response to new environments and new threats ^(307, 308). There have been many examples in *S. aureus*, where regulatory genes such as *ica* and *agr* have demonstrated increased gene expression after changes in environments ^{(308) (309)}. Both phase variation and decrease in colony size may also be due to carryover of residual NX-AS-401 into the inoculum, resulting in a change of expression in genes that restrict growth size or NX-AS-401 mediated restriction of growth.

This has been observed previously in *S. aureus* where small colonies occur after the bacteria are replaced under a selective pressure by an antibiotic ⁽³⁰⁶⁾. The development of *S. aureus* from its regular phenotype to a smaller more persistent colony is an adaptation to environmental stress and an effort to protect itself from any hostile environmental factors such as antibiotics, changes in pH or reactive oxygen species ⁽³⁰⁶⁾. However, the development of smaller colonies and whether it is a potential permanent adaptation is debated as different *S. aureus* strains have different responses to the same environmental pressure ⁽³¹⁰⁾. Different environmental pressures can also cause their own unique response such as: reduction of *S. aureus* metabolism, arrested cell division to prevent internalisation of an antibiotic ^(291, 310). However environmental pressure can also decrease cell size but increase metabolism causing increased production of extracellular components such as matrix and enzymes that can protect *S. aureus* from the hostile environment ⁽³⁰⁶⁾. These small colonies are often responsible for the persistence of infection in chronic wounds, sub-effective antibiotic concentration can cause small colony development either through genetic mutations or due to limiting the expression of genes linked to the electron transport chain and in *S. aureus* genetic regulators such as *agr*, *sarA* and *sigB* ⁽³¹⁰⁾. These changes alter the membrane of the

colonies making them less permeable to antibiotics and other harmful components such as hydrogen peroxide ⁽³¹⁰⁾.

However, as with antibiotic treated *S. aureus* the smaller colonies seen after treatment with NX-AS-401 were not a permanent change in the *S. aureus* phenotype. Increased incubation to 40 hours or sub-culture of the colonies onto antibiotic free media caused the colonies to revert to the same size as the control / untreated cells. Without knowledge of the effects of antibiotic pressure results like this could indicate that sub-MICs of an antibiotic causes an increase in the number of colony forming unit (CFU) as more are present despite being smaller. However, the opposite is more likely as the colonies diminished size indicates that there are fewer cells within them. This would require enumeration of the bacteria in both the smaller and larger CFU ⁽³¹¹⁾ but currently no studies have enumerated the cells within colonies on agar plates and CFU counts are the standard method to enumerate bacteria.

Clinically these results could indicate that an antibiotic is not effective and that the bacteria persist and even grow further under the selected antibiotic therapy ⁽²²⁾. This may not be applicable directly to topical wounds such as burns or abrasions where tests based on presence/absence of known pathogenic bacteria are needed ⁽³¹²⁾. However, it would be important in tests where infection is based on a CFU count, for example surgical wounds that involve sterile sites of the human body such as bones and joints where the bone and synovial fluid itself is usually free of bacteria ⁽²⁾.

Figure 4.5 shows the results of *S. aureus* growth curves, these were performed by incubating the EUCAST broth-microdilution plates in a spectrophotometer for 24 hours. EUCAST broth microdilution methods require end-point absorbance readings at 18-20 hours after exposure to antibiotics. In the growth curves this exposure was extended to 24 hours to identify if any effect occurred after the standard EUCAST treatment times.

However, the extension of the incubation period does not explain the difference seen in strains UHW 8 (D), UHW 15 (E) and UHW 18 (F) that match neither the EUCAST broth microdilution nor the TVC counts in Figure 4.3. In these three strains NX-AS-401 concentrations of 64-256 µg/ml only inhibited growth by 50 % as opposed to the ≥90 % seen in EUCAST broth microdilution and TVC counts. This could possibly be caused by

changes in growth conditions as incubation in the spectrophotometer has a different environment than an incubator and the use of a plate seal instead of incubating with the manufacturer's lid may also cause changes in growth patterns due to changes in atmosphere⁽³¹³⁾. Differences between these results could also be due to the method of measurement. While NX-AS-401 does not precipitate like NBR 26-6A, its presence likely causes an environmental pressure on *S. aureus* cells increasing the production of secreted material⁽²⁹⁰⁾ as previously discussed in Chapter 3 (**Section 3.5.1**)⁽²⁹¹⁾. These effects may be more pronounced in strains UHW 8, UHW 15 and UHW 18 especially under different growth conditions, therefore increasing turbidity and absorbance readings. While turbidity is used to measure bacterial growth, an increase in cell number is not the only reason for increased turbidity. The production of extracellular proteins, polysaccharide and dead cell debris can also increase turbidity and absorbance values. This could explain why only growth curves show this pattern while MIC and TVC tests that were grown under similar environment conditions and demonstrated that NX-AS-401 inhibited the growth of UHW 8, UHW 15 and UHW 18 at NX-AS-401 concentrations $\geq 128 \mu\text{g/ml}$.

Despite variability between the three methods NX-AS-401 does inhibit growth of *S. aureus in vitro*. The MIC for *S. aureus* has been defined as $\geq 128 \mu\text{g/ml}$ as seen in most strains across all three methods. Since NX-AS-401 demonstrates the same MIC as NBR 26-6A it suggests that the difference in the percentage of ajoene in these two formulations has little impact on the effects of these two compounds to inhibit *S. aureus* growth and some of its activity may be caused by the unknown components of NX-AS-401. The antibacterial effects of ajoene may also be enhanced by other garlic components as suggested by Jakobsen *et al*⁽¹⁹⁴⁾ and this may also explain the more pronounced activity seen in garlic preparations such as oils and aqueous extract that contain yet unidentified molecules⁽²¹⁰⁾.

This established MIC $>128 \mu\text{g/ml}$ is higher than the previously mentioned studies where the ajoene MICs were identified as $16 \mu\text{g/ml}$ by Naganawa *et al*⁽²¹⁷⁾ and a bacteriostatic effect was seen at concentrations $> 5 \mu\text{g/ml}$ by Jakobsen *et al*^(194, 241). As discussed in Chapter 3 (**Section 3.5.1**) the MIC values are high in comparison to current standard of care antibiotic such as gentamicin and ciprofloxacin where their MIC values are $1 \mu\text{g/ml}$ according to EUCAST clinical breakpoint version 9.0⁽²⁴⁷⁾. While EUCAST no

longer provide clinical breakpoints for sulphonamide antibiotics alone, the common trimethoprim/sulphamethoxazole is 2 µg/ml indicating that NX-AS-401 is not as active as the structurally similar sulphonamide class on antibiotics. EUCAST clinical breakpoints are not solely based on the concentrations that kills bacteria but also consider the antibiotic concentrations that are toxic to the host. Therefore a bacterium may be susceptible to antibiotic at a concentration greater than the clinical breakpoint, however these concentrations may be difficult or impossible to achieve in a host without causing adverse effects ⁽²⁹⁶⁾. Therefore, further investigation into the potential toxic effects of NX-AS-401 could identify whether the NX-AS-401 MIC is achievable *in vivo*. Since the MIC for NX-AS-401 is relatively high a potential application for NX-AS-401 would also be a topical agent for wounds, in these formulations antibiotics not suitable for systemic use or that require higher concentrations can be used, for example mupirocin which is used in effective topical ointments at 20mg/g but if given systemically is immediately broken down into monic acid ⁽³¹⁴⁾.

This MIC is also high when molar mass is considered as ajoene has a mass of 234.4 g/mol while other drugs such as tetracycline and gentamicin are only slightly bigger at 444.4 g/mol and 477.6 respectively ⁽³¹⁵⁾.

The growth of *S. aureus* was inhibited at similar NX-AS-401 concentrations >128 µg/ml across all strains regardless of resistance mechanisms. This indicates a consistent mechanism of action that is effective across multiple strains that is not impeded by any of the identified resistance mechanisms. However, the strain variable reaction of *S. aureus* to NX-AS-401 in regard to biofilm formation, virulence and gene expression indicate that there may be multiple targets or alternate pathways that can limit the secondary effects of NX-AS-401.

Although these concentrations were higher than anticipated, NX-AS-401 was being considered as a potential topical therapy for chronic infections associated with wounds. In this instance, higher concentrations may be achievable as topical application however, more research into its toxic effects are required, due to the variability seen between HaCaT cells and *G. mellonella* (**Chapter 6**). High concentrations may also not be necessary if used in combination with other antibiotics, considering the synergistic effects of NX-AS-401 (**Section 4.5.5**).

Figures 4.2, 4.3 and 4.5 and also show that NX-AS-401 elicits a bactericidal effect at concentration of 2048 µg/ml after 18-20 hours. This value is 16 times the MIC and identifies NX-AS-401 as a bacteriostatic drug against *S. aureus* ⁽²⁸³⁾. While bacteriostatic drugs do not directly kill bacteria, they inhibit growth allowing for eradication by host immune phagocytes. This can help protect host microflora and prevent secondary infection ⁽¹²⁰⁾.

To understand the effects of NX-AS-401 on *S. aureus* also requires identifying whether intrinsic mechanisms such as efflux pumps or the known resistance mechanism can increase tolerance to NX-AS-401 increasing the MIC beyond what has been established. It is also necessary to identify whether *S. aureus* can develop or already contains a resistance mechanism that can completely nullify its action making the *S. aureus* resistant to its effects.

4.5.3 NX-AS-401 Tolerance and Resistance

Emerging antimicrobial resistance has not only caused a necessity to develop new antibiotics, but it is also the biggest threat to developing new antibiotics. Resistance can be obtained intrinsically through changes in genetic locations, such as single nucleotide polymorphism (SNP) in gene loci or by the acquisition of genetic material through horizontal gene transfer conjugation, DNA transformation and phage transduction ⁽²⁹⁶⁾. Tolerance is the ability of the bacterial cell to survive in the presence of an antibiotic without a specified resistance mechanism, this may be through reducing metabolic activity or through the secretion of a matrix that prevents antibiotics from reaching the cell ⁽³¹⁶⁾.

To identify any increase in tolerance to NX-AS-401 or the development of a resistance mechanism, *S. aureus* cells were subject to repeated exposure to sub-MIC NX-AS-401. This experiment was designed to see if cells adapted in the presence of higher concentrations of NX-AS-401 and used to current clinical best practice guidelines that recommend antibiotic treatment for a maximum of 14 days before switching to a new antibiotic ⁽⁸⁾.

Therefore *S. aureus* were exposed to NX-AS-401 or gentamicin for 14 days to mimic current clinical wound care guidelines for topical antibiotics ⁽⁸⁾. Infections that do not respond to the current antibiotic after 14 days are treated with a different antibiotic class. These guidelines allow for treatment of undetected secondary pathogens and are employed to prevent the spread of AMR ⁽⁸⁾.

EUCAST guidelines⁽²⁴⁸⁾ allow for a two-fold difference in the MIC obtained, due to errors that can occur in that methodology, such as inoculum preparation and pipetting errors ⁽²⁸³⁾. The blue dotted lines on Figure 4.6 indicate the two-fold increase in MIC, any points above that line are considered outside the acceptable margin of error and indicate that an organism becoming more tolerant/resistant to the antibiotic.

Figure 4.6 shows that *S. aureus* demonstrated no significant ($p < 0.05$) increase in tolerance to NX-AS-401, the maximum MIC was 512 $\mu\text{g/ml}$ seen on day eight for strains UHW 18 (F), UHW 19 (G) and CRI 2 (H). However, tolerance to gentamicin increased rapidly with the MIC rising from 1 $\mu\text{g/ml}$ to 16 or 32 $\mu\text{g/ml}$ by day eight for all strains. This is above the accepted EUCAST margin of error and demonstrates a significant increase in antibiotic tolerance. While tolerance to gentamicin reaches its maximum after eight days, the increase was transient and unstable as the MIC dropped to 8 and 16 $\mu\text{g/ml}$ for all strains by day 12 though this was still above the two-fold threshold. An unexpected result occurred with UHW 19 (F) on day 12 as the strain failed to grow in all wells containing gentamicin and only survived in antibiotic free media.

This could be due to the strain sacrificing viability for a temporary antibacterial resistance as seen with other bacteria such as vancomycin Intermediate *Staphylococcus aureus* (VISA) ^(154, 155, 291). In VISA, the bacterial cells viability is sacrificed for a transient resistance to vancomycin, cell metabolism is often reduced, and cell division decreased to prevent the action of vancomycin against the cells. This puts them in a viable but non-culturable state to protect them ^(108, 155, 317). Although effective against one agent this can leave the bacteria more susceptible to additional antibiotics and host immunity ⁽¹⁵⁵⁾.

In UHW 19 exchange of viability for gentamicin tolerance was seen until day 10, tolerance decreased at day 11 and cells were eradicated by day 12. This exchange may

have led to an increase in susceptibility that caused eradication of all UHW 19 cells even at low gentamicin concentration in strain UHW 19.

Increases in gentamicin tolerance could also be caused by antibiotic pressure resulting in a stress response slowing cell division and metabolism, thus causing increased bacterial tolerance^(108, 291, 316) or through point mutations in the target genes reducing the action of an antibiotic but not completely disabling its effect⁽³¹⁶⁾. An additional explanation could also be the presence of a heterogenous resistance gene⁽²⁶⁾. However, gene sequencing did not identify any aminoglycoside resistance genes in any of the isolates. Heterogenous resistance in VRSA strains suggests only a small portion of the population carry one copy of the *vanA* gene that confers vancomycin resistance that is only expressed in the presence of vancomycin⁽¹⁵⁴⁾, similar to the aforementioned *ermC* gene that confers resistance once cells have been exposed to erythromycin⁽³⁰³⁾. The presence of hetero-resistance can be responsible for antibiotic treatment failure *in vivo* where *in vitro* tests have shown susceptibility⁽²⁶⁾. However, clinical diagnosis of heterogenous resistance is difficult as it requires labour intensive population analysis profiling performed on agar microdilution⁽²⁶⁾. This method requires the creation of multiple agar plates containing different antibiotic concentrations and is too time consuming/labour intensive for most clinical laboratories⁽³¹⁸⁾. During gene sequencing no gentamicin resistance gene was identified in any of the *S. aureus* strains (**Section 4.4.1**) and no SNP was identified in all eight strains that included the 30S ribosomal subunit that gentamicin targets, this indicates that the increased tolerance to gentamicin was due to environmental pressure changing the *S. aureus* metabolism. These effects require further investigation through the use of metabolic assays to monitor cell metabolism after gentamicin exposure, the use of technology such as mass spectroscopy may also identify whether the non-specific bacterial efflux pumps such as the Multidrug and Toxic Compound Extrusion (MATE)⁽¹⁶⁵⁾ group become more active when *S. aureus* is exposed to sub-inhibitory antibiotic concentrations and thus increased tolerance by removing the antibiotic before it could take effect.

Day 15 began a “wash-out” period where *S. aureus* cells were grown in antibiotic free media and then subjected to MIC testing a day later. This was repeated daily with a new inoculum created from the previous culture grown in antibiotic free media. Figure

4.6 shows that all strains returned to the original or starting MIC after 1 day in antibiotic/MIC free MHB, indicating no permanent increase in antibiotic tolerance and no generation of spontaneous resistance mechanisms against both gentamicin and NX-AS-401. This also fits with what other studies have shown that sub-inhibitory antibiotic concentrations elicit an environmental pressure reducing *S. aureus* growth and metabolism without killing the cells or causing the development of antibiotic resistance ^(154, 191, 317). However, the development of antibiotic resistance based on antibiotic pressure varies as some bacteria have developed a resistance over time ⁽³¹⁹⁾, as seen with *E. coli* which has shown it can become resistant to ciprofloxacin as repeated exposure to sub-inhibitory concentrations causes homologous recombination of DNA conferring resistance ⁽³¹⁹⁾. In some cases sub-inhibitory antibiotic concentrations may not cause the spontaneous generation of resistance mechanisms but can exacerbate horizontal gene transfer of antibiotic resistance genes from resistant bacteria to susceptible bacteria ^(142, 191).

The implications of the result seen here are that *S. aureus* cells find it difficult to increase their tolerance to NX-AS-401 within a clinically relevant timeframe and as far as it is known NX-AS-401 resistance has not yet been found in nature. This may be due to the presence of non-ajoene components within NX-AS-401 as resistance to combinations and mixtures are not often seen, hence the effectiveness of combination therapies *in vivo* ^(111, 230, 244).

However, to confirm this AST testing and genetic analysis with more bacterial strains encompassing many resistance mechanisms would be required.

In comparison to NX-AS-401 other sulphur based antibiotics, the sulphonamides are a broad spectrum antibiotic, that have demonstrated activity against a variety of bacteria by inhibiting folic acid synthesis, a precursor to nucleic acid synthesis ⁽¹³⁴⁾. Sulphonamide drugs are completely synthetic with potentially 1000s of permutations of sulphonamides available ⁽¹⁸²⁾. However, since they were developed early in the 1930s resistance to them has become common ⁽¹⁸²⁾ due to mutation in the gene encoding for dihydropteroate synthase (DHPS) a precursor to folic acid synthesis making sulphonamides ineffective on its target site ⁽¹⁶¹⁾.

Prevalent resistance is one of the reasons sulphonamide based antibiotics are not commonly prescribed in modern healthcare practices ⁽¹⁸²⁾. However, there are also problems with side effects as a high portion of the population experiencing adverse effects when treated with sulphonamide based drugs ⁽¹³³⁾. The side effects for sulphonamide drugs have varied from lesser adverse reactions such as rashes, itching and nausea to severe reactions such as liver damage and pulmonary disorders ⁽¹³³⁾. These are thought to be caused by the metabolites of sulphonamide drugs that include, hydroxylamine and nitroso sulfamethoxazole ⁽¹³³⁾.

Sulphonamide resistance mechanisms were not identified in any of the eight *S. aureus* strains via gene sequencing, with no SNPs forming in folate synthesis pathways and no resistance genes identified via CARD or Resfinder indicating that all eight strains were susceptible to sulphonamides. The most commonly identified resistance mechanism is called *folP* and causes a change in the dihydropteroate synthase protein conferring sulphonamide resistance ⁽²⁶²⁾. In future studies sulphonamide resistant *S. aureus* strains should be used to determine if resistance mechanisms such as *folP* also prevent the activity of NX-AS-401.

In other garlic derived compounds such as allicin, it has been shown that susceptibility varies, especially in Gram-positive where MDR strains without sulphonamide resistance have a much higher MIC than their more susceptible counterparts ⁽²¹⁴⁾. This may be due to the activity of a known resistance mechanism of allicin, or it could be the presence of an unknown resistance mechanism that acts against allicin and has the potential to act on ajoene and any potential unidentified molecules in NX-AS-401. Wound infections are often polymicrobial in nature containing a mixture of Gram-negative and Gram-positive organisms ⁽²²⁾. The bacteria present can originate from both the host skin microflora and from the source of the wound such as dog bites causing *Pasteurella* species and punctures from rusted tools causing *Clostridium* species infections ⁽³²⁰⁾. Due to the polymicrobial nature found in both acute and chronic wounds further studies would require identifying the effects of NX-AS-401 on both Gram positive and Gram-negative organisms, currently there have been more studies into the effects of NX-AS-401 and ajoene on *P. aeruginosa*, however these indicate that while NX-AS-401 can prevent and disrupt *P. aeruginosa* biofilms it does not directly eradicate or cause inhibition of its growth ^(179, 194).

In future studies experiments would require the use of polymicrobial cultures or at least extended to include different bacteria commonly associated with wounds and a mix of both Gram-positive, Gram-negatives and fungi such as *Candida* species. These studies could determine whether a resistance mechanism to NX-AS-401 is already present in nature and whether NX-AS-401 exposure can cause resistance through spontaneous mutation in different bacteria species. These investigations may also identify whether NX-AS-401 exposure can increase dissemination of resistance mechanisms between bacterial strains and species.

4.5.4 Gene Sequencing and analysis.

Full information of sequenced isolates and assemble can be found in appendix 1.6. Only 1 isolate demonstrated poor sequencing with CRI 2 NX-AS-401 showing a full genome length of 64137, much lower than the >250000 genome length of the other sequenced isolates. Genome coverage appears to be in line with other *S. aureus* isolate as reference genome *S. aureus* 8325 has a known genome length of 2821361.

The phylogenetic tree identified that the seven of the eight isolates remained similar to the control strains after resistance evolution experiments. The genome for reference isolate *S. aureus* 8325 was also included to ensure that all strains were *S. aureus* and similarly related despite coming from different sources (**Figure 4.7**). In creation of the phylogenetic tree local bootstrapping values appeared >0.99 for most isolates. Bootstrapping use the established sequence data to create fictional data and reform the tree multiple times, each time placing the isolate on the node according to the artificially created data set. The more consistently the isolate is placed in the same node on the phylogenetic tree the higher the bootstrapping score to a value of 1. Therefore, scores of >0.99 indicate high bootstrapping support and high likelihood that the isolate it where it belongs.

Unfortunately, isolated CRI 2 NX-AS-401 did not sequence correctly (**Appendix 1.6**), resulting in an incorrect assembly a low total genome of 64137. This in combination with apparent contamination or mislabelling of isolate CRI 2 Gentamicin to spread throughout the phylogenetic tree (**Figure 4.7**) rather than form one node. The cause of poor sequencing is unknown but likely causes are contamination or mis-labelling

caused after the resistance training experiment. The problems with sequencing directly result in the poor bootstrapping value of 0.414 given to isolate CRI 2 NX-AS-401.

Three other isolates also demonstrated lower bootstrapping values despite having genome sizes and N50 values comparable to other isolates (**Appendix 1.6**), including NCTC 12973 and UHW 18, according to Hillis and Bull values lower than 0.7 could be considered poor bootstrapping support ⁽³²¹⁾. Despite having low boot strap values (0.628 and 0.668) these genomes have also grouped with the control isolate and other experimental genomes indicating they are in the correct place, in future repeated sequencing would be performed to ensure the isolates are in the correct node on the phylogenetic tree.

The isolates also appear clustered based on their antibiotic susceptibilities, with NCTC 13142 and UHW 3 clustered together and carrying the *mecA* cassette. NCTC 12973, UHW 15, UHW 18 and UHW 19 remained closely linked and contain one or both of the *fosB* or *blaZ* resistance genes. UHW 8 which was identified as the most genetically divergent strain, carries the resistance genes *glpT* and *murA* that were not identified in any other strain.

In comparison to the AST (**Section 4.4.1 and 4.5.1**) the resistance mechanisms identified via sequencing match with the phenotypic resistance seen in EUCAST disc diffusion and broth microdilution. There were additional resistance mechanisms identified against antibiotics that were not used throughout this study such as *glpT*, *murA* and *fosB* that confer resistance to fosfomycin as describe in Table 4.2 A ⁽²⁶²⁾.

In the resistance training experiment, gentamicin tolerance was increased in all strains, genetic analysis has shown that this was not caused by the presence of a heterogenous resistance mechanism. However, CARD analysis of the genome did identify the presence of intrinsic *S. aureus* efflux pumps that may have an effect on gentamicin tolerance and potentially NX-AS-401 such as *mepR*, *ImrS* and *norA* which was accompanied by promoters *arlS* and *arlR* and regulator *mgrA* ⁽²⁶²⁾.

The *mepR* gene is part of the multidrug and toxin extrusion (MATE) complex that codes for the efflux pump *mepA*. The pump does not specifically target antibiotics but does remove toxic components from inside the cell ⁽¹⁶⁵⁾. The function of *mepR* is to reduce

the expression of itself and only increase *mepA* when augmented with a specific substrate caused by exposure to toxic compounds and antibiotics ⁽¹⁶⁵⁾. The *mepR* gene is often found in the genome of *S. aureus* isolates but the other components of the MATE complex, *mepA* and *mepB* were not found in any of the eight isolates indicating its lack of action. In these isolates *mepR* was identified indicating there was no efflux pump to activate ⁽¹⁶⁵⁾.

The *lmrS* gene codes for a multi-drug efflux pump that is linked with *S. aureus* resistance to lincomycin and linezolid ^(262, 322). It has been shown to be a causative agent for multi-drug resistance (MDR) in Gram-positives if the gene has been acquired from *S. aureus* ⁽³²²⁾. It has also been shown to provide resistance to trimethoprim, chloramphenicol and sodium dodecyl sulphate (SDS) in *S. aureus* ⁽³²²⁾. SDS is often used in cleaning and hygiene products but its activity is greatly reduced by the presence of *lmrS*, the activity of *lmrS* on a product containing a sulphate bond may indicate that *lmrS* has activity on the components of NX-AS-401. Whether this was seen in this study cannot be confirmed as *lmrS* was identified in all strains. In the future, the development of a *lmrS* mutant would be utilised to identify whether the presence of *lmrS* has an effect on NX-AS-401 and if its absence increases the susceptibility of *S. aureus* to NX-AS-401.

The multi-drug efflux pump *norA* was identified in all eight of the *S. aureus* isolates, this was not unusual as it has been shown to be part of the *S. aureus* core genome ⁽³²³⁾. The *norA* efflux pump is known to cause fluoroquinolone resistance when expression is increased, while basal expression increases tolerance to drugs such as ciprofloxacin it does not cause antibiotic therapy failure ⁽¹⁶⁴⁾. The expression of *norA* is controlled by a two-component regulatory system containing *arIS* and *arIR* and *norA* expression is reduced in strains that are missing or have a mutation in the *arIS* component ⁽³²⁴⁾. In four (UHW 3, UHW 8 UHW 15 and CRI 2) of the eight isolates utilized in this study the *arIS* promoter was not identified indicating that *norA* expression could not be increased and cause fluoroquinolone resistance. However, in the remaining 50 % of the isolates all parts of the *norA* complex were present but fluoroquinolone resistance was not detected phenotypically. While *norA* has been studied extensively ^(164, 323-325) few of the disparities between its presence in the genome and its appearance phenotypically have been determined.

The lack of promoter regions is one explanation for the lack of function of *norA*, there are also mutations that prevent *norA* from being assembled correctly and there are various *norA* alleles with some showing stronger activity than others ⁽³²³⁾. Another explanation are changes in the global regulator *mgrA* that was also identified in all eight *S. aureus* isolates. Usually global regulator *mgrA* that controls expression of *norA*, however, in the presence of another global regulator *sigB* it can lose the ability to promote *norA* expression ⁽³²⁵⁾. Therefore, while *norA* is part of the core genome it appears that its expression is not as ubiquitous. Further genetic and transcriptomic studies may determine why strains NCTC 13142, NCTC 12973, UHW 18 and UHW 19 contain *norA* and the relevant promoters and regulators but do not demonstrate fluoroquinolone resistance. However, it is likely due to incorrect assembly or that the pump is not present in high enough numbers to bestow fluoroquinolone resistance to *S. aureus* ^(323, 324).

These three potential resistance mechanisms/genes were unknown prior to genetic analysis since they did not appear in the phenotype, either due to lack of the target antibiotic or due to lack of expression. However, their presence in all eight *S. aureus* strains demonstrates how ubiquitous they are and whether they affect NX-AS-401 performance is unknown. Future experiment with NX-AS-401 should use *S. aureus* wild-types and knock-out mutants without *mepR*, *lmrS* and *norA* to determine if these efflux pumps act on NX-AS-401.

In isolates UHW 3 and CRI 2 single point mutations in genes *parC*, *parE* (UHW 3 only) and *gyrA* were detected under all experimental conditions. These point mutations confer fluoroquinolone resistance and were only found by analysis of the sequences using CARD database, that highlighted the responsible single point mutations and not only presence of the gene.

The identified resistance mechanisms (**Table 4.2 B**) for specific antibiotic classes were different for each *S. aureus* isolate used in this study. As shown in Table 4.2 resistance mechanisms mostly remained consistent between control isolates and those repeatedly exposed to sub-inhibitory NX-AS-401, gentamicin or those that underwent 14-day passage in antibiotic free media.

The *tet(38)* gene found in NCTC 12973 was also not present in another *S. aureus* strain. The most likely explanations for the acquisition/presence of *blaZ* in NCTC 13142 and UHW 3 is the presence of a sub-population within the original culture that carries the *blaZ* gene. This sub-population then thrived under the antibiotic pressure of NX-AS-401 or gentamicin and general passage ⁽²⁶⁾. Although some resistance mechanisms such as vancomycin resistance come with bacterial fitness costs none have been attributed to *blaZ* ⁽¹⁵⁴⁾. The increased presence of resistant sub-populations has also been well documented after treatment with antibiotics or passage ^(26, 144, 154). The presence of a sub-population may have also been present in all isolates but was not gathered or present in high enough numbers for identification in the sweeps of bacteria taken for DNA extraction, this may also occur if the bacteria contain a heterogenous resistance mechanism.

The acquisition of *tet(38)* is likely to have caused misidentification via CARD as *S. aureus* does contain a transmembrane transporter “SA0132” that has a similar genetic code to *tet(38)* this may also explain why it was not identified in Resfinder ⁽²⁶²⁾.

CRI 2 is the potentially contaminated isolate that clustered with the other UHW 19 isolates. This explains the “acquisition” of *fosB* since UHW 19 does contain that resistance element. This is most likely the only isolate that may have been subject to contamination during the experiment or subsequent sequencing. Comparison of CRI 2 gentamicin isolate to the UHW 19 control via Snippy could not be performed as the isolates were different, whereas comparison of the CRI 2 isolate to the CRI 2 control identified 16 SNPs. This indicates that while *fosB* was present, other parts of the UHW 19 genome was not indicating a low level contamination. This infers that the acquisition of the *fosB* gene was likely due to contamination via mobile genetic element that confers *fosB* resistance. This could not be confirmed in the phenotype as fosfomycin was not tested, however in future this should be confirmed.

In summary the inconsistent presence of these resistance elements across isolates and their lack of presence in the phenotype may also be explained by the presence of heterogenous resistance genes, or problems with sequencing, assembly, or alignment. The outcomes of this analysis could have been improved through repeated sequencing of the control isolates to ensure that the genomes were assembled correctly.

Though few resistance genes were acquired, there were no consistent antibiotic resistance conferring mutations identified across experimental conditions indicating that repeated NX-AS-401 and gentamicin exposure did not cause the mutation of a specific resistance gene. However, it has been shown that resistance genes can develop in response to antibiotics, for example in *Salmonella* species exposure to sub-MIC streptomycin caused the evolution of novel high-level resistance mechanisms due to mutations in the antibiotics target site ⁽³²⁶⁾. This is often based on the mutability of the genomic DNA and may be caused by either mutations such as SNPs that cause a change in target proteins, or due to epigenetic factors such as DNA methylation ⁽³²⁷⁾.

To identify if the exposure to sub-inhibitory NX-AS-401 and gentamicin is responsible for specific genetic mutations an analysis of the single nucleotide polymorphisms (SNPs) that occurred in each isolate was performed (**Figure 4.8**), the Venn diagrams compare the number of SNPs that have occurred in each condition as well as how many are repeated in all three conditions and those that have only occurred in two conditions.

As shown in Figure 4.8 SNPs that occurred under all three environmental conditions occurred between 37-75 % of the isolates overall. This indicates that the treatment was unlikely to be responsible for the formation of SNPs and that the SNPs have likely occurred in areas highly mutable parts of the genome where SNPs are not uncommon ⁽³²⁸⁾. This is also identified in the median and average number of SNPs per isolate identify as no treatment option increased or decreased the number of SNPs.

Certain isolates such as NCTC 12973 and UHW 3 seemed more prone to mutation with total SNP number of 119 in both while, CRI 2 seemed more genetically stable with a total of 40. The number of SNPs that can occur in the genome over a year, can be referred to as the rate of diversification. The study by Benoit *et al*, 2018 determined that the rate of diversification of *S. aureus* can vary wildly between strain ⁽³²⁹⁾.

Treatment with sub-MIC NX-AS-401 or gentamicin did not cause a SNP in the same gene in all eight *S. aureus* strains. This indicates that NX-AS-401 and gentamicin do not cause specific SNP mutations in the same parts of the genome when used at sub-MIC levels for 14 days continuously. Whether this is specific to these two compounds requires further investigation, the resistance training experiment would have to be

applied to other bacterial species such as other members of the *Staphylococcus* genus and other Gram positives to identify whether NX-AS-401 does cause specific mutations.

The genetic sequencing also shows that increase in gentamicin tolerance seen in Figure 4.6 is not caused by mutation in the target site as no SNPs were detected within the 30S subunit (**Appendix 1.5**). This means that increased tolerance to gentamicin is likely caused by antibiotic pressure resulting in decreased growth and division ⁽³³⁰⁾. Other sub-MIC challenge studies have shown that *S. aureus* exposed to sub-MIC gentamicin or gentamicin at MIC levels for short time periods, <4 hours has resulted in altered growth, metabolism, virulence, and changes in antibiotic sensitivity, however whether these changes were sustainable over time has not been identified ⁽³³¹⁻³³³⁾.

How NX-AS-401 mediates changes in phenotype that were previously identified via AST testing, metabolic assays ⁽³³²⁾ and growth curves ⁽³³¹⁾ requires more in-depth investigations such as transcriptomics and metabolomics to understand the full effects of gentamicin induced antibiotic pressure on *S. aureus*. These techniques have been used in some studies such as Schelli *et al* that demonstrate sub-MIC aminoglycosides ability disrupt multiple pathways such as, pyrimidine and amino acid metabolism using mass spectroscopy indicating that these techniques could be employed for monitoring changes in resistance mechanisms ⁽³³³⁾.

Understanding the full effect of NX-AS-401 may also require a more genetically diverse representation of the *S. aureus* genome, this would identify whether NX-AS-401 is effective against all *S. aureus* isolates and not just these select few. Since NX-AS-401 has demonstrated the ability to inhibit growth of *S. aureus* it is important to identify where it could be used effectively in clinical situations. This could include its use as a solo agent or whether adding secondary antibacterial agents can increase the efficacy of both agents.

4.5.5 Antibiotic Interactions

It is important to identify antibiotic interactions, as combination therapy becomes more common in the treatment of antibiotic resistant infections, or infections in areas where immune function is limited ⁽¹¹⁰⁾. Preliminary tests on NX-AS-401 supplemented agar was used to identify potential antibiotic interactions before performing antibiotic checkerboards.

As shown in Table 4.3 zone sizes increased on the media containing NX-AS-401 compared with NX-AS-401 free medium, p-values were obtained via Mann Whitney tests and determined that increases in zone sizes >2 mm were significant ($p > 0.05$). Combination treatments with NX-AS-401 and gentamicin, ciprofloxacin, clindamycin, erythromycin, and tetracycline demonstrated increased antibiotic activity unless a previous resistance was present and identified (**Section 4.4.1**). The beta-lactam cefoxitin was the only antibiotic to show indifference with all strains, however synergy has been seen with cefoxitin in other studies, such as in combination with aminoglycosides ⁽³³⁴⁾.

Supplemented disc diffusion was used as preliminary testing to identify potential antibiotic interaction; however, this method could be subject to criticism as the effect of NX-AS-401 on agar composition is unknown. The diffusion rate of antibiotic discs can be altered by changes in agar thickness and viscosity, NX-AS-401 may allow for a greater diffusion rate and thus increase zone sizes ⁽²⁴⁶⁾. This could be tested via agar cell diffusion test ⁽³³⁵⁾, to monitor the permeability of acids and bases in MHB with and without NX-AS-401 supplementation.

FICI values were determined by the calculation provided in Section 2.3.10. To determine the FICI wells where growth was inhibited by $\geq 90\%$ and contained the lowest concentration of both NX-AS-401 and antibiotic were chosen. However, this method was not ideal as selecting one well from the entire plate can bias results, giving a synergistic result where more broadly across the plate there may be limited interaction. To mitigate this bias and to prevent reporting incorrect antibiotic interactions three different wells containing different NX-AS-401 and antibiotic concentrations were chosen from each replicate and the values averaged to produce a more accurate FICI value.

Determination of synergy was based on the final value, as shown in Table 4.5. The data matched with what was determined in disc diffusion with most antibiotic classes demonstrating synergy with NX-AS-401 apart from those with pre-existing antibiotic resistance. NX-AS-401 also had indifferent interactions in combination with cefoxitin in both susceptible and resistant strains apart from NCTC 13142 where synergy was detected. Gene sequencing (**Table 4.3**) identified that all isolates resistant to cefoxitin carried the *mecA* gene, however NCTC 13142 was the only *mecA* strain that displayed synergy. This could be due to an increased NX-AS-401 susceptibility, but this was not seen in MIC testing. Therefore, the synergy here may be due to changes in how NX-AS-401 affects NCTC 13142 in comparison to other *mecA* positive strains, UHW 3 and CRI 2. However, confirmation of the synergy was required before this was investigated further.

To confirm the synergistic trends a template was obtained (MacSynergy™ II) ⁽²⁵⁶⁾ that allowed for interactions to be determined according to the Bliss independence model. Unlike the FICI calculation the Bliss model accounted for the whole antibiotic checkerboard within the calculation and provided values for both synergy and antagonism. Table 4.5 provides the outcomes of the Bliss independence analysis, with most NX-AS-401 and antibiotic combination showing the same synergy identified under disc diffusion and FICI calculation.

The only differences between FICI and Bliss results that occurred were that UHW 19 and CRI 2 did not demonstrate synergy with ciprofloxacin and all strains were indifferent in cefoxitin/NX-AS-401 combinations. These results seem likely to be more accurate as CRI 2 and NCTC 13142 were resistant to ciprofloxacin and cefoxitin respectively, however the reason for an indifferent result with NX-AS-401 and ciprofloxacin in strain UHW 19 is unknown as no potential resistance mechanisms were discovered via gene sequencing. This may be due to combination therapy causing increased expression of the previously discussed *norA* efflux pump that can mitigate the effects of ciprofloxacin, however expression changes would need to be identified via RT-qPCR after exposure UHW 19 was exposed to both antibiotics ⁽³²⁴⁾.

The antibiotic clindamycin also displayed synergy with NX-AS-401 on all strains apart from UHW 3, which has an intrinsic resistance. *S. aureus* strain CRI 2 also demonstrated synergy between clindamycin and NX-AS-401 despite having an

inducible resistance. Whether synergy occurs in the presence of erythromycin, clindamycin and NX-AS-401 was not tested. The difference in synergy result may also be down to the genomic variant of *ermC* present, as it requires induction if it lacks the promoter sequence, whereas if the promoter sequences is present it confers intrinsic resistance to clindamycin ⁽²⁶²⁾. However, this does indicate that NX-AS-401 does not activate expression of the *ermC* gene that confers resistance to both macrolides and lincosamides.

The synergy identified in tables 4.3-4.5 shows that NX-AS-401 could have potential as an antibiotic adjuvant. While all three methods indicated synergy between NX-AS-401 and the different antibiotic classes, the Bliss independence model appears to be the most conservative and accurate as it considers all concentration combinations of NX-AS-401 and antibiotic. The values obtained through the Bliss model also indicate the likelihood of the synergy being replicated *in vivo*. The synergistic properties of ajoene have also been detected *in vivo* and *in vitro* previously when ajoene and the aminoglycoside tobramycin were utilised against *in vitro Pseudomonas aeruginosa* biofilms ^(194, 244).

Synergism with antibiotics is a positive indicator for the clinical application of NX-AS-401 where combination therapies have become a standard clinical practice for the treatment of multi-drug resistant (MDR) infections ⁽³³⁶⁾. However,

Antibiotic synergy between current antibiotic classes is quite rare, most remain indifferent to each other due to similar mechanisms of action ⁽³³⁷⁾. Known combination therapies include the use of beta-lactams and aminoglycosides or more specific drug combination such as colistin and tigecycline that work due to different mechanisms of action ^(111, 337). In these cases beta-lactams and colistin break down the cell wall/membrane allowing for increased permeability of aminoglycosides and tigecycline that both interact with the 30S ribosomal subunit ⁽¹¹¹⁾.

One of the major concerns in the development of new compounds and their efficacy in combination therapies is whether the interactions seen *in vitro* will apply *in vivo*, for example the idea that bactericidal and bacteriostatic antibiotics would be antagonistic ⁽²⁹⁸⁾. While this was thought to make sense, the actuality is more nuanced, with synergy between bacteriostatic and bactericidal drugs instead based on the

mechanism of action. Uncovering a mechanism of action can help identify whether antibiotic combinations are potentially synergistic ⁽¹²¹⁾.

Additionally, it is unclear whether combination therapies may also increase the occurrence of antibiotic associated side effects, such as kidney and liver disorders ⁽³³⁶⁾. This is because the use of two antimicrobial agents in combination means that there are two metabolic processes required for clearance and excretion from the host ⁽³³⁸⁾. However, if the combination therapy contains synergistic antibiotics the concentrations required can be reduced, easing the burden on the host filtration / elimination system ⁽³³⁸⁾.

Antibiotics that are potentially similar to NX-AS-401 have also been shown to work well in combination with drugs such as sulphamethoxazole combined with trimethoprim still utilised ⁽¹⁸²⁾. This combination is used as both agents act on the folate synthesis pathway and their combined efficacy is much greater than each antibiotic individually ⁽³³⁹⁾.

Molecules from garlic such as allicin have also demonstrated potential synergy *in vitro* with antibiotics such as beta-lactams ⁽²³⁰⁾ and vancomycin against *S. aureus* ⁽²³²⁾ and through to *in vivo* studies where one study by Sharifi-Rad *et al* demonstrated that allicin had synergy with silver nano-particles against wound infections in mice ⁽³⁴⁰⁾. Overall, synergy data between antibacterial and individual garlic derived molecules is limited. These limitations are likely due to the unknown mechanism and the high concentrations required in comparison to standard of care antibiotics.

Since the mechanism of action for garlic derived drugs has yet to be determined it has been suggested that their activity and contribution in antibiotic synergy could be due to the ability of compounds such as allicin to easily pass through the phospholipid membranes ⁽²²⁷⁾. This allows allicin to act on thiol groups within the cell and may cause metabolic disruptions that enhance the effects of other antibiotics ⁽²²⁷⁾. This could be confirmed for NX-AS-401, through the use of the Agilent Seahorse analyser, that can measure changes in metabolic pathways. Whether ajoene is also able to easily pass through phospholipid membranes has yet to be determined and would require testing using phospholipid vesicles ⁽²²⁷⁾. If ajoene also demonstrated phospholipid membrane permeability this may indicate potential for synergy but may also indicate the ability to

cause adverse effects *in vivo* if it readily transfers into host cells and interferes with proteins ⁽²³²⁾.

Synergy seen with other garlic derived compounds *in vivo* and the results of the Bliss model for NX-AS-401, indicates that the synergistic effects of NX-AS-401 may be reproducible in future *in vivo* studies.

Understanding the true potential for NX-AS-401 as a secondary agent in combination therapy will require identifying its mechanism of action, any additional effects it has on *S. aureus* and any potential toxic effects if utilised *in vivo*. Future studies to identify the mechanism of action would require many molecular based techniques based on the suspected target. Reverse transcription quantitative polymerase chain reaction (RT-qPCR) or transcriptomic studies such as DNA/RNA sequencing can be utilised to identify potential genetic targets of NX-AS-401. This has already been done with ajoene and *P aeruginosa* that identified NX-AS-401 targeting the genes associated with rhamnolipid production ⁽¹⁹⁴⁾. Changes in protein production and metabolism could be identified via polyacrylamide gel electrophoresis (PAGE), chromatographic methods and mass spectrometry, as done by V. N. Loi *et al* have identified how allicin causes thiol stress in *S. aureus* ⁽²²⁸⁾.

A combination of these methods would not only directly provide a mechanism of action or data to indicate it but may also provide information on secondary effects and whether the NX-AS-401 formulation also disrupts additional *S. aureus* mechanisms involved with virulence factor production and biofilm formation.

4.6 Conclusions

Aim: To identify the MIC and MBC of NX-AS-401 against *S. aureus* in comparison to NBR 26-6A.

NX-AS-401 inhibited growth and prevented an increase in cell numbers of all *S. aureus* strains regardless of their antibiotic susceptibility. The MIC was identified as 64-128 µg/ml and the MBC was 2048 µg/ml for all *S. aureus* strains. These results are similar to NBR 26-6A, however, an MBC was identified after 24 hours. In comparison to current standard of care antibiotics the MIC is relatively high, however more data is required to identify whether the NX-AS-401 MIC is achievable *in vivo*.

Aim: To identify the mode of action (bacteriostatic/ bactericidal) of NX-AS-401 against *S. aureus*.

The data provided by broth microdilutions (**Section 4.4.3**), identifies NX-AS-401 as a bacteriostatic drugs as the MBC is greater than four times the MIC. This was confirmed in time/kill curves (**Section 4.4.4**) and growth curves (**Section 4.4.5**) where a similar number of *S. aureus* cells were present at both zero and 20 hour timepoints when treated with 32-128 µg/ml of NX-AS-401.

Aim: To identify potential resistance and tolerance to NX-AS-401.

Repeated exposure to NX-AS-401 did not result in a permanent increase in tolerance or the spontaneous generation of a resistance to NX-AS-401. However, gentamicin tolerance was increased above the two-fold margin of error on day eight. Both gentamicin and NX-AS-401 MICs reverted to their original level once the selective pressure was removed. This does indicate that *S. aureus* developing a tolerance to NX-AS-401 is unlikely to occur within normal treatment time frames. However, more strains, species and resistance mechanisms need to be tested to determine if resistance to NX-AS-401 exists.

Aim: To identify whether exposure of *S. aureus* to sub-inhibitory concentration of NX-AS-401 or gentamicin causes mutations in specific gene sites or increased the generation of single nucleotide polymorphisms (SNPs).

Repetitive exposure to sub-MIC levels of NX-AS-401 and gentamicin over 14 days did not cause loss of identified resistance mechanisms or cause the development of mutations within specific parts of the *S. aureus* genome.

Aim : To identify interactions of NX-AS-401 with current standard of care antibiotics.

Combination therapies with NX-AS-401 and current standard of care antibiotics show high levels of synergy which could potentially be replicated *in vivo*. This would reduce the required concentration of NX-AS-401 making it more achievable *in vivo*. However, synergistic effects were unable to overcome identified antibiotic resistance.

5.0 Chapter 5: Identifying the mode of action of NX-AS-401 on *S. aureus* biofilms.

5.1 Introduction

5.1.1 Anti-Biofilm Targeting Antibiotics

Biofilms are defined as a 3D structure formed by bacteria either as a floating aggregate or bound to surface ^(86, 288). The formation of a biofilm is a critical survival strategy for many bacteria, and the development of these structures can lead to the development of chronic infections ⁽²⁸⁸⁾. As previously discussed, (**Chapter 1 Section 1.2.3**) *S. aureus* biofilm formation is a multi-factorial process, beginning with the early stages of attachment and following through to the development of a 3D structure and release of bacterial cells ⁽⁸⁹⁾. The many stages of biofilm development provide a plethora of potential antimicrobial targets. However, targeting one mechanism or pathway does not often prevent biofilm formation as bacteria either have secondary biofilm formation processes or can manipulate host immune factors such as clotting agent fibrinogen into a scaffold for building a biofilm ^(89, 341).

Once formed the biofilm matrix contains a series of channels within the matrix allowing the passage of nutrients to bacterial cells deeper within the biofilm. These channels can also prevent the action of antibiotics via electrostatic interaction and increase antibiotic tolerance, thus restricting the use of current standard of care antibiotics ^(89, 288) either by preventing antibiotic action due to the extracellular matrix, or through overwhelming cell numbers preventing complete eradication. The minimum biofilm eradication concentrations of current standard of care antibiotics are often 100-1000 times their MIC against planktonic cells ⁽¹¹³⁾.

Therefore, the treatment of chronic wounds and the associated biofilms requires the development of new biofilm targeting antibiotics or combination therapies that would increase the efficacy of current antibiotics ⁽⁸⁹⁾. Modern biofilm eradication practices include combination therapies consisting of two or more antibiotics at high concentrations and the removal of contaminated in-dwelling devices such as catheter tips and prosthetics ⁽⁸⁹⁾. Antibiotic lock therapy can also be used on in-dwelling devices,

this involves instilling high concentrations of antibiotic into the indwelling device such as a catheter lumen ⁽³⁴²⁾. This treatment involves removal of the bacteria from the device surface and does not interact with the patient causing the adverse effect associated with high antibiotic use such as renal failure ⁽³⁴²⁾. While these therapies may eradicate biofilms, they can cause additional problems, the high doses can disrupt normal microflora and after therapy the bacteria-free surface can be colonised by other pathogenic bacteria. Although the biofilm may be eradicated potentially harmful extracellular components and toxins can remain ^(89, 342). In situations where antibiotics fail in the removal of biofilms that have formed on host tissues more invasive procedures such as debridement and tissue removal are required ⁽⁸⁹⁾.

Given the difficulties in removing established biofilm the best practice approach is to prevent biofilms from forming rather than trying to disrupt or remove them once they are established ⁽¹⁰⁴⁾. This has led to the investigation of biofilm inhibiting drugs and novel non-drug-based approaches that prevent bacterial adherence and subsequent biofilm formation ⁽¹⁰⁴⁾. New medical device surfaces are in development that can prevent adherence through molecular interaction or by acting directly as antimicrobial surfaces killing bacteria that come into contact either through small molecules or by acting as reservoirs for antibiotics/disinfectants ⁽³⁴³⁾.

As seen in Table 5.1 various anti-biofilm drug types are in development and have progressed to the clinical stage ⁽⁸⁹⁾. The reduced efficacy of standard of care antibiotics against biofilms can require a 100-1000-fold increase from the planktonic MIC in order to have an effect ⁽¹¹³⁾, this has led to a growing demand for antibiofilm drugs that can assist in the treatment of chronic infections. There are many different anti-biofilm drugs in development ⁽⁸⁹⁾ each with their own mechanism of action. Table 5.1 provides a broad description of the drugs that either target the extracellular matrix (ECM) or the bacterial cell directly.

Table 5.1 Potential new anti-biofilm drugs.

The table lists the different anti-biofilm drugs in development, as well as their targets and stage of development. The table was originally provided in a review of anti-biofilm drugs by Koo *et al* 2017 ⁽⁸⁹⁾.

Types	Biofilm Target	Biofilm phase	State of Development
Antibiotics	Microbial cell	All stages	Clinical
Antimicrobial peptides	Microbial cell	All stages	Pre-clinical
Antimicrobial oligonucleotides	Microbial cell	Early/Mature biofilm	<i>In vivo</i>
Nanoparticles	Microbial cell, ECM	All stages	<i>In vivo</i> , pre-clinical, clinical
Other antimicrobials/ oxidizers/ antiseptics	Microbial cell	All stages	Clinical
Persister /dormant cells targeting	Microbial cell	Early/Mature biofilm	<i>In vivo</i>
Antibody/Vaccines	Microbial cell, ECM	Initial attachment, early biofilm	<i>In vivo</i>
Adhesin inhibitors/binding	ECM	Initial attachment	Pre-clinical
Bacteriophages	Microbial cell	Early/Mature biofilm	<i>In vivo</i>
Detergent/ Surfactant irrigants	Microbial cell, ECM	All stages	Clinical
Dispersal Inducers	Microbial cell	Mature biofilm	<i>In vitro</i> , <i>In vivo</i> , pre-clinical, clinical
Degradative Enzymes	ECM	Early/Mature biofilm	Clinical, pre-clinical
Extracellular Polysaccharide	ECM	Initial attachment, early biofilm	<i>In vivo</i> , <i>In vitro</i>

synthesis inhibitors			
Natural products	Microbial cell, ECM	All stages	<i>In vivo</i> , clinical
Photodynamic substances	Microbial cell	Early/Mature biofilm	<i>In vivo</i>
Metabolic interference	Microbial cell	Early/Mature biofilm	<i>In vivo</i> , <i>In vitro</i>
QS inhibitors	Microbial cell	All stages	Pre-clinical, <i>In vivo</i>
Probiotics	Microbial cell	Initial attachment, early biofilm	<i>In vitro</i> , Pre-clinical (in oral), clinical

Targeting the ECM has potential as an effective prophylactic treatment by inhibiting synthesis and secretion or can be used to disrupt pre-established biofilms by targeting the chemical composition ⁽⁸⁹⁾, this can include the use of enzymes such as DNase and proteases to breakdown the extracellular DNA and proteins respectively. However, while these have not been listed in Table 5.1 plant and bacterial proteases and DNases have been identified and found to break down *S. aureus* biofilms without affecting host tissues during *in vitro* tests ^(89, 344, 345). Breakdown of the extracellular polymeric (EPS) matrix can occur through multiple paths, including EPS inhibitors, glycopeptides hydrolases, manufactured antibiotics and drugs such as Dispersin B that can breakdown the matrix, dispersing the biofilm and restoring antibiotic efficacy by removal of the matrix ^(89, 104). However, removal of the ECM may cause dissemination of the bacteria, transforming a localised infection into a system one, this has been seen in cases of poor dental hygiene where the bacterial biofilm plaque on the teeth can break away and enter the blood stream through wounds in the mouth ⁽¹⁰¹⁾. The movement of parts of the biofilm has been linked to systemic infections such as sepsis as well as the build-up of biofilms at other host sites such as plaques in heart valves ⁽¹⁰¹⁾. Therefore, if matrix targeting drugs are used a strong secondary antibiotic is required to eradicate the dispersed bacterial cells ^(89, 346).

Anti-biofilm targets can include preventing biofilm formation by inhibiting the production of or directly attacking the extracellular polysaccharide, protein and/or eDNA ^(89, 104). Targets can also focus on encouraging the production of factors associated with biofilm dispersal such as autolysin ⁽¹⁰⁴⁾. Another potential target is the accessory gene regulatory system that controls quorum sensing (**Chapter 1 Section 1.2.3**) the method by which *S. aureus* cells communicate and work together to form biofilms ⁽⁸⁹⁾. The ajoene component of NX-AS-401 has already been shown to interrupt the quorum sensing pathways in *Pseudomonas aeruginosa* ⁽¹⁹⁴⁾, however its effects against Gram-positive biofilms has yet to be determined.

While eradication of the biofilm is necessary and can help eliminate a chronic infection it can be difficult as the biofilm may reform due to the presence of dormant or persister cells. Bacterial biofilms often contain persister cells that have severely reduced metabolic activity that prevents the action of antibiotics ^(81, 86, 107, 288). These can be seen in Figure 5.1 that shows how biofilms can be treated with antibiotics but not completely eradicated. This allows persister cells, that are usually more tolerant to antibiotics (due to reduced metabolism) to repopulate and reinfect the site ^(107, 288).

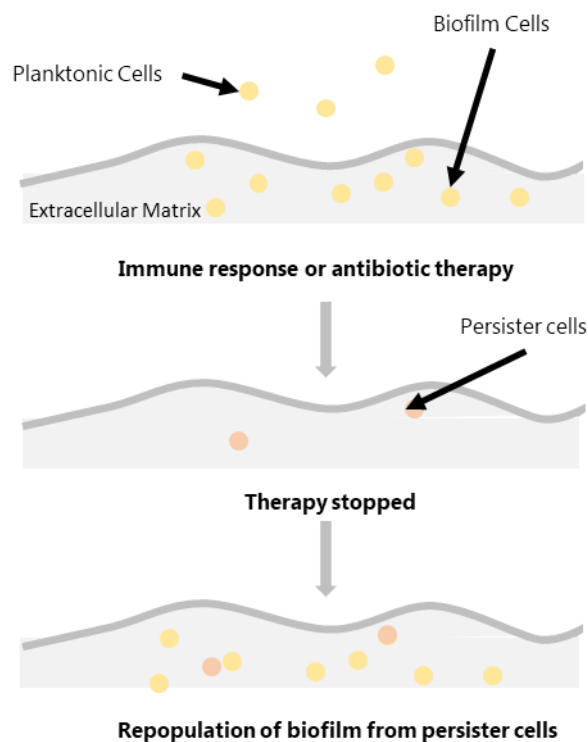


Figure 5.1 Image showing how antibiotic treatment can leave behind residual biofilm matrix and persister cells ⁽¹⁰⁷⁾

To completely remove persister cells and the biofilm matrix shown in Figure 5.1 novel drugs are in development that specifically target the dormant or persister cells causing death of the biofilm and prevent re-establishment of an infection once antibiotics have been stopped ⁽⁸⁹⁾. These have included novel antibiotic classes such as acyldepsipeptide antibiotics that can still penetrate dormant cells and activate metabolic pathways that encourage autophagy resulting in cell death ⁽⁸⁹⁾.

As previously mentioned, (**Chapter 1, Section 1.2.3**) due to biofilm electrostatic interaction and ECM sequestering antibiotic efficacy is greatly reduced. Therefore, restoration of antibiotic efficacy is another approach to biofilm eradication, approaches to this have included the use of nanoparticles bound to antibiotics, and man-made microcapsules that contain antibiotics ^(89, 346). These strategies have allowed active agents to move through the channels in extracellular matrix and allows antibiotic penetration into the deeper biofilm layers ⁽⁸⁹⁾. This allows for more targeted delivery of the antibiotic to the target site and reduced the antibiotic tolerance conferred by the formation of a biofilm ⁽³⁴⁶⁾.

5.1.2 The potential of NX-AS-401 as an anti-biofilm drug.

Molecules such as sulphonamides and other garlic components (allicin, oils and extracts) contain similar functional components to those found in NX-AS-401, however data on their effect on biofilms is limited. Garlic derived components such as alcoholic and aqueous garlic extracts, allicin and ajoene have shown different anti-biofilm effects dependent on the target organism, however research is limited. For example, on both methanol and ethanol based garlic extracts there is one study into their effects on biofilms, with limited data ⁽³⁴⁷⁾. More robust studies by Girish *et al* ⁽²⁰⁶⁾ Jakobsen *et al* ^(194, 241) and the Mohsenipour and Hassanshahian study ⁽³⁴⁷⁾ all agree that garlic based extracts have anti-biofilm properties, reducing mass, matrix amount and metabolism of both Gram positive and negative bacteria ⁽²⁰⁶⁾. The study by Girish *et al* ⁽²⁰⁶⁾ not only identified antibiotic biofilm effects of garlic based solutions but also how the effects can be enhanced by loading nano-particles with garlic extracts allowing for greater penetration into the biofilm.

However, the study by Girish *et al* primarily focuses on the percentage of allicin found within the extract, which is not the only active component within garlic ^(135, 206). The study of Allicin is useful for comparison and assists in understanding the effects of NX-AS-401, as ajoene is created from thermal rearrangement of three allicin molecules and therefore contains similar chemical functional groups ⁽¹³⁵⁾. Studies have shown that allicin can prevent biofilm formation in Gram-negative bacteria such as *P. aeruginosa* ⁽²²⁹⁾ and *Proteus mirabilis* ⁽²¹⁵⁾. The effects of allicin against *P. aeruginosa* identified by Lihua *et al* ⁽²²⁹⁾ are also similar to the results identified by Jakobsen *et al* when ajoene was utilised against *P. aeruginosa* ^(194, 241) in that both agents were able to reduce mass and prevent biofilm growth at sub-MIC concentrations.

Although allicin may be a good indicator for hypothesizing the mechanism of action for NX-AS-401 there are not many investigations into its effects on Gram-positive organisms, specifically *S. aureus*. A study by Zainal *et al* has shown an anti-biofilm effects of allicin against *S. aureus* biofilms, however this focused on changes in biomass via crystal violet and demonstrated reduced mass, however it did not focus on the mechanism of action for allicin against *S. aureus* biofilms ⁽¹⁸⁰⁾.

Targeting bacterial biofilms and their associated mechanisms is one of the methods for treating chronic infections, however, care should be taken to prevent secondary infection by bacterial cell dissemination or reinfection due to the presence of persister cells. The effects of NX-AS-401 on biofilms requires study to determine if it can be used as an anti-biofilm therapy on its own or as part of an anti-biofilm combination therapy using current standard of care antibiotics.

5.2 Aims

- Determine if all eight *S. aureus* strains can form a biofilm and identify the strength and biofilm phenotype for each strain.
- Identify the effects of NX-AS-401 on the formation and disruption of *S. aureus* biofilms, in terms of mass, metabolism and viable cells.
- Identify whether the antibiotic interactions seen in planktonic cultures are replicated in pre-established biofilms.
- Visually identify changes in biofilm structure and cell morphology after exposure to NX-AS-401 using scanning electron microscopy (SEM) and confocal microscopy.
- Identify changes in gene expression of *S. aureus* biofilms after exposure to NX-AS-401 using RT-qPCR.

5.3 Materials and Methods

No changes have been made to the materials and methods provided in Chapter 2.

5.4 Results

5.4.1 Biofilm Characterisation

S. aureus can produce a biofilm via multiple mechanisms, each *S. aureus* strain used in this study underwent biofilm phenotyping (Section 2.3.9) to determine the mechanism each strain uses (Table 5.2).

Table 5.2 Results of OD^{cut} and Biofilm Phenotyping.

These results identify the mechanism of each *S. aureus* strain uses to create a biofilm in a tissue culture treated 96 well plate in MHB. Biofilm methods and formation may vary based on adherent surface and media composition. OD^{cut} values measure the ability of a strain to form a biofilm. Values identify a strain as a (0-2) weak, (2-4) moderate or (4+) strong biofilm former.

Strain	OD ^{cut}		Biofilm Phenotype
	Value	Interpretation	
NCTC 13142	2.19	Moderate	Proteinaceous
NCTC 12973	2.20	Moderate	Proteinaceous
UHW 3	1.55	Weak	Proteinaceous
UHW 8	1.41	Weak	Proteinaceous
UHW 15	2.81	Moderate	Proteinaceous
UHW 18	1.83	Weak	Proteinaceous
UHW 19	2.65	Moderate	Proteinaceous
CRI 2	3.92	Moderate	Proteinaceous

5.4.2 Effects of NX-AS-401 on *S. aureus* biofilm formation.

The effects of NX-AS-401 on the ability to inhibit *S. aureus* biofilms was measured with three outputs including, biomass (crystal violet) (Figure 5.2), metabolic activity (resazurin) (Figure 5.3) and total viable cell (TVC) counts (Figure 5.4).

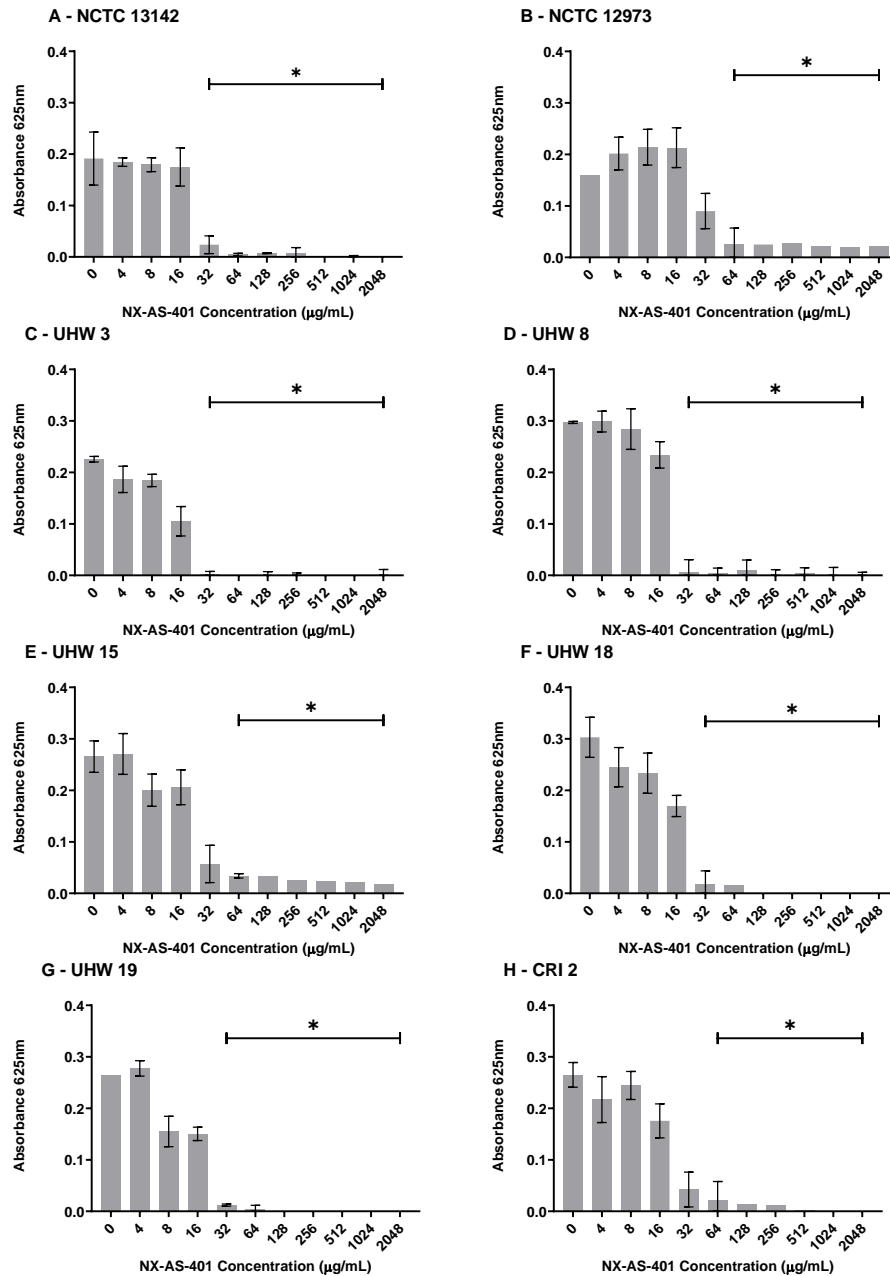


Figure 5.2 Changes in biomass caused by exposing *S. aureus* to NX-AS-401.

Statistically significant ($p < 0.05$) >90 % reduction in biomass is indicated by an asterisk (*). Error bars represent the standard error of the mean.

The minimum biofilm inhibitory concentrations (MBIC) were identified as a 90 % reduction in biomass in comparison to the untreated control. *S. aureus* strains NCTC 13142, UHW 3, UHW 8, UHW 18, and UHW 19 had MBIC of 32 µg/ml according to biomass. The remaining three strains, NCTC 12973, UHW 15 and CRI 2 demonstrated an MBIC of 64 µg/ml.

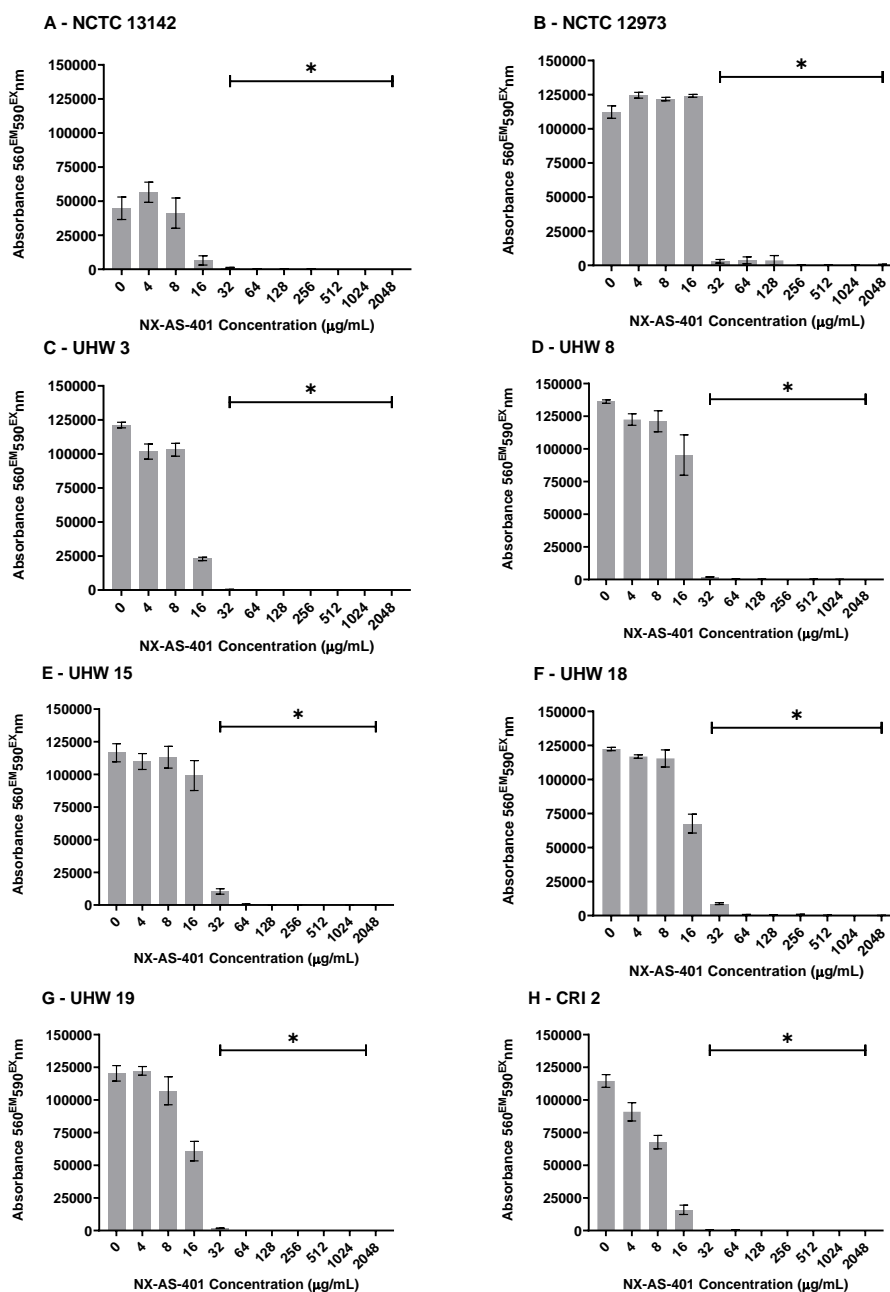


Figure 5.3 Changes in biofilm metabolism caused by exposing *S. aureus* to NX-AS-401. Statistically significant ($p < 0.05$) >90 % reduction in metabolism is indicated by an asterisk (*). Error bars represent the standard error of the mean.

MBIC values according to bacterial metabolism of resazurin was identified as 32 µg/ml for all the eight *S. aureus* strains.

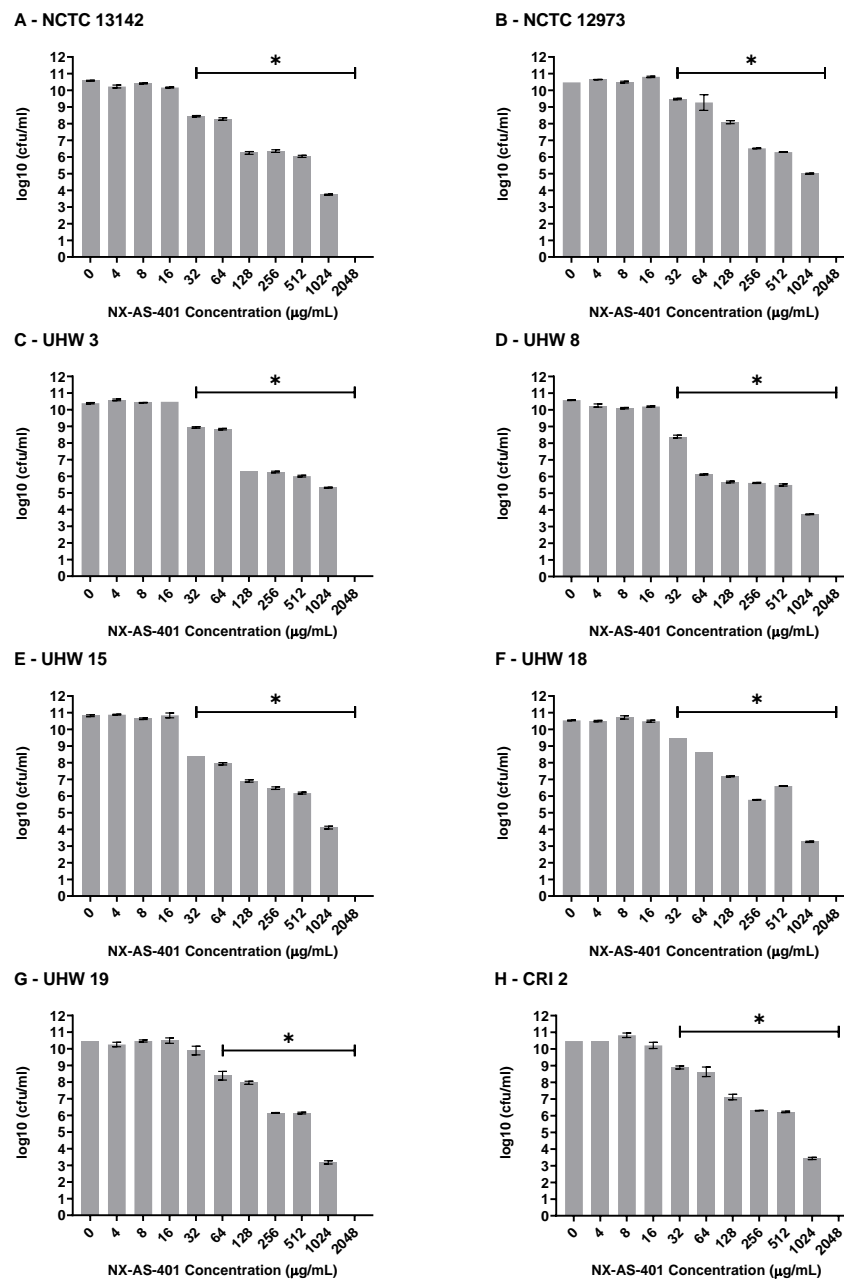


Figure 5.4 Changes in cell number caused by exposing *S. aureus* to NX-AS-401. Statistically significant ($p < 0.05$) >90 % reduction in cell number is indicated by an asterisk (*). Error bars represent the standard error of the mean.

MBIC of NX-AS-401 according to TVC counts was 32 µg/ml for seven out of eight *S. aureus* strains with strain UHW 19 demonstrating an MBIC of 64 µg/ml

5.4.3 Effects of NX-AS-401 on pre-established *S. aureus* biofilms.

The ability of NX-AS-401 to disrupt *S. aureus* biofilms established over 48 hours and treated for 20 hours was monitored via biomass (Figure 5.5), metabolic activity (Figure 5.6) and TVC counts (Figure 5.7). An MBEC of 50 % was used to account for leftover cell debris and extracellular matrix stained by crystal violet.

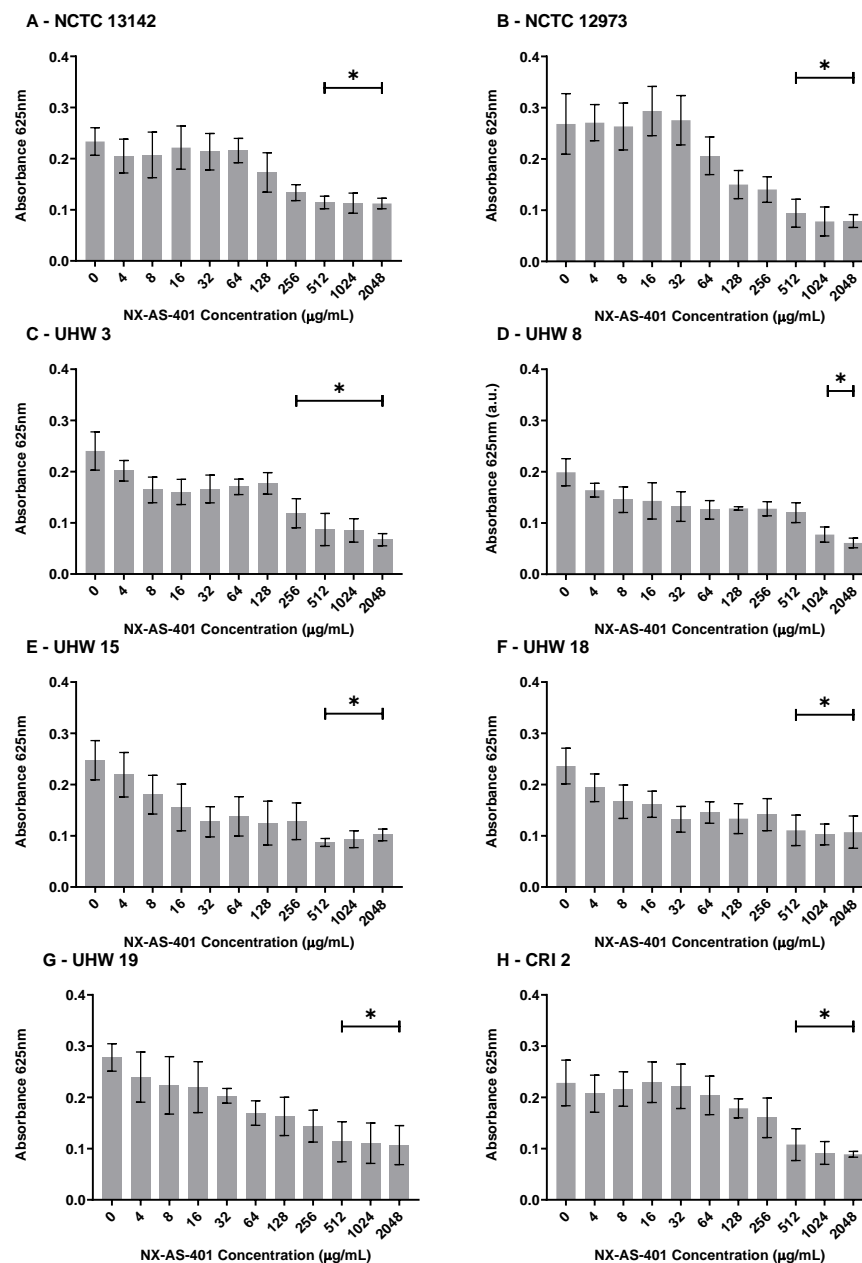


Figure 5.5 Changes in the biomass of pre-established 48-hour *S. aureus* biofilms caused by NX-AS-401.

Statistically significant ($p < 0.05$) >50 % reduction in biomass is indicated by an asterisk (*). Error bars represent the standard error of the mean.

MBEC⁵⁰ of NX-AS-401 according to crystal violet assay was 512 µg/ml for seven out of eight *S. aureus* strains with strain UHW 3 demonstrating an MBEC⁵⁰ of 1024 µg/ml.

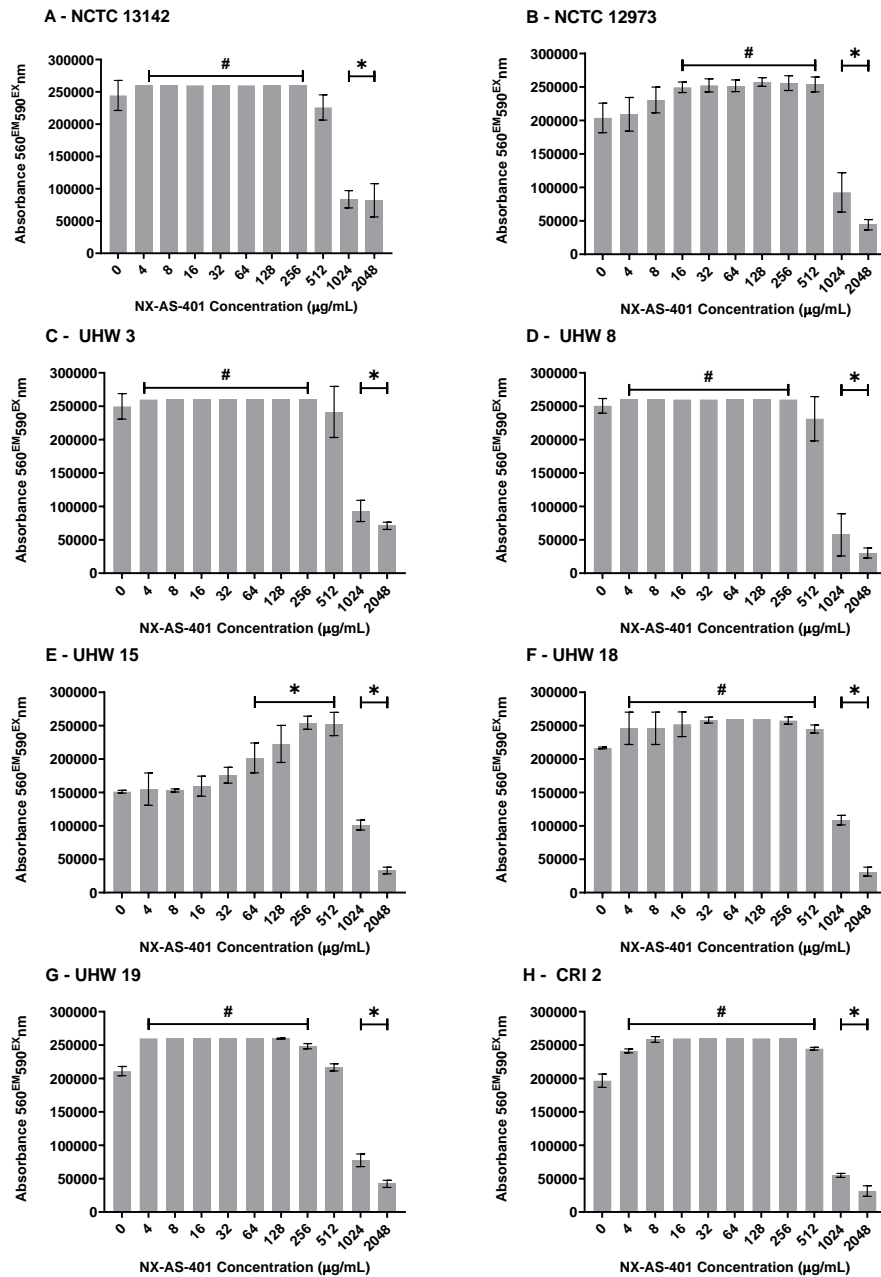


Figure 5.6 NX-AS-401 mediated changes in resazurin metabolism of *S. aureus* biofilms pre-established over 48 hours.

Statistically significant ($p < 0.05$) > 50 % reduction in metabolic activity is indicated by an asterisk (*), increases in metabolism caused by sub-MBEC concentrations are marked with (#). Error bars represent the standard error of the mean.

MBEC⁵⁰ of NX-AS-401 according to Celltiter blue assay was 1024 µg/ml for all eight *S. aureus* strains. All strains exhibited a statistically significant ($p < 0.05$) increase in metabolic activity at concentration < 1024 µg/ml.

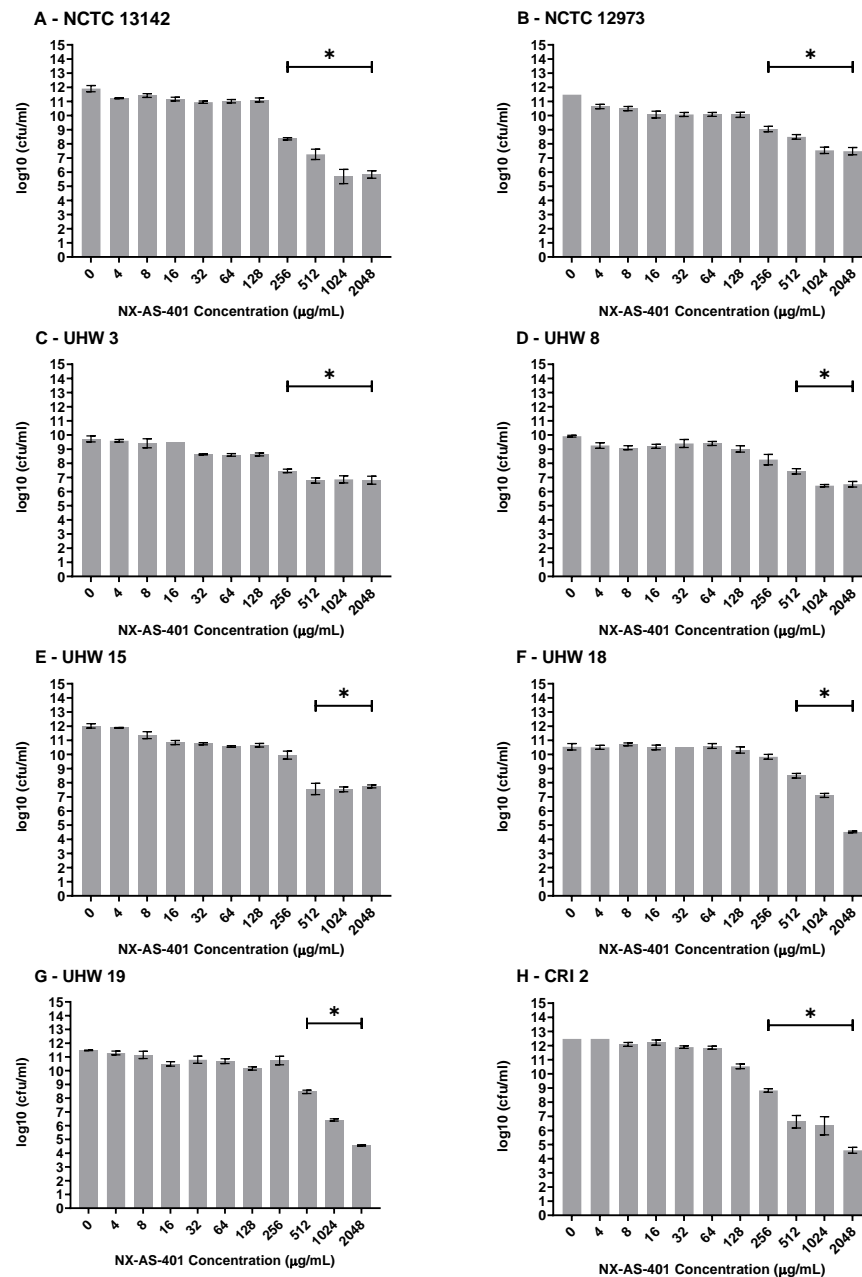


Figure 5.7 NX-AS-401 mediated changes in biofilm cell number.

Statistically significant ($p < 0.05$) > 50 % reduction in cell number is indicated by an asterisk (*). Error bars represent the standard error of the mean.

An MBEC of 90 % was used for TVC counts as this is indicated by a two-fold decrease in log₁₀ values. Therefore, ~ 99 % reduction in cell numbers was caused by NX-AS-401

concentrations >256 µg/ml in strains NCTC 13142, NCTC 12973, UHW 3 and CRI 2. In strains UHW 8, UHW 15, UHW 18 and UHW 19 cells were reduced by 99 % at an NX-AS-401 concentration >512 µg/ml.

Table 5.3 Summary of MBIC and MBEC results obtained from figures 5.2-5.7.

The Table contains the NX-AS-401 MBIC and MBEC₅₀ values obtained for each strain under each biofilm measuring method.

Strain	MBIC (µg/ml) based on:			MBEC ⁵⁰ (µg/ml) based on:		
	Crystal Violet	Resazurin	TVC	Crystal Violet	Resazurin	TVC
NCTC 13142	32	32	32	512	1024	256
NCTC 12973	64	32	32	512	1024	256
UHW 3	32	32	32	256	1024	256
UHW 8	32	32	32	1024	1024	512
UHW 15	64	32	32	512	1024	512
UHW 18	32	32	32	512	1024	512
UHW 19	32	32	64	512	1024	512
CRI 2	64	32	32	512	1024	256

5.4.4 Antibiotic Interactions

Antibiotic interactions against pre-formed 48-hour biofilms were identified via TVC counts after treatment with sub MBEC concentrations of NX-AS-401 (128 µg/ml) and sub-MBEC concentrations of gentamicin (256 µg/ml), tetracycline (512 µg/ml) and ceftiofur (512 µg/ml) for 20 hours (**Table 5.5**).

Table 5.4 Changes in viable cell number when treated with antibiotics alone and in combination.

Numbers represent the log₁₀ CFU/ml under each testing condition. Statistical significance (p <0.05) was identified by Kruskal-Wallis tests and highlighted in grey. Strains that were resistant to a selected antibiotic according to AST (**Chapter 4 Section 4.4.1**) have a thick border highlighting both the log₁₀ CFU/ml when exposed to the agent alone and in combination with NX-AS-401.

Log ₁₀ (CFU/ml) of <i>S. aureus</i> strains treated with:							
Strain	NX-AS-401	Gentamicin	NX-AS-401 & gentamicin	Tetracycline	NX-AS-401 & tetracycline	Ceftiofur	NX-AS-401 & ceftiofur
NCTC 13142	11.12	7.79	6.87	5.53	3.83	10.65	10.18
NCTC 12973	11.05	7.83	6.84	8.88	6.36	11.21	10.20
UHW 3	9.84	10.62	5.30	7.07	5.73	11.12	7.53
UHW 8	9.06	6.84	3.10	7.32	0.00	7.04	6.52
UHW 15	11.51	10.68	6.43	6.39	0.00	12.00	8.43
UHW 18	10.11	8.53	5.40	5.67	0.00	10.99	7.97
UHW 19	10.16	7.42	0.00	8.52	0.00	10.33	8.32
CRI 2	12.09	5.98	0.00	5.26	0.00	10.55	8.27

As shown in Table 5.4. all strains displayed synergy between NX-AS-401 and gentamicin and NX-AS-401 and tetracycline, with the latter combination able to overcome the resistance mechanism. A reduction in *S. aureus* cell numbers were significant with some combinations, such as NX-AS-401 and tetracycline able to kill all *S. aureus* cells. While synergy was seen in ceftiofur, no strains were eradicated by the combination of NX-AS-401 and ceftiofur.

5.4.5 Scanning Electron Microscopy (SEM) and Confocal Laser Scanning Microscopy (CLSM)

Visualization of *S. aureus* biofilms by CLSM, was performed to identify the effects of NX-AS-401 on biofilm structure and cell morphology. The FilmTracer live kit (Thermofisher, UK) containing propidium iodide (PI) and SYTO 9 stain was used to distinguish between dead and live *S. aureus* cells, propidium iodide was also used to bind extracellular DNA and give an indication of biomass. Comstat 2.0 was used to obtain biofilm values that could be statistically analysed. All *S. aureus* strains underwent both SEM, confocal microscopy and Comstat analysis. The different values obtained, and their definitions have been provided in Table 5.5. Figures 5.8 – 5.15 display three representative SEM and CLSM image of the nine taken. Tables 5.6 to 5.13 show the results of the Comstat analysis of the CLSM images.

Table 5.5 Defined values provided by Comstat analysis of CLSM images.

Value Name	Definition
Biomass ($\mu\text{m}^3/\mu\text{m}^2$)	The amount of biofilm present in all three dimensions. Overall biofilm size. The value obtained does not differentiate between cells and extracellular matrix, however if SYTO 9 is related to cell numbers, while propidium iodide is related to dead cells and extracellular matrix.
Thickness (μm)	The height of the biofilm from the base of the glass coverslip to the top.
Roughness Coefficient	The roughness of the biofilm layer refers to whether the biofilm has formed a uniform layer or if there are patches missing. A decrease indicates that the top layer of the confocal image is a uniform density, while an increase indicates an uneven surface.
Surface Area (μm^2)	The amount of space taken up in the biofilm in all layers in two dimensions rather than three used for biomass. Increases indicate more biofilm, while decreases indicate less biofilm.
Surface to Biovolume Ratio ($\mu\text{m}^2/\mu\text{m}^3$)	The ratio of biofilm free surface to biofilm presence, increased values indicate there is more free surface and less biofilm.
% of base layer occupied by Biofilm &	Percentage or value of the base layer occupied by the biofilm, often decreases as biofilm decrease, can be used to measure the antibiotic penetration in thick biofilms.
Base layer area occupied (μm^2)	Occupancy of the biofilm on the base layer closest to adherent surface.

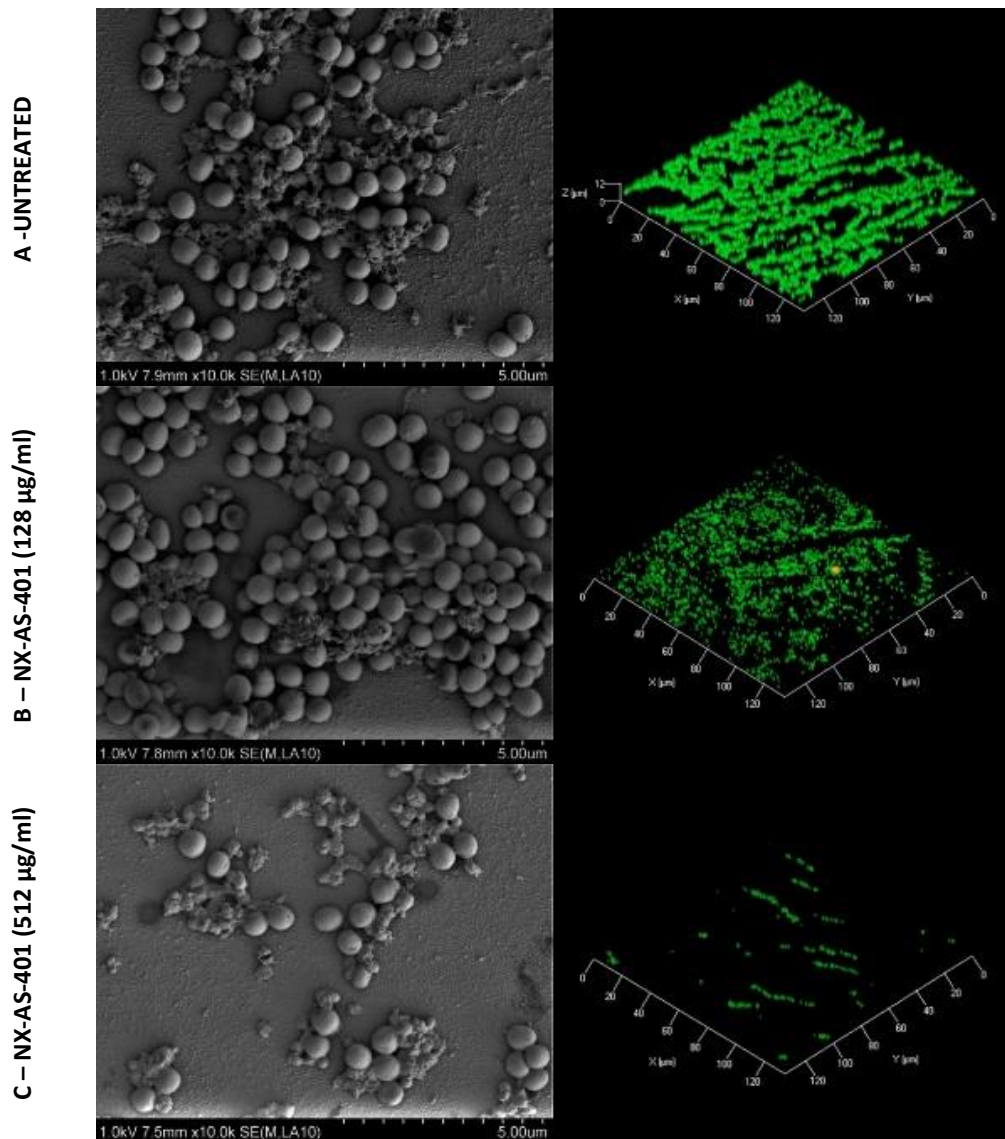


Figure 5.8 Representative SEM (Left) and CLSM (Right) images of NCTC 13142 biofilms treated with NX-AS-401.

CLSM indicates that *S. aureus* biofilms were disrupted as concentration increased, with an NX-AS-401 concentration of 512 µg/ml causing reduced biomass. SEM imaging show that in an untreated biofilm NCTC 13142 seems to create more EPS than a biofilm treated with 128 µg/ml. The SEM images indicate no change between untreated *S. aureus* biofilms and those treated with 128 µg/ml NX-AS-401.

Table 5.6 Comstat analysis of NCTC 13142 Biofilm CLSM images:

The table is composed of average values from the analysis of three CLSM images that best represented the biofilm under each test condition. Statistical significance was identified by p-values (p <0.05 *, p <0.01 **, p <0.001 ***).

		Biomass ($\mu\text{m}^2/\mu\text{m}^3$)	Thickness (μm)	Roughness Coefficient	Surface Area (μm^2)	Surface / Biovolume Ratio ($\mu\text{m}^2/\mu\text{m}^3$)	% of base layer occupied by Biofilm	Base layer area occupied (μm^2)	
NX-AS-401 Concentration ($\mu\text{g}/\text{ml}$)	0	Syto 9 (Green)	4.03	4.00	0.92	545221	7.44	43.19	7865.06
		Propidium Iodide (Red)	1.10	4.00	1.36	176396	8.80	13.37	2435.78
	128	Syto 9 (Green)	0.87***	3.5*	1.19*	129631***	8.14**	23.01***	4190.72***
		Propidium Iodide (Red)	0.19***	3.5*	1.68**	32681***	9.24*	9.19**	1674.22**
	512	Syto 9 (Green)	0.47***	3.5*	1.54**	81165***	9.39***	9.13***	1662.62***
		Propidium Iodide (Red)	0.14***	3.5*	1.83**	25602***	9.91***	2.68***	488.18***

Comstat analysis confirmed that biomass, thickness, surface area and base layer occupation decreased significantly compared to the untreated control after exposure to both 128 and 512 $\mu\text{g}/\text{ml}$ NX-AS-401. Roughness co-efficient and the surface to biofilm ratio significantly increased due to removal of the biofilm.

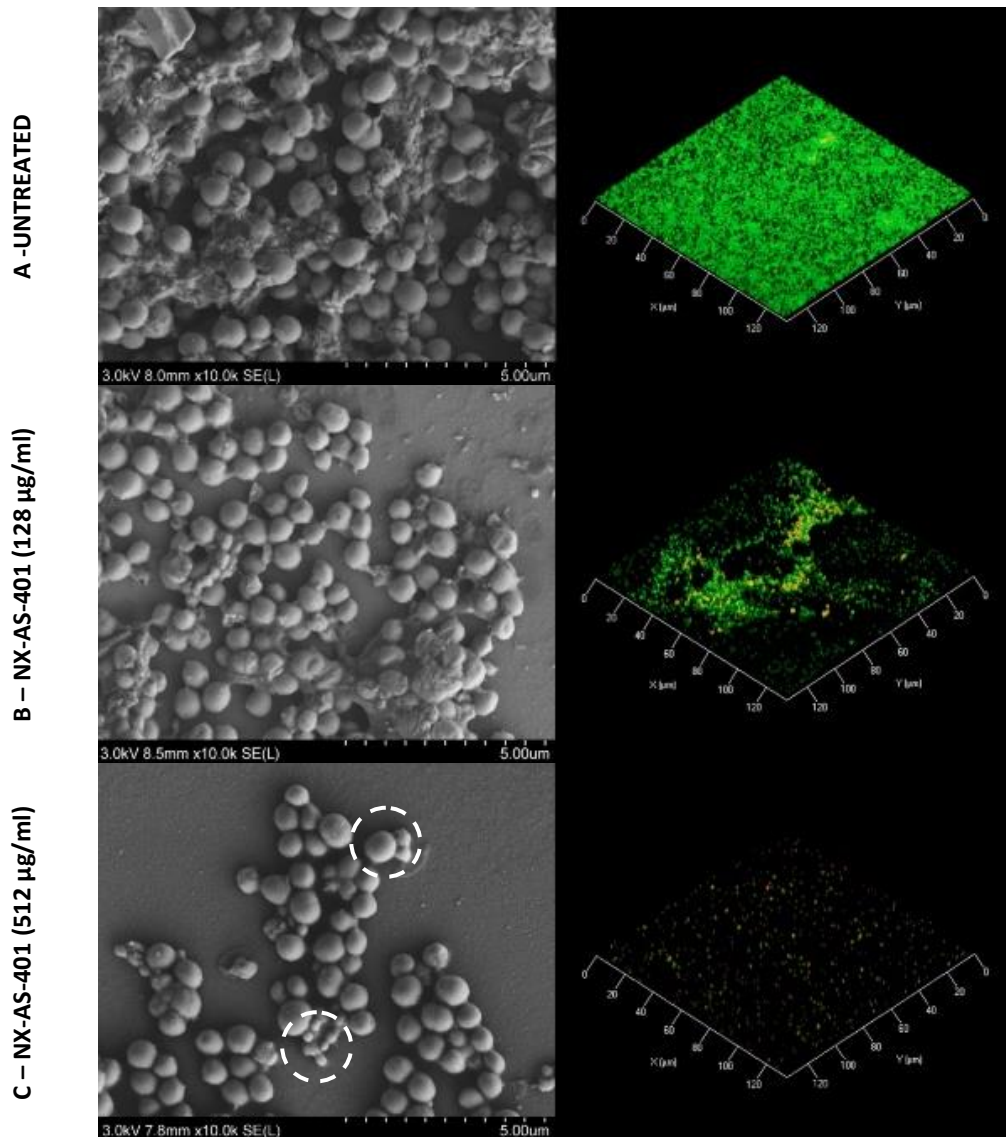


Figure 5.9 Representative SEM (Left) and CLSM (Right) images of NCTC 12973 biofilms treated with NX-AS-401. Dashed circles highlight examples of *S. aureus* cells with unusual morphology in comparison to untreated cells

SEM and CLSM identified that *S. aureus* biofilm mass was reduced in a concentration dependent manner with 128 µg/ml reducing biomass, and even greater disruption of the established biofilm at 512 µg/ml NX-AS-401.

The abnormal morphology highlighted was only seen in the 512 µg/ml sample and only in this strain, it is more likely that this was caused by SEM sample processing rather than exposure to NX-AS-401.

Table 5.7 Comstat analysis of NCTC 12973 Biofilm CLSM images.

The table is composed of average values from the analysis of three CLSM images that best represented the biofilm under each test condition. Statistical significance was identified by p- values ($p < 0.05$ *, $p < 0.01$ **, $p < 0.001$ ***).

		Biomass ($\mu\text{m}^2/\mu\text{m}^3$)	Thickness (μm)	Roughness Coefficient	Surface Area (μm^2)	Surface / Biovolume Ratio ($\mu\text{m}^2/\mu\text{m}^3$)	% of base layer occupied by Biofilm	Base layer area occupied (μm^2)	
NX-AS-401 Concentration ($\mu\text{g}/\text{ml}$)	0	Syto 9 (Green)	4.16	5.50	0.55	415720	5.49	100.00	19669.62
		Propidium Iodide (Red)	1.71	5.50	0.96	245111	7.86	34.12	6213.69
	128	Syto 9 (Green)	2.06**	4.5*	0.99**	263367**	7.02**	45.04***	8202.07**
		Propidium Iodide (Red)	0.19***	4.5*	1.75**	29803***	8.42**	7.07***	1287.81***
	512	Syto 9 (Green)	0.43***	3.5**	1.44***	67370***	8.61***	15.92***	2899.58***
		Propidium Iodide (Red)	0.13***	3.5**	1.78**	21590***	9.20***	4.66***	848.12***

Comstat analysis confirmed that biomass, thickness, surface area and base layer occupation decreases significantly compared to the untreated control after exposure to both 128 and 512 $\mu\text{g}/\text{ml}$ of NX-AS-401. Roughness co-efficient and the surface to biofilm ratio significantly increases due to removal of the biofilm.

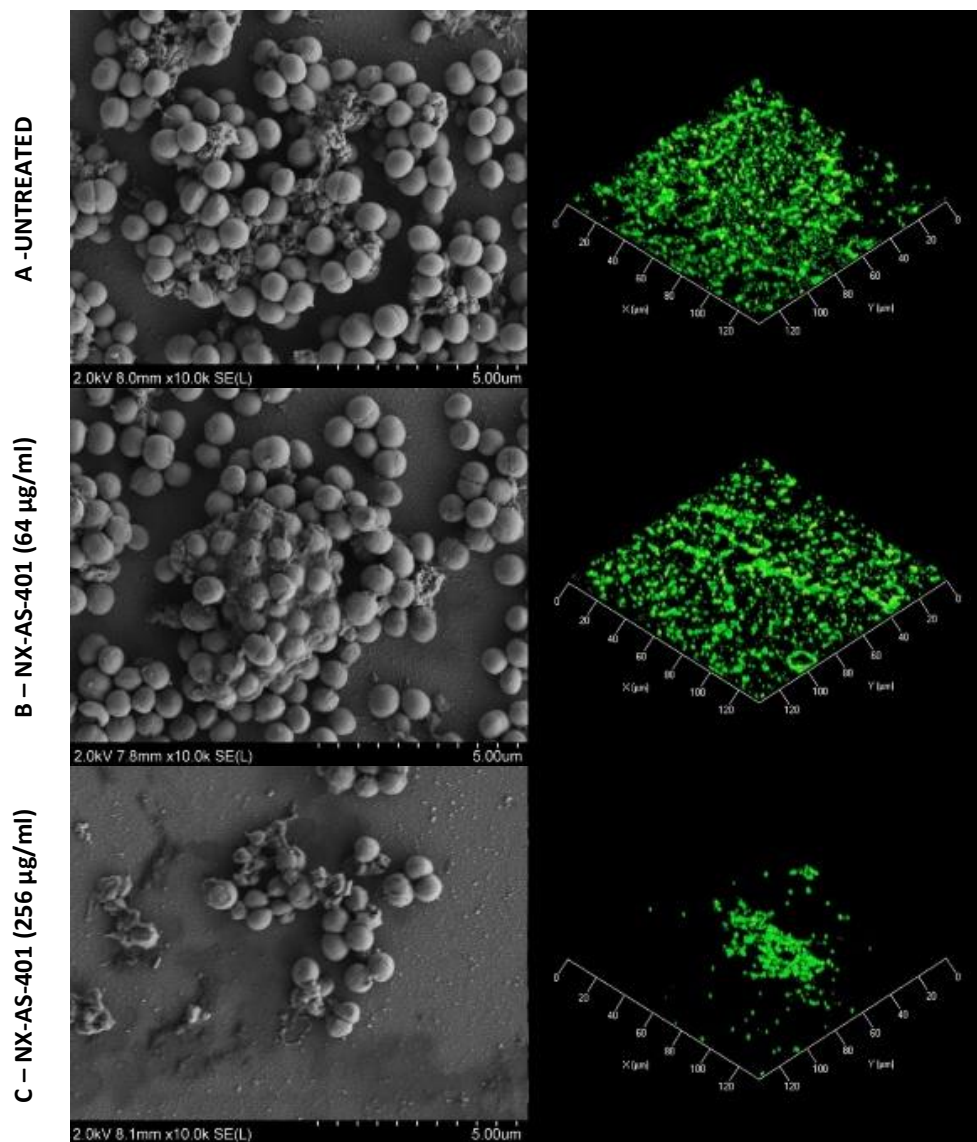


Figure 5.10 Representative SEM (Left) and CLSM (Right) images of UHW 3 biofilms treated with NX-AS-401:

Since isolate UHW 3 demonstrated increased susceptibility to NX-AS-401's anti-biofilm properties during MBEC tests, lower NX-AS-401 concentrations were used. In these images both SEM and CLSM reach the same conclusion, NX-AS-401 concentrations of 64 µg/ml did not disrupt pre-established UHW 3 biofilms. However, a higher concentration of 256 µg/ml was able to disrupt the biofilm effectively.

Table 5.8 Comstat analysis of NCTC UHW 3 Biofilm CLSM images.

The table is composed of average values from the analysis of three CLSM images that best represented the biofilm under each test condition. Statistical significance was identified by p- values ($p < 0.05$ *, $p < 0.01$ **, $p < 0.001$ ***).

		Biomass ($\mu\text{m}^2/\mu\text{m}^3$)	Thickness (μm)	Roughness Coefficient	Surface Area (μm^2)	Surface / Biovolume Ratio ($\mu\text{m}^2/\mu\text{m}^3$)	% of base layer occupied by Biofilm	Base layer area occupied (μm^2)	
NX-AS-401 Concentration ($\mu\text{g}/\text{ml}$)	0	Syto 9 (Green)	1.61	5.1	0.3	89598	3.06	71.73	13064.03
		Propidium Iodide (Red)	0.01	4.1	1.96	2672	13.26	0.55	99.69
	64	Syto 9 (Green)	1.51	5.40*	0.60**	84628*	3.08	59.23**	10786.38*
		Propidium Iodide (Red)	0.01	4.45*	1.98	1684	14.35*	0.0004**	0.07***
	256	Syto 9 (Green)	0.29***	4.40**	1.76***	14559***	2.74*	11.24***	2046.45***
		Propidium Iodide (Red)	0.002*	3.49**	1.99*	515*	15.55*	0.0015**	0.28***

Comstat analysis confirmed that an NX-AS-401 concentration of 64 $\mu\text{g}/\text{ml}$ did not significantly change the biomass or surface to biovolume ratio of UHW 3 when measured with SYTO 9. UHW 3 biofilms treated with 256 $\mu\text{g}/\text{ml}$ biomass, thickness, surface area and base layer occupation were decreased significantly with an increase in the roughness co-efficient and the surface to biofilm ratio caused by biofilm removal.

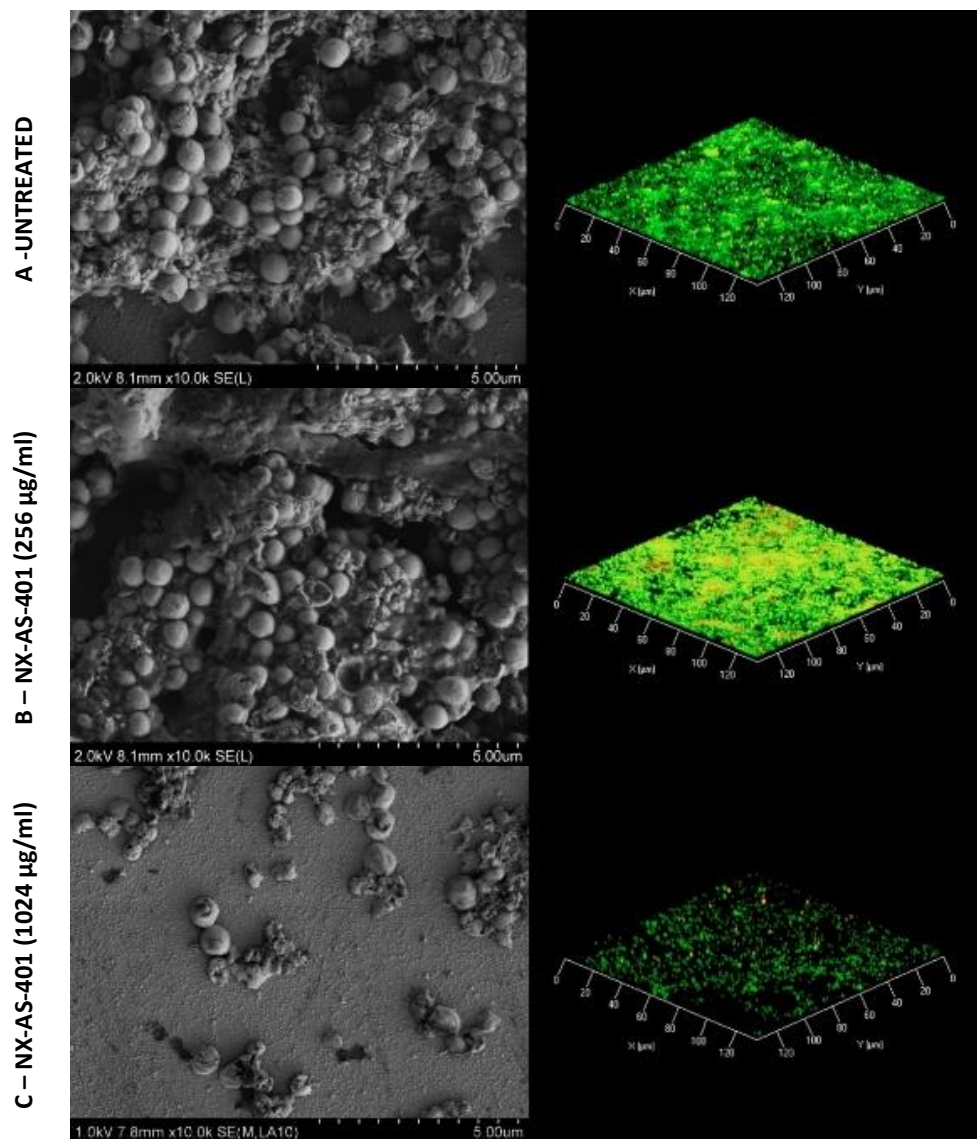


Figure 5.11 Representative SEM (Left) and CLSM (Right) images of UHW 8 biofilms treated with NX-AS-401:

Overall isolate UHW 8 produced more extracellular matrix than the other seven *S. aureus* isolates. NX-AS-401 at a concentration of 256 µg/ml appeared to increase biomass and the production of extracellular matrix according to CLSM. In SEM there was no change in the appearance of untreated *S. aureus* biofilms and those treated with 256 µg/ml NX-AS-401. Both CLSM and SEM did show that an increased NX-AS-401 concentration of 1024 µg/ml reduced the biomass of the UHW 8 biofilm.

Table 5.9 Comstat analysis of UHW 8 Biofilm CLSM images.

The table is composed of average values from the analysis of three CLSM images that best represented the biofilm under each test condition. Statistical significance was identified by p- values ($p < 0.05$ *, $p < 0.01$ **, $p < 0.001$ ***).

		Biomass ($\mu\text{m}^2/\mu\text{m}^3$)	Thickness (μm)	Roughness Coefficient	Surface Area (μm^2)	Surface / Biovolume Ratio ($\mu\text{m}^2/\mu\text{m}^3$)	% of base layer occupied by Biofilm	Base layer area occupied (μm^2)	
NX-AS-401 Concentration ($\mu\text{g}/\text{ml}$)	0	Syto 9 (Green)	2.36	5.40	0.17	82250	1.91	98.40	17919.75
		Propidium Iodide (Red)	0.03	4.45	1.92	6075	11.60	0.84	153.74
	256	Syto 9 (Green)	2.10*	5.40	0.11**	62989**	1.64*	97.78	17806.72
		Propidium Iodide (Red)	0.44*	5.08**	0.95**	58481***	7.29***	23.48***	4276.87***
	1024	Syto 9 (Green)	1.79*	4.5**	1.03***	23843***	7.31***	39.41***	7176.38***
		Propidium Iodide (Red)	0.52***	4.50	1.36***	81000***	8.60***	22.45***	4087.9***

Comstat analysis confirmed that in comparison to the untreated control, a NX-AS-401 concentration of 256 $\mu\text{g}/\text{ml}$ significantly decreased the biomass the UHW 8 biofilm according to SYTO 9 staining, however, biomass increased according to propidium iodide staining. When NX-AS-401 treatment was increased to 1024 $\mu\text{g}/\text{ml}$ biomass, roughness co-efficient and surface to biofilm ratio was decreased according to SYTO 9. For propidium iodide the same but lesser pattern occurred at 1024 $\mu\text{g}/\text{ml}$ as 256 $\mu\text{g}/\text{ml}$

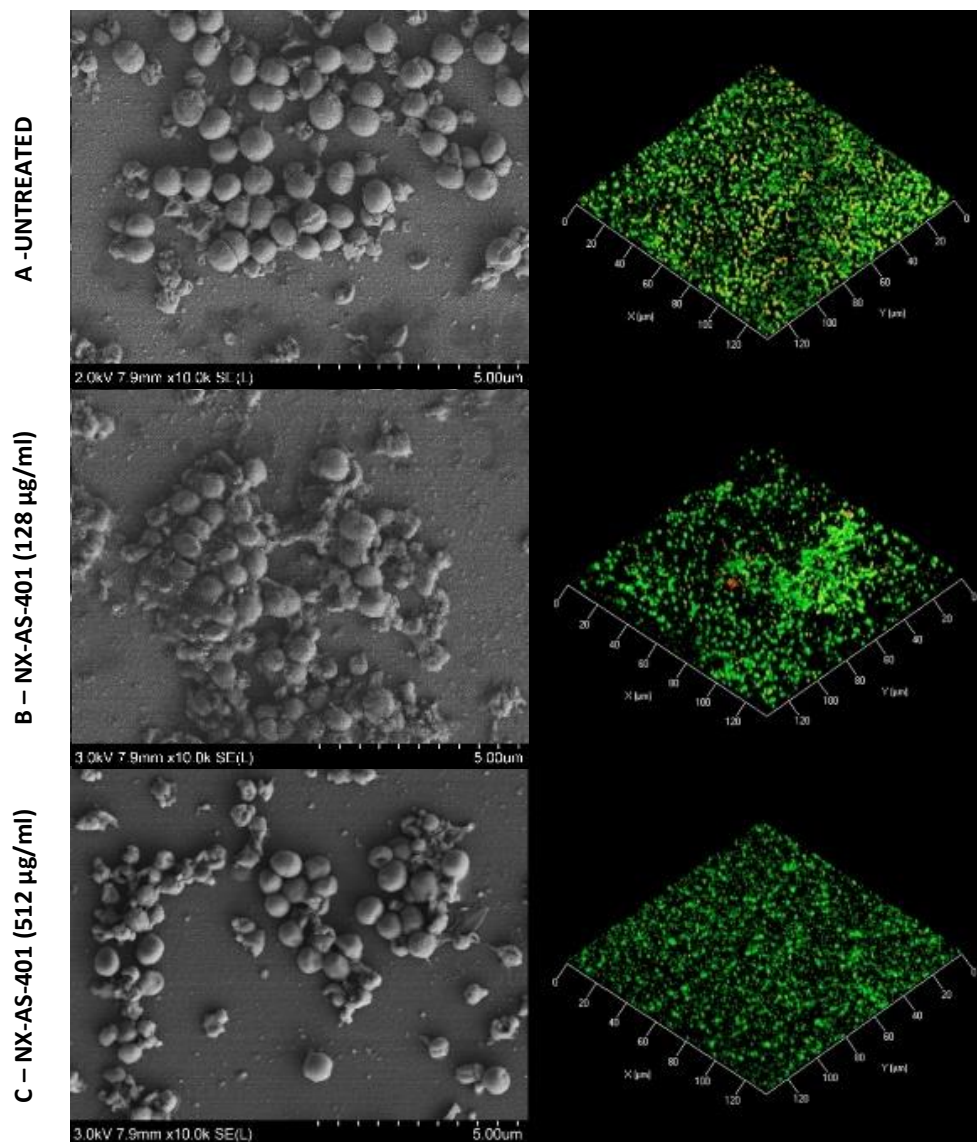


Figure 5.12 Representative SEM (Left) and CLSM (Right) images of UHW 15 biofilms treated with NX-AS-401:

Biofilm disruption of UHW 15 was dependent on NX-AS-401 concentration with a slight decrease in biomass when treated with 128 µg/ml and a further reduction at NX-AS-401 concentrations of 512 µg/ml according to CLSM and viability staining. SEM images seem to indicate that UHW 15 remained unaffected by any NX-AS-401 treatment with poorly formed biofilms in all images.

Table 5.10 Comstat analysis of UHW 15 Biofilm CLSM images.

The table is composed of average values from the analysis of three CLSM images that best represented the biofilm under each test condition. Statistical significance was identified by p- values ($p < 0.05$ *, $p < 0.01$ **, $p < 0.001$ ***).

		Biomass ($\mu\text{m}^2/\mu\text{m}^3$)	Thickness (μm)	Roughness Coefficient	Surface Area (μm^2)	Surface / Biovolume Ratio ($\mu\text{m}^2/\mu\text{m}^3$)	% of base layer occupied by Biofilm	Base layer area occupied (μm^2)	
NX-AS-401 Concentration ($\mu\text{g}/\text{ml}$)	0	Syto 9 (Green)	1.64	5.08	0.58	89392	3.00	62.26	11339.10
		Propidium Iodide (Red)	0.15	5.08	1.74	21105	7.76	7.03	1280.45
	128	Syto 9 (Green)	1.08**	5.40*	0.99**	64833**	3.31*	43.87**	7990.11***
		Propidium Iodide (Red)	0.06**	4.77**	1.88	9969***	9.49**	1.13***	205.85***
	512	Syto 9 (Green)	0.15***	4.13**	1.70***	20023***	7.41***	13.58***	2472.81***
		Propidium Iodide (Red)	0.03***	3.81***	1.92*	6259***	13.28***	1.55***	282.75***

Comstat analysis confirmed that an NX-AS-401 concentration of 128 $\mu\text{g}/\text{ml}$ significantly reduced biomass, surface area and base layer occupancy of the UHW 15 biofilm, while roughness coefficient, thickness and surfaces to biofilm ratio were all decreased according to SYTO 9, the same results were seen with propidium iodide, however thickness was also reduced. These effects were more pronounced when NX-AS-401 treatment was increased to 512 $\mu\text{g}/\text{ml}$.

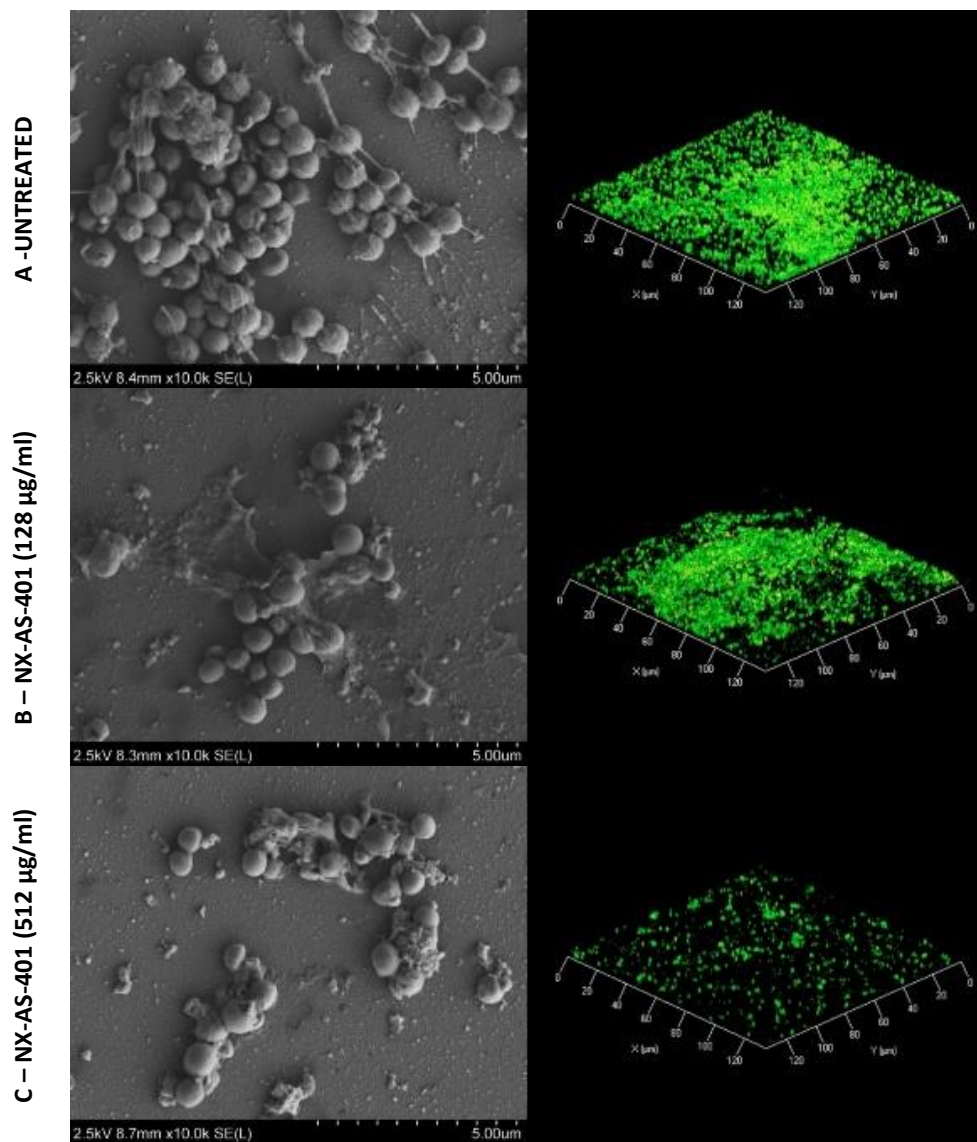


Figure 5.13 Representative SEM (Left) and CLSM (Right) images of UHW 18 biofilms treated with NX-AS-401:

Biofilm disruption of UHW 18 was NX-AS-401 concentration dependent with disruption occurring at 128 $\mu\text{g/ml}$ and biomass was further reduced at NX-AS-401 concentrations of 512 $\mu\text{g/ml}$. This is more clearly seen in CLSM where fluorescence does decrease as NX-AS-401 concentration increases. However, in SEM imaging there is little difference between the biofilms treated with either 128 or 512 $\mu\text{g/ml}$ NX-AS-401 .

Table 5.11 Comstat analysis of UHW 18 Biofilm CLSM images.

The table is composed of average values from the analysis of three CLSM images that best represented the biofilm under each test condition. Statistical significance was identified by p- values ($p < 0.05$ *, $p < 0.01$ **, $p < 0.001$ ***).

		Biomass ($\mu\text{m}^2/\mu\text{m}^3$)	Thickness (μm)	Roughness Coefficient	Surface Area (μm^2)	Surface / Biovolume Ratio ($\mu\text{m}^2/\mu\text{m}^3$)	% of base layer occupied by Biofilm	Base layer area occupied (μm^2)	
NX-AS-401 Concentration ($\mu\text{g}/\text{ml}$)	0	Syto 9 (Green)	2.25	6.04	0.38	98724	2.41	78.71	14334.76
		Propidium Iodide (Red)	0.03	4.77	1.89	8328	14.39	0.12	22.30
	128	Syto 9 (Green)	0.82***	5.40**	1.05***	52048**	3.48**	44.41***	8088.76***
		Propidium Iodide (Red)	0.07**	5.40**	1.81	14070***	11.37**	3.45***	628.1***
	512	Syto 9 (Green)	0.12***	4.45***	1.84***	11031***	5.08***	7.09***	1291.63***
		Propidium Iodide (Red)	0.002***	3.49***	1.99*	453***	13.55***	0.02**	4.17***

Comstat analysis confirmed that an NX-AS-401 concentration of 128 $\mu\text{g}/\text{ml}$ significantly reduced biomass, thickness, surface area and base layer occupancy of the UHW 18 biofilm. Propidium iodide staining showed an increase in biomass, thickness, surface area and base layer occupancy. Significant decreases in biomass, thickness, surface area and surface to biofilm ratio were seen via both SYTO 9 and propidium iodide in UHW 18 biofilms treated with 512 $\mu\text{g}/\text{ml}$ NX-AS-401.

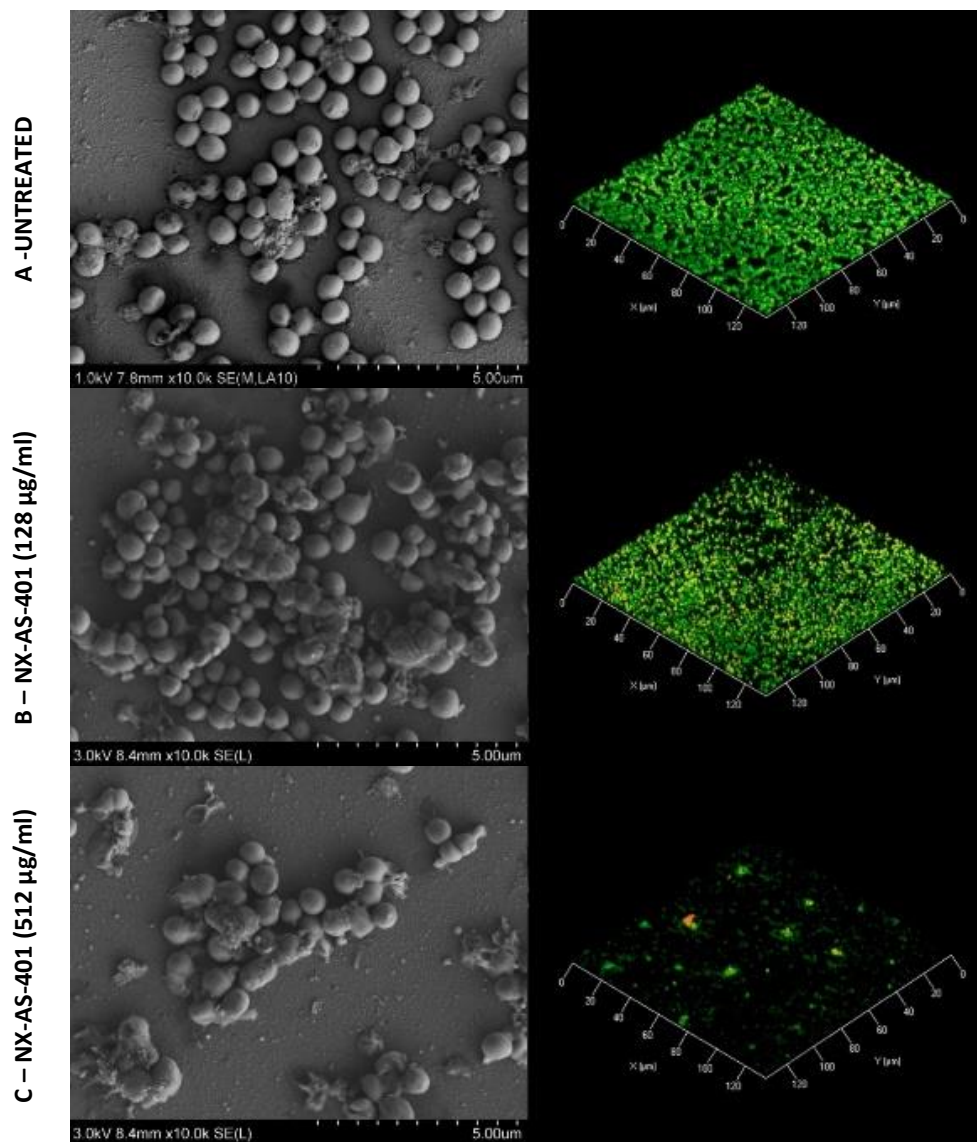


Figure 5.14 Representative SEM (Left) and CLSM (Right) images of UHW 19 biofilms treated with NX-AS-401:

Biofilm disruption of UHW 19 was NX-AS-401 concentration dependent with a low level disruption occurring at 128 $\mu\text{g/ml}$ according to CLSM. In SEM images there was no difference in untreated *S. aureus* biofilms and those treated with 128 $\mu\text{g/ml}$ NX-AS-401. Both SEM and CLSM confirmed NX-AS-401 mediated disruption to biofilm when treated with 512 $\mu\text{g/ml}$ leading to decreased biomass.

Table 5.12 Comstat analysis of UHW 19 Biofilm CLSM images.

The table is composed of average values from the analysis of three CLSM images that best represented the biofilm under each test condition. Statistical significance was identified by p- values ($p < 0.05$ *, $p < 0.01$ **, $p < 0.001$ ***).

		Biomass ($\mu\text{m}^2/\mu\text{m}^3$)	Thickness (μm)	Roughness Coefficient	Surface Area (μm^2)	Surface / Biovolume Ratio ($\mu\text{m}^2/\mu\text{m}^3$)	% of base layer occupied by Biofilm	Base layer area occupied (μm^2)	
NX-AS-401 Concentration ($\mu\text{g}/\text{ml}$)	0	Syto 9 (Green)	3.39	5.40	0.33	109838	1.78	88.50	16117.14
		Propidium Iodide (Red)	0.05	4.13	1.84	11416	12.85	1.14	207.45
	128	Syto 9 (Green)	1.47***	5.08*	0.70**	79461**	2.96*	61.78**	11251.29**
		Propidium Iodide (Red)	0.08*	4.13	1.81	15085**	10.41*	1.22	222.17
	512	Syto 9 (Green)	0.13***	4.13***	1.78***	12099**	5.19***	9.82***	1787.88***
		Propidium Iodide (Red)	0.01**	4.13	1.98*	1302***	7.22***	0.59**	107.47**

Comstat analysis confirmed that an NX-AS-401 concentration of 128 $\mu\text{g}/\text{ml}$ significantly reduced biomass, thickness, surface area and base layer occupancy of the UHW 19 biofilm. Propidium iodide staining showed significant increase in biomass and surface area while surface to biofilm ratio was reduced. Significant decreases in biomass, surface area and surface to biofilm ratio were seen via both SYTO 9 and propidium iodide when UHW 19 biofilms were treated with 512 $\mu\text{g}/\text{ml}$ NX-AS-401.

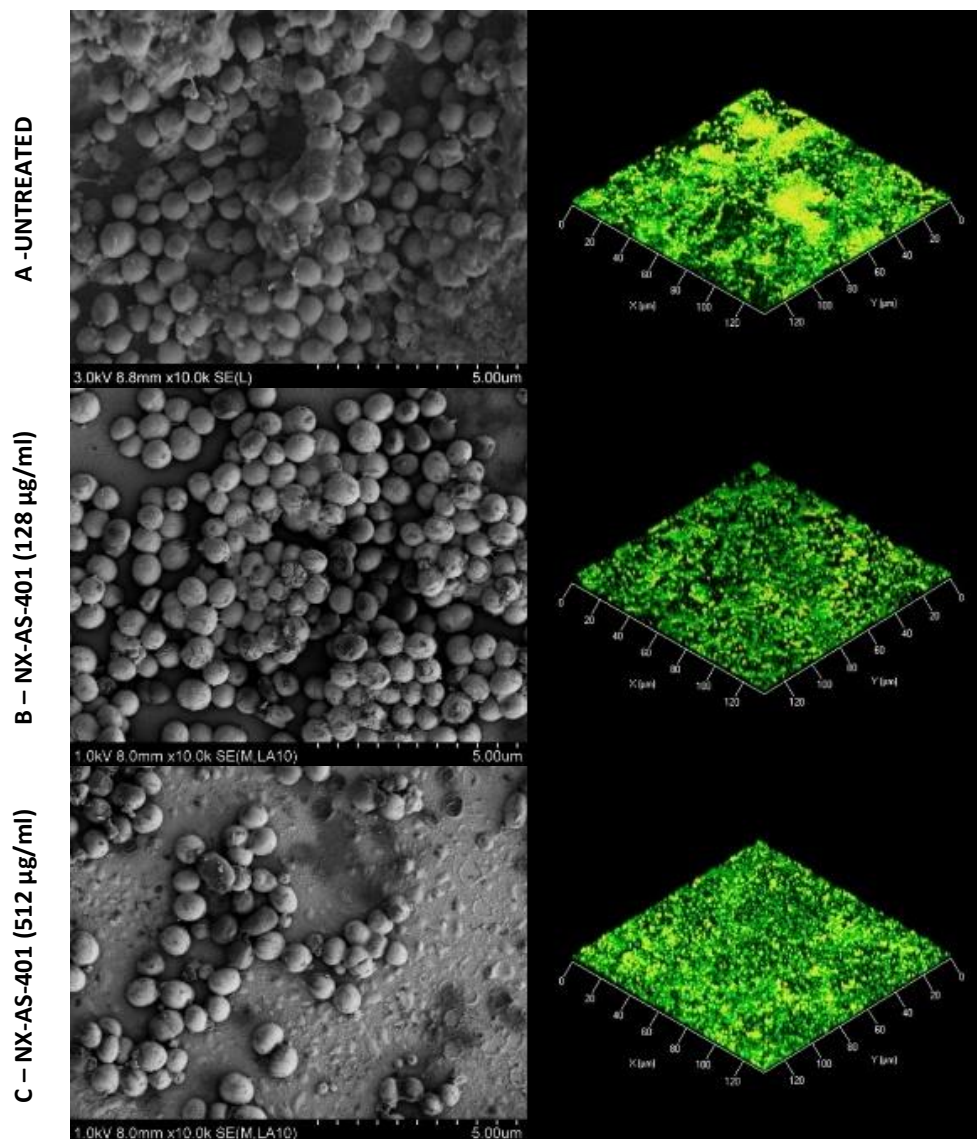


Figure 5.15 Representative SEM (Left) and CLSM (Right) images of CRI 2 biofilms treated with NX-AS-401:

Low-level biofilm disruption of the CRI 2 biofilm occurred at an NX-AS-401 concentration dependent of 128 µg/ml according to CLSM with little difference seen in biofilm structure according to SEM. Biomass reduced at NX-AS-401 concentrations of 512 µg/ml shown in SEM but not CLSM. The SEM images clearly show a reduction in the number of cells, however, there appears to be a coating of extracellular matrix on the substrate surface that may have an effect on live/dead staining of the biofilm.

Table 5.13 Comstat analysis of CRI 2 Biofilm CLSM images.

The table is composed of average values from the analysis of three CLSM images that best represented the biofilm under each test condition. Statistical significance was identified by p- values ($p < 0.05$ *, $p < 0.01$ **, $p < 0.001$ ***).

		Biomass ($\mu\text{m}^2/\mu\text{m}^3$)	Thickness (μm)	Roughness Coefficient	Surface Area (μm^2)	Surface / Biovolume Ratio ($\mu\text{m}^2/\mu\text{m}^3$)	% of base layer occupied by Biofilm	Base layer area occupied (μm^2)	
NX-AS-401 Concentration ($\mu\text{g}/\text{ml}$)	0	Syto 9 (Green)	5.79	5.72	0.03	90209	0.48	99.99	18210.84
		Propidium Iodide (Red)	0.08	4.77	1.78	16733	11.11	7.75	1411.89
	128	Syto 9 (Green)	1.23***	6.35**	0.65***	72126**	3.22***	64.77***	11795.81**
		Propidium Iodide (Red)	0.27***	6.67**	1.48*	39894**	8.05***	0.49***	88.79***
	512	Syto 9 (Green)	1.48***	5.08***	0.72***	64378***	2.40***	55.89***	10177.8***
		Propidium Iodide (Red)	0.23***	4.77	1.48*	34625***	8.37***	12.14***	2211.8***

Comstat analysis confirmed that an NX-AS-401 concentration of 128 $\mu\text{g}/\text{ml}$ significantly reduced biomass, surface area and base layer occupancy of the CRI 2 biofilm, while propidium iodide biomass, thickness, surface area was increased. Significant decreases in biomass, thickness, surface area and base layer occupied were seen in CRI 2. Comparatively biomass, surface area and base layer occupancy was all increased according to propidium iodide, while surface to biovolume ratio decreased.

5.4.6 Reverse Transcription - quantitative Polymerase Chain Reaction (RT-qPCR)

Changes in gene expression were monitored in 48-hour biofilms treated at a range of time points to see whether NX-AS-401 alters the expression of biofilm associated genes (Figures 5.16, 5.17 and 5.18).

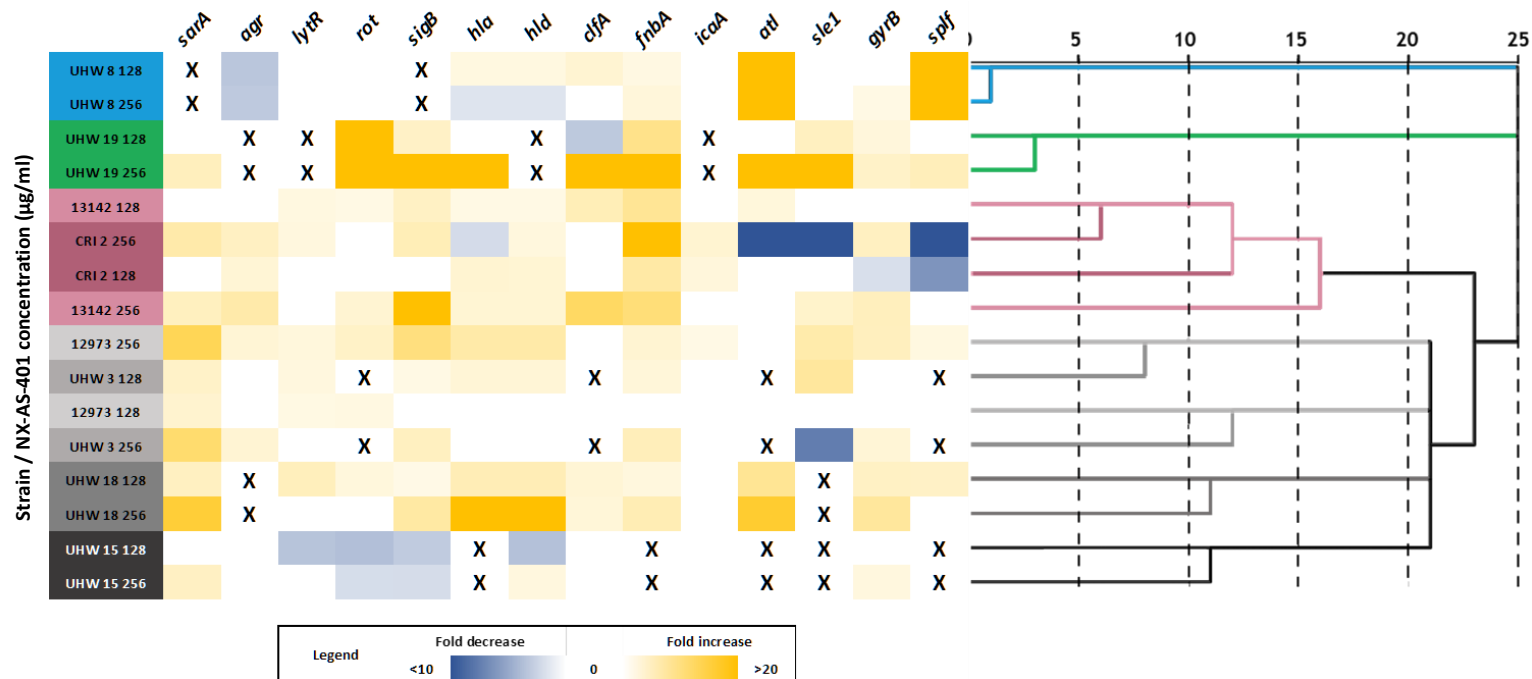


Figure 5.16 Gene expression changes in pre-established 48 hours *S. aureus* biofilms after exposure to 128 or 256 µg/ml NX-AS-401 for two hours.

Changes in gene expression are indicated via colour gradient with white indicating no change in expression and colour intensity increasing as gene expression is increased (Yellow) or decreased (Blue) in comparison to the untreated control. X's indicate primers with an efficiency <90 % after optimization and were deemed to have no target in those *S. aureus* strains. The values on the dendrogram (right) X axis denote squared Euclidean distance and indicate how closely related the cluster are to each other based on RT-qPCR results

According to HCA, at the two hour time-point clusters were strains dependent. Treatment with NX-AS-401 for two hours upregulated expression of most genes in the majority of the *S. aureus* strains used in this project. Noticeable trends include the increased expression of *sarA* and *gyrB* when treated with 256 µg/ml NX-AS-401 in all strains where the primers were efficient. Strains UHW 8, UHW 15 and CRI 2 provided unusual responses as for UHW 8 as *agrA* was down-regulated at both NX-AS-401 concentration while 50 % of the strains have shown no change or an increased at 256 µg/ml. Haemolysin related genes *hla* and *hld* are also downregulated at 256 µg/ml whereas other strains show increased expression or no change. UHW 15 demonstrated an unusual result with downregulation of *lytR*, *sigB*, *rot* and *hld* when treated with 128 µg/ml and decreased *sigB* and *rot* at 256 µg/ml. The biggest expression changes occurred in strains UHW 8 and CRI 2 for the *atl* and *splf* genes which showed an increase and decrease in their gene expression, respectively. There were also trends such as increases in the expression of *agr*, *lytR*, *hla* and *hld* in strains NCTC 13142, NCTC 12973 and CRI 2 when treated 256 µg/ml NX-AS-401. While strains UHW 18 and UHW 19 showed increased expression of *hla*, *atl* and *splf* when treated with 256 µg/ml.

Another interesting result is that in some cases NX-AS-401 concentrations caused opposite responses. For example, in strain UHW 8 concentrations of 128 µg/ml NX-AS-401 causes increased expression of *hla* and *hld* while 256 µg/ml NX-AS-401 caused reduced expression, and this was also seen in UHW 3 for *sle1*.

The opposite was also identified were 128 µg/ml NX-AS-401 causes reduced expression and 256 µg/ml NX-AS-401 caused increased expression of *hld* in UHW 15 and *clfA* in UHW 19.

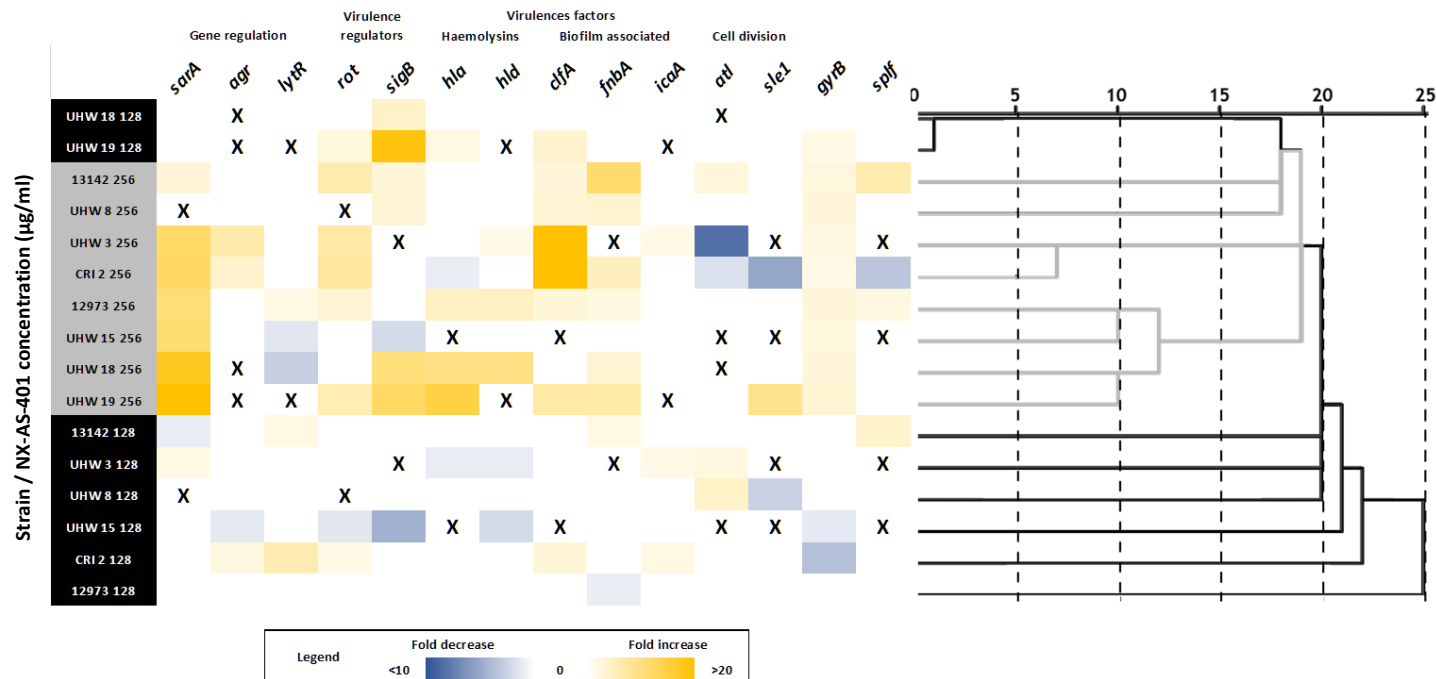


Figure 5.17 Gene expression changes in pre-established 48 hours *S. aureus* biofilms after exposure to 128 or 256 µg/ml NX-AS-401 for four hours. Changes in gene expression are indicated via colour gradient with white indicating no change in expression to and colour intensity increasing as gene expression is up (Yellow) or down (Blue) regulated in comparison to the untreated control. X's indicate primers with an efficiency <90 % after optimization and were deemed to have no target in those *S. aureus* strains. The values on the dendrogram (right) X axis denote squared Euclidean distance and indicate how closely related the cluster are to each other based on RT-qPCR results. Strains treated with 128 µg/ml NX-AS-401 are coloured black while treatment with 256 µg/ml is coloured grey.

Unlike the two hour time point HCA determined that the data is clustered based on NX-AS-401 concentration rather than strain dependently. Changes in gene regulation of isolates treated for four hours include upregulation of accessory gene regulator *sarA* in all strains apart from UHW 8 when treated with 256 µg/ml, upregulation of DNA transcription gene *gyrB* expression in all strains at 256 µg/ml while upregulation of *fnba*, *clfa* and *sigB* was seen in six out of the eight strains. Other genes show cluster specific trends such as the down-regulation of *hld* at NX-AS-401 concentration 128 µg/ml in cluster two and upregulation of *rot* and *hla* in cluster three at NX-AS-401 concentration of 256 µg/ml.

Similar to the two hour timepoint, there were also areas where 128 µg/ml NX-AS-401 caused reduced expression while 256 µg/ml NX-AS-401 caused increased expression of specific genes. This occurred in *gyrB* in strains UHW 15 and CRI 2, *sarA* in NCTC 13142 and in *clfA* of NCTC 12973.

The same effect also occurred in UHW 3 where 128 µg/ml NX-AS-401 causes increased expression and 256 µg/ml NX-AS-401 caused reduced expression of *sle1*. However, the fold change is lower than the two hour timepoint.

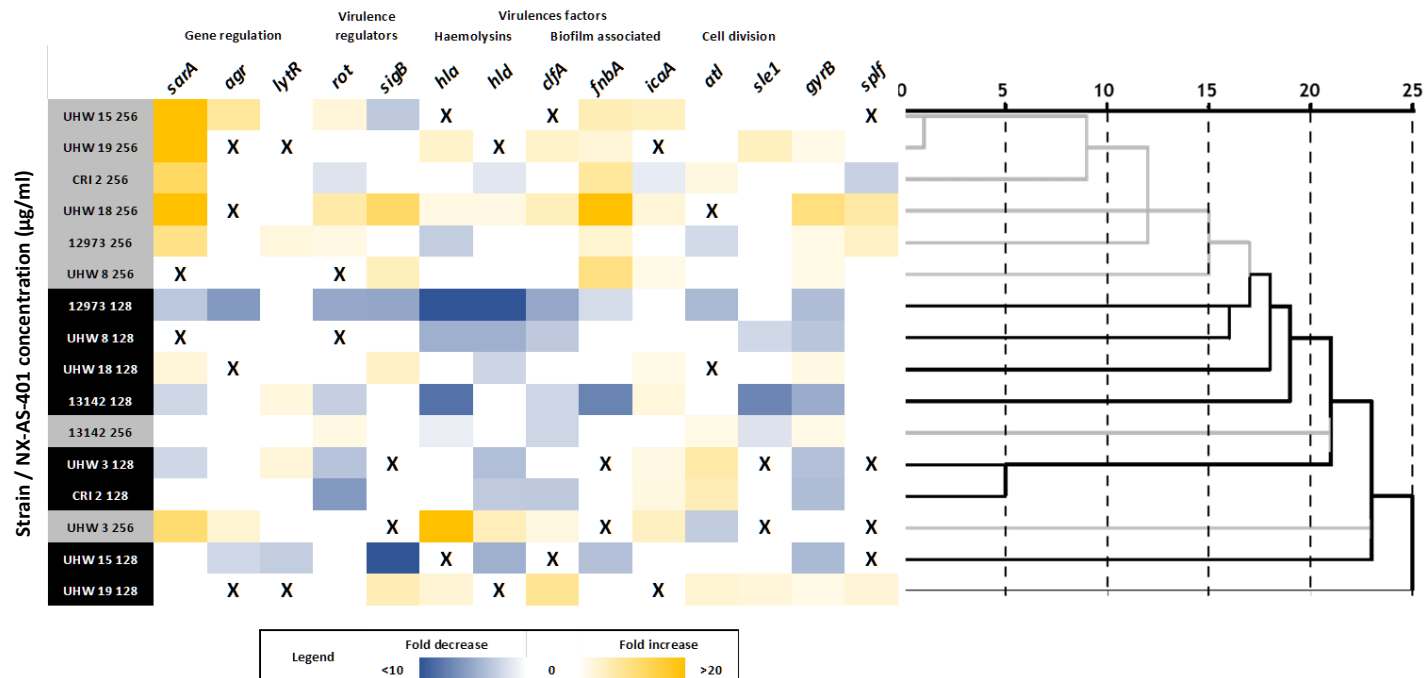


Figure 5.18 Gene expression changes in pre-established 48 hours *S. aureus* biofilms after exposure to 128 or 256 µg/ml NX-AS-401 for four hours. Changes in gene expression are indicated via colour gradient with white indicating no change in expression to and colour intensity increasing as gene expression is up (Yellow) or down (Blue) regulated in comparison to the untreated control. X's indicate primers with an efficiency <90 % after optimization and were deemed to have no target in those *S. aureus* strains. The values on the dendrogram (right) X axis denote squared Euclidean distance and indicate how closely related the cluster are to each other based on RT-qPCR results. Strains treated with 128 µg/ml NX-AS-401 are coloured black while treatment with 256 µg/ml is coloured grey.

Unlike the two hour time point but similar to the 4 hour timepoint HCA determined that the data is clustered based on NX-AS-401 concentration rather than strain dependently .Trends identified in *S. aureus* biofilms treated with NX-AS-401 for 24 hours, include upregulation of accessory gene regulator *sarA* in all strains apart from UHW 8 when treated with 256 µg/ml. NX-AS-401 concentrations of 256 µg/ml caused down regulation of DNA transcription gene *gyrB* expression in six strains, but not in UHW 19 and 18. Trends are also seen in specific clusters such as in cases where all primers were successful (NCTC 12973, NCTC 13142 and CRI 2) and downregulation of both *sigB* and *fnbA* was observed when treated with 128 µg/ml. Both *agrA* and *icaA* were upregulated when UHW three and UHW 15 were exposed to 256 µg/ml NX-AS-401. In strains UHW 18 and UHW 19 where *agrA* primers failed had the most similarity amongst strains, as *gyrB* increased at both NX-AS-401 concentrations 128 and 256 µg/ml, *rot* expression is also increased at 128 µg/ml, while *hla* and *clfa* were increased at NX-AS-401 concentration of 256 µg/ml.

Once again UHW 3 showed that 128 µg/ml NX-AS-401 caused increased expression and 256 µg/ml NX-AS-401 caused reduced expression of *sle1*. The 24 hour timepoint also contains more example of NX-AS-401 concentrations causing opposite responses to gene regulation. NCTC 12973, NCTC 13142 and UHW 3 all demonstrated reduced expression of *sarA* when treated with 128 µg/ml NX-AS-401 and increased expression with 256 µg/ml NX-AS-401. This was also seen with *gyrB* and *sigB* in NCTC 12973 and NCTC 13142 while UHW 3 demonstrated the same effect in *hld*. Additional strains such as UHW 15, UHW 19 and UHW 8 also had the same effect in different genes.

5.5 Discussion

Chronic wound infections with associated bacterial biofilms are difficult to treat due to the production of extracellular matrix, presence of persister cells and increased horizontal gene transfer ^(74, 288). These components inhibit the action of current standard of care antibiotics and allow for infections to persist and deteriorate ^(74, 288).

Current treatment methods vary, with combination therapies or high dose antibiotic lock therapy used for wounds or chronic infection caused by indwelling medical device colonisation ^(218, 342). If antibiotic treatment is not sufficient more invasive procedures such as the removal of indwelling medical devices such as catheter tips, or the removal of infected tissue i.e. debridement is required ^(89, 104).

5.5.1 *S. aureus* biofilm characterisation

The ability of *S. aureus* to form a biofilm varies per strain in terms of mechanism and strength ⁽³⁴⁸⁾ with biofilm formation and maintenance regulated by genes such as staphylococcal accessory gene regulator (*sar*), polysaccharide intercellular adhesin (*ica*) and *hld/RNA* II and III complexes, These are known to be involved in the generation of biofilms both *in vitro* and *in vivo* ⁽¹⁰⁹⁾. Due to this *S. aureus* biofilms can be grouped based on their biofilms forming mechanism and whether it is based on extracellular matrix containing protein, polysaccharide or extracellular DNA (eDNA) ⁽¹⁰⁹⁾. Crystal violet assays can also be employed to identify the biofilm forming strength, indicating how well these strains form biofilm *in vitro* ⁽²⁵¹⁾.

In this chapter all strains formed biofilms via the proteinaceous mechanism and were identified as weak or moderate biofilms according to the OD^{cut} values that identify how strong a bacterial strains form a biofilm using biomass as an indicator (**Table 5.2**).

As discussed in Chapter 1 Section 1.2.3, *S. aureus* biofilm formation is variable and can be based on antibiotic resistance for example, methicillin sensitive *S. aureus* tends to form biofilms with extracellular polysaccharide due to reliance on polysaccharide intracellular adhesin (PIA) production whereas MRSA tends to form more protein based biofilms with increased fibronectin binding protein ⁽¹⁰⁹⁾. This seems to be caused by suppression of the production of PIA when the methicillin resistance is introduced into the organism, however the full mechanism for why this occurs is unknown ⁽¹⁰⁹⁾.

Since five of the eight strains used in this project were MSSA it is unusual that all have been identified as proteinaceous biofilm formers and were unaffected by sodium metaperiodate. This could be due to the fact that all strains are genetically similar as indicated in Chapter 4 (**Section 4.5.4**) and are protein-based biofilm formers. This genetic similarity could explain why all strains were identified as weak-moderate biofilm formers as polysaccharide is identified as the stronger biofilm forming mechanism in *S. aureus* ⁽³⁴⁹⁾. The lack of polysaccharide formation and weak biofilm formation may be caused by their growth in MHB without additional supplementation such as NaCl or glucose. Additionally *in vitro* *S. aureus* biofilm development is often dependent on media composition ⁽³⁵⁰⁾ with additional supplementation such as 2 % NaCl or glucose beneficial for MSSA and MRSA biofilm development respectively ⁽¹⁰⁹⁾. Media composition can also affect biofilm associated gene expression, for example Ca²⁺ is required for fibronectin protein gene (*fnb*) expression ⁽⁹²⁾, Supplementation was not used in this project as the aim was to identify the effects of NX-AS-401 without adding additional variables.

The effects of media on the biofilm phenotype of *S. aureus* should have been confirmed by the Congo Red agar method, this utilised a saccharide supplementation with *S. aureus* strains that produce polysaccharide base biofilms forming black slime like colonies ⁽⁸⁰⁾. This could be performed in future studies along with tests in more physiologically relevant media such as artificial wound fluid ⁽³⁵¹⁾. This would identify the impact of additional host components could result in changes to *S. aureus* biofilm formation as well as NX-AS-401 efficacy.

Overall the interaction of *S. aureus* extracellular matrix components is not fully understood, with both polysaccharides and protein having independent function in biofilm formation and eDNA commonly found in all biofilm types ⁽³⁵²⁾.

5.5.2 The effects of NX-AS-401 on biofilm formation and disruption.

When treating biofilms prophylactic options are the best, by preventing the biofilm from forming you not only manage the present infection but may prevent subsequent re-infection from persister cells and practice antibiotic stewardship by limiting antibiotic use ^(89, 104). However, it is not always possible to prevent biofilm formation,

therefore the effects of novel antibiotics on established biofilms must also be considered ^(89, 104).

In Figures 5.2 to 5.4 the effects of NX-AS-401 on biofilm inhibition identified the minimum biofilm inhibition concentration (MBIC) of NX-AS-401 to be 32 -64 µg/ml for all eight *S. aureus* strains. This is different from the results seen in Chapter 3 (**Section 3.4.2**) with the NX-AS-401 predecessor NBR 26-6A, which only demonstrated biofilm inhibition at a concentration of 128 µg/ml. This suggests that the increase in the percentage of ajoene within NX-AS-401 may be responsible for the anti-biofilm effects associated with NX-AS-401.

Figure 5.2 also shows that all *S. aureus* strains produced a crystal violet reading at a concentration of 2048 µg/ml which was identified as the MBC in Chapter 4 (**Section 4.5.2**), this reading was not caused by the presence of viable *S. aureus* cells but by the staining of extracellular material and adherent cell debris as demonstrated in Figure 5.4 where no viable cells were discovered. This indicates that at an NX-AS-401 concentration of 2048 µg/ml *S. aureus* is unable to produce a biofilm and is eradicated as seen in the MBC.

The antibiofilm effects of ajoene against *S. aureus* have been identified previously, however, the study utilized pure ajoene in a 1:4 ratio of E and Z isomers ^(194, 241), this is a 25 % increase in the Z isomer over NX-AS-401. The Z-isomer of ajoene has been documented as the more active isomer which may explain differences between the MBIC/MBEC of ajoene seen in this experiment and the work by Jakobsen *et al* ^(194, 241). The antibiofilm effects have also been seen in alcohol based ⁽³⁴⁷⁾ and aqueous garlic extracts where anti-biofilm effects have been identified but at higher concentrations compared to NX-AS-401, for example 20 mg/ml for alcoholic based garlic extracts ⁽³⁴⁷⁾ and a concentration of 16 µg/ml aqueous garlic extracts caused ~55 % biofilm inhibition ⁽²¹⁸⁾. The greater efficacy may be due to the presence of multiple anti-biofilm molecules such as allicin, alliin and potential synergy between them ^(210, 219).

A sub-MIC dose of NX-AS-401 in its current formulation can prevent the biofilm formation of *S. aureus*, this would make NX-AS-401 a useful compound for prophylactic wounds such as surgical sites and could prevent the development of both acute and chronic wound infections similarly to topical antibiotics and antiseptics ⁽³⁵³⁾.

The effects of NX-AS-401 on pre-established biofilms was identified in Figures 5.4-5.6, as previously identified in Chapter 3 (**Section 3.5.2**) *S. aureus* biofilms grown over 24 hours were weakly formed and prone to destruction via pipetting, so NX-AS-401 48 hour biofilms were utilized for greater density and biofilm strength and were used in all experiments.

Figure 5.4 demonstrated that the minimum biofilm eradication concentration that could eliminate 50 % of the biofilm (MBEC⁵⁰) varied per strain, with MBEC values between 256 and 1024 µg/ml. This differed from the results obtained with formulation NBR 26-6A (**Chapter 3, Section 3.4.4-5**) where concentrations of >32 µg/ml disrupted established biofilms. Unlike inhibition which seemed linked to ajoene content, biofilm disruption may be mediated by the presence of the small, unidentified compounds present within all NX-AS-401 formulations. This is likely due to the small molecules ability to penetrate into the deeper layers of the biofilm by avoiding the electrostatic inhibition caused by the extracellular polymeric substances or by using the biofilm “water” channels as seen with other small molecules ^(89, 90). This observations means that further investigation should be performed into the smaller components of NX-AS-401 and their potential antimicrobial /antibiofilm activity.

This was not completely consistent in the metabolic assay, (**Figure 5.5**) where the MBEC was identified as 1024 µg/ml for all eight *S. aureus* strains and metabolic activity was increased at sub-MBEC⁵⁰ concentrations. Unfortunately for most strains the colour change that resulted from resazurin metabolism was beyond the limit of detection for the spectrophotometer (Fluostar, BMG) but based on the data obtained for UHW 15 (**Figure 5.5 E**) and the trends seen at concentrations 4-16 µg/ml in strains NCTC 12973, UHW 18 and CRI 2 (**Figure 5.5 B, F and G**) it appears that metabolism increased alongside the concentration of NX-AS-401 up until 512 or 1024 µg/ml. This corresponds with studies where increased metabolism is seen in the presence of sub-MIC antibiotics or in the presence of toxic compounds ^(25, 113, 354). This was also seen in Chapter 3 (**Section 3.4.4**) and still likely caused by the presence of NX-AS-401 inducing a stringent stress response, increasing metabolism through activation of efflux pumps. This reaction has been seen in *S. aureus* planktonic cultures and biofilms challenged with antibiotics compounds previously ^(25, 113, 291, 354). In some cases an increase in biofilm metabolism can be caused by an increase in the production of extracellular

matrix as a means to prevent the action of antibiotics ⁽²⁵⁾. However, since an increase was identified in metabolism and not in biomass it appears the former option is more likely and that while metabolism was increased, NX-AS-401 did not influence the production of extracellular matrix as confirmed via SEM.

The increased metabolic activity was also not likely to be related to the division of *S. aureus* cells as Figure 5.6 indicates that cell numbers were not significantly ($p < 0.05$) increased or decreased in comparison to the untreated control at NX-AS-401 concentrations less than the MBEC⁵⁰. TVC counts shown in Figure 5.6 also identified a lower MBEC⁵⁰ than both crystal violet and resazurin metabolism with concentration between 256-512 $\mu\text{g/ml}$ identified as the MBEC⁵⁰.

These experiments have shown that a single method cannot be used to quantify the effects of an antibiotic gradient against *S. aureus* biofilms. All three methods should be taken into consideration to understand the effects of an anti-biofilm agent. In this case it showed that NX-AS-401 can reduce cell number and biomass at concentrations between 256-512 $\mu\text{g/ml}$ for all biofilms studied, however it caused an increase in *S. aureus* metabolism. While sub-MIC doses can prevent biofilm formation, NX-AS-401 concentrations need to be double or quadruple the MIC (128 $\mu\text{g/ml}$) to disrupt established biofilms.

In comparison, current standard of care antibiotics often requires between 100-1000-fold increase in concentration above the MIC to elicit an effect against biofilms. This is due to biofilms specifically preventing the action of antibiotics in multiple ways including ⁽⁷⁴⁾, production of extracellular matrix which sequesters antibiotics via electrostatic interaction thus preventing antibiotics from reaching their targets ⁽⁹²⁾. The extracellular matrix and proximity of cells within a biofilms can also increase transfer of antibiotic resistance genes ⁽¹⁶⁷⁾. Formation of biofilms also leads to a reduction in cell metabolism and division preventing the influx of antibiotics into the target cell and reducing availability to the target site ^(317, 346).

These combined biofilm resistance strategies can vastly reduce antibiotic efficacy; therefore, a higher concentration is required to reach the cells and overcome these barriers. It is unusual that NX-AS-401 only requires an increase of two or four times the MIC to elicit an effect. This indicates that the molecule may not be inhibited by the

extracellular matrix as much as other antibiotics or may act on the extracellular matrix itself. This could be due to the smaller size of ajoene that has a molar mass of 234.4 g/mol in comparison to drugs such as gentamicin and clindamycin that have molar mass of 477.6 g/mol and 425 g/mol respectively ⁽³¹⁵⁾. The size difference could allow ajoene to move down the water channels within the biofilm matrix. These channels are often 10 µm across and allowing for the movement of nutrients further into the deeper layers of the biofilm, and therefore allow for compound penetration ⁽³⁵⁵⁾. However this has yet to be proven as studies that have identified small molecules with antibacterial effects have not tested if the channels are used ^(88, 356). It is known that small molecules can pass through the channels unimpeded as this is part of the bacterial biofilms quorum sensing system for both Gram-negative and Gram-positive organisms ^(76, 88).

The use of small molecules and nano-particles to assist in bacterial biofilm eradication is a common strategy and an effective one with many small molecules such as antimicrobial peptides and nano-particles of gold or silver have been used to disperse established biofilms ^(206, 340, 355).

Compounds that are structurally similar to NX-AS-401 have shown similar effects on biofilm formation with garlic extracts and individual compounds such as allicin able to inhibit biofilm formation in both Gram-positive and Gram-negative organisms ^(194, 206, 215, 226). The closest example for NX-AS-401 is the study by Jakobsen *et al* ⁽²⁴¹⁾, that demonstrated that ajoene caused down-regulation of the gene encoding haemolysin delta (*hld*). The *hld* gene is not only responsible for the production of haemolysin but serves as a molecular switch as it is part of the gene that codes for RNA III an important molecule in the regulation of exoproteins and cell wall-associated proteins important for biofilm formation and maintenance ^(64, 241). This may be a potential mechanism for NX-AS-401 based on its high ajoene content but since NX-AS-401 contains other compounds there could be multiple *S. aureus* pathways affected. It has been shown that other garlic extracts have been able to inhibit or disrupt *S. aureus* biofilms, for example allicin has proven highly effective with MBICs identified between 6 -12 µg/ml ^(180, 226). In contrast, other garlic extracts have shown potential antibiofilm effects at concentrations of 32 µg/ml ⁽³⁵⁷⁾. Both allicin and whole garlic extraction have demonstrated greater efficacy than NX-AS-401 in the disruption of biofilms, however

like NX-AS-401 the mechanism by which they eliminate *S. aureus* biofilms have yet to be determined. Molecules such as allicin have also shown low molecular stability and the molecules may have already degraded before reaching the deep layers of the biofilm ⁽²³¹⁾. The instability also makes them difficult to use clinically as they cannot be stored effectively ⁽²³¹⁾. The anti-biofilm effects of the sulphonamide class of antibiotics, that contain similar functional groups to NX-AS-401, have also never been determined since it is no longer employed clinically.

In terms of clinical relevance these results indicate that NX-AS-401 may have a role in the treatment of infections which have a biofilm component, however further investigations into how NX-AS-401 affects biofilm and what concentrations of NX-AS-401 are non-toxic to the host would need to be carried out. This could require the employment of both 2D and 3D cell models as well as animal studies to identify the toxic concentrations of NX-AS-401.

5.5.3 Antibiotic Interactions

Identifying whether the synergy displayed between NX-AS-401 and standard of care antibiotics against planktonic cells (**Chapter 4, Section 4.4.5**) was reproducible in biofilms was problematic. Since biofilms cannot be measured by standard light spectroscopy, measuring changes in biomass and metabolism are taken from crystal violet staining or metabolic assays, respectively. These methods are incompatible with the Bliss model and MacSynergy II software ^(255, 298). These results are also difficult to interpret in a checkerboard assay as metabolic activity may increase at lower NX-AS-401/antibiotic concentration due to an antibiotic induced stress response seen in Figure 5.5, that can mask the effects of NX-AS-401 and prevent identifying if cells are eradicated or the biofilm is dispersed ⁽²⁹⁴⁾. Crystal violet staining can also provide difficult to interpret results as it stains extracellular matrix and dead cells which can falsely indicate the presence of biofilm such as those seen in Figure 5.1 ⁽⁷¹⁾. TVC counts were the best representative of both number the of viable cells, however, this method does not detect whether combination therapy causes dispersal of the biofilm as the removal of media and washing steps would remove any non-adherent biofilm cells.

Despite these issues TVC counts were employed to estimate whether NX-AS-401 displays the same synergistic interactions against *S. aureus* biofilms as it does towards planktonic cells. If this experiment were repeated, TVC counts would also be performed on the biofilm supernatant to see whether overall cell numbers were reduced and whether combination therapies resulted in both dissemination and cell death.

Only three antibiotics were used for biofilms synergy testing, these included gentamicin that was synergistic with NX-AS-401 on all strains, tetracycline which was the only antibiotic to overcome a resistance mechanism, and ceftiofur did not demonstrate any synergy in planktonic studies. The combination therapies used sub-MBEC concentrations and were utilized for both NX-AS-401 and antibiotics in combination therapies (**Antibiotic MBEC are provided in Appendix 1.2**). These tests indicate that NX-AS-401 was synergistic against biofilms as all strains exposed to combinations of NX-AS-401 with either gentamicin or tetracycline caused a significant ($p < 0.05$) reduction in the number of viable cells or caused complete biofilm eradication, as seen with strains UHW 19 and CRI 2. This result is unusual for UHW 19 as it had demonstrated resistance against tetracycline, however NX-AS-401 and tetracycline synergy against UHW 19 was identified via the Bliss model (**Chapter 4, Section 4.5.5**). The results for NX-AS-401 in combination with ceftiofur showed seven of the eight *S. aureus* isolates demonstrated significant synergy. Strains NCTC 13142, UHW 3 and CRI 2 also demonstrated synergy despite resistance to ceftiofur due to the presence of the *mecA* gene. Out of all the *S. aureus* strains used in this chapter only UHW 8 demonstrated an indifferent response to combination exposure to NX-AS-401 and ceftiofur. This is different to what was seen in planktonic studies where no synergy between NX-AS-401 and ceftiofur was identified in both FICI and Bliss calculations (except in strain UHW 18).

Antibiotic synergy between NX-AS-401 and ceftiofur in *S. aureus* biofilm may be caused by reduced expression of *mecA* and therefore the synthesis of PBP2A. It has been shown that the presence of *mecA* within an *S. aureus* strain can change biofilm formation as it becomes reliant on fibronectin binding protein rather than polysaccharide intracellular adhesin and this change in biofilm structure may lead to a vulnerability to ceftiofur ⁽¹⁰⁹⁾. However, this would require further investigation,

utilizing RT-qPCR to look for expression changes in *mecA* and the genes for fibronectin binding protein and polysaccharide intercellular adhesin.

These results indicate interactions of NX-AS-401 with current standard of care antibiotics may also occur against biofilm, and in the case of ceftiofur to greater effect than seen in planktonic cells. While synergy against planktonic phase cells has been noted for other garlic-based components ^(230, 232, 340) and ajoene, no studies have focused on the potential synergy of garlic-based compounds and antibiotics against biofilms. Neither the planktonic or biofilm studies have identified antagonism between NX-AS-401 and any of the tested antibiotic classes, this indicates that the mechanism of action for NX-AS-401 does not inhibit the action of the other antibiotic classes tested so far.

Understanding the mechanism of action for NX-AS-401 would also increase the likelihood of using NX-AS-401 as a topical antibiotic if utilized in combination therapies with already used topical agents such as mupirocin and fusidic acid against MRSA ⁽¹⁵⁾. Since the synergistic effects were seen against planktonic cells (**Chapter 4, Section 4.4.8**) and biofilms (**Chapter 5, Section 5.5.3**) it would imply that a combination NX-AS-401 and antibiotic topical therapy could be used against acute wounds and due to its strong antibiofilm effects, chronic infections.

In order to understand the clinical relevance of the synergy indicated, further work is also required to identify the toxicity of NX-AS-401 and whether the combination therapies can be employed against cell lines and animal models.

5.5.4 Scanning Electron Microscopy (SEM) and Confocal Laser Scanning Microscopy (CLSM) Imaging

In these experiments *S. aureus* biofilms were pre-established onto glass coverslips rather than the tissue culture treated plastic used in the biofilm inhibition and biofilm disruption experiments. Therefore, the biofilm strength differs in comparison to those identified in Table 5.2, for example strains NCTC 12973 (**Figure 5.9**), UHW 8 (**Figure 5.11**) and CRI 2 (**Figure 5.15**) formed the thickest biofilms according to both SEM and CLSM, this was confirmed via Comstat analysis where these strains occupied >95 % of the base layer (**Tables 5.6, 5.8 and 5.12**). This is likely due to the substratum effect and

the ability of bacterial strain to form a biofilm dependent on the surface and whether it is hydrophilic/hydrophobic ^(71, 73).

SEM imaging indicated that biofilms produced by all *S. aureus* strains apart from strains UHW 8 (**Figure 5.11**) and CRI 2 (**Figure 5.15**) were reduced when treated with 64 - 128 µg/ml NX-AS-401, with biomass further reduced when concentrations were increased to 256 µg/ml for UHW 3 (**Figure 5.10**) and 512 µg/ml for all others strains apart from UHW 8. SEM images also confirmed that NX-AS-401 exposure did not result in any obvious morphological changes to *S. aureus* cells. While there were a few cells with different morphology in NCTC 12973 (**Figure 5.9**), these were probably caused by dehydration of the SEM samples. However, in future to confirm whether the changes in NCTC 12973 cells were caused by NX-AS-401 or SEM sample preparation further microscopy techniques could be employed such as atomic force microscopy.

In these tests the 2 imaging methodologies demonstrated the same results for strains NCTC 12973, UHW8 and UHW 15. In other strains there were discrepancies between SEM and CLSM. In NCTC 13142, UHW 3 and UHW 19 there was no disruption seen at the quarter MBEC concentrations according to SEM, however there was disruption seen in CLSM. In strain UHW 18 the SEM samples show much greater disruption than the CLSM samples when the biofilm was treated with 128 µg/ml NX-AS-401. Similarly strain CRI 2 shows greater disruption in SEM when treated with NX-AS-401 at a concentration of 512 µg/ml in comparison to CLSM images.

The different results are likely due to different sample preparation techniques, with SEM requiring fixation and live/dead staining utilising multiple wash steps. Results may also vary as SEM requires taking multiple images around the sample and determining the level of disruption visually, whereas CLSM and live/dead staining allow for large sections of the sample to be taken and analysed. Strain specifically, the anomalous result for CRI 2 was likely due to the live/dead stain being retain in the extracellular products that have coated the substrate as seen in the SEM images (**Figure 5.15**).

While most strains displayed biofilm disruption and correlated with increases in NX-AS-401 concentration, two strains provided different results. SEM and CLSM results for CRI 2 showed that biomass remained similar for both untreated control and biofilms

treated with 128 µg/ml NX-AS-401 while UHW 8 had an increase in biofilm when treated with sub-MBEC⁵⁰ NX-AS-401 concentration of 256 µg/ml.

SEM indicated that NX-AS-401 caused biofilm dispersal but could not identify any if it also caused *S. aureus* cell death. CLSM was performed with live/dead staining and analysed using Comstat 2.0 to determine if NX-AS-401 caused *S. aureus* cell death. Live/dead staining utilised two different fluorescent dyes, SYTO 9 and propidium iodide (PI) which both bind to DNA ⁽³⁵⁸⁾. When bound to DNA both dyes provide greater fluorescence with PI having greater affinity for DNA and should provide a stronger signal than SYTO 9 once bound to DNA ⁽³⁵⁸⁾. However, PI cannot enter viable cells and therefore can only bind with the DNA within permeable cells or eDNA within the extracellular matrix ⁽³⁵⁸⁾ which allows the determination of the percentage of live to dead cells and the presence of eDNA within the matrix.

As seen with SEM in all strains apart from UHW 8 (**Figure 5.11**) and CRI 2 (**Figure 5.15**) a decrease in both biomass according to SYTO 9 and PI occurred when biofilms were treated with NX-AS-401. For strains NCTC 13142, NCTC 12973, UHW 3, UHW 15, UHW 18, UHW 19 and CRI 2 (**Tables 5.6 – 5.8 & 5.10 – 5.13**) biomass was reduced by >90 % when treated with 256 - 512 µg/ml according to SYTO 9 stain and biomass was decreased by >80 % in these strains according to PI. This indicates that a majority of the biofilm was removed when treated with NX-AS-401. The impact of NX-AS-401 on cell death is difficult to determine as parts of the biofilm that have broken away were washed away during the staining process so whether they were alive, or dead could not be determined. In the biofilm that remained there was a decrease in signal from both SYTO 9 and PI in relation to the positive control, this implies that while NX-AS-401 was able to reduce biomass it may not increase cell death. This is confirmed using the SYTO 9 to PI ratio that did not increase for any of the strains apart from NCTC 12973 and UHW 8, for NCTC 12973 there is an increase in dead cells at sub-MBEC⁵⁰ NX-AS-401 concentration of 128 µg/ml (**Figure 5.9 B**) which is the only incidence of increased cell death caused by NX-AS-401. These findings do not match the TVC results obtained in Section 5.4.3, but this may be due to the different surfaces in each experiment.

UHW 8 (**Figure 5.11 and Table 5.9**) demonstrated an increase in biomass when treated with sub-MBEC⁵⁰ NX-AS-401 concentration of 128 µg/ml. However, while overall biomass increased the largest increases occurred in the PI stained portions of the

biofilm. The 128 µg/ml was ~15 times higher, surface area was ~10 times higher and the biofilm was 0.6 µm thicker than the positive control. This indicates that when NX-AS-401 treatment is sub-optimal it could cause an increase in biomass most likely caused by dead cells, debris, or an increase in extracellular matrix. In strain UHW 8 exposure to sub-MBEC⁵⁰ NX-AS-401 concentration may have caused a shift in biofilm phenotype and more eDNA is either present or produced. An increase in eDNA would explain the increase of PI stain in Figure 5.10 B. There is also a suggestion that eDNA may protect the degradation of the extracellular proteins, therefore an increased presence may be for protection of the biofilm ⁽³⁵⁹⁾. This could be examined by using DNase on UHW 8 biofilms and staining with crystal violet to see if it has the ability to destroy the biofilm, other methods could use other DNA specific fluorescent dyes such as cell impermeant TOTO-1 and CLSM to confirm the presence of extra eDNA ⁽³⁶⁰⁾.

These results confirm that NX-AS-401 was capable of reducing *S. aureus* biofilm regardless of the surface it was adhered too, however these techniques did not assist in specifying whether NX-AS-401 has an effect on the matrix or bacterial cells. SEM did not show any changes in cell morphology, such as membrane depressions or holes within the membrane seen with other antibiotics such as penicillins, lincosamides and macrolides ⁽³⁶¹⁾. There were also no observable changes in cell division, such as a high number of cells arrested during the final separation stage of division as seen with other naturally derived compound such as manuka honey ⁽¹⁹⁸⁾.

Unfortunately, the biofilms formed were not thick enough to determine how well NX-AS-401 can penetrate into a biofilm. If the experiments were repeated a different media such as artificial wound fluid or additional MHA supplementation would be used to allow for greater biofilm formation. The development of a more stratified biofilm combined with CLSM can then be used to identify how NX-AS-401 permeates through the biofilm layers. These techniques have been used with other antibiotics such as vancomycin to identify whether glycopeptides can reach the biofilm base layer ⁽³⁶²⁾.

One potential mechanism of action for NX-AS-401s anti-biofilm properties may be that it acts on the extracellular matrix, causing dissemination. This would be related to the hypothesis that NX-AS-401 interferes with proteins, since all biofilms in this experiment produced protein based biofilms.

In both the biofilm disruption experiments (**Section 5.4.3**) and CLSM biofilm was reduced but cell numbers remained high, the current theory is that NX-AS-401 may cause biofilms to break apart but the cells that are removed may still be alive. Current antibiofilm agents tested for their ability to target the biofilm matrix have included the use of enzymes, antibodies and phages that break down polysaccharides, protein or nucleic acids ⁽⁸⁹⁾ as are displayed in Figure 5.19.

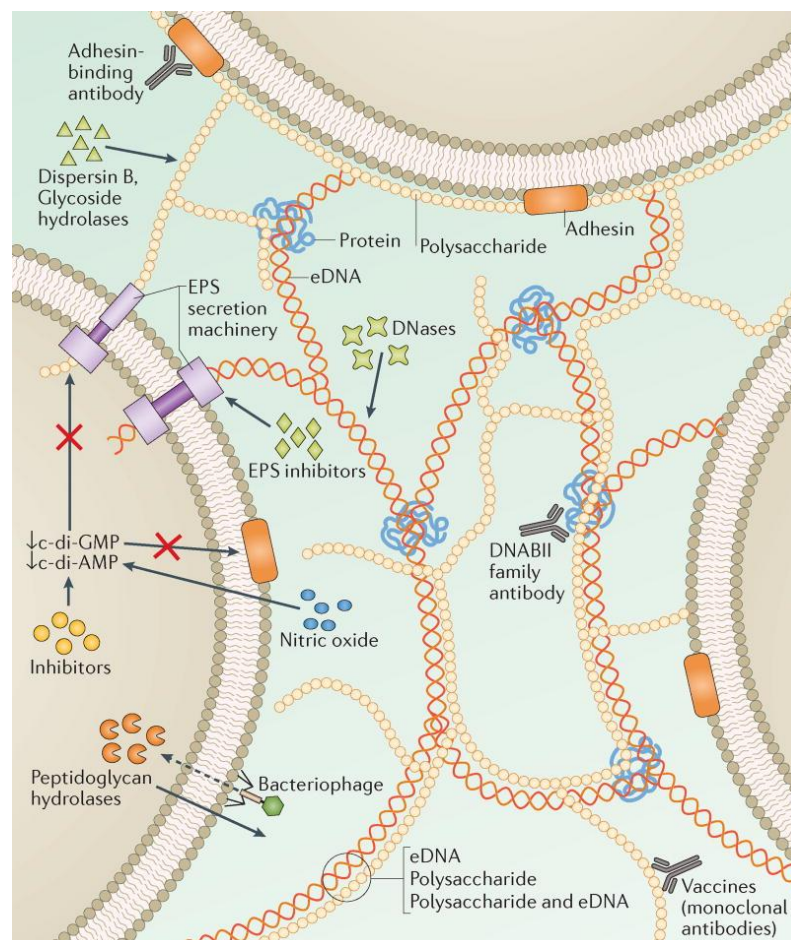


Figure 5.19 The components in an extracellular biofilm matrix and potential biofilm matrix disruptors. Image obtained from Koo *et al* 2017 ⁽⁸⁹⁾.

Figure 5.19 demonstrates the multiple pathways that can be disrupted in *S. aureus* biofilm matrix by anti-biofilm agents. It also shows the role of proteins with the biofilm, as they serve as a binding mechanism between eDNA and polysaccharide as well as forming their own bridges. Figure 5.19 only identifies one mechanism for protein degradation and that is the use of antibodies. This is not the only known mechanism as proteases can also be used, the major issue with this approach is finding

highly specific enzymes that will only interact with the specific bacterial proteins and not interact with host proteins causing an adverse reaction ⁽³⁴⁵⁾.

The removal of proteins and eDNA from the biofilm matrix is difficult as both seem interconnected. Currently there are no drugs that specifically target biofilm associated proteins unlike polysaccharides which have drugs such as dispersin B. This may be due to lack of demand, as most bacteria form polysaccharide biofilms, or due to protein targeting drugs interfering with host proteins.

5.5.5 Reverse transcription - quantitative polymerase chain reaction (RT-qPCR) of biofilm associated *S. aureus* genes.

The time points chosen for RT-qPCR in this project were selected to show initial the reaction of *S. aureus* to NX-AS-401. Time points were selected from TVC counts and growth curves (**Chapter 4, Section 4.4.4-5**) where cell growth was altered due to the presence of NX-AS-401. Inhibition of *S. aureus* growth primarily occurred between 2-4 hours for all eight strains so these time points were chosen as well as a 24 hour timepoint to identify if gene expression returned to normal.

S. aureus 16S rRNA gene was used as a housekeeper gene to standardize relevant expression based on usage in many studies ^(70, 292, 324, 363). In this work, no changes in 16S expression were seen between untreated controls or NX-AS-401 treated biofilms at 2, 4 and 24 hour time points. The 16s gene is often selected as a housekeeper gene as it is easily identifiable, the genome can maintain multiple copies and its expression tends to be stable under most testing conditions ⁽³⁶⁴⁾. DNA gyrase b (*gyrB*) was initially utilized as a secondary housekeeper, due its stable expression, however *gyrB* expression was altered causing an increase at two and four hours and decreased expression at 24 hours ⁽³⁶⁵⁾.

Strains were divided into clusters based on HCA analysis, however there were flaws to this method. HCA is often employed where there are only 2 variables, the target gene and the strain. Additional concentrations as a variable may have caused clustering to occur via concentration gradients. Additionally HCA can only be performed on complete data sets, in areas where primers were unsuccessful against a strain and no

results were obtained a zero value was placed otherwise the analysis could not be performed. It was not determined how the 0 value would cause problems during clustering as the zero would denote no change in gene expression which could not be proven using these primers. HCA is also often employed against larger data sets to identify trends, this may explain why this method of analysis did not identify trends in these experiments.

RT-qPCR was performed to monitor changes in the expression of biofilm associated genes, however *S. aureus* gene expression control is complex, with regulators such as *sarA*, *agrABCD*, *lytR/S* and sensor histidine kinase (*sae*) affecting multiple genes. A regulatory pathway provided in Figure 5.20 demonstrates how the genes studied here affected transcription of relevant target genes. However, this is not a complete regulatory map and there are other factors that can alter expression of these genes.

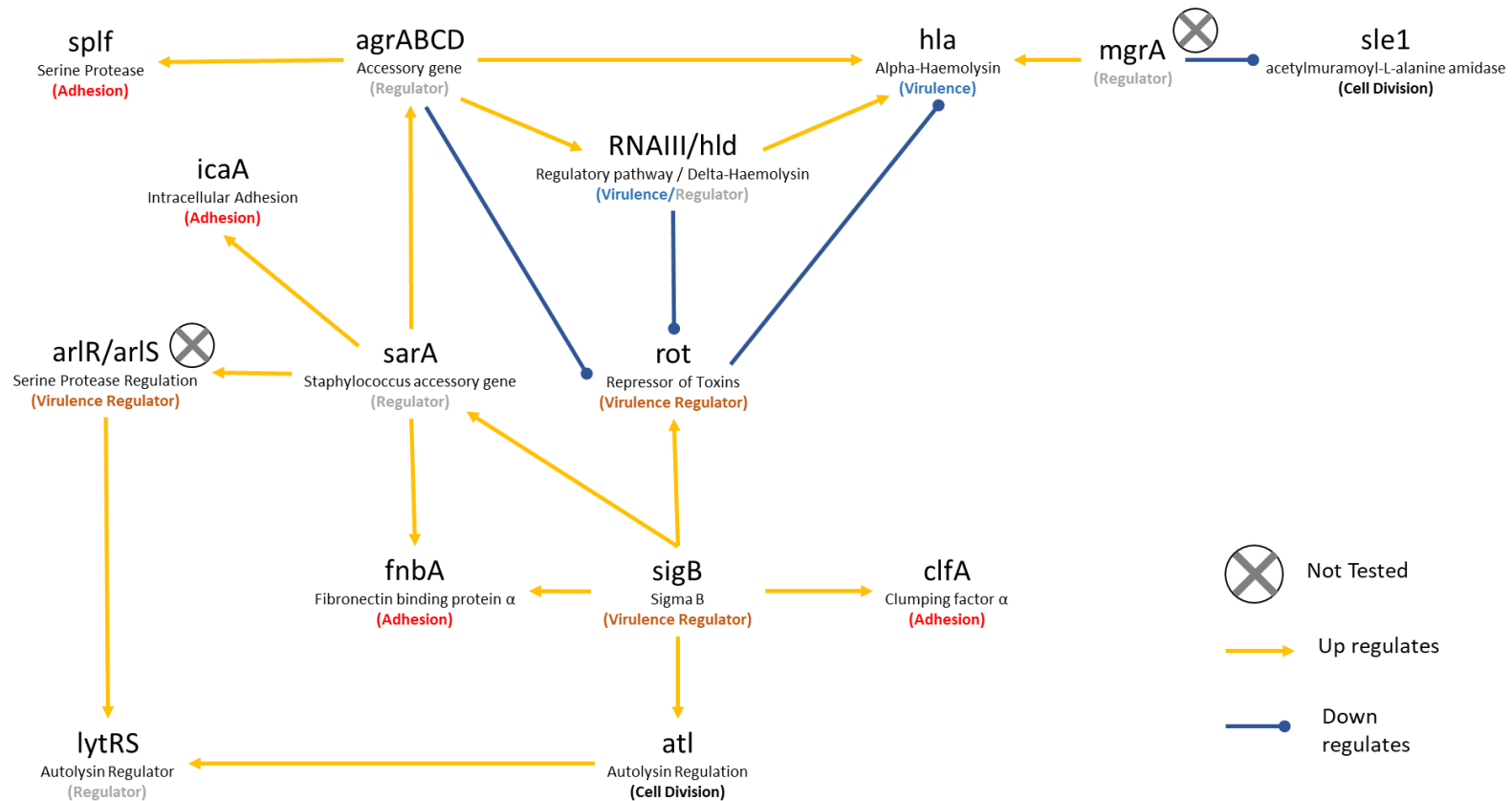


Figure 5.20 Transcription regulation of *S. aureus* virulence genes during normal cell function.

The regulatory map was created ^(42, 76, 366) to identify the interactions between target genes and to indicate whether they increased or decreased the expression of other target RT-qPCR genes measured in this chapter. DNA transcription gene *gyrB* is not included as it is not associated with other genes and is often used as a housekeeper.

5.5.5.1 Gene expression changes in *S. aureus* biofilms treated with NX-AS-401 for two and four hours.

In biofilms that were treated with NX-AS-401 for two hours (**Figure 5.16**) the most significant changes across all strains occurred in the global regulator *sarA* and *gyrB* that both demonstrated an 5-15- and 2-5-fold increase in expression when treated with 256 µg/ml respectively. HCA clustering determined that the effects of NX-AS-401 after 2 hours were strain dependent, but this changed to concentration dependent at 4 hours. HCA indicates that reactions to NX-AS-401 are both strain and concentration dependent and that there may not be a definite gene target as no trends can be clearly seen at either the two or four hour timepoint after the analysis.

In Figure 5.16 shows that in *S. aureus* strains, NCTC 13142, NCTC 12973 and CRI 2 where all primers demonstrated >90 % efficiency, the known regulation pathway (**Figure 5.20**) could be followed completely. For example, increased expression of *sigB* caused increased *sarA* expression and that in turn increased *icaA*, *agrA* and *fnbA* and indicates a potential shift in to more biofilm focussed expression ⁽⁵⁶⁾.

However, expression of virulence associated genes such as *hla* and *hld* were also increased 3-6-fold. The pattern in the isolates NCTC 13142, NCTC 12973 and CRI 2 indicates an increase in overall gene expression in response to NX-AS-401 after two hours which is not uncommon in biofilms when challenged with antibiotics or put under environmental stress. Since biofilms contain *S. aureus* cells at different metabolic stages, such as persister cells, exposed cells on the biofilm surface, and base layer cells, that may all react differently to the presence of NX-AS-401 ^(70, 367).

The increase expression of *rot* is also following the regulatory pathway in Figure 5.20 and was likely caused to the 10-20-fold increase in the expression of *sigB* that overrides the down regulation that should be caused by the 3-6-fold increase of *agrA* and *hla*.

In strain CRI 2 expression of *atl* and *spIF* are strongly down regulated with 27- and 20-fold change respectively and this does not fit with the expected response where increased *sigB* and *agrA* expression should increase expression of *atl* and *spIF*. The gene *atl* codes for autolysin an important enzyme in cell division that lyses the peptidoglycan between cells ⁽³⁶⁸⁾. Meanwhile *spIF* codes for a serine protease, a

virulence factor that aids in colonization and adhesion ^(67, 369). Down-regulation of all these genes could be linked to additional gene regulators that have not been tested such as *mgrA* and the two-component *saeRS* regulator that have shown to have an effect on *spIF* and *atl* ^(36, 370).

In Figure 5.16 strains UHW 3 and UHW 15 where the *atl* and *spIF* primer efficiency was <90 % there was a three-fold increase in the expression of *sarA* and *gyrB* at 256 µg/ml at the two hour time point.

Unusually increased *sarA* expression did not lead to the increased expression of genes in the known regulatory pathway. The *S. aureus sar* complex controls many host functions particularly during cell growth, an increase in its expression may be directly related to virulence factors such as those known in Figure 5.20, but it also regulates the expression of genes associated with virulence, autolysis, biofilm formation and stress responses ^(363, 371). Therefore, a three-fold increase may not have been strong enough to elicit changes in the genes studied here but may have caused changes in the expression of other genes ⁽³⁶³⁾. Due to the vast number of genes controlled by *sarA* it is difficult to speculate on how it is affecting function without further data on other target genes ⁽³⁶³⁾. This could be identified through the use of more global RNA analysis such as RNA sequencing, that could determine the effects of NX-AS-401 on global gene regulation.

Strains UHW 18 and UHW 19, contains the greatest number of genes with increased expression such as *sarA*, *gyrB*, *sigB*, *fnbA*, *clfA* *spIF* when treated with 256 µg/ml. However, for UHW 18 expression was increased between 5 and 15-fold for these genes, isolate UHW 19 had five-fold increases for *sarA* and as high as 240-fold increases for *clfA*. In strains UHW 18 and UHW 19 the selected primer for *agrA* demonstrated less than 90 % efficiency. However, since the *agrABCD* complex is responsible for *hla* and *spIF* expression and that was increased in both strains it suggested that the complex was still present. This was confirmed via BLAST alignment of the primers against the sequence of those two strains (yielding a <90 % match with the *agrA* primer) indicating potential presence but lack of primer specificity due to a variation in the sequence.

UHW 8 was the only strain where optimization of the *sarA* primer failed. Isolate UHW 8 was also unusual in its reaction compared to the other strains as it was the only isolate that demonstrated a six-fold decrease in *agrA* expression and followed the known regulatory pathway (**Figure 5.20**) by causing a three-fold decrease in the expression of both *hla* and *hld*. However, surprisingly while *agrA* expression was decreased there was a 40-fold increase in the expression *spIF* that is directly controlled by *agr*. Unfortunately, this result is difficult to explain as while studies have shown the *spIF* is directly controlled by *agrABCD* ^(50, 97), others have also linked it to the *sar* complex ⁽³⁷²⁾. Since the primer for *sar* was inefficient against this strain this will require further RT-qPCR with primers designed via primer blast.

One of the most interesting results that matches with biofilm disruption studies is the changes in expression of the *agrA* gene as reduced expression of *agrABCD* complex has been linked to increased biofilm formation and when the complex is activated in biofilms it can cause biofilm separation and dissemination ^(97, 373). This is due to the *agrABCD* complex acting as both encoder and as a receiver for cyclic autoinducing peptides (AIPs) ^(97, 373). The AIPs are associated with the *S. aureus* quorum sensing system as well as virulence factor expression and can act as a switch between phenotypes ^(97, 373). The results shown in the two hour timepoint are particularly interesting regarding *agrA* expression as in the strains where the *agrA* primer functioned a pattern emerges that matches with previous studies such as SEM and CLSM despite a different treatment timepoint.

For example, the strains NCTC 13142, NCTC 12973, CRI 2 and UHW 3 all demonstrated increased *agrA* expression when treated with NX-AS-401 at a concentration of 256 µg/ml. These strains also demonstrated decreased biomass during SEM and CLSM after 20 hours of treatment with 128-512 µg/ml. Meanwhile isolate UHW 8 demonstrated a decreased expression of *agrA* after two hour treatment and is also the only isolate that had increased biomass during SEM and CLSM when treated with 256 µg/ml confirming the effects of NX-AS-401 on *agrABCD*. Unfortunately, this did not apply to strains UHW 18 and UHW 19 where a new primer design is required for confirmation or UHW 15 where there was no change in *agrA* expression.

It is also unknown whether NX-AS-401 targets *agrA* expression directly or has an effect on the production of AIP, as previously mentioned the disulphide bonds present in NX-245

AS-401 can react with thiol groups on cysteine residues. Synthesis of AIP requires catalysis of a thiolactone ring by a cysteine containing side chain, this process may be interrupted by NX-AS-401 causing problems in the formation of functional AIP ^(43, 97). This would require mass spectroscopy and molecular docking techniques that could determine if the presence of NX-AS-401 causes a decrease in the amount of AIP present or whether NX-AS-401 interaction with the protein causes inactivation. These techniques could also be applied to other virulence factors to uncover potential mechanisms of action for NX-AS-401. In *S. aureus* strains where *agrA* was deleted or AIP recognition decreased there was a decrease in the production of exoproteins and lytic enzymes ⁽³⁷³⁾. While the reduction in lytic enzymes may prevent biofilm dispersal it also attenuates virulence with virulence factors such as Panton-Valentine leukocidin also decreased ⁽³⁷³⁾.

Another trend that links to changes in *agrA* expression are the changes in expression of both *hla* and *hld*. In all strains where both primers were efficient the expression of *hla* and *hld* are the same, for example in strain NCTC 12973 both strains had a three-fold increase in expression when treated with 256 µg/ml for two hours. This also occurs with strain UHW 8 where downregulation of *agrA* has caused a three-fold decrease in *hla* and *hld* expression.

As seen in the RT-qPCR two hour results and in other studies ^(42, 63, 65, 76, 366) there is a direct relationship between *agr*, *hld* and *hla*. Changes in the expression of *hld* may also explain the antibiofilm activity of NX-AS-401 as the *hld* gene is part of the RNA III ⁽⁶³⁾. RNA III is large regulatory RNA that controls the production of proteins associated with cell attachment and plays a role in *S. aureus* quorum sensing that leads biofilm formation ^(63, 65). RNA III also acts as phenotypic switch for *S. aureus* and can change the phenotype between biofilm formation and virulence, it achieves this by blocking the translation of *rot* and increasing the production of exotoxins ^(63, 65). The study by Jakobsen *et al* utilized *S. aureus* reference strain 8325 and found that ajoene was directly responsible for a 77-fold decrease in *hld/RNAIII* expression and was independent of *agr*. Reduction of *hld/RNAIII* expression is also responsible for the decreased expression of other virulence genes such as *hla* and *spIF* ⁽²⁴¹⁾. The finding of the Jakobsen *et al* study ⁽²⁴¹⁾ could not be replicated during the two hour timepoint and instead the effects of NX-AS-401 seem more prominent on the *agr* system. Neither

increases nor decrease in the expression of *hld* caused changes in the production of virulence factors. Whether the effects of *hld* affected the translation of *rot* is unknown, but there were no trends seen between the expression of *hld* and *rot*. These results may differ for multiple reasons. Firstly, these are strain dependent actions of NX-AS-401 as well as difference in compound formulation, 1:4 E to Z ajoene isomer as opposed to 1:1, and concentrations of 5 µg/ml as opposed to the 128 and 256 µg/ml used in this study.

The changes in expression for *sarA*, *sigB* and *gyrB* remained the same at four hours as they did for the two hour timepoint. However, while baseline expression was increased it was equal or less than the expression change seen at two hours. This may indicate that the effects of NX-AS-401 had begun to subside due to metabolism, efflux of NX-AS-401 out of the cells or the two hour response was stress related and the expression in *S. aureus* was reducing to normal levels. Time dependent responses have been seen with other antibiotics such as daptomycin which elicits its effect after six hours but only causes changes in gene expression after 24 hours of exposure ⁽³⁷⁴⁾, whereas other studies have shown that chemicals that interfere with the *agrA* operon can induce changes in gene expression an hour after exposure ⁽³⁷⁵⁾.

Overall, the changes in expression remain strain dependent, with no novel changes in comparison to the two hour time-point. It would suggest that the four hour response is most likely the aftermath of the initial two hour response, with no unique change in expression caused. This has been shown for ajoene in the study by Jakobsen *et al* ⁽²⁴¹⁾ where the greatest changes in gene expression occurred between 15 minutes and an hour.

5.5.5.2 Gene expression changes in *S. aureus* biofilms treated with NX-AS-401 for 24 hours.

The exposure of *S. aureus* to NX-AS-401 for 24 hours demonstrated the greatest global down regulation of genes in comparison to the untreated control. The expression was inversed compared to the two hour time point, with down regulation of genes such as *gyrB*, *hld* and *sigB*, specifically at the 128 µg/ml treatment. HCA clustered the data according to NX-AS-401 concentration, though with strains NCTC 13142 and UHW 3 as outliers in comparison to the four hour timepoint. Overall NX-AS-401 effects seem both concentration and strain dependent with greater down-regulation seen with 128 µg/ml NX-AS-401 at this timepoint.

A 10-40-fold increased expression of *sarA* occurred in seven of the eight strains when treated with 256 µg/ml of NX-AS-401. This indicating that while the expression of the other genes tested remained unchanged under the 256 µg/ml NX-AS-401 testing conditions, there may have been an increase in the expression of other untested genes.

In relation to the Jakobsen study ⁽²⁴¹⁾, this was the only time point where the data matched and all of the strains using the *hld* primer were successful. Expression was downregulated 2-10-fold in comparison to the untreated control. This result only occurred at the 128 µg/ml but also occurred independently of *agrA*, which had little change in expression. This was also the only timepoint where *hla* and *hld* expression did not follow the same pattern except for strains NCTC 12973 and UHW 8. This may replicate the findings in other studies ⁽²⁴¹⁾ where NX-AS-401 effects *hld* expression. The changes in formulation and ajoene isomer may explain why this effect occurs later.

The isolates, NCTC 12973, NCTC 13142 and CRI 2 within demonstrated down regulation of most genes with 2-5-fold decreases in the expression of *gyrB*, *sigB* and *fnbA* at 128 µg/ml. This pattern follows the know regulatory pathways (**Figure 5.20**) and indicates an overall down regulation when treated with 128 µg/ml NX-AS-401. This could indicate a transformation of the cells to a less active phase and the creation of a persister phenotype. This may explain the lack of changes in gene expression with isolates NCTC 13142, NCTC 12973 and CRI 2 as they may have either reverted to a persistent cell type with reduced metabolic activity to protect themselves from the

higher NX-AS-401 concentration ⁽³⁷⁶⁾. This reaction has been seen with other antibiotics including trimethoprim-sulphamethoxazole ^(376, 377). However, this does not explain the increased expression of *sarA* that would usually be down-regulated, this could indicate that the cells are resuming normal activity due to reduced NX-AS-401 in the environment.

Isolates UHW 3 and UHW 15 also demonstrated either no change or down regulation of most genes when treated with 128 µg/ml of NX-AS-401. The only difference in comparison to isolates NCTC 13142, NCTC 12973 and CRI 2 is that exposure to 256 µg/ml NX-AS-401 for 24 hours increased *agrA* and *icaA* expression, two regulatory mechanisms that have according to Figure 5.20 no effect on each other. Once again this may be due to revival of the cell after NX-AS-401 or to regulate the expression of untested genes. UHW 3 was also the only strain that showed a 30-fold increase in expression of *hla*, however there is no current hypothesis on why this has occurred and may require further experimental repeats and further RT-qPCR of other virulence factors to determine if this is a strain specific reaction to NX-AS-401.

Isolates UHW 19 and UHW 18 showed very little changes in expression in any of the test genes when treated with 128 µg/ml for 24 hours, indicating that either the NX-AS-401 has degraded or the cells had grown less susceptible to its effects. In contrast to the other strains, UHW 19 and UHW 18 were the only strains that showed increased gene expression overall when treated with 256 µg/ml. According to gene sequencing (**Chapter 4, Section 4.4.1**) these isolates are very closely related but their reaction is different from any other strain in this thesis. The 10-20-fold increase in the expression of regulatory genes *sarA* and *gyrB* indicate that the known regulatory pathway (**Figure 5.20**) has been followed since there is a 4-20-fold increase in the expression of the virulence factors *hla*, *hld*, *fnbA* and *clfa* in both strains. However why these two strains have this response is unknown and without more data it is difficult to speculate.

The final strain UHW 8 demonstrated similar downregulation as seen in the NCTC 13142, NCTC 12973 and CRI 2, however since the *sarA* primer was unsuccessful it requires a new primer to identify if the response was similar.

Overall, the effects of NX-AS-401 on the gene expression of *S. aureus* at 24 are strain dependent. The upregulation of *sarA* in all strains when treated with 256 µg/ml could

indicate that NX-AS-401 or a metabolite has a direct action on *sarA* however, a NX-AS-401 concentration of 128 µg/ml did not produce a similar or weaker result. If *sarA* expression was directly affected there should have also been an increase in the expression of other genes. This might indicate that while NX-AS-401 does not affect the gene directly it may influence *sarA* translation or on other members of the *sar* complex that prevents increased expression of other genes. This study may have been clearer by focusing on more linear pathways or overall changes in global expression.

5.5.5.3 RT-qPCR Overview and implication in wounds.

Overall, the effects of NX-AS-401 on the gene expression of *S. aureus* are dependent on strain, concentration, and time.

A major observation noted during all timepoints was that NX-AS-401 altered gene expression in a concentration dependent manner, in some cases the dose led to opposite changes in expression where in the target gene concentration of 128 µg/ml NX-AS-401 caused increased expression and 256 µg/ml NX-AS-401 caused decreased expression or vice versa. This effect occurred five times in both the two and four hour timepoints, before occurring 13 times in the 24 hour timepoint. In all of these only one occurred at all three timepoints and that was expression of *sle1* in *S. aureus* strain UHW 3. The explanation for this effect has yet to be determined, one hypothesis is that the decrease in expression seen at the 24 hour timepoint is due degradation/metabolism of the compound in the 128 µg/ml NX-AS-401 tests. The reduced presence of NX-AS-401 therefore reduces the antibiotic pressure and rather than return to gene expression similar to untreated biofilms the gene expression is reduced. This has been seen in transcriptional studies that show antibiotic pressure can increase gene expression during initial exposure, but expression can be reduced below baselines >16 hours after antibiotic exposure ^(378, 379).

This may explain the effects seen at 24 hours but not the ones seen at the two and four hour timepoints. The current theories are based around the undetermined mechanism of actions for NX-AS-401. It could be caused concentration dependently

with lower concentration unable to elicit the same response as higher concentration and therefore a different effect occurred. These reactions could have also been due to the theory that NX-AS-401 does not act on a single specific target and therefore the effects are strain and concentration dependent leading to a few anomalous results. This effect has been seen with other antibiotic such as ceftaroline where gene expression was increased at 1/4 MIC and decreased with 1/6 MIC ⁽³⁷⁹⁾ and for multiple antibiotics such as cefazoline, erythromycin, rifampicin and tigecycline where both concentration and exposure time caused opposite responses ⁽³⁸⁰⁾.

At two hours concentrations of 128 µg/ml caused few changes in gene expression, while a NX-AS-401 concentration of 256 µg/ml increased overall expression. This response seems similar to spontaneous stress reaction seen with other antibiotics. During this the cells increase the activity of efflux pumps to remove any harmful substance and increase virulence factor production to acquire resource and begin biofilm formation. This is not an unusual response to antibiotics or environmental stress and while this may seem bad in infection as long as the pressure is maintained it would still allow for clearance of the infection.

The initial response seems to lapse after four hours, and expression levels seem to return to those of untreated cells. This may be where NX-AS-401 has started to elicit its effects, causing down regulation of the genes seen at 24 hours and this may agree with the study by Jakobsen *et al* ⁽¹⁹⁴⁾ where *hld* is a target. This could be confirmed by the addition of timepoint between four and 24 hours, to see if down regulation is a trend over time. In terms of wounds, this timepoint is still allowing for the NX-AS-401 to take effect and assist in bacterial clearance. More RT-qPCR would have also focused on additional virulence factors including leukocidins that assist in immune system evasion. This would help identify whether NX-AS-401 would aide in the clearance of infection by assisting the immune system.

Overall NX-AS-401 effects on the gene expression of *S. aureus* are varied, it appears that the compound has more effects on regulatory mechanisms such as *sarA*, *agrA*, *sigB* and *hld* and does not specifically target resistance mechanisms or biofilm associated genes such as *hla*, *clfA*, *fnbA* and *icaA*. It may be due to low expression of *icaA* in these strains that they form proteinaceous biofilms rather than with polysaccharide coded for by *ica* ⁽³⁸¹⁾. Since NX-AS-401 did not change regulation of *ica*

the effects of NX-AS-401 on PIA dependent biofilms cannot be determined, however, the study by Jakobsen ⁽²⁴¹⁾ utilised *S. aureus* strains 8325-4 which is shown to PIA dependent ⁽³⁸²⁾. This indicates that NX-AS-401 may have an effect on both polysaccharide and protein-based biofilms. To confirm the effects on the final eDNA type biofilm a known eDNA based biofilm forming strain will need to be studied. If NX-AS-401 can affect all biofilm types, this would be very beneficial in the treatment of chronic wounds where NX-AS-401 could assist in their disruption and subsequent eradication. Since none of the target genes for qPCR covered the production of eDNA it does not confirm whether the increase in biomass seen in UHW 8, when treated with 128 µg/ml NX-AS-401, during SEM and CLSM experiments was caused by increased eDNA production. This requires further investigation using specific cell impermeable DNA probes/dyes specificity such as TOTO-1. Additionally DNase 1 could also be added alongside NX-AS-401 treatment to see if the anti-biofilm effects are enhanced.

The effects of NX-AS-401 on gene expression seen here are similar to other garlic derived compounds such as allicin that have been shown to induce a thiol stress response in *S. aureus* cells that changes the transcription of many regulators and represses genes associated with the *sigB* regulator ⁽²²⁸⁾. The effect of NX-AS-401 during the 2hr and 24hr timepoints indicates that ajoene may not be the only active component within in NX-AS-401 and that the unidentified components may cause similar effects to what has been seen with other garlic extracts.

In total there was no decreased expression of biofilm related genes at two and four hours. However, after 24 hours expression, biofilm gene regulators and genes that code for biofilm proteins were significantly reduced. Additional timepoints may confirm when NX-AS-401 causes a reduction in virulence gene expression and how long the effects last. A decrease in virulence gene expression may result in a decrease in virulence and damage to the host, however this will require confirmation via proteomics, specifically mass spectroscopy targeting known virulence factors such as those associated with biofilms and toxins such as haemolysins and leukocidins ⁽³⁸³⁾. Expansion on the effects of NX-AS-401 on *S. aureus* gene expression will either have to focus on specific linear pathways to completely understand the effects or a more global action should be taken, such as RNA sequencing that could identify how NX-AS-401 effect global gene expression.

This is important for wound care as it would determine whether increased expression results in increased production of virulence factors and what the impact would be on wound care. If NX-AS-401 increases virulence factor production for 12 hours post treatment, this may cause more damage to the host before the healing process can begin. However, this effect may only occur at sub-MIC/sub-MBEC NX-AS-401 concentrations similar to how sub-MIC concentrations of beta-lactams can increase virulence factor production ⁽³⁸⁴⁾.

5.5.6 NX-AS-401 as an anti-biofilm agent

Overall, these results indicate that NX-AS-401 has the potential to be used therapeutically as an option for preventing/disrupting biofilm associated with chronic wounds. Results in this chapter have demonstrated the ability to inhibit biofilms at sub-MIC concentrations and disrupt biofilms at only 2-4-fold higher than MIC concentrations. In addition, the concentration needed could be reduced due to synergy with current standard of care antibiotics.

The mechanism of action of NX-AS-401 is still to be identified, while there were many changes in gene regulation, no specific target was determined. Whether this was due to the limited number of genes tested or whether it does not have a specific gene target can only be identified using mass expression techniques such as RNA-sequencing. Experiments monitoring gene expression should also include planktonic cells to determine how NX-AS-401 inhibits biofilm formation and whether a specific gene or pathway is regulated.

If NX-AS-401 interacts with AIP to destabilised biofilms, it would be a unique mechanism of action as most other antibiotics such as aminoglycosides, macrolides, and tetracycline target protein synthesis rather than proteins directly. The development of new antibiotics has led to some molecules such as Acyldepsipeptide antibiotics that act on proteins, specifically proteases directly ⁽³⁸⁵⁾. If NX-AS-401 does act on proteins, techniques such competition assays, chromatography and fluorescence spectroscopy should be used to determine if NX-AS-401 irreversibly binds to specific proteins or whether it is inactivated by host protein binding similar to other antibiotics ⁽¹²⁷⁾. Whether interactions with host proteins nullify the action of NX-AS-253

401 or if NX-AS-401 acts against them is important for wound care as actions against host proteins may cause adverse reactions, this has been seen in other disulphide compounds particularly the sulphonamide class of antibiotics ⁽¹⁸²⁾.

If action on proteins such as AIP is the mechanism of actions for NX-AS-401 this explains its activity against these proteinaceous biofilms, ideally strains that produce polysaccharide and eDNA based biofilms should have been utilised to determine if NX-AS-401 has the same antibiofilm effects.

In future modification to the biofilm experiments performed here would provide more information, Modification such as the use of more biologically relevant media such as artificial wound fluid could determine whether the effects of NX-AS-401 would occur in an environment more like those *in vivo*. ⁽²⁰⁴⁾. The use of different media may also allow for the formation of stronger biofilms with potentially different phenotypes, this would test the anti-biofilm action of NX-AS-401 and determine whether its efficacy remains despite challenge with a more robust biofilm. Artificial wound media and serum would also help to determine the compound stability as garlic constituents such as allicin have shown low stability in heparinised blood, leading to degradation of the compound within five minutes, and inactive allyl mercaptan only persist for an hour ⁽³⁸⁶⁾.

The use of alternative media and preparing more biofilms could then allow for expansion of the tests to include polymicrobial biofilms that are more representative of those *in vivo*, and this could include multiple strains of the same bacteria or different bacterial species. Based on the known anti-biofilm activity of NX-AS-401 it would identify whether the presence of multiple species in a biofilm are still susceptible or more tolerant to the actions of NX-AS-401. The biofilms may be more tolerant either due to the presence of more proteins for NX-AS-401 to interact with, or due to differences in ECM composition that prevent the movement of NX-AS-401 into the biofilm. Polymicrobial biofilms would need to be grown and the activity could be measured using the same approaches taken in this thesis, including biomass, metabolism, TVC as well as SEM.

5.6 Conclusion

Aim: Determine if all eight *S. aureus* strains can form a biofilm and the biofilm phenotype for each strain.

All *S. aureus* strains were able to generate biofilm, however biofilm density was substratum dependent with results varying based on whether biofilms were developed in tissue culture treated well plates or glass coverslips. All *S. aureus* strains produced a proteinaceous biofilm; however, this may be due to the use of media free of supplementation such as NaCl and glucose rather than a strict biofilm phenotype.

Aim: Identify the effects of NX-AS-401 on the formation and disruption of *S. aureus* biofilms, in terms of mass, metabolism and viable cells.

NX-AS-401 can inhibit biofilm formation at $\frac{1}{4}$ of the MIC. Disruption of pre-established biofilms occurs at NX-AS-401 concentrations 2-4 times higher than the MIC (256-512 $\mu\text{g/ml}$). This is much lower than current standard of care antibiotics that often require 100-1000-fold increase in concentration indicating that NX-AS-401 has a strong anti-biofilm effect and may be effective in the treatment of chronic biofilm associated wounds.

Aim: Identify whether the antibiotic interactions seen in planktonic cultures are replicated in pre-established biofilms

The synergistic effects of NX-AS-401 and current antibiotics that were identified against planktonic cells (**Chapter 4, Section 4.5.4**) are also achievable against biofilms. If the combination therapies between NX-AS-401 and antibiotics seen *in vitro* are reproducible *in vivo* this may allow for more effective treatment of biofilms and reduce antibiotic usage on chronic infections.

Aim: Visually identify changes in biofilm structure and cell morphology after exposure to NX-AS-401 using scanning electron microscopy (SEM) and confocal microscopy.

SEM and CLSM did not establish that NX-AS-401 can alter *S. aureus* cell morphology as part of its mechanism of action. SEM and CLSM indicate that NX-AS-401 concentrations reduce pre-established biofilm biomass and cell number, however, the effects can be strain variable when sub-MBEC⁵⁰ concentrations are used. This corroborates with the MBEC studies further identifying how NX-AS-401 can assist in biofilm eradication and may assist in chronic wound healing.

Aim: Identify changes in gene expression of *S. aureus* biofilms after exposure to NX-AS-401 using RT-qPCR.

NX-AS-401 mediated modulation of the *S. aureus* genes tested was strain dependent with no specific mechanism of action determined. Initial exposure to NX-AS-401 did increase global gene expression, however the virulence factors genes in this study were down-regulated after 24 hours. This indicates that NX-AS-401 can alter gene expression and may reduce the ability of *S. aureus* to produce/maintain biofilms and virulence factors after the initial exposure.

6.0 Chapter 6: NX-AS-401 as a potential anti-virulence agent

6.1 Introduction:

6.1.1 *S. aureus* virulence factors as therapeutic targets

S. aureus produces a variety of virulence factors that can assist in the development of localised wound infections in wound types such as abrasions and burns ^(30, 387). Specific *S. aureus* virulence factors can also be associated with specific diseases such as Panton-Valentine leukocidin (PVL) with impetigo or toxic shock syndrome toxin (TSST) with toxic shock syndrome ^(30, 348, 387). However, not all *S. aureus* strains produce all known virulence factors, therefore only certain strains can cause these specific diseases ⁽³⁸⁸⁾. For example, PVL is only produced in <5 % of *S. aureus* strains ⁽³⁸⁾ while TSST production is produced by approximately 50 % ⁽³⁸⁹⁾.

The presence or absence of certain virulence factors is not the only feature that defines the virulence potential of an *S. aureus* strain. The amount of virulence factor (for example, haemolysin) produced by each strain is also variable and therefore important ⁽³⁴⁸⁾. Virulence factor production is regulated by gene expression, involving gene regulators such as *sigB* and *RNAIII* while also requiring the virulence factor encoding gene ^(42, 43). *S. aureus* strains are capable of acquiring new virulence factors through horizontal gene transfer or extracellular genetic material from other lysed bacterial cells, for example staphylococcal enterotoxins are often disseminated through a bacterial population through plasmid transfer ⁽⁴⁵⁾. These multiple pathways can all affect the production of different virulence factors and expression can themselves be modulated by many different factors ⁽⁵²⁾. Differences in the environment of *S. aureus* such as nutrition, aerobic/anaerobic atmosphere, temperature and other environmental pressures, such as antibiotics or enzymes (such as proteases) have demonstrated an impact on *S. aureus* metabolism ^(52, 87). Expression of the major *S. aureus* virulence regulators *saeRS* is an example of how changes can occur due to environmental pressure, as *saeRS* expression is modulated by changes in pH, NaCl concentration and sub-inhibitory antibiotic concentration ⁽³⁹⁰⁾. Unlike other global regulators (*sar*, *agr* and *sigB*) *saeRS* directly binds to the promoter regions of

virulence factors, such as alpha and beta haemolysins and coagulase. Therefore, changes in *saeRS* can heavily impact *S. aureus* virulence ⁽³⁹⁰⁾.

The ability for *S. aureus* to become pathogenic through changes in regulation is what places it in the category of 'opportunistic pathogen'. While *S. aureus* can cause infection it is also a common species found in the human skin microbiota and has been estimated to be on 30 % of the population ⁽³⁹¹⁾. As a skin colonizer its presence is often passive, demonstrating no ill effects to the host until a change in environment or host health status give *S. aureus* an opportunity to causes infection ⁽³⁹¹⁾. However, this can vary as skin conditions such as psoriasis and eczema can cause breakdown of the outer layers of the skin resulting in *S. aureus* becoming pathogenic and causing further degradation of the dermis ^(9, 57). Conditions such as eczema have also been linked to the density of *S. aureus* colonisation, indicating that overgrowth of *S. aureus* can also be the cause of infection and turn it from a commensal to a pathogen, however this has yet to be conclusively proven ⁽⁵⁷⁾.

Since *S. aureus* is considered part of the healthy human microbiota complete eradication may not be desirable. Removal of commensal *S. aureus* is only performed when necessary such as on surgical sites prior to an operation as precautionary measure to prevent post-operative infection ⁽¹¹⁰⁾. This is because complete eradication can also allow for colonization by different potentially more antibiotic resistant/virulent bacterial species ⁽¹¹⁰⁾.

Therefore, an alternative approach to the development of antibiotics is the targeting of virulence factor production with the purpose being to reduce the amount of damage *S. aureus* can cause and allow for removal by the host ⁽³⁹²⁾. Some of these drugs in development have been listed in Table 6.1 and focus on altering virulence production/efficacy potentially reducing the severity of the infection's symptoms ^(42, 43, 393). This strategy allows for eradication of the infection by the host immune system or secondary antibiotic agent while reducing discomfort for the patient by reducing symptom severity ^(42, 43). The additional benefits for this include reducing the potential adverse effects of antibiotics such as dysbiosis that can allow for secondary infections of a different organism ⁽³⁹³⁾. A common example of this is the gastrointestinal *Clostridium difficile* infection that can be caused by oral antibiotics eliminating commensal bacteria in the gut ⁽³⁹⁴⁾.

Table 6.1 Virulence factors and targeted in-development drugs provided by Kane *et al*, 2018 ⁽³⁹²⁾.

Virulence Factor	Mechanism of Action	Inhibition Mechanism
<i>agr</i> system	AgrA increases transcription of various virulence factors	<ul style="list-style-type: none"> • Savirin: Small molecule that down regulates <i>agr</i> and subsequent downstream virulence factors ^(392, 395). • Solonamide B: Natural product. Reduced expression of <i>agrA</i> ^(392, 395).
α -toxin (<i>hla</i>)	Binds to eukaryotic cells and oligomerizes, forming pores and lysing the cell.	<ul style="list-style-type: none"> • Baicalin: Natural product that prevents the oligomerization of α-toxin ^(392, 396). • LC10: Antibody specific to α-toxin, increases murine survival when combined with antibiotics ^(392, 395). • HlaH35L: Mutated form of α-toxin. Used to immunize prior to challenge with <i>S. aureus</i>, reduced lesions in murine model of infection. ^(392, 396).
Phenol Soluble Modulins (PSM)	Ability to lyse a variety of cells including leukocytes and erythrocytes.	<ul style="list-style-type: none"> • Antibodies: PSMs tend to be very immunogenic, and antibodies raised to them can confer protection by reducing dissemination during infection ^(392, 396). • Block PMT transporter: PMT is responsible for the transport of all types of PSM ⁽³⁹²⁾.
Protein A	Protein that binds to IgG antibodies and Variable Heavy 3 idiotype B-cell receptors.	<ul style="list-style-type: none"> • SpAKKAA: Mutated protein A that when administered prior <i>S. aureus</i> challenge increases survival and host antibody production ^(392, 395). • Photothermaltherapy: Antibodies specific to protein A that contain gold rods ⁽³⁹²⁾.
Panton-Valentine Leukocidin (PVL)	PVL subunits oligomerizes and form a cell lysing pore.	<ul style="list-style-type: none"> • Chemotaxis Inhibitory proteins: Staphylococcal protein which has specific binding to the C5aR. Similar effects could be realized using antibodies ⁽³⁹²⁾.
Staphylococcal Enterotoxins (SE)	SEs bind MHC class II receptors on T-cells and hyper stimulate the T-cells.	<ul style="list-style-type: none"> • Antibodies: Immunizing mice against one form can provide protection against other forms ^(392, 396). • Toxoid: Use of mutated SEs can elicit immune responses to the native SE ⁽³⁹²⁾.
Two-Component System	A kinase which senses environmental signals and a response regulator which binds DNA to affect transcription.	<ul style="list-style-type: none"> • AFN-1252: Type 2 fatty acid synthesis inhibitor. Significantly reduces <i>saeS</i> and <i>saeR</i> expression ⁽³⁹²⁾. • Walkmycin & Waldiomycin: Natural product that inhibits Walk and kills <i>S. aureus</i>. ^(392, 397)

Staphyloxanthin	Pigment responsible for some strains of <i>S. aureus</i> golden colour. Protects the bacterium from oxidative stress.	<ul style="list-style-type: none"> • BPH-652: Derived from human cholesterol inhibitor drugs. Inhibits the CrtM enzyme which is in staphyloxanthin biosynthesis pathway ^(392, 398). • Naftifine: Antifungal drug that inhibits CrtN enzyme in staphyloxanthin biosynthesis pathway ^(392, 398).
-----------------	---	--

However, while there has been promising development in anti-virulence drugs none of them have been successful enough to use clinically ⁽³⁹⁹⁾. There have been trials using antibodies against specific bacterial toxins however their efficacy has yet to be confirmed ⁽³⁹⁹⁾. Table 6.1 demonstrates how *S. aureus* virulence can be diminished through various drugs and their respective targets, these include drugs that alter the gene expression of virulence associated genes such as haemolysin alpha (*hla*), or the overarching regulatory mechanism (*agr*) ⁽³⁹⁹⁾ or drugs that targets synthesis of virulence factors and oligomerization of proteins into a toxin ⁽³⁹⁹⁾.

The variety of drugs in development demonstrate how anti-virulence drugs are viewed as promising for the treatment of AMR bacteria and how their ability to attenuate virulence is important in the treatment of *S. aureus* specific infections. Despite none of them being used clinically their proof of concept activity *in vitro* can be easily identified.

Phenotypic studies can be used to identify the effects of potential anti-virulence drugs or whether sub-MIC antibiotics can causes an increase or decrease in the activity or production of specific virulence factors ⁽³⁸⁴⁾. However, while *S. aureus* produces a variety of virulence factors only a few can be quantified via phenotypic assays, these include but are not limited to:

6.1.2 Colonising Factors

These factors are associated with colonization of a host site by *S. aureus*, either as a commensal organism or prior to the establishment of an infection. The largest groups of virulence factors associated with *S. aureus* are called adhesins and invasins.

6.1.3 Adhesins and Invasins

S. aureus has been shown to have a wide variety of different cell surface proteins that have a range of functions in host colonisation and subsequent infection ^(58-60, 400). The largest group of adhesins are microbial surface component recognising adhesive matrix molecules (MSCRAMM) group ⁽⁵⁹⁾. MSCRAMM is the term used for molecules that allow bacterial cells to adhere to host cells and tissues. The term is used for all bacteria ⁽⁵⁸⁾, however it is not known whether they are essential for binding, due to their variety both within and across species. No studies have produced a complete MSCRAMM free mutant. MSCRAMM mutants are likely unachievable because the MSCRAMM group is very large, removing all MSCRAMM would likely prevent normal cells function ⁽⁵⁹⁾. Single mutants have been made or strains that lack multiple MSCRAMMS but not all ⁽⁴⁰¹⁾. The MSCRAMM group contains many virulence factors including protein A, clumping factor A, fibronectin binding protein A (FnBPA) and many others ^(58-60, 400).

MSCRAMMs have high affinity for extracellular matrix components such as collagen and members of the complement cascade found on the surfaces of host cells allowing for bacterial cell attachment to host cells. ^(58-60, 400). Once attached the *S. aureus* cell can be internalised into a host cell, this allow for evasion and protection from phagocytosis by the host immune system ⁽⁶⁰⁾.

One of the most important mechanisms for host cell internalisation is through the MSCRAMM FnBPA which is mediated by FnBPA binding to integrin $\alpha_5\beta_1$ through fibrinogen within host cell walls (**Figure 6.1 A**) ^(61, 402). This pathway is specific to *S. aureus* while other *Staphylococcus* species use other equivalent pathways such as *S. pseudintermedius* using SpsD/L and *S. epidermidis* using Embp ⁽⁶¹⁾. The production and expression of FnBPA has also been linked to a worse prognosis in sepsis patients as it assists in abscess formation and causes embolisms as it gathers host platelets together ⁽⁶¹⁾. The increased expression of FnBPA causes *S. aureus* internalisation into host cells to occur at a faster rate and therefore allows for greater immune system invasion and causes damage to host ⁽⁴⁰²⁾. While there are additional MSCRAMMS that allow for cellular invasions, FnBPA has been identified as the most important ⁽⁴⁰²⁾. Figure 6.1 shows some of the additional methods of adhesion and invasion for *S. aureus*.

Generally adhesion and invasion is measured phenotypically through gentamicin protection assays, but other methods include clumping assays, static adherence and flow adherence that requires human plasma, coated well plates and human cell lines with a constant flow of bacteria/media respectively ⁽⁴⁰³⁾.

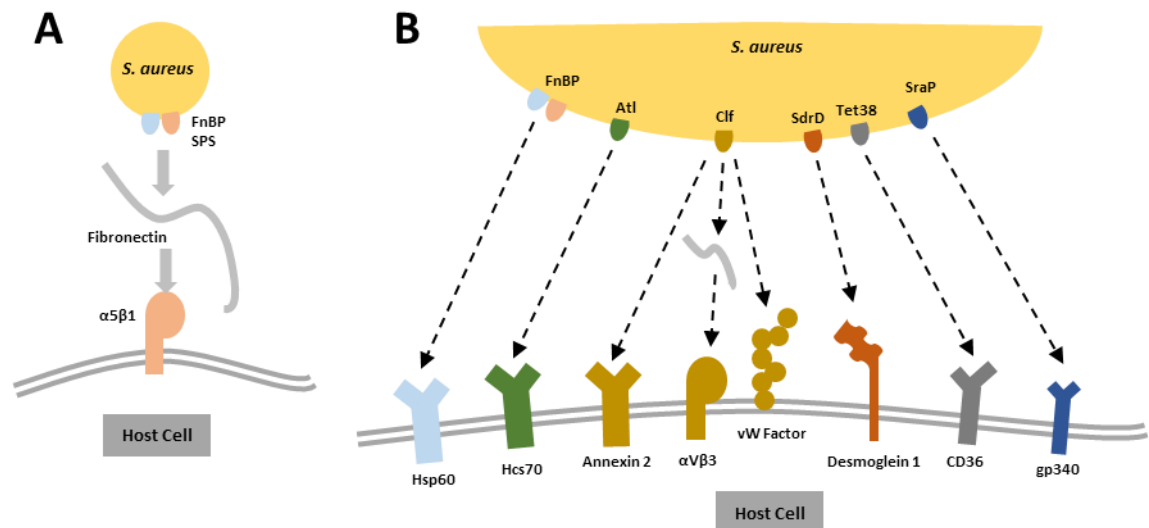


Figure 6.1 The role of membrane bound proteins on the internalisation of *S. aureus* into human epithelial cells, image obtained from Josse *et al*, 2017 ⁽⁶¹⁾.

A – Highlights the adherence of *S. aureus* to host cells via the fibronectin pathway. B - Indicates the multiple other MSCRAMMs that are used and their specific receptors.

Secondary invasion mechanisms are based on the various membrane bound proteins found on both host cells and *S. aureus* cells as seen in Figure 6.1 B ⁽⁶¹⁾. These are linked to additional MSCRAMMs such as clumping factor A and enzymes such as autolysin ⁽⁶¹⁾. The important role of MSCRAMMs in host colonisation makes them an ideal target for the development of treatments or potential vaccines ⁽⁵⁹⁾. However, due to the variety of MSCRAMMs a single target is not possible and the elimination/prevention of one colonisation pathway may reduce adhesion and invasion due to a secondary pathway ⁽⁵⁹⁾. This can help identify whether novel drugs that target these mechanisms are effective *in vitro*.

6.1.4 Lipases

All *S. aureus* strains are capable of producing a type of lipase that has been shown to play a role in host colonisation before assisting in biofilm formation ⁽⁴⁰⁴⁾. Lipase is utilised by *S. aureus* in multiple pathways such as metabolism of fats, but also to protect itself from linoleic acid ⁽⁴⁰⁴⁾. Linoleic acid is part of the human innate immune system that acts as both a barrier to colonisation and antibacterial agent, however its direct antibacterial effects are unknown ⁽⁴⁰⁵⁾. Similarly lipase appears to play an important role in biofilm formation, with biofilms reduced in *S. aureus* mutants where lipase was removed, however the mechanism has yet to be fully characterised ⁽⁴⁰⁴⁾. As well as helping during colonisation lipase production has also been linked to the formation of abscesses during infections ⁽⁶²⁾. A function of the human innate immune system is the use of triglycerides that contain lipids such as lauric acid which have antibacterial properties ⁽⁴⁰⁶⁾. The role of lipase is to degrade these lipids preventing their action and protecting the *S. aureus* cells ⁽⁴⁰⁶⁾. While *S. aureus* produces general lipases it can also produce enzymes with high specificity such as lecithinase which acts upon the phospholipid lecithin ⁽⁴⁰⁷⁾. The membrane of human cells contains lecithin which may be a target of *S. aureus* lecithinase however, the current action is unknown but the current hypothesis is it assists in immune system evasion and nutrient acquisition ⁽⁴⁰⁷⁾.

Once *S. aureus* has colonised a target site, it may remain as a harmless commensal or develop into an infection ⁽¹¹⁾. *S. aureus* infections vary in their severity based on both the type and amount of virulence factors produced ^(388, 408).

6.1.5 Haemolysins and Leukocidins:

Haemolysins are toxins that specifically target host blood components, including both red and white blood cells ⁽⁴⁰⁹⁾. They allow *S. aureus* to acquire iron from red cells and cause lysis of white blood cells serving as a method of evading the host immune system ⁽⁴⁰⁹⁾. *S. aureus* produces a variety of different haemolysins and leukocidins each with their own function and specificity.

- **Alpha (α) haemolysin (α -toxin)**

The initial function of α -toxin is the lysis of red blood cells but it has the ability to bind with the outer membrane of various nucleated cell types causing cell death ⁽⁴¹⁰⁾. The ability to cause the lysis of various cell types within the host can lead to the development of serious clinical conditions such as severe pneumonia and bacteraemia due to tissue necrosis ⁽⁴¹⁰⁻⁴¹²⁾. Although α -toxin is commonly identified in *S. aureus* the amount produced varies per strain, as some strains have the gene but do not produce the toxin. This may be due to a problem with its synthesis, low expression or mutations in the regulatory *agr* gene that controls haemolysin production ^(409, 413). However, due to its ubiquitous nature and severity of the diseases caused by high α -toxin production, it is a target for the development of a vaccine and anti-virulence drug as shown in Table 6.1 ⁽⁴¹³⁾.

- **Beta (β) haemolysin (β -toxin)**

While categorised as a haemolysin, β -toxin is a sphingomyelinase, this toxin targets cells which have sphingomyelin on their cells surface and causes lysis of those cells ^(414, 415). Most human host leucocytes have this present on their cell surface making them a target for β -toxin ⁽⁴¹⁶⁾. Studies into the effects of the toxin are variable due to species specific susceptibility, with *in vitro* activity only seen on sheep blood and not on commonly used laboratory blood media containing horse or rabbit blood ^(414, 417). It also has unusual functional characteristics based on exposure to different temperatures giving it an unusual moniker of “Hot-Cold” haemolysin ^(414, 415, 417, 418). However, while these studies vary on the effects *h/b* has on red blood cells, they agree that it can inhibit host neutrophils and other immune cells. Studies have shown that the toxin lyses proliferating human lymphocytes^(415, 417) and can cause lysis of the affected cells, but if it fails to lyse them it will leave them in a more vulnerable condition sensitizing them to other toxins such as phenol-soluble modulins that are also produced by *S. aureus* ⁽⁴¹⁴⁾.

- **Delta (δ) haemolysin (δ -toxin)**

S. aureus produces δ -toxin in large quantities but demonstrates only a moderate cytolytic effect against both red and white blood cells ^(417, 419, 420). The toxin itself is a phenol-soluble modulin that may have greater effect when produced alongside β -toxin ⁽⁴¹⁷⁾. The effects of δ -toxin are similar to others in that it lyses both red and while cells,

however it is also known to affect the human immune system through mast cell activation and is therefore associated with immune conditions such as atopic dermatitis and can cause an inflammatory response while reducing the adaptive immune response ⁽⁴¹⁹⁾. These effects allow *S. aureus* to evade the immune system and prolong infection.

- **Gamma (γ) haemolysin (γ -toxin)**

The γ -toxin is another haemolysin that has been poorly studied despite the genetic locus being present in 99 % of *S. aureus* strains ⁽⁴²¹⁾. Though most strains possess the genetic potential to produce the toxin it may not always be produced ^(419, 421, 422). The few studies that have looked into its effects seem to indicate that it is pro-inflammatory and that it may play a role in clinical conditions such as Toxic Shock Syndrome (TSS) as it was produced in 100 % of TSS associated isolates while production of other haemolysins varied from 0 – 66 % ^(409, 421).

Haemolysins are important in *S. aureus* pathogenicity, and for most of them their roles have been clearly defined and functions identified ⁽⁴²³⁾. They are one of the main targets for virulence modulation as preventing haemolysin production or their mechanism of action may allow for easier eradication by the host immune system ⁽³⁹³⁾. Changes in the production or activity can also be monitored phenotypically using different blood types and spectrophotometric methods.

6.1.6 Deoxyribonuclease (DNase)

Production of DNase can be identified by specialised DNA containing media that produces a zone of clearance or a colour change after DNA in the media is broken down ⁽⁴²⁴⁾. DNase is a nuclease that specifically targets deoxyribonucleic acid, it is often used to differentiate *S. aureus* from other *Staphylococcus* species alongside the coagulase test ^(424, 425). Its role is the breakdown of DNA into usable nucleotides and studies have shown that other nucleases aid infection by promoting evasion of host cells, specifically neutrophils ^(426, 427) that can kill target organisms through extracellular traps. The traps contain antimicrobial peptides and protease bound to a DNA backbone. DNase can act on these traps breaking them apart providing another mechanism for *S. aureus* to evade the immune system ⁽⁴²⁷⁾.

6.1.7 Protease

Proteases are enzymes that have the ability to breakdown proteins, and *S. aureus* can produce a variety of extracellular proteases that are important for both *S. aureus* cell growth⁽⁴²⁸⁾ and pathogenicity⁽⁵²⁾. Proteases can assist in infection development by breaking down antimicrobial peptides and prevent phagocytosis of *S. aureus* by host leukocytes, though the mechanism has not been identified⁽⁵²⁾. Protease deficient *S. aureus* strains have also shown that they play an important role in disease development as in mutant strains pathogenicity, abscess formation and organ penetration was significantly reduced^(52, 428). This is most likely due to being unable to break down host proteins that both protect cells as antimicrobial peptides or make up parts of cells and tissues⁽⁴²⁸⁾.

6.1.8 NX-AS-401 Anti-virulence

Since many environmental factors can alter virulence factor production and based on changes in gene expression it is important to identify whether exposure to NX-AS-401 only alters gene expression or if it alters the effects of virulence factors directly.

Previous studies have shown that garlic and garlic derived compounds such as allicin and ajoene have the ability to modulate virulence factor expression, however, these have mostly focused on their effects on biofilm development and the quorum sensing cellular communication systems in *P. aeruginosa*^(194, 219, 229). The effects of garlic and the derived component on Gram-positive bacteria have yet to be identified with no papers reporting whether garlic derived antibiotics can alter virulence factor production in bacteria such as *Staphylococcus* and *Streptococcus* species.

Studies that have focused on garlic extracts, have provided a little more information, and focused on reducing quorum sensing and inhibiting biofilm formation, but some have indicated the ability to reduce *S. aureus* enterotoxin production while also looking at the immunomodulatory effects of garlic and how it can reduce inflammation^(184, 202, 226). There has been one study on the effects of allicin on *S. aureus* haemolysin production that indicates the compounds are effective at reducing haemolysin expression and therefore production⁽⁶⁶⁾. This indicates that there is potential for garlic and garlic derived compounds to be used as anti-virulence drugs.

6.2 Aims

- To identify the virulence factor phenotype of *S. aureus* strains and identify changes in production after exposure to subinhibitory concentrations of NX-AS-401.
- To identify the toxic effects of NX-AS-401 on the human skin cell line (HaCaT) and in the experimental moth model *Galleria mellonella*.
- To determine if NX-AS-401 could increase the survival rate of *Galleria mellonella* larvae infected with *S. aureus*.
- To determine if NX-AS-401 alters the ability of *S. aureus* to adhere and invade HaCaT skin epithelial cells.

6.3 Methods

No changes have been made to the materials and methods provided in Chapter 2.

6.4 Results

6.4.1 NX-AS-401 Supplementation in solid media

Liquid MHA plates were supplemented with different concentrations of NX-AS-401 to determine which NX-AS-401 concentrations prevented growth on solid media.

Table 6.2 Average TVC counts from agar plates containing different concentrations of NX-AS-401.

Results displayed are the average log CFU/ml of 9 replicates.

MHA Plate NX-AS-401 concentration (µg/ml)	Average TVC count (LOG ₁₀ CFU/ml)							
	NCTC 13142	NCTC 12973	UHW 3	UHW 8	UHW 15	UHW 18	UHW 19	CRI 2
128	0	0	0	0	0	0	0	0
64	0	0	0	0	0	0	0	0
32	0	0	0	0	0	0	0	0
16	8.2	7.8	6.2	3.4	4.1	6.4	9.2	8.1
12	10	10	10	10	10	10	10	10
8	10	10	10	10	10	10	10	10
4	10	10	10	10	10	10	10	10
0	10	10	10	10	10	10	10	10

MHA supplemented with NX-AS-401 inhibited *S. aureus* growth for all strains at concentrations ≥ 16 µg/ml. This result is much lower than the MIC established in broth micro-dilution but is likely due to diffusion rates of NX-AS-401 in agar, as well as a change in ratio of NX-AS-401 molecules per bacterial cell.

6.4.2 Phenotypic Virulence

S. aureus was inoculated onto MHA plates supplemented with sheep and horse blood, egg yolk, lipids (tributylin and tween) and skimmed milk powder. Samples were inoculated onto MHA with and without 12 µg/ml NX-AS-401 supplementation. NX-AS-401 supplementation was the highest NX-AS-401 concentration that could be achieved in MHA without effecting *S. aureus* growth (**Section 6.4.1**). Zones of lytic activity were measured to identify base levels and changes mediated by NX-AS-401 (**Table 6.2**).

6.4.2.1 The effects of NX-AS-401 on beta (β) and gamma (γ) haemolysin produced by *S. aureus*.

Two batches of Mueller-Hinton agar, one containing 5 % sheep blood (pictured) and another containing 5 % defibrinated horse blood (not pictured) were used to monitor effects of NX-AS-401 on haemolysin activity. On horse blood agar, *S. aureus* was able to produce a small zone of lysis, but zones of lysis were difficult to visualise (Figure 6.2).

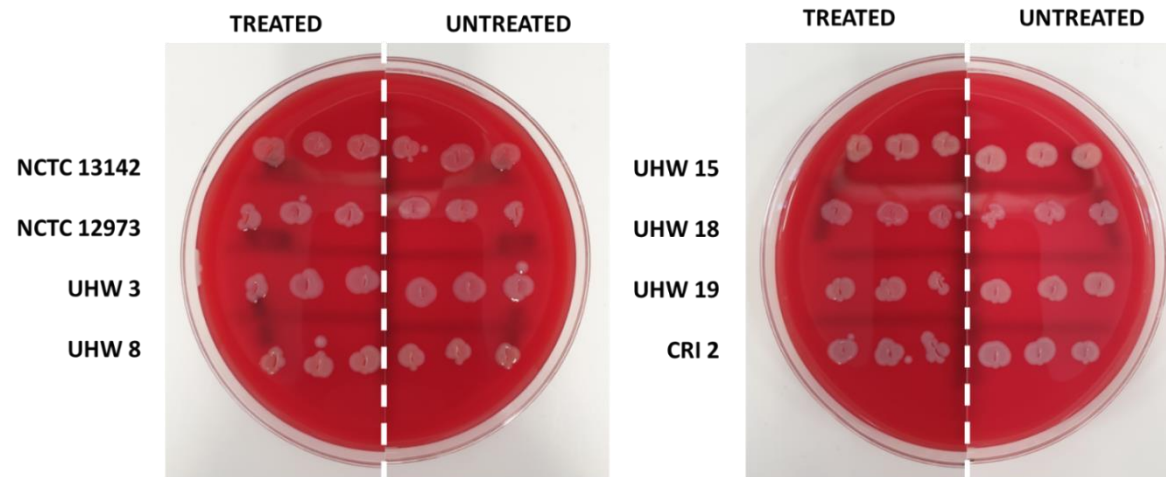


Figure 6.2 The activity of *S. aureus* haemolysin after exposure to NX-AS-401 on sheep blood agar.

No haemolytic activity was seen on Columbia sheep blood agar after inoculation with all eight *S. aureus* strains. No significant ($p > 0.05$) differences in zone size could be determined in horse blood agar with or without NX-AS-401 as lytic zones were measured as 1-2 mm for all strains. This indicates that the eight strains of *S. aureus* used in this project had low levels of haemolytic activity on the blood obtained from horses and sheep and the activity was not affected by NX-AS-401.

6.4.2.2 The effects of NX-AS-401 on the production and activity of *S. aureus* lipase.

Agar containing a 5 % egg yolk mixture (not pictured) and another containing 2.5 % of both tributyrin and tween (**Figure 6.3**) was utilised to monitor the effect of NX-AS-401 against *S. aureus* lipase production and activity. Egg yolk agar was also used to monitor lecithinase production. Images from egg yolk agar did not show zones of lytic activity due to the iridescent sheen caused by lipid degradation.

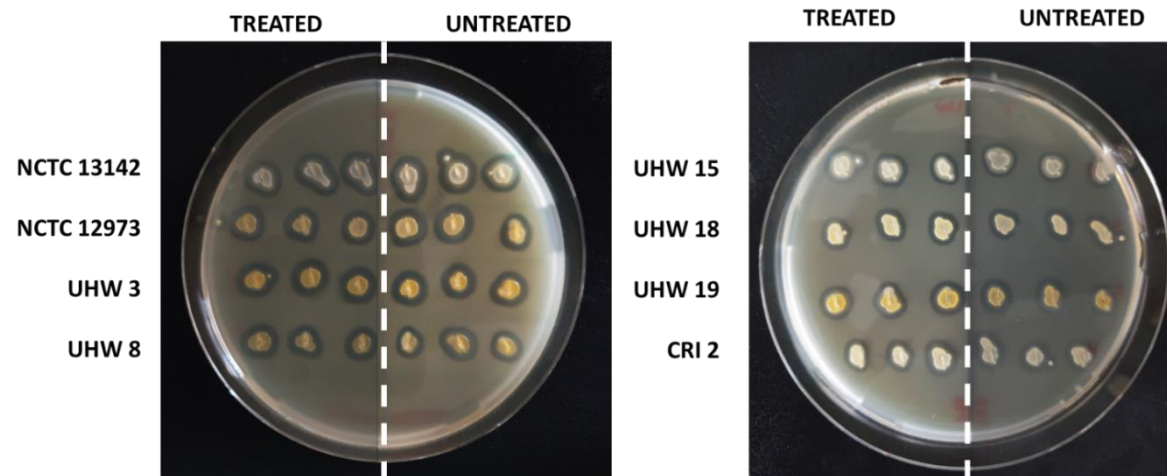


Figure 6.3 *S. aureus* lipase activity on cells with and without exposure to NX-AS-401.

All *S. aureus* strains demonstrated lipase activity with no significant ($p > 0.05$) difference in activity with NX-AS-401 supplementation. Zone sizes remained consistent on under both test conditions with lipase activity ranging from 1-2 mm from the *S. aureus* colonies.

6.4.2.3 The effects of NX-AS-401 on the production and activity of *S. aureus* DNase.

DNase agar (Oxoid) was used to monitor the effects of NX-AS-401 on DNase activity shown in Figure 6.4

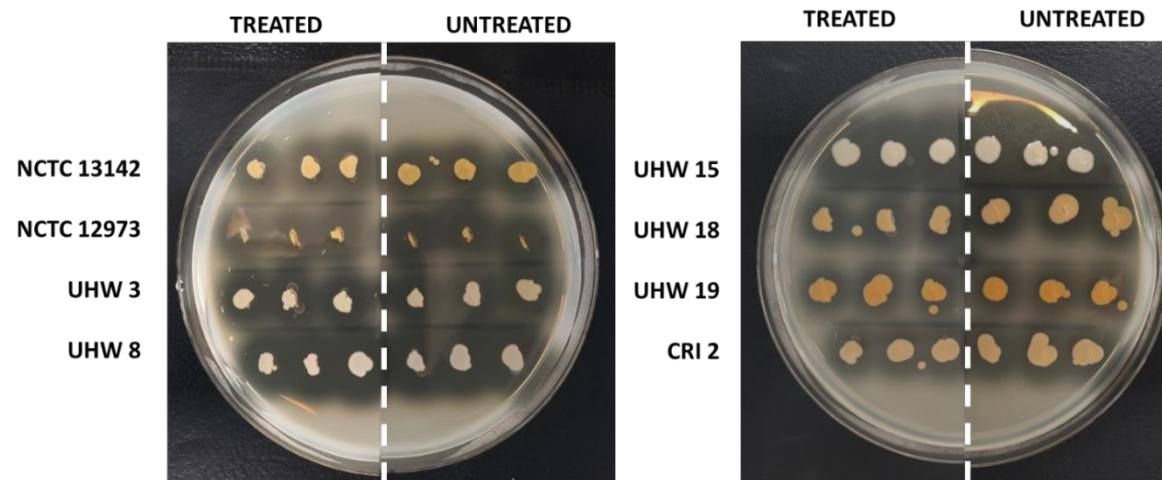


Figure 6.4 *S. aureus* DNase activity on cells with and without exposure to NX-AS-401.

All *S. aureus* strains demonstrated DNase activity.

DNase activity varied per strain. Isolate UHW 15 demonstrated increased DNase production with larger zone sizes of 4-5 mm in comparison to NCTC 13141, NCTC 12973, UHW3, UHW 8, UHW 18 and UHW 19 with lytic zone sizes of 3-4 mm and isolate CRI 2 where lytic zones measured between 2-3 mm. Comparison between zones sizes of NX-AS-401 treated and untreated cells showed no significant ($p > 0.05$) difference in DNase activity.

6.4.2.4 The effects of NX-AS-401 on the production and activity of *S. aureus* protease

100 ml of skimmed milk was added to 100 ml of double strength MHA to monitor the effects of NX-AS-401 on protease activity (Figure 6.5).

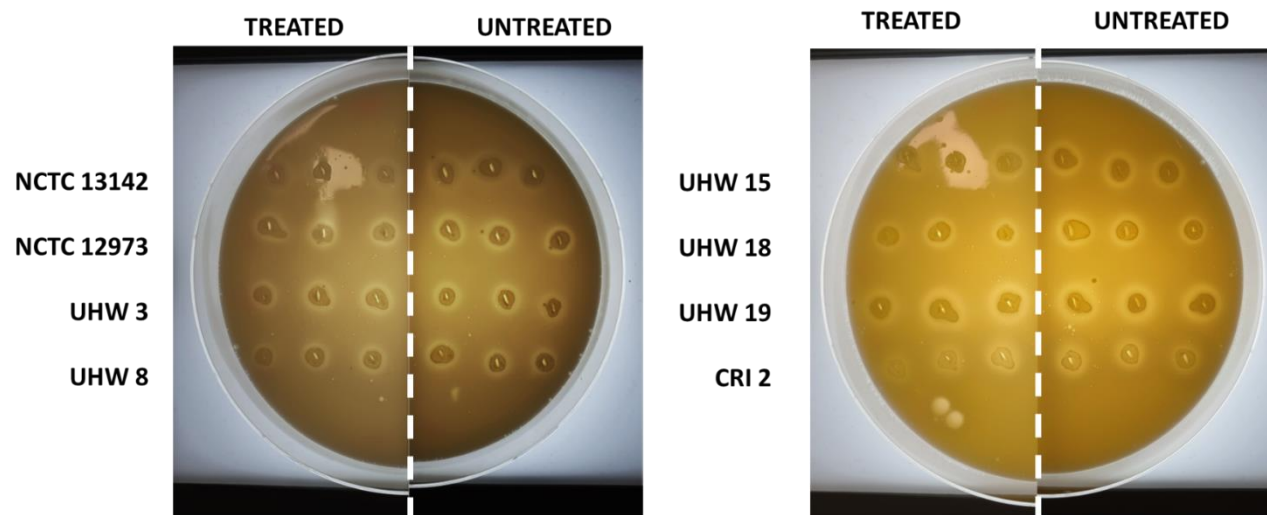


Figure 6.5 *S. aureus* Protease activity on cells with and without exposure to NX-AS-401.

All *S. aureus* strains demonstrated protease activity which varied per strains.

Strain UHW 19 had higher levels of protease activity than other strains with larger zone sizes of 3-4 mm when compared to all other strains which were measured as 1-2 mm. However, exposure to NX-AS-401 did not significantly ($p < 0.05$) change the activity of protease in any of the *S. aureus* strains.

Table 6.3 Summary of virulence factors produced by each *S. aureus* strain:

This table displays the virulence phenotype of each isolate; positive lysis is indicated by + and no activity/lysis is indicated by -.

		Virulence Factor / Media					
Strain		β-toxin (Sheep Blood)	γ-toxin (Horse Blood)	Lipase (Tributyryn and Tween)	Lecithinase (Egg Yolk)	Protease (Skim Milk Powder)	DNase (DNase)
	NCTC 13142	-	+	+	+	+	+
	NCTC 12973	-	+	+	+	+	+
	UHW 3	-	+	+	+	+	+
	UHW 8	-	+	+	+	+	+
	UHW 15	-	+	+	+	+	+
	UHW 18	-	+	+	+	+	+
	UHW 19	-	+	+	+	+	+
	CRI 2	-	+	+	+	+	+

All strains were able to produce the same virulence factors, however, virulence factor activity or amount produced varied per strains. NX-AS-401 did not modulate virulence in any of the strains.

6.4.3 *In vivo* virulence modulation of *S. aureus* by NX-AS-401 in *Galleria mellonella* (*G. mellonella*)

G. mellonella larvae were used to measure the toxicity of NX-AS-401 in a whole organism. They were also used to determine if NX-AS-401 could increase survival of *G. mellonella* after infection with *S. aureus*. All *G. mellonella* larvae were monitored for five days post injection.

6.4.3.1 NX-AS-401 toxicity

NX-AS-401 was injected into *G. mellonella* larvae at range of concentrations to determine if NX-AS-401 caused any adverse effects or host death (Figure 6.6).

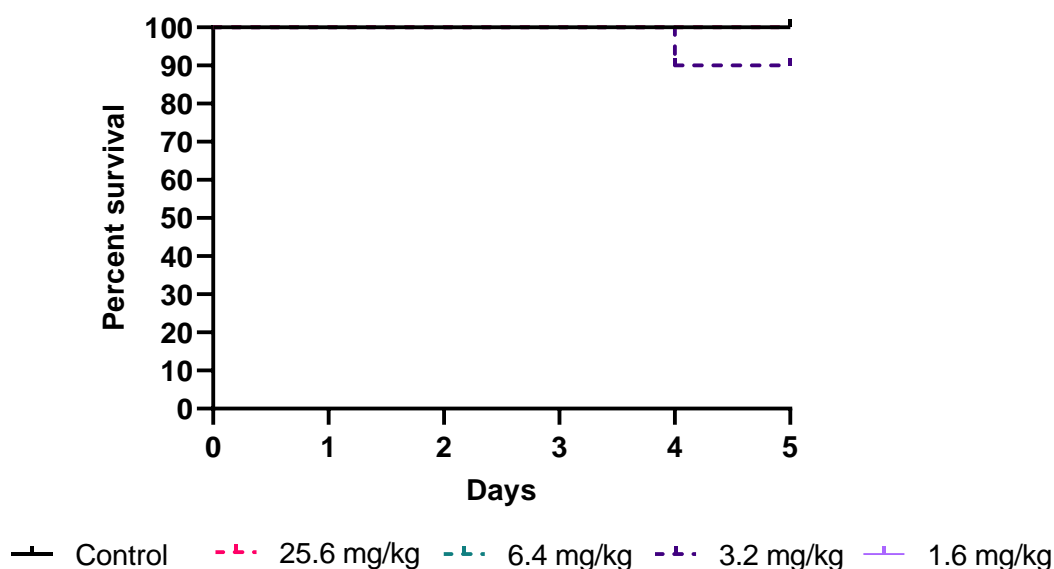


Figure 6.6 The toxic effects of NX-AS-401 on *G. mellonella* larvae over 5 days.

The graph shows that NX had no toxic effects when inoculated into *G. mellonella* larvae at any of the concentrations tested (range between 0-512 $\mu\text{g/ml}$).

6.4.3.3 Optimisation of the lethal dose of *S. aureus*.

G. mellonella were infected with different *S. aureus* CFU/ml suspensions and their survival was monitored over five days to determine the lethal dose (CFU/ml) (Figure 6.7).

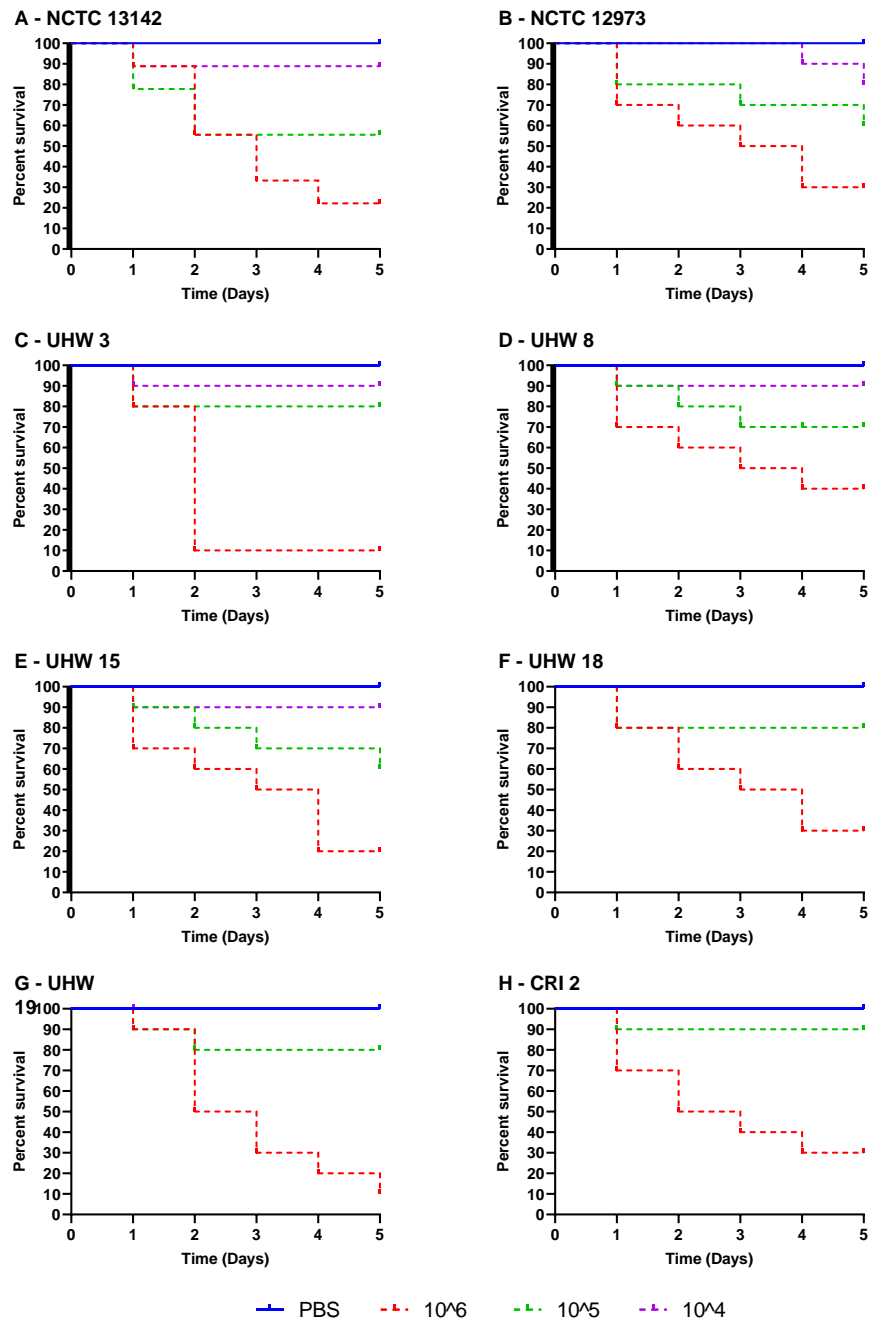


Figure 6.7 The effects of *S. aureus* cell density on the survival of *G. mellonella*.

S. aureus dose was directly linked to mortality in *G. mellonella* larvae for all strains ($p < 0.05$). Increases in the *S. aureus* (dose) CFU/ml reduced the life span of *G. mellonella* over five days.

An *S. aureus* inoculum of 10^4 CFU/ml decreased survival of *G. mellonella* by a maximum of 20 % (NCTC 12973), five days after injection however most strains (NCTC 13142, UHW 3, UHW 8 and UHW 15) demonstrated a 10 % decrease in survival while other *S. aureus* strains (UHW 18, UHW 19 and CRI 2) demonstrated no effect at a 10^4 CFU/ml inoculum. An increase in *S. aureus* dose to 10^5 CFU/ml decreased *G. mellonella* survival to 40 % for strains NCTC 13142, NCTC 12973 and UHW 15, while UHW, 3 UHW 18 and UHW 19 decreased survival by 20 %. UHW 8 and CRI 2 reduced survival by 30 % and 10 % respectively. The highest *S. aureus* dose of 10^6 CFU/ml decreased survival between 60-90 % of *G. mellonella* across all strains. UHW 3 and UHW 19 caused a 90 % decrease in survival, NCTC 13142 and UHW 15 reduced survival by 80 % and NCTC 12973, UHW 18 and CRI 2 reduced *G. mellonella* survival by 70 %. The least lethal strain at a 10^6 CFU/ml dose was UHW 8 that reduced survival by 60 %.

6.4.3.4 The effects of NX-AS-401 on *S. aureus* lethality in *G. mellonella*

The ability of NX-AS-401 to increase survival of *G. mellonella* infected with *S. aureus* was monitored by injecting *G. mellonella* larvae with 10 μ l of *S. aureus* 10⁶ CFU/ml and 10 μ l NX-AS-401 at concentrations of 128 μ g/ml. Positive control *G. mellonella* received 10 μ l of *S. aureus* inoculum and 10 μ l of PBS, while negative control received two x 10 μ l of PBS injections (**Figure 6.8**).

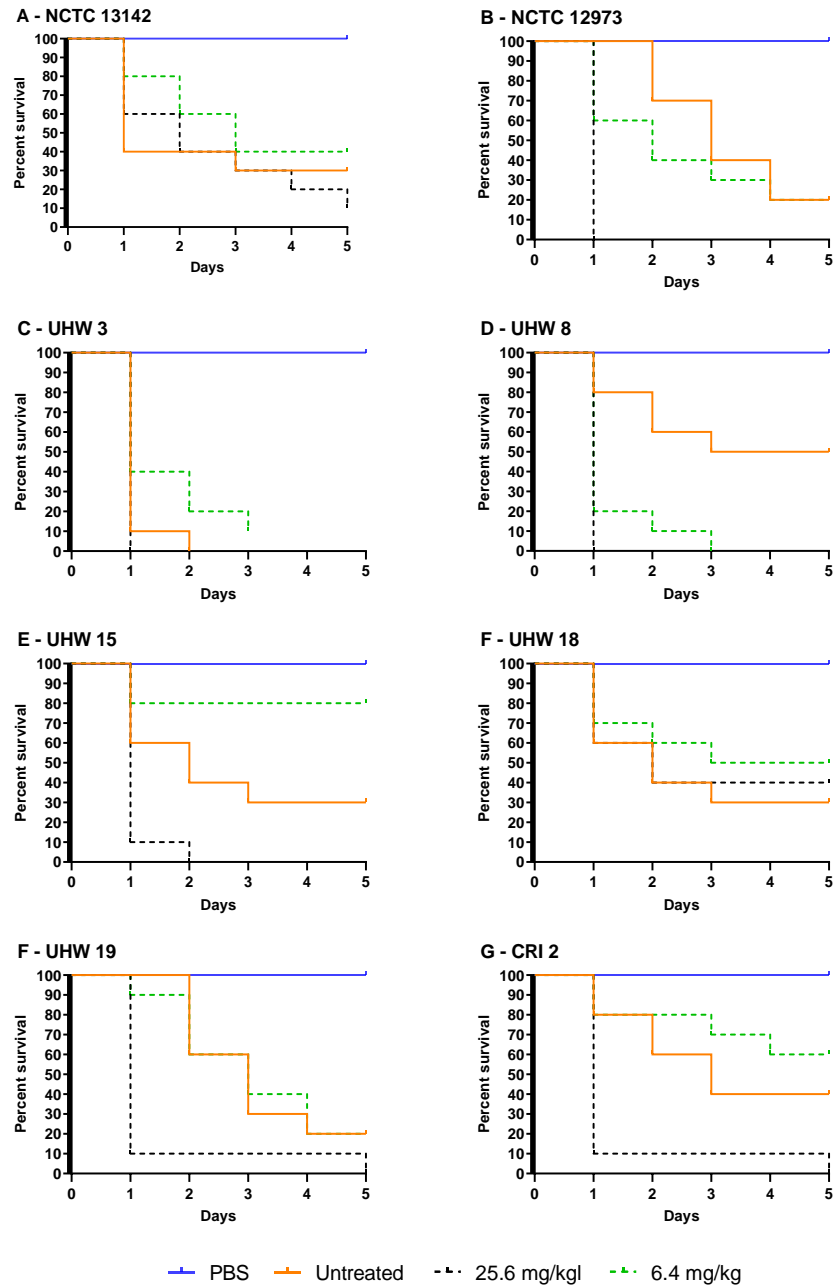


Figure 6.8 The effects of NX-AS-401 on infected *G. mellonella* survival.

The effects of NX-AS-401 on the survival of *G. mellonella* infected with *S. aureus* varied per strain. Significant ($p > 0.001$) values are highlighted with triple asterisk (***)

Responses of infected *G. mellonella* treated with 6.4 mg/kg NX-AS-401 were strain dependent. Most strains demonstrated no statistically significant ($p < 0.05$) change in survival when treated with 6.4 mg/kg NX-AS-401, *G. mellonella* infected with strains UHW 8 showed a significant ($p < 0.05$) decrease in survival when injected with 6.4 mg/kg of NX-AS-401.

UHW 15 was the only strain that exhibited a statistically significant ($p < 0.05$) increase in survival when infected with both 10^6 CFU/ml of *S. aureus* and 6.4 mg/kg of NX-AS-401.

Infected *G. mellonella* were treated with NX-AS-401 25.6 mg/kg which demonstrated similar effect to 6.4 mg/kg with *G. mellonella* death occurring at similar rates. Only two strains reacted differently, UHW 8 where the higher NX-AS-401 increased *G. mellonella* fatality while UHW 15 was the only strain where more *G. mellonella* recovered from the infection.

6.4.4 *In vitro* virulence in human skin epithelial cells

HaCaT human skin epithelial cells were used to assess toxicity of NX-AS-401. Then they were used to assess *S. aureus* adherence and invasion (Figures 6.9 & 6.10).

6.4.4.1 Cytotoxicity

HaCaT cell were treated with a concentration gradient of NX-AS-401 to identify concentrations toxic to human skin epithelial cells. Cytotoxicity was measured via AlamarBlue metabolic assay after confluent cells were treated with NX-AS-401 for 24 hours (Figure 6.9).

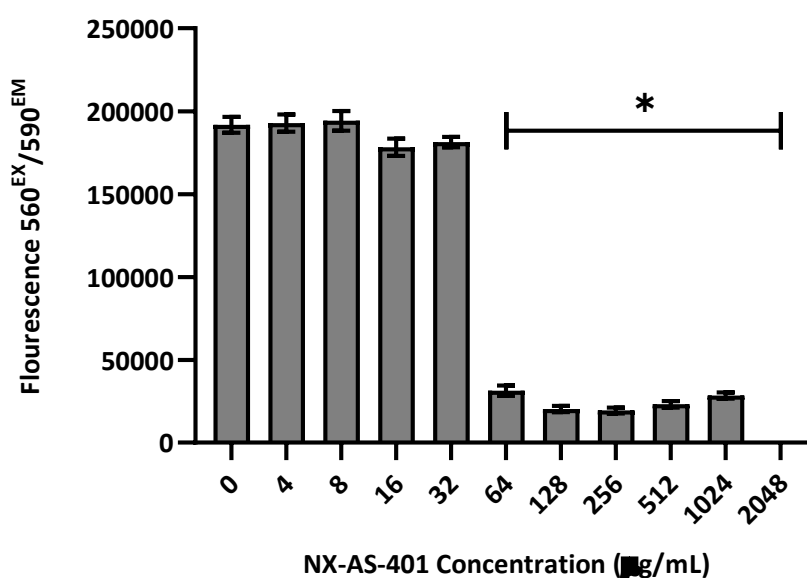


Figure 6.9 The effects NX-AS-401 on HaCaT cell viability.

Statistical significance ($p < 0.05$) is indicated by an asterisk (*), error bars show the standard error of the mean.

NX-AS-401 demonstrated a statistically significant ($p < 0.05$) ability to reduce cell metabolism at concentrations ≥ 64 µg/ml. Concentrations of 2048 µg/ml completely inhibited the metabolism of HaCaT cells in comparison to the positive control.

6.4.4.2 Adhesion/Invasion

To identify the effects of NX-AS-401 on the ability of *S. aureus* to adhere and invade human keratinocytes, *S. aureus* cells were added to cultures of HaCaT cells at a multiplicity of infection ratio of 200:1. NX-AS-401 was added to the *S. aureus* and HaCaT cells at a concentration of 16 or 32 µg/ml. An NX-AS-401 free control was used as a control.

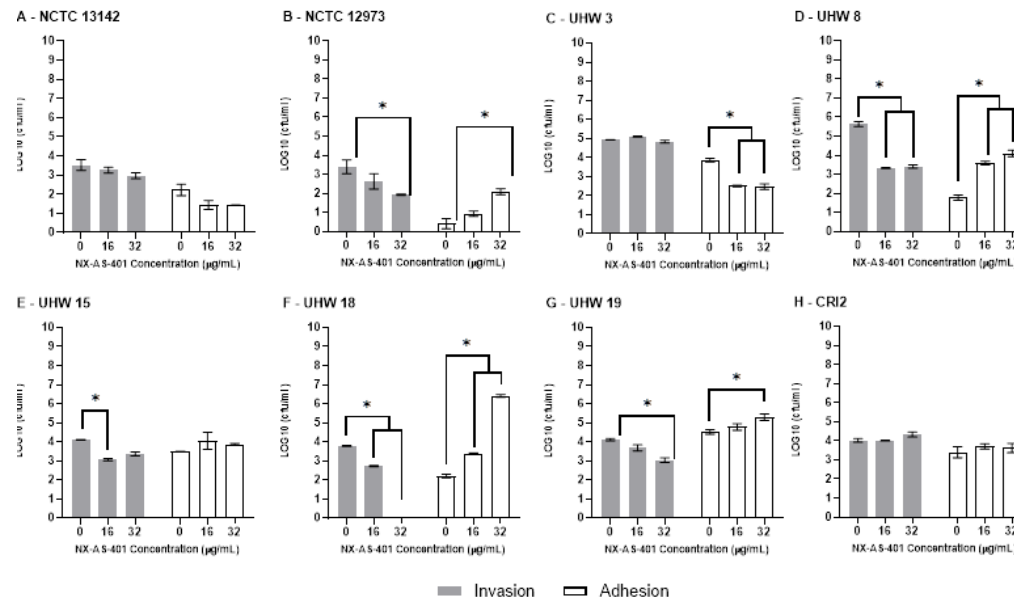


Figure 6.10 Alterations in the ability of *S. aureus* to adhere and invade HaCaT cells.

NX-AS-401 mediated changes in the ability of *S. aureus* to adhere and invade human cells was strain dependent. Statistical significance ($p < 0.05$) is indicated by an asterisk (*), error bars show the standard error of the mean.

Two strains, NCTC 13142 (A) and CRI 2 (H) showed no statistically significant ($p < 0.05$) change in the adherence or invasion of HaCaT cells when treated with 16 or 32 $\mu\text{g/ml}$ NX-AS-401. Strains NCTC 12973 (B), UHW 8 (D), UHW 18 (F) and UHW 19 (G) exhibited significant ($p < 0.05$) increases in adherence at NX-AS-401 concentrations of 32 $\mu\text{g/ml}$, while UHW 8, UHW 15 and UHW 18 displayed increased adherence at 16 $\mu\text{g/ml}$. Strains NCTC 12973, UHW 8, UHW 18 and UHW 19 demonstrated a significant ($p < 0.05$) decrease in the number of invaded *S. aureus* cells at NX-AS-401 concentration of 32 $\mu\text{g/ml}$, a decrease in HaCaT cell invasion was also seen at 16 $\mu\text{g/ml}$ in strains UHW 8, UHW 15 and UHW 18. In UHW 3 (C) adherence to HaCaT cells was significantly reduced ($p < < 0.05$) at NX-AS-401 concentrations of 16 and 32 $\mu\text{g/ml}$.

6.5 Discussion

The presence and production of *S. aureus* virulence factors is linked to both specific diseases states and severity of disease ⁽⁸⁷⁾. When developing new antibiotics or drugs that have an effect on bacteria it is important to consider whether they might affect virulence factor expression and production ^(384, 393). For example, when antibiotic concentrations reach sub-effective doses (due to metabolism or protein binding) the bacterial eradication effects are reduced but the environmental antibiotic pressure can remain, causing increased production of virulence factors such as toxins and extracellular polysaccharide ⁽¹²⁷⁾. It was important to identify whether the pressure exerted by NX-AS-401 at sub-MIC concentrations was going to modulate virulence factor expression and production ^(384, 393).

Modulating virulence factor production can also be used in a positive way, as MIC and sub-MIC antibiotics can also reduce the production of harmful enzymes and products involved in biofilm formation therefore reducing disease severity and improve patient outcomes ^(62, 184, 375, 399). Therefore, anti-virulence drugs have become a more favourable avenue of research for fighting bacteria as they may also provide additional effects such as reducing the impact on the host microbiota in comparison to standard of care antibiotics, thereby preventing dysbiosis and secondary infections ^(62, 184, 399).

6.5.1 Impact of NX-AS-401 on *S. aureus* virulence factor production *in vitro*.

S. aureus produces a variety of virulence factors that can be measured phenotypically. As indicated in Figures 6.2 – 6.5 sub-inhibitory concentrations of NX-AS-401 had no effect on the activity of haemolysin, lipase, protease, and DNase when produced from *S. aureus*.

The eight isolates used in this study underwent alignment via BLAST ⁽⁴²⁹⁾ to determine if *hlyB* was present. In all eight isolates *hlyB* was present with a greater >82 % match to the *hlyB* sequence obtained from UniProt ⁽⁴³⁰⁾ indicating that all strains had the capability of producing β -toxin. This is not uncommon as while the β -toxin gene may be found in the *S. aureus* genome, it is commonly inactivated by bacteriophage ϕ Sa3 that exists in 77-93 % of the *S. aureus* population and prevents β -toxin production ⁽⁴³¹⁾.

The presence of the ϕ Sa3 bacteriophage was confirmed in isolate NCTC 12973 using phage search tool, PHASTER ^(432, 433) but not in the other strains. An explanation as to why strains not carrying the ϕ Sa3 phage did not produce haemolysin beta was identified after the experiment. While β -toxin does affect sheep erythrocytes lysis is not seen unless the plate is incubated at 4 °C after incubation at 36 °C, to activate the hot-cold mechanism of β -toxin ⁽⁴²³⁾. This requires further optimisation of the experiment to identify whether NX-AS-401 mediates β -toxin production.

Haemolytic activity against horse blood cells was strain dependent (**Image not shown**), this is due to the specificity of each haemolysin toxin produced by *S. aureus* and lack of production in γ -toxin that affects horse blood cells ⁽⁴²³⁾. This haemolysin is found within 99 % the *S. aureus* populations genome, which explains why eight *S. aureus* strains were able to produce a zone of lysis ⁽⁴²¹⁾. Variability in production could be due to changes in promoters, regulatory pathways or based on the number of γ -toxin genes within each strain's genome. Understanding this would require whole genome sequencing and RT-qPCR looking at different rates of expression between strains.

However regardless of the amount of γ -toxin produced the addition of sub-inhibitory NX-AS-401 did not cause any changes in the activity of haemolysin in all eight strains.

All eight *S. aureus* strains demonstrate lytic activity on the other media types, showing production of lipase, protease, and DNase but production/activity was strain dependent. In all eight strains NX-AS-401 did not cause any observable difference in lipase activity the zones of lysis on both tributyrin/tween media (**Figure 6.3**) and egg yolk media (Image not shown) indicating no change in lipase activity. Additionally no strain exhibited lecithinase activity in the egg yolk agar that is usually identified by a white opaque zone around the edge of the colony ⁽⁴⁰⁷⁾. DNase (**Figure 6.4**) and protease (**Figure 6.5**) production/activity also remained unchanged when all eight *S. aureus* strains treated with NX-AS-401. This would indicate that NX-AS-401 would not prevent identification of *S. aureus* via DNase plate in current clinical laboratories.

The results complement current literature that confirm *S. aureus* virulence factor production is strain dependent ^(348, 402, 434-436). Whether NX-AS-401 can modulate the expression and activity of other virulence factors is still yet to be determined and requires further investigation. The limitations of agar diffusion tests also include the

unknown properties of NX-AS-401, such as its ability to diffuse through agar and its stability when added to MHA. This could be monitored through agar pH diffusion tests that could measure changes in the ability of small molecules to pass through the agar ⁽³³⁵⁾.

Optimisation studies (**Section 6.4.1**) did conclude that agar supplemented with NX-AS-401 concentrations ≥ 16 $\mu\text{g/ml}$ caused a significant decrease in the size of *S. aureus* colonies and on MHA supplemented with ≥ 32 $\mu\text{g/ml}$ NX-AS-401 *S. aureus* failed to grow. This indicates that NX-AS-401 does have an effect on *S. aureus* colonies when placed in solid media. These values seem to differ from those seen in EUCAST broth microdilution in terms of MIC but these changes are likely due to difference in the diffusion of NX-AS-401 through solid and liquid media. The other explanation is that NX-AS-401 concentrations ≥ 32 $\mu\text{g/ml}$ are inhibiting growth as seen with time/kill curves (**Section 4.4.4.**) and growth curves (**Section 4.4.5.**).

Based on these current tests NX-AS-401 does not fit in with the list of anti-virulence drugs shown in Table 6.1. NX-AS-401 has demonstrated no effect on the lytic enzymes that are often targeted.

However, it is also important that while NX-AS-401 does not demonstrate the ability to decrease virulence factor production at sub-MIC concentrations it also did not increase virulence factor production. This is positive for NX-AS-401 as current standard of care antibiotics, such as vancomycin, clindamycin and gentamicin at sub-MIC levels have increased *S. aureus* virulence factor production *in vitro*, especially leucocidin ED (*LukED*) ^(384, 437). In cases where antibiotics are unable to reach the infection site at a therapeutic dose this could cause further deterioration of the patient ⁽³⁸⁴⁾.

Studies that have focused on the anti-virulence effects of garlic derived compounds have also proven little anti-virulence activity in terms of toxins and enzymes ⁽²¹⁵⁾, but it has been shown that allicin reduced production of *S. aureus* α -toxin by >70 % at concentrations of 16 $\mu\text{g/ml}$ by acting directly on *agrA* and *hla* expression ⁽⁶⁶⁾. Indeed, some studies have established the effects of allicin and ajoene as quorum sensing inhibitors to prevent biofilm formation ^(194, 219, 229, 241, 244).

This was reproduced for NX-AS-401 in the RT-qPCR (**Chapter 5 Section 5.4.7**) but higher concentrations (128 $\mu\text{g/ml}$) were required, and the effect was strain variable.

This does indicate that NX-AS-401 has the capability to modulate virulence in a similar mechanism to allicin, however the effects are reduced, and higher concentrations are required. This indicates that the lack of anti-virulence effects of NX-AS-401 do not make it a viable virulence targeting antibiotic. These investigations were also limited to these phenotypic virulence factors, however, there are many others that could have been investigated employing different methods such as broth haemolysis assays, coagulase and catalase tests ⁽⁴³⁸⁾. More robust investigations utilising proteomic studies (mass spectroscopy and 2D page) to monitor changes in protein production/efficacy to understand the total effect NX-AS-401 has on *S. aureus* would be the best approach to identify changes in virulence factors that causes more severe symptoms such as toxic shock syndrome toxin and the entero/exfoliative toxins ⁽³⁴⁸⁾.

6.5.2 The effects of NX-AS-401 on *G. mellonella* and larvae infected with *S. aureus*

G. mellonella is an insect model used in many studies to determine antibiotic and toxic effects of potential new drugs ⁽²⁷²⁾. The ability for *G. mellonella* to tolerate NX-AS-401 was identified before further *in vivo* studies could be performed involving *S. aureus* infection.

Concerns with NX-AS-401 were due to it containing ≥ 90 % ajoene, a molecule derived from *Allium sativum* commonly known as garlic which has been subject to many studies due to its unique properties in regard to healthcare ⁽²¹⁷⁾. However, historically it has also been used as a pest deterrent and natural insecticide ⁽⁴³⁹⁾. The effects of garlic oil have not been determined against *G. mellonella*, however against other insects such as *Tenebrio molitor* the LD₅₀ for garlic oil was determined at approximately 50 mg/ml for a 1 μ l drop on the insects thorax ⁽⁴⁴⁰⁾.

To determine toxicity, *G. mellonella* larvae were injected with NX-AS-401 concentrations equal to the established MIC (128 μ g/ml), $\frac{1}{2}$ MIC, $\frac{1}{4}$ MIC and 4x MIC for *S. aureus*. Meanwhile, experimental positive controls included *G. mellonella* larvae injected with 10 μ l of PBS to ensure that any deaths were caused by exposure to NX-AS-401 or *S. aureus* infection instead of trauma caused by the injection. Figure 6.6 showed that *G. mellonella* larvae were able to survive at all concentrations of NX-AS-

401 indicating that NX-AS-401 either demonstrates no toxic effect against *G. mellonella* or that any toxic effects did not cause fatality of *G. mellonella* larvae.

Figure 6.7 demonstrates how *S. aureus* dose affects the *G. mellonella* survival ⁽²⁷⁰⁾. In *G. mellonella* experiments an LD₅₀ would usually be calculated for each strain specifically, this was not possible during this experiment due to a small time frame and low budget for the project. In future this experiment would be repeated with more optimisation experiments to ensure an accurate LD₅₀ for each strain. In this experiment this inaccuracy makes strain to strain comparison more difficult, however, whether NX-AS-401 alters *S. aureus* virulence and recovery from infection could still be determined.

S. aureus pathogenicity was strain dependent in as shown in Figures 6.2 to 6.5, this has also been seen with other organisms ⁽⁴⁴¹⁾.

The ability of NX-AS-401 to allow *G. mellonella* to recover from a lethal *S. aureus* infection varied per strain. *G. mellonella* larvae injected with 25.6 mg/kg experienced increased fatality with all strains apart from NCTC 13142 and UHW 18. There are two potential hypotheses for the increased fatality of *G. mellonella* infected with 25.6 mg/kg.

The first is that NX-AS-401 at a dose of 25.6 mg/kg. increased *S. aureus* virulence factor production therefore increasing *G. mellonella* fatality. While this effect has not been well documented, it has been seen with sub-MIC tedizolid that increases the expression of toxin and biofilm associated genes in *G. mellonella* ⁽⁴⁴²⁾. The dose of 25.6 mg/kg NX-AS-401 may be reduced due to dilution of NX-AS-401 by the *G. mellonella* hemolymph or activity may be reduced due to protein binding. Similar to human protein binding, *G. mellonella* protein may bind to NX-AS-401 reducing concentration and thus efficacy ⁽⁴⁴³⁾.

The second hypothesis is while *G. mellonella* tolerated any potential toxic effects associated with NX-AS-401 at high concentrations when given alone, the combination of NX-AS-401 and an *S. aureus* infection overwhelmed the *G. mellonella* larvae reducing survival. This has been shown in studies where *G. mellonella* larvae inoculated with just penicillin G have an increase in oxidative stress in their gut ⁽⁴⁴⁴⁾. While penicillin did not decrease *G. mellonella* survival on its own, the oxidative stress did make the *G. mellonella* more susceptible to bacterial infection and increased fatalities

(^{441, 444}). This may also be caused by activation of inflammation mechanisms due to reactive oxygen species (⁴⁴⁵).

2D-PAGE could be employed as well to identify changes in *G. mellonella* proteins. Since the disulphide bond with ajoene is known to react with cysteine residues and thiol groups the more likely option is that *G. mellonella* proteins are affected. This may be where NX-AS-401 reduces the ability of *G. mellonella* to fight infections as NX-AS-401 may react on the smaller protein chains of antimicrobial peptides (AMPs) that make up a part of the *G. mellonella* innate immune system. This could be investigated through reversed-phase chromatography that has been used to isolate AMPs from *G. mellonella* previously (⁴⁴⁶). Confirmation of whether NX-AS-401 can effect AMPs can also be performed by using In synthesised AMPs or on *S. aureus* infections in *ex vivo* skin models using infected pig skin that produces AMP, the changes can then be identified using mass spectroscopy (⁴⁴⁷).

When *G. mellonella* received a 6.4 mg/kg dose of NX-AS-401 survival was strain dependent and indicates that NX-AS-401 influenced the progress of the *S. aureus* infection during the infection process. No significant changes in survival were identified with NCTC 13142, NCTC 12973, UHW 18, UHW 19 and CRI 2 indicating that the NX-AS-401 concentration was too low to elicit an effect but could not be used at higher concentrations based on the effect seen with 25.6 mg/kg of NX-AS-401.

Increased sensitivity to NX-AS-401 was identified in isolate UHW 8, with an MIC of 64 µg/ml instead of 128 µg/ml according to broth micro dilution (**Chapter 4, 4.4.3**). However, this did not seem to be the same in the *G. mellonella* model as *G. mellonella* infected with UHW 8 and NX-AS-401 demonstrated decreased survival when infected and treated with both NX-AS-401 concentrations. *G. mellonella* were also more susceptible to isolate UHW 3 showing decreased survival rates when infected with *S. aureus* and injected with NX-AS-401. This was most likely caused by UHW 3 being identified as the most virulent strain in optimization tests (**Figure 6.7**) and virulence was increased with a sub inhibitory dose of NX-AS-401. Along with the previously mentioned mass spectroscopy looking at changes in *G. mellonella* proteins expression, mass spectroscopy and RT-qPCR could be employed to identify changes in the expression and production of virulence factors from *S. aureus* during *G. mellonella*

infection ⁽⁴⁴²⁾. However, based on the result obtained it appears that NX-AS-401 demonstrates no anti-virulence attributes and would be used differently.

Direct comparisons between the RT-qPCR data obtained in Chapter 5 and *G. mellonella* cannot be drawn due to the many differences in growth conditions and NX-AS-401 concentrations. However, both UHW 3 and UHW 8 that were shown to be more lethal to *G. mellonella* during infection did not show similar changes in virulence factor production in comparison to each other during the RT-qPCR testing. This may be due to limited number of virulence genes tested during the RT-qPCR and therefore more virulence genes require investigation.

Isolate UHW 15 was the only strain that demonstrated a significant ($p < 0.05$) ability to increase *G. mellonella* survival during *S. aureus* infection when treated with 6.4 mg/kg of NX-AS-401. Further confirmation that the effects of NX-AS-401 on *S. aureus* during *G. mellonella* infection are strain dependent. However, comparison to the RT-qPCR data (**Chapter 5**) does show that UHW 15 exposed to NX-AS-401 showed decreased expression of virulence factor regulators *sigB* and *rot* under all test conditions, although *sigB* expression returned to normal after 24 hours when exposed to both NX-AS-401 concentrations (128 and 256 µg/ml). The repression of *sigB* may explain changes in virulence but raises further questions as *rot* is the gene that represses toxin production and down-regulation should cause an increase in virulence factor production. This is the opposite of what has been seen phenotypically in these *G. mellonella* studies.

It is difficult to compare the effects of NX-AS-401 against *S. aureus* within the *G. mellonella* model with other garlic based extracts, as others have not been tested, the closest available study monitored the effects of the sulphonamide, Sulphamethoxazole (SMX) on the survival of *G. mellonella* infected with *S. aureus* ⁽¹⁶¹⁾. This study did show that daily treatment with SMX did allow for recovery of the *G. mellonella* when they were infected with *S. aureus* strains sensitive to SMX ⁽¹⁶¹⁾. This does indicate that NX-AS-401 is not as effective for systemic infections as the sulphonamide class of antibiotic, however this was never the intention as the proposed application of NX-AS-401 is a topical wound treatment. The effects of *S. aureus* infection and subsequent antibiotic treatment on *G. mellonella* has been identified in other studies via shotgun proteomics and chromatography of the *G. mellonella* haemolymph to identify changes

291

in both *S. aureus* virulence factor production and alteration to the *G. mellonella* immune response ^(270, 448). These methods could be used in the future to identify changes caused by NX-AS-401 in *G. mellonella* and what role NX-AS-401 has during *S. aureus* infection. Expanding the testing parameters by including more timepoints, and repeating treatment with NX-AS-401 may also assist in identifying whether NX-AS-401 can increase *G. mellonella* survival. In future research it might be useful to test NX-AS-401 on human cell line scratch tests to see what effects has on the healing of non-infected wounds. Since ajoene alone has demonstrated anti-inflammatory properties ⁽²³⁹⁾ and can alter cell function in cancerous cells ⁽²⁰⁸⁾, its effects on how it effects non-infected wounds is also important before moving on to infected wounds and more complex tests such as *Ex vivo* infected wound models.

Overall, the effects of NX-AS-401 on *S. aureus* infections appears to be strain variable but high doses of NX-AS-401 can decrease the survival of infected *G. mellonella*. This is not unexpected as studies that have used multiple strains have also shown that *G. mellonella* survival is strain dependent for organisms such as *S. aureus* ^(161, 449) and *Streptococcus pneumoniae* ⁽⁴⁵⁰⁾. Although many studies have used *G. mellonella* as a model for determining antibiotic efficacy it has also been noticed that they are highly variable ^(270, 272, 451) and are susceptible to changes in their environment with alterations to heat, light and food sources causing changes to their immune response ⁽⁴⁵¹⁾.

6.5.3 The ability of NX-AS-401 to modify adherence and invasion of *S. aureus* to human skin cells

Human cell line studies assist in identifying the potential effects of novel compounds *in vitro* before *in vivo* studies commence ⁽⁴⁵²⁾. Keratinocyte cell lines such as HaCaT or HeKa are easily cultured in laboratory conditions and can be often used to identify both phenotypic and molecular changes that occur when exposed to potential drugs such as antibiotics ^(452, 453). Phenotypic changes can often be identified through microscopy and metabolic assays while changes to genetic regulation, chemokine and cytokine production can be identified via PCR and enzyme-linked immunosorbent assays respectively ^(452, 453).

Keratinocytes were chosen for this experiment for better understanding of how NX-AS-401 interacts with the most common cell type found in the human dermis and in both acute and chronic wounds ⁽⁴⁵³⁾. Keratinocytes have been shown to play an important role in the healing of wounds and prevention of infection ⁽⁴⁵³⁾, therefore it is vital to understand whether NX-AS-401 assists, inhibits or has no effect on their ability to manage opportunistic pathogens such as *S. aureus*. HaCaT cells were chosen due to their ease of culture, widespread use and their use in many studies based around *S. aureus* adhesion and invasion.

In the HaCaT cell lines used for cell culture studies NX-AS-401 demonstrated toxicity at a concentration ≥ 64 $\mu\text{g/ml}$ (**Figure 6.9**). This initial assessment indicated that achieving a therapeutic dose close to the MIC (128 $\mu\text{g/ml}$) of NX-AS-401 against *S. aureus* would not be achievable *in vivo*. However, this data does not correlate with the cytotoxicity studies performed in *G. mellonella* larvae (**Figure 6.8**) where no lethal toxic effects were seen when NX-AS-401 was injected up to a concentration of 512 $\mu\text{g/ml}$. Further work may entail the use of ELISAs to monitor cytokine production as a method of determining whether NX-AS-401 causes an inflammatory response, assisting in both immune response and cytotoxicity identifications ⁽⁴⁵⁴⁾.

Discrepancies between these two methods have not been fully studied, while there is a known difference between single cell line and *G. mellonella* cytotoxicity tests and many have been performed using other cell lines, none have specifically used HaCaT cells or identified the reason for the differences ^(270, 272, 455). These studies have shown that the single layer cell model can overestimate the cytotoxic effect of low toxicity compounds, whereas *G. mellonella* may provide a more accurate model due to being a whole system ^(270, 272, 455). The discrepancies between the two models could be caused by multiple issues such as molecules having specific interactions to the species or cell types, for example, *S. aureus* does produce virulence factors that can affect specific cells such as the haemolysins that are species specific and other toxins that effect immune cells such as monocytes but have no effect on keratinocytes ^(421, 452, 456). Another explanation for the discrepancy between the models is the limitations of monolayer cell cultures. Single cell monolayer cultures do not replicate the stratified nature of host tissues and the absence of other host cells, immunity potentially alters the normal reaction of the test cell type in response to a challenge by bacteria or a

toxic compound ⁽⁴⁵⁷⁾. Limitations with measuring cytotoxicity in single cell models also arise due to the single cell type and a loss of tissue structure that allows whole organisms to tolerate higher doses of potentially toxic chemicals ⁽²⁸⁹⁾. Due to the discrepancies in cytotoxic doses for both immortalized human cell lines and *G. mellonella* further investigations would be required to uncover how NX-AS-401 elicits an effect in both models. This would be begin with 3D cell culture using 3D generated cell models from pluripotent stem cell ⁽⁴⁵⁸⁾, pig and mouse skin models ⁽⁴⁵⁹⁾, epithelium tissue inserts that would identify toxic effects on a model with greater similarity to its *in vivo* application.

Monolayer human cell line models do have other applications when determining properties of potential antimicrobials, while NX-AS-401 has demonstrated no anti-virulence effects in phenotypic tests, it has demonstrated anti-biofilm properties (**Chapter 5**) whether the mechanisms that NX-AS-401 affected could also alter the adherence and invasion of *S. aureus* in human cells was measured using the HaCaT cell line. The ability of *S. aureus* cells to adhere and invade HaCaT cells was strain dependent (**Figure 6.10**). This could be attributed to a change in phenotype that has been seen with other antibiotics, for example when treated with sub-inhibitory concentrations of oxacillin *S. aureus* can change into both a hyper-adherent or hypo-adherence phenotype based strain. This is brought about through modulation of fibronectin binding protein ⁽⁴⁶⁰⁾ a main facilitator of cell adherence and internalisation. Modification to this protein or the corresponding receptor $\alpha 5\beta 1$ integrin on the HaCaT cells can cause changes in adhesion and invasion ^(61, 460). A similar reaction seen with NX-AS-401 indicates that it may have an effect on fibronectin binding protein which may explain its effects on *S. aureus* biofilms (**Chapter 5**). However, adhesion and biofilm formation are not dependent on fibronectin binding protein.

While adherence was increased in NCTC 12973, UHW 8, UHW 15, UHW 18 and UHW 19, invasion was decreased in a dose dependent manner with NX-AS-401 concentrations of 32 $\mu\text{g/ml}$ responsible for the larger decrease in invaded cells in all strains apart from UHW 15. This response is likely not toxicity and is most likely caused a similar effect to sub-inhibitory concentrations of antibiotics such as oxacillin and rifampicin demonstrated the ability to block *S. aureus* invasins and prevent internalization of the bacterial cell ⁽⁴⁶⁰⁾ so a similar effect could be present with NX-AS-

401. While *S. aureus* cells can adhere to host cells, preventing *S. aureus* internalisation retains *S. aureus* on the host cell surface where they are more vulnerable to host immune components such as phagocytes and NK cells, complement and antibodies⁽⁴⁶¹⁾. Therefore, preventing internalisation may reduce *S. aureus* cell numbers and increase the chance of eradicating the infection^(274, 462).

Isolate UHW 3 was the only strain that exhibited a dose dependent decrease in the number of adherent cells, and no increase in *S. aureus* invasion was seen. This was different to other studies that identified isolate UHW 3 as the more virulent strain as it was more lethal to *G. mellonella* and produced a moderate amount of biofilm (**Chapter 5**). However, while the presence of NX-AS-401 increased UHW 3 virulence in *G. mellonella* (**Figure 6.8**), the same effect was not seen here as the cells ability to adhere to the HaCaT cell was reduced. This appears to be a strain specific effect and further studies into why UHW 3 reacted differently to NX-AS-401 in comparison to other strains would require more in-depth molecular techniques such as RNA microarray and 2D-PAGE to identify whether NX-AS-401 mediates changes in gene expression/transcription or effects the protein itself, the latter option is more likely due to the known action of the disulphide bond on cysteine residues.

6.5.4 NX-AS-401 as an anti-virulence agent.

Unfortunately, comparison between NX-AS-401, ajoene and other garlic constituents against *S. aureus* cannot be made as there is little information available on the anti-virulence effects of these compounds against *S. aureus*. However, compounds from other natural sources have demonstrated anti-virulence effects, these include phenolic compounds such as catechin from tea and a robust review by Silva *et al*⁽¹⁸⁹⁾ identified many plant based compounds with anti-virulence activity. The only anti-virulence activity attributed to garlic based compounds is the ability of allicin to reduced urease expression in *Proteus mirabilis*, and to neutralise the toxin PLY in *Streptococcus pneumoniae* that can damage all cell types⁽¹⁸⁹⁾. These effects are also due to the activity of allicin on the enzyme and toxin itself rather than through altering expression of the toxin⁽¹⁸⁹⁾, this strengthens the hypothesis that allicin and ajoene act on proteins directly.

The only demonstrated anti-virulence effect of a garlic derived components against *S. aureus* are the effects of allicin on *hla* production ⁽⁶⁶⁾ and changes in biofilm formation ^(194, 347) and other tests have focused on Gram-negative organisms such as *P. aeruginosa* ⁽¹¹³⁾. Due to the wide-spread resistance and side effects associated with sulphonamide class antibiotics they have also not been used for any published anti-virulence studies at sub-MIC levels for comparison against di-sulphide containing NX-AS-401.

The anti-virulence effects of NX-AS-401 varied dependent on methodology used, *S. aureus* strain and NX-AS-401 concentration. Low NX-AS-401 concentrations of <16 µg/ml have no effect on virulence according to phenotypic virulence tests, however concentrations of 16-32 µg/ml can modify the ability of *S. aureus* cells to adhere and invade human epithelial cells. *In vivo* studies indicate that changes in bioavailability or due to additional toxicity NX-AS-401 increases *S. aureus* virulence at higher concentrations of 128-512 µg/ml.

Given additional time and resources it would have been beneficial to expand the tests and look at other virulence factors that had not been tested. Since NX-AS-401 demonstrated no action against the activity of enzymes, future studies would primarily focus on the anti-biofilm effects. As the ability of NX-AS-401 to alter adhesion and invasion has been seen in one cell line and one organism and that it has shown the ability to inhibit and disrupt biofilms (**Chapter 5**), it indicates that NX-AS-401 acts on pathways related to both systems such a fibronectin binding protein production. If given the opportunity additional studies would employ more molecular based analysis of proteins such as 2D-protein agarose gel electrophoresis (2D-PAGE) and mass spectroscopy that could monitor changes in virulence factors associated with biofilms and cellular adhesion ⁽³⁷⁾ Future studies would also include specific *S. aureus* mutants that lack specific biofilm/adhesin virulence factors.

Future work would also focus on the impact of NX-AS-401 on host immunity, focusing on how NX-AS-401 modulates the host immune systems through measurement of cytokine networks by ELISAs. Since the major component ajoene has already proven anti-inflammatory effects ^(209, 239) it would be important to understand how NX-AS-401

changes immune components such as the anti-inflammatory cytokine Interleukin-10 that is produced during bacterial infection and plays a role in immune tolerance.

6.7 Conclusion

Aim: To identify virulence factor phenotype of *S. aureus* strains and identify changes in production after exposure to subinhibitory concentrations of NX-AS-401.

Sub-inhibitory concentrations of NX-AS-401 had no effect production or activity of *S. aureus* haemolysins, lipases, proteases, or DNase. Concentrations were limited in agar plates to 12 µg/ml as higher concentration inhibited *S. aureus* growth (**Section 6.4.1**)

Aim: To identify the toxic effects of NX-AS-401 against both single cell human cell lines (HaCaT) and the whole organism model *G. mellonella*.

The *G. mellonella* model demonstrated that NX-AS-401 did not have any toxic effects against the wax moth larvae. When injected by itself NX-AS-401 did not lead to decreased survival indicating that it is a low toxicity compound. However, in contrast NX-AS-401 demonstrated a cytotoxic effect on HaCaT cells at concentrations >32 µg/ml. Therefore, further investigation is required to identify the full toxic effects and identify whether NX-AS-401 is suitable for infection management in wounds.

Aim: To determine if NX-AS-401 could increase the survival rate *Galleria mellonella* larvae infected with *S. aureus*.

Results were strain dependent when *G. mellonella* were infected with *S. aureus* and treated with NX-AS-401. Injection of 6.4 mg/kg of NX-AS-401 in *S. aureus* infected *G. mellonella* did not lead to increased survival of *G. mellonella* in comparison to untreated controls in six out of 8 strains. In isolate UHW 8 the 6.4 mg/kg NX-AS-401 injection increased lethality and the opposite was seen in UHW 15 where survival was significantly increased. Higher NX-AS-401 doses (25.6 mg/kg) resulted in decreased *G. mellonella* survival when injected with all *S. aureus* strains. This indicated that NX-AS-401 does not have the potential to be used as a systemic infection treatment.

Aim: To determine if NX-AS-401 alters the ability of *S. aureus* to adhere and invade HaCaT cells.

Both 16 and 32 $\mu\text{g/ml}$ NX-AS-401 concentration were able to alter the ability of *S. aureus* cells to adhere and invade HaCaT cells. In these experiments modification of adherence and invasion was both strain and concentration dependent with invasion decreased in six out of eight strains and adherence increased in five out eight strains when treated with 32 $\mu\text{g/ml}$ of NX-AS-401. This demonstrates the strain dependent effects of NX-AS-401 to prevent internalisation of the cells.

Overall NX-AS-401 does not seem to have an effect on *S. aureus* virulence, further testing is required to understand where NX-AS-401 elicits its effects on factors that contribute to adherence and biofilm formation.

7.0 General Discussion:

7.1 NX-AS-401, garlic derived molecules and protein disruption.

The aims of this thesis were to identify the effects of the novel compound NX-AS-401 against the important pathogen *Staphylococcus aureus*. Due to rapid development of antibiotic resistance in bacteria, current antibiotics are becoming less effective ^(132, 146). Predictions indicate that without intermediate intervention there will be approximately 10 million deaths per year by 2050 due to antibiotic resistance ^(132, 146). Therefore, new antibiotics and treatment options are required before treatable infections become untreatable once more.

While there are many avenues for potential antibiotics, this thesis has focused on NX-AS-401, a formulation created by Neem Biotech Ltd. NX-AS-401 derived from garlic, a historical infection treatment and source of compounds such as diallyl polysulphides, allicin and ajoene ⁽¹³⁵⁾. These molecules have already demonstrated a wide array of health benefits, but little research has focused on their antibacterial properties. The main component of NX-AS-401 is the garlic derived molecule ajoene, and this molecule has already been shown to have many health benefits acting as an antithrombotic, anti-inflammatory and anti-tumorigenic agent ^(207, 208, 213, 239). Its effects in microbiology have been varied, previously showing it has anti-fungal and anti-viral effects ^(220, 238, 463). Ajoene has also been studied previously, however information on how it works is limited and mainly focuses on its effects against Gram-negative organisms ^(135, 179, 241).

Although NX-AS-401 does contain >90 % ajoene there were other components present that may have provided additional additive effects when compared to the action of ajoene alone, unfortunately many of these small molecules have not been identified and whether they have been utilized in other studies is unknown. Due to their low levels in NX-AS-401 the likelihood is that the effects demonstrated in this thesis are due to ajoene due to its high presence within NX-AS-401.

Studies by Naganawa *et al* (1996) ⁽²¹⁷⁾, Bjarnsholt *et al* (2015) ⁽²¹⁹⁾ and Jakobsen *et al* (2012 & 2017) ^(194, 241) have previously shown that ajoene has activity on various bacterial species including *Bacillus species*, *E. coli* and *Pseudomonas aeruginosa* (*P. aeruginosa*). The studies by Naganawa ⁽²¹⁷⁾ *et al* and Jakobsen *et al* ^(194, 241) also

contained work into *S. aureus*, however this was limited to growth kinetics and employed different ajoene isomers (primarily Z-ajoene) as well as different growth techniques. Despite the differences in methods, they also concluded that ajoene could inhibit the growth of *S. aureus* but none of the studies uncovered the underlying mechanism of action.

Based on previous literature and how garlic derived components react with other cell types the running hypothesis throughout this thesis was that ajoene and subsequently NX-AS-401 has an effect on bacterial proteins due to the presence of the disulphide bond within ajoene (**Figure 7.1**) which according to Naganawa *et al* is the only source of antimicrobial activity.

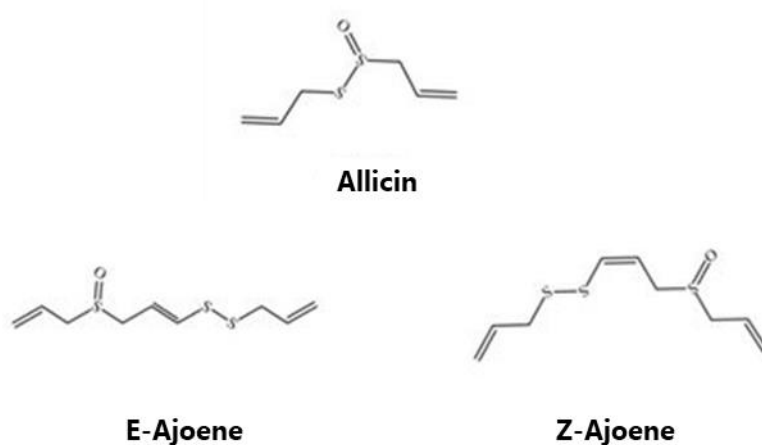


Figure 7.1 The molecular structure of Allicin and both ajoene E-Z isomers.

This hypothesis has been formed because of another garlic derived antimicrobial molecule, specifically allicin. While ajoene remains fairly unresearched, allicin is a well-documented garlic derived antimicrobial (66, 135, 180, 214-216, 222, 226-232, 234, 235, 340, 464). It has a broad spectrum of activity and can easily permeate through cell membranes, the molecule contains a disulphide bond this causes thiol and sulphur stress within the cell (228). However, it is biologically unstable, and activity is lost quickly making it an unviable therapeutic agent.

While allicin and ajoene are derived from garlic, they are structurally different (**Figure 7.1**) and previous studies have identified that they have different mechanisms of activity, that are all dependent on the disulphide bond. Disulphide bonds can interfere

with the bonds that often form between thiol groups of cysteine residues during protein folding, and the presence of additional bonds can interfere with that process causing protein mis-folding (**Figure 7.2**)^(136, 213).

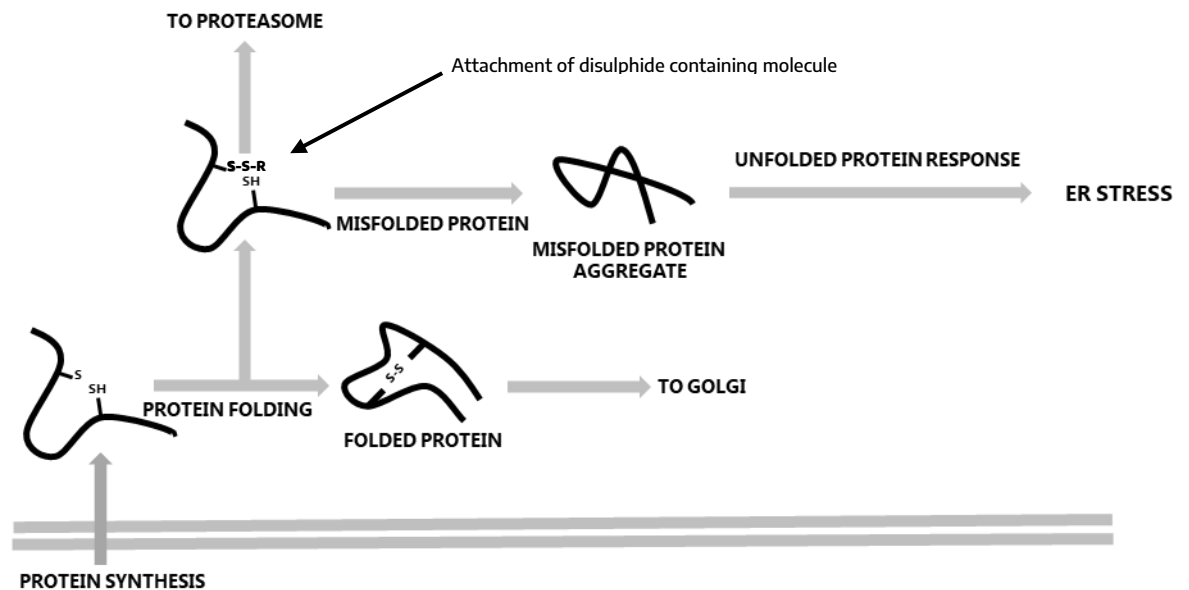


Figure 7.2 The S-thiolation of cysteine thiols by disulphide bonds in cancer cells.

Image created based on data Kaschula *et al* 2015⁽²⁴⁰⁾.

Although the mechanism of action for garlic derived components against bacteria have yet to be understood, there have been studies that indicate how allicin and ajoene cause the death other cell types^(208, 220, 227, 234, 239, 240). In these studies, both molecules are responsible for activity on enzymes vital for cells to function and other proteins^(213, 240). Ajoene caused mis-folding of proteins causing protein aggregates to form and causing apoptosis in cancer cells⁽²⁴⁰⁾. This is due to the disulphide bond causing sulphur thiolation of free cysteines on proteins causing misfolding as shown in Figure 7.2⁽²⁴⁰⁾.

A similar effect was also identified in fungi where ajoene has shown action against the synthesis of phosphatidylcholine, a membrane protein not found in bacterial pathogens^(243, 245). Allicin has shown the ability to inhibit glutathione in fungi, a product seen that is also found in the oxidative stress responses of bacteria^(233, 234). However, *S. aureus* lack the ability to produce glutathione, removing it as a potential target for ajoene⁽²³³⁾.

Stress response to mis-folded proteins not only provides an indication of the mechanisms of action for NX-AS-401 but also explains the increased metabolism caused by sub-inhibitory concentrations. Increases in metabolism during metabolic assays and crystal violet assays were thought to be caused by stress responses. If NX-AS-401 causes a mis-folding of proteins within the bacterial cell this can cause a metabolic stress response, as the cells try to produce more protein, degrade misfolded proteins or use alternative pathways ⁽⁴⁶⁵⁾. This would also fit in with the bacterial response to allicin, that can cause a thiol stress response due to modification of protein cysteines as seen in *E. coli* ⁽⁴⁶⁶⁾. At sub-inhibitory doses NX-AS-401 may not provide a large enough response for cell apoptosis but may cause a significant stress response. This is one possible explanation for the inhibitory and bactericidal effects of NX-AS-401 but requires further confirmation via protein studies, and this could include fluorescence microscopy to physically observe and labels protein aggregates or mass spectroscopy ⁽⁴⁶⁷⁾.

The protein disruption hypothesis may also explain the synergistic effects of NX-AS-401 when used in combination with standard of care antibiotics. In a study by Rendu *et al* (1989) ⁽²³⁹⁾ they determined that ajoene's anti-thrombotic effect was caused by changes in the micro viscosity on the internal side of the artificial and platelet lipid membranes, this resulted in a physical change without the loss of osmotic pressure or changes to the outer side of the membrane ⁽²³⁹⁾. The loss of membrane potential can inhibit the exchange of ions, leading to cell death, similar to antibiotics such as daptomycin, however with a different mechanism as daptomycin form membrane pores ⁽⁴⁶⁸⁾. It is known that the garlic derived components easily permeate through cell membranes without causing cell leakage ⁽²²⁷⁾. This allows for a greater build-up of molecules such as allicin into the cell interior ⁽²²⁷⁾.

Alterations to membrane permeability have also been identified in anti-cancer studies as ajoene has shown the ability to covalently bind to the protein vimentin, where it prevents the migration of metastatic cells ⁽²⁰⁸⁾. In human cells vimentin plays a role in the cytoskeleton by maintaining cell shape and integrity ^(208, 469). It is also known to play a role in the pathogenesis of both bacterial and viral infections, with bacteria such as *E. coli* and *Klebsiella species* using it for internalization ⁽⁴⁶⁹⁾. Unfortunately, the role of vimentin in *S. aureus* infection is not known, but it also assists in the invasion of *S.*

aureus cells into human cells, this potentially indicates why treatment with NX-AS-401 prevented the internalization of *S. aureus* cells into the HaCaT cells in some strains. However, whether this is due to an effect on *S. aureus* or due to HaCaT cells is unknown, but as the effect is strain specific it indicates that *S. aureus* is more likely effected. Using the methods described by Kaschula *et al* ⁽²⁰⁸⁾ may help to identify whether NX-AS-401 has an effect on HaCaT cells. While the presence of vimentin in the *S. aureus* cytoskeleton has not been documented, there are similar intermediate filament proteins that NX-AS-401 may act on ⁽⁴⁷⁰⁾.

Changes in membrane permeability, either through micro viscosity or alteration to the bacterial cytoskeleton require confirmation via fluorescent molecular rotors ⁽⁴⁷¹⁾. These specific fluorescent molecules allow for determination of membrane potential via spectrophotometer detection with an increase in fluorescence that would indicate a loss of membrane potential ⁽⁴⁷¹⁾. This change in viscosity may not only lead to cell death, but may explain antibiotic synergy, as while it may not cause cell leakage an increase in permeability may allow for greater antibiotic penetration. If the effect is nonspecific it may explain why there was synergy with many different antibiotic classes ⁽⁴⁷¹⁾.

Ajoene mediated disruption of protein may also occur at other stages of molecule synthesis such as protein prenylation ⁽²¹³⁾. Protein prenylation a post-translational protein modification that often attaches proteins to lipid molecules ⁽²¹³⁾. This method is used in bacteria to attach proteins to the cell membrane ⁽⁴⁷²⁾, specifically for the MSCRAMM group, a series of proteins essential for *S. aureus* biofilm development. This effect could prevent MSCRAMM mediated cell to cell and extracellular matrix (ECM) attachment ^(58, 59). Acting on protein prenylation rather than the MSCRAMM folding itself may explain the anti-biofilm activity as the MSCRAMM group contains multiple proteins with similar mechanisms of action and it is unlikely NX-AS-401 has an effect on all of them ^(58, 59). The ability to interfere with cell to cell attachment via MSCRAMMS may also explain the strain specific adhesion/invasion effects seen after NX-AS-401 exposure. This may be based on which MSCRAMMS are present as not all strains produce all MSCRAMMS ^(58, 59).

Overall, the current hypothesis that NX-AS-401 reacts with *S. aureus* proteins remains valid and more likely. Another indication of alteration of biological proteins may also

explain the increased virulence of *S. aureus* against *G. mellonella* when treated with 512 µg/ml NX-AS-401. This may be due to NX-AS-401 reacting with innate immune proteins within the *G. mellonella* limiting its capability to manage the infection, or NX-AS-401 treatment may cause over reaction of the immune system leading to *G. mellonella* death.

7.2 Future perspectives.

Future study of NX-AS-401 should continue developing a greater understanding of the NX-AS-401 mechanism of action. Since current hypothesis lays with action of ajoene on cysteine residues a confirmatory test can be performed by performing MICs with added cysteine, if NX-AS-401 does react with cysteine residues its action will be nullified by free cysteine as seen with molecules such as allicin. Another method to determine thiol disruption may be the addition of thiol bond inhibitors such as iodoacetamide that could be applied to *S. aureus* before NX-AS-401 treatment ⁽⁴⁷³⁾.

However, a negative test does not completely disprove the protein disruption theory as other mechanisms may involve proteins.

Identifying which proteins are affected and whether they act on protein synthesis, protein folding or protein prenylation requires further research. In order to determine the wherein protein development and the specificity of NX-AS-401 proteomic studies are required. Unfortunately, the protein experiments planned, specifically 2D-polyacrylamide gel electrophoresis, were not completed due to time and availability of resources. In the future numerous techniques could be employed to identify changes in protein development and function, these have been shown in Table 7.1

Table 7.1 Methods for identifying changes in protein in bacteria.

Technique & References	Details	Potential Outcome	Problems
2 dimensional sodium dodecyl sulphate poly-acrylamide gel electro-phoresis (2D-SDS-PAGE) ⁽⁴⁷⁴⁾	Mass based protein separation via pH and electrical charge,	Quantitative measure that could identify whether NX-AS-401 changes protein production	Second dimension electrophoresis requires application of a reagent (SDS) that unfolds proteins . Therefore, whether NX-AS-401 causing mis-folds and protein aggregate formation would be missed.
Mass spectroscopy ^(474, 475)	Identification of protein sequences via mass and charge. Proteins are identified via database or using genome sequences	This would be performed after 2D-page and would identify which proteins have been modified by NX-AS-401.	Would not detect mis-folded proteins. Requires a good database and highly reproducible 2D-PAGE.
Western blotting ^(474, 476)	Transfer of SDS-PAGE to a membrane, followed by application of protein specific antibodies, and chemically labelled for analysis.	Performed after SDS-PAGE, useful for quantification of specific protein targets.	Highly specific and requires specific antibodies, only selective for one protein at a time, though some methods can strip antibodies allowing the membrane to be re-used.
Enzyme linked immune - sorbent assay (ELISA) ⁽⁴⁷⁷⁾	Can be used on treated cell cultures after sonication or cell lysis. Involves capture and detections of specific ligands and proteins using antibodies. Can be used to detect toxin production.	Quantification of specific protein targets in supernatants and after cell lysis. Does not require treatment of protein and can detect low protein production and indicate protein mis-folding.	Requires specific protein markers.
Fluorescent reporters ⁽⁴⁷⁸⁾	Attachment of green fluorescent protein to specific proteins or split over multiple target. Can be used to target specific proteins or misfolded aggregates, detection of misfolded can be determined via spectroscopy or confocal microscopy.	Identification of mis-folded proteins or the formation of protein aggregates within the cell. Correctly formed proteins will demonstrate more fluorescence than misfolded counterparts.	Is either highly specific or non-specific, requires known targets to selectively bind GFP or will only identify aggregates without indicating which proteins are misfolded

If confirmed direct protein disruption would be a novel mechanism of action as while disruption of protein synthesis is the mechanism for drugs such as glycyclines and tetracycline it usually occurs pre-translation through the 30S subunit ⁽¹⁸²⁾. This different mechanism of action may also explain the high levels of antibiotic synergy as the antibiotic and NX-AS-401 are not in competition for the same binding site. Another future investigation into the antibiotic synergy of NX-AS-401 is determining if NX-AS-401 can cause misfolding of enzymes that cleave specific antibiotics, such as penicillinases ⁽¹¹⁶⁾. This could determine if NX-AS-401 could be used in combination therapies to overcome known resistance mechanisms.

7.3 Other components of NX-AS-401

The proposed purpose of NX-AS-401 is as a topical antibiotic agent, and this has been seen with previous garlic-based remedies, however, no garlic based treatment has made it into the clinic. Garlic and garlic containing poultices, ointments and salves have been used historically as treatments for various ailments and infections ^(205, 211). A recent study has looked at the role of the traditional Bald's eyesalve that utilized allium plants, onion and garlic to act as antimicrobial agents ⁽²⁰⁵⁾. This salve was primarily applied as a topical agent for eye infections and have proven antibacterial effects ⁽²⁰⁵⁾. On further investigation the activity was majorly attributed to the presence of garlic, and while the study claimed no anti-biofilm effects for garlic, the anti-biofilm effects were identified with NX-AS-401 ^(205, 223). This may indicate that there is synergism between the components or that the antibacterial effects of garlic are not solely due to the presence of allicin and ajoene.

Since ajoene is the primary component of NX-AS-401, the thesis has focused on how this molecule affects *S. aureus*. However, NX-AS-401 also contains other compounds. Currently they are small and unidentifiable, so it is difficult to speculate on their mechanisms of action or the role they have in the anti-bacterial effect of NX-AS-401. In other antibiotic agents that are either derived from or composed of natural products such as plants, the activity is not solely attributed to one molecule but several and in some cases the removal of certain molecules can inhibit the antibacterial activity ^(201, 479).

For example other plants such as ginger⁽²⁰¹⁾ and essential oils of thyme, peppermint, lavender and lemon⁽⁴⁷⁹⁾ have multiple antibacterial constituents that can demonstrate activity on their own but appear more active when used in combination. This is also seen in non-plant derived natural products such as honey⁽¹⁹⁹⁾. This may be due to an intrinsic synergistic effect between all the compounds present. Whether this is the same for NX-AS-401 will require further chemical analysis, identification of the small components and separate antimicrobial sensitivity testing. Exploring the chemical side of NX-AS-401 could allow for greater refinement of the potential antibacterial role and reduce the effective concentration, this increased efficacy could then support the role of NX-AS-401 in wound care.

7.4 Further work:

Since the MIC for NX-AS-401 is high (128 µg/ml) in comparison to other antibiotics (1 µg/ml) and based on the limited human cytotoxicity tests (**Chapter 6.5.3.1**) where NX-AS-401 reduced HaCaT cell metabolic activity at 32 µg/ml, that concentration may not be viable for a topical treatment. However, toxicity doses of NX-AS-401 in *G. mellonella* systemically was much higher (512 µg/ml). Confirmation of the potential toxic effects of a compound often involve *in vivo* animal models. This would be required to determine the toxicity of NX-AS-401 as the HaCaT cell monolayer is inaccurate for toxicity studies due to the limitation such as osmosis, shearing and lack of stratification^(452, 453). While *G. mellonella* are comparable for low toxic compounds they are not as accurate with high toxicity compounds⁽⁴⁵⁵⁾ therefore other tests such as animal models are required.

Despite some limitations, *in vitro* cell culture methods could also be employed to understand how NX-AS-401 affects normal wound healing. This can begin with the standardised epithelial scratch assay, where an established monolayer of cells is scratched to form a mock wound⁽⁴⁸⁰⁾, NX-AS-401 could then be applied both singularly and in antibiotic combination before monitoring wound healing via microscopy⁽⁴⁸⁰⁾. Latter tests can then incorporate *ex-vivo* models such as porcine skin models where wounds can be generated through different measures, including freeze shock and surgical cuts^(480, 481). Once wounded the skin can undergo healing through re-

epithelisation in cell culture medium, this can determine the effects of NX-AS-401 on the healing of a stratified dermis ^(480, 481). The advantages of the *ex vivo* porcine skin model is that the wounds can also be made to replicate diabetic wounds through the addition of glucose and can also be infected with different bacteria allowing for greater understanding of the role of NX-AS-401 against chronic and acute wound infections ⁽⁴⁸⁰⁾. These studies can also help identify any effects NX-AS-401 might have on certain host responses by looking at cytokine production from porcine skin during wound healing/infection ^(480, 481).

These investigations can then be expanded to the role of NX-AS-401 on the immune response. Identifying whether NX-AS-401 modifies production/action of interleukins (IL) associated with bacterial infection such as IL-6, IL-7 and IL-10 that are involved in inflammation and b-cell proliferation ^(41, 482). The role of NX-AS-401 on other cytokines such as tumour necrosis factor and interferon-gamma may provide insight as to whether NX-AS-401 has other effects, than hinder or enhance the host immune response to infection ⁽⁴⁸²⁾.

For other experiments performed further clarification is required, this includes the addition of confocal microscopy to visualise *S aureus* invaded HaCaT cells ⁽⁴⁸³⁾. This would require a fluorescence tagged *S. aureus* strain ^(483, 484). Confirmation of internalisation of the *S. aureus* into the HaCaT cell would ensure the invasion phenotype and help to limit the potential errors when enumerating bacteria according the TVC methodology used. This is due to limitations of cell adhesion/invasion assays and the use of chemicals that lyse human cells can also cause lysis of bacterial cells leading to false enumeration. For example triton X-100 can lyse *S. aureus* cells at an 0.5 % concentration ⁽⁴⁸⁵⁾.

Gene expression studies should also be performed on planktonic cells and employ the use of more global approaches such as RNA sequencing. This may further the understanding of NX-AS-401 on *S. aureus* gene expression and help understand the changes seen here on two component pathways that were not tested such as *saeRS*, *srrAB* and *arIRS*. This may require further investigation if proteomic studies do not confirm the current hypothesis of action on proteins.

Finally, optimisation of the formulation is required, this project began during the infancy of NX-AS-401 development, since more information has become available and there are known differences between ajoene isomer function it would be important to develop the most effective formulation of NX-AS-401. However, this may be easier once the underlying mechanism of action is determined.

Hopefully with further research and development drugs such as NX-AS-401 can assist in combating the growing threat posed by antimicrobial resistance.

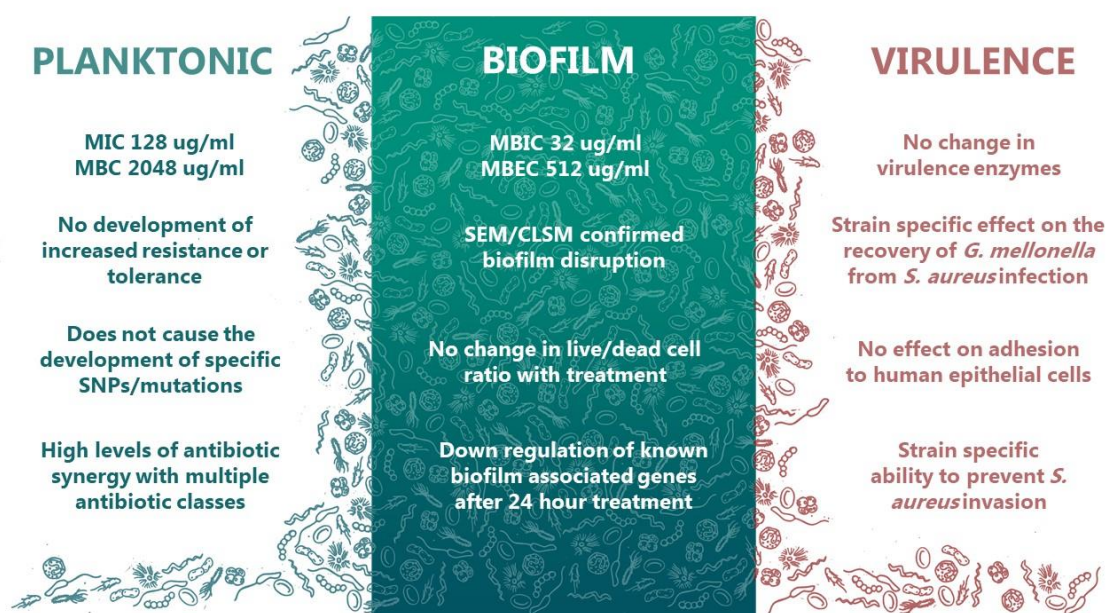


Figure 7.3 The effects of NX-AS-401 against methicillin resistant *Staphylococcus aureus* (MRSA).

A summary of all the findings of this project and the identified effects of NX-AS-401.

8.0 References

1. Guest JF, Ayoub N, McIlwraith T, Uchegbu I, Gerrish A, Weidlich D, et al. Health economic burden that wounds impose on the National Health Service in the UK. *BMJ Open*. 2015;5(12):e009283.
2. Bowler PG, Duerden BI, Armstrong DG. Wound microbiology and associated approaches to wound management. *Clin Microbiol Rev*. 2001;14(2):244-69.
3. Giacometti A, Cirioni O, Schimizzi AM, Prete MSD, Barchesi F, D'errico MM, et al. Epidemiology and Microbiology of Surgical Wound Infections. *Journal of Clinical Microbiology*. 2000;38(2):918-22.
4. Posnett J, Franks PJ. The Burden of Chronic Wound in the UK. *Nursing Time*. 2008;104(3):44-5.
5. Spencer RC. Predmoninant pathogens found in the European prevalence of infection in intensive care study. *European Journal of Clinical Microbiology and Infectious Diseases*. 1996;15(4):281-5.
6. Kawasumi A, Sagawa N, Hayashi S, Yokoyama H, Tamura K. Wound Healing in Mammals and Amphibians: Toward Limb Regeneration in Mammals. *Current topics in microbiology and immunology*. 2012;367.
7. Guo S, Dipietro LA. Factors affecting wound healing. *J Dent Res*. 2010;89(3):219-29.
8. UK W. Best practice statement: The use of topical antimicrobial agents in wound management. In: UK W, editor. 3rd ed. London: Wounds UK; 2013.
9. Dryden M. Complicated skin and soft tissue infection. *Journal of Antimicrobial Chemotherapy*. 2010;65(3):35-44.
10. Ford M. *Medical Microbiology*. 2nd ed. Oxford: Oxford University Printing Press; 2014. 484 p.
11. Ziebuhr W, Hennig S, Eckart M, Kränzler H, Batzilla C, Kozitskaya S. Nosocomial infections by *Staphylococcus epidermidis*: how a commensal bacterium turns into a pathogen. *International Journal of Antimicrobial Agents*. 2006;28, Supplement 1:14-20.
12. Cronquist AB, Jakob K, Lai L, Della Latta P, Larson EL. Relationship between skin microbial counts and surgical site infection after neurosurgery. *Clin Infect Dis*. 2001;33(8):1302-8.
13. Neopane P, Nepal HP, Shrestha R, Uehara O, Abiko Y. In vitro biofilm formation by *Staphylococcus aureus* isolated from wounds of hospital-admitted patients and their association with antimicrobial resistance. *Int J Gen Med*. 2018;11:25-32.
14. James GA, Swogger E, Wolcott R, Pulcini Ed, Secor P, Sestrich J, et al. Biofilms in chronic wounds. *Wound Repair and Regeneration*. 2008;16(1):37-44.
15. Team NGU. National Institute for Health and Care Excellence: Clinical Guidelines. Surgical site infections: prevention and treatment. London: National Institute for Health and Care Excellence (UK); 2019.

16. Team NGU. National Institute for Health and Care Excellence: Clinical Guidelines. Cellulitis and erysipelas: antimicrobial prescribing. London: National Institute for Health and Care Excellence (UK); 2019.
17. Muhammed Ameen S RJ, Le Poullain MN,. Orally Administered Trimethoprim-Sulfamethoxazole for Deep Staphylococcal Infections. *Clinical Infectious Diseases*. 2017;58(11):iii-iv.
18. Internal Clinical Guidelines t. National Institute for Health and Care Excellence: Clinical Guidelines. Diabetic Foot Problems: Prevention and Management. London: National Institute for Health and Care Excellence (UK); 2015.
19. Internal Clinical Guidelines t. National Institute for Health and Care Excellence: Clinical Guidelines. Antimicrobial stewardship: systems and processes for effective antimicrobial medicine use. London: National Institute for Health and Care Excellence (UK); 2015.
20. Lipsky BA, Hoey C. Topical Antimicrobial Therapy for Treating Chronic Wounds. *Clinical Infectious Diseases*. 2009;49(10):1541-9.
21. Frykberg RG, Banks J. Challenges in the Treatment of Chronic Wounds. *Adv Wound Care (New Rochelle)*. 2015;4(9):560-82.
22. Bowler PG, Duerden BI, Armstrong DG. Wound microbiology and associated approaches to wound management. *Clinical microbiology reviews*. 2001;14(2):244-69.
23. Band VI, Crispell EK, Napier BA, Herrera CM, Tharp GK, Vavikolanu K, et al. Antibiotic failure mediated by a resistant subpopulation in *Enterobacter cloacae*. *Nat Microbiol*. 2016;1(6):16053-.
24. Ventola CL. The antibiotic resistance crisis: part 1: causes and threats. *P T*. 2015;40(4):277-83.
25. Song T, Duperthuy M, Wai SN. Sub-Optimal Treatment of Bacterial Biofilms. *Antibiotics (Basel, Switzerland)*. 2016;5(2):23.
26. Band VI, Weiss DS. Heteroresistance: A cause of unexplained antibiotic treatment failure? *PLOS Pathogens*. 2019;15(6):e1007726.
27. Murray PR, Rosenthal KS, Pfaller MA. *Medical Microbiology E-Book: Elsevier Health Sciences*; 2015.
28. Foster T. *Staphylococcus*. *Medical Microbiology 4th Edition*. Galveston, Texas: University of Texas Medical Branch at Galveston; 1996.
29. Gosbell, Gosbell IB. Methicillin-Resistant *Staphylococcus aureus*. *American Journal of Clinical Dermatology*. 2004;40(5):239-59.
30. Sisirak M, Zvizdic A, Hukic M. Methicillin-resistant *Staphylococcus aureus* (MRSA) as a cause of nosocomial wound infections. *Bosn J Basic Med Sci*. 2010;10(1):32-7.
31. Grif K, Heller I, Prodinger WM, Lechleitner K, Lass-Flörl C, Orth D. Improvement of detection of bacterial pathogens in normally sterile body sites with a focus on orthopedic samples by use of a commercial 16S rRNA broad-range PCR and sequence analysis. *Journal of clinical microbiology*. 2012;50(7):2250-4.

32. Grice EA, Segre JA. The skin microbiome. *Nature Reviews Microbiology*. 2011;9(4):244-53.
33. Otto M. Staphylococcus colonization of the skin and antimicrobial peptides. *Expert Rev Dermatol*. 2010;5(2):183-95.
34. Lacey KA, Geoghegan JA, McLoughlin RM. The Role of Staphylococcus aureus Virulence Factors in Skin Infection and Their Potential as Vaccine Antigens. *Pathogens*. 2016;5(1):22.
35. Schlievert PM, Strandberg KL, Lin Y-C, Peterson ML, Leung DYM. Secreted virulence factor comparison between methicillin-resistant and methicillin-sensitive Staphylococcus aureus, and its relevance to atopic dermatitis. *J Allergy Clin Immunol*. 2010;125(1):39-49.
36. Geiger T, Goerke C, Mainiero M, Kraus D, Wolz C. The virulence regulator Sae of Staphylococcus aureus: promoter activities and response to phagocytosis-related signals. *Journal of bacteriology*. 2008;190(10):3419-28.
37. Mandell GL. Catalase, superoxide dismutase, and virulence of Staphylococcus aureus. In vitro and in vivo studies with emphasis on staphylococcal-leukocyte interaction. *Journal of Clinical Investigation*. 1975;55(3):561-6.
38. Adler A, Temper V, Block CS, Abramson N, Moses AE. Pantone-Valentine Leukocidin-producing Staphylococcus aureus. *Emerging Infectious Diseases*. 2006;12(11):1789-90.
39. Vandenesch F, Naimi T, Enright MC, Lina G, Nimmo GR, Heffernan H, et al. Community-acquired methicillin-resistant Staphylococcus aureus carrying Pantone-Valentine leukocidin genes: worldwide emergence. *Emerg Infect Dis*. 2003;9(8):978-84.
40. Löffler B, Hussain M, Grundmeier M, Brück M, Holzinger D, Varga G, et al. Staphylococcus aureus Pantone-Valentine Leukocidin Is a Very Potent Cytotoxic Factor for Human Neutrophils. *PLOS Pathogens*. 2010;6(1):e1000715.
41. Kobayashi SD, Malachowa N, DeLeo FR. Pathogenesis of Staphylococcus aureus abscesses. *The American journal of pathology*. 2015;185(6):1518-27.
42. Bronner S, Monteil H, Prevost G. Regulation of virulence determinants in Staphylococcus aureus: complexity and applications. *FEMS Microbiol Rev*. 2004;28(2):183-200.
43. Wang B, Muir TW. Regulation of Virulence in Staphylococcus aureus: Molecular Mechanisms and Remaining Puzzles. *Cell Chem Biol*. 2016;23(2):214-24.
44. Fitzgerald JR, Monday SR, Foster TJ, Bohach GA, Hartigan PJ, Meaney WJ, et al. Characterization of a putative pathogenicity island from bovine Staphylococcus aureus encoding multiple superantigens. *J Bacteriol*. 2001;183(1):63-70.
45. McCarthy AJ, Lindsay JA. The distribution of plasmids that carry virulence and resistance genes in Staphylococcus aureus is lineage associated. *BMC Microbiol*. 2012;12:104.
46. Xia G, Wolz C. Phages of Staphylococcus aureus and their impact on host evolution. *Infection, Genetics and Evolution*. 2014;21:593-601.
47. Mishra AK, Yadav P, Mishra A. A Systemic Review on Staphylococcal Scalded Skin Syndrome (SSSS): A Rare and Critical Disease of Neonates. *Open Microbiol J*. 2016;10:150-9.

- 48.Ladhani S, Joannou CL, Lochrie DP, Evans RW, Poston SM. Clinical, Microbial, and Biochemical Aspects of the Exfoliative Toxins Causing Staphylococcal Scalded-Skin Syndrome. *Clinical Microbiology Reviews*. 1999;12(2):224-42.
- 49.Jenul C, Horswill AR. Regulation of *Staphylococcus aureus* Virulence. *Microbiol Spectr*. 2018;6(1):10.1128/microbiolspec.GPP3-0031-2018.
- 50.Tegmark K, Morfeldt E, Arvidson S. Regulation of agr-dependent virulence genes in *Staphylococcus aureus* by RNAIII from coagulase-negative staphylococci. *Journal of bacteriology*. 1998;180(12):3181-6.
- 51.Oogai Y, Matsuo M, Hashimoto M, Kato F, Sugai M, Komatsuzawa H. Expression of virulence factors by *Staphylococcus aureus* grown in serum. *Applied and environmental microbiology*. 2011;77(22):8097-105.
- 52.Kolar SL, Ibarra JA, Rivera FE, Mootz JM, Davenport JE, Stevens SM, et al. Extracellular proteases are key mediators of *Staphylococcus aureus* virulence via the global modulation of virulence-determinant stability. *Microbiologyopen*. 2013;2(1):18-34.
- 53.Kong C, Neoh H-m, Nathan S. Targeting *Staphylococcus aureus* Toxins: A Potential form of Anti-Virulence Therapy. *Toxins*. 2016;8(3):72.
- 54.Roberts C, Anderson KL, Murphy E, Projan SJ, Mounts W, Hurlburt B, et al. Characterizing the effect of the *Staphylococcus aureus* virulence factor regulator, SarA, on log-phase mRNA half-lives. *Journal of bacteriology*. 2006;188(7):2593-603.
- 55.Tuchscher L, Bischoff M, Lattar SM, Noto Llana M, Pfortner H, Niemann S, et al. Sigma Factor SigB Is Crucial to Mediate *Staphylococcus aureus* Adaptation during Chronic Infections. *PLOS Pathogens*. 2015;11(4):e1004870.
- 56.Subrt N, Mesak LR, Davies J. Modulation of virulence gene expression by cell wall active antibiotics in *Staphylococcus aureus*. *J Antimicrob Chemother*. 2011;66(5):979-84.
- 57.Gong JQ, Lin L, Lin T, Hao F, Zeng FQ, Bi ZG, et al. Skin colonization by *Staphylococcus aureus* in patients with eczema and atopic dermatitis and relevant combined topical therapy: a double-blind multicentre randomized controlled trial. *Br J Dermatol*. 2006;155(4):680-7.
- 58.Walsh EJ, Miajlovic H, Gorkun OV, Foster TJ. Identification of the *Staphylococcus aureus* MSCRAMM clumping factor B (ClfB) binding site in the α C-domain of human fibrinogen. *Microbiology*. 2008;154(Pt 2):550-8.
- 59.Ghasemian A, Najar Peerayeh S, Bakhshi B, Mirzaee M. The Microbial Surface Components Recognizing Adhesive Matrix Molecules (MSCRAMMs) Genes among Clinical Isolates of *Staphylococcus aureus* from Hospitalized Children. *Iranian journal of pathology*. 2015;10(4):258-64.
- 60.Foster TJ, Geoghegan JA, Ganesh VK, Hook M. Adhesion, invasion and evasion: the many functions of the surface proteins of *Staphylococcus aureus*. *Nat Rev Microbiol*. 2014;12(1):49-62.
- 61.Josse J, Laurent F, Diot A. Staphylococcal Adhesion and Host Cell Invasion: Fibronectin-Binding and Other Mechanisms. *Frontiers in Microbiology*. 2017;8(2433).
- 62.Kong C, Neoh HM, Nathan S. Targeting *Staphylococcus aureus* Toxins: A Potential form of Anti-Virulence Therapy. *Toxins (Basel)*. 2016;8(3).

63. Boisset S, Geissmann T, Huntzinger E, Fechter P, Bendridi N, Possedko M, et al. Staphylococcus aureus RNAIII coordinately represses the synthesis of virulence factors and the transcription regulator Rot by an antisense mechanism. *Genes Dev.* 2007;21(11):1353-66.
64. Gupta RK, Luong TT, Lee CY. RNAIII of the Staphylococcus aureus agr system activates global regulator MgrA by stabilizing mRNA. *Proceedings of the National Academy of Sciences of the United States of America.* 2015;112(45):14036-41.
65. Korem M, Gov Y, Kiran MD, Balaban N. Transcriptional profiling of target of RNAIII-activating protein, a master regulator of staphylococcal virulence. *Infection and immunity.* 2005;73(10):6220-8.
66. Leng B-F, Qiu J-Z, Dai X-H, Dong J, Wang J-F, Luo M-J, et al. Allicin reduces the production of α -toxin by Staphylococcus aureus. *Molecules.* 2011;16(9):7958-68.
67. Tam K, Torres VJ. Staphylococcus aureus Secreted Toxins and Extracellular Enzymes. *Microbiol Spectr.* 2019;7(2):10.1128/microbiolspec.GPP3-0039-2018.
68. Newstead LL, Varjonen K, Nuttall T, Paterson GK. Staphylococcal-Produced Bacteriocins and Antimicrobial Peptides: Their Potential as Alternative Treatments for Staphylococcus aureus Infections. *Antibiotics (Basel, Switzerland).* 2020;9(2):40.
69. Foster TJ, Geoghegan JA, Ganesh VK, Höök M. Adhesion, invasion and evasion: the many functions of the surface proteins of Staphylococcus aureus. *Nature reviews Microbiology.* 2014;12(1):49-62.
70. Beenken KE, Dunman PM, McAleese F, Macapagal D, Murphy E, Projan SJ, et al. Global gene expression in Staphylococcus aureus biofilms. *Journal of bacteriology.* 2004;186(14):4665-84.
71. Merritt JH, Kadouri DE, O'Toole GA. Growing and analyzing static biofilms. *Curr Protoc Microbiol.* 2005;Chapter 1:Unit-1B.
72. Stoodley P, Sauer K, Davies DG, Costerton JW. Biofilms as complex differentiated communities. *Annual review of microbiology.* 2002;56:187-209.
73. Donlan RM. Biofilms: microbial life on surfaces. *Emerging infectious diseases.* 2002;8(9):881-90.
74. Donlan RM, Costerton JW. Biofilms: Survival Mechanisms of Clinically Relevant Microorganisms. *Clinical Microbiology Reviews.* 2002;15(2):167-93.
75. Balamurugan P, Praveen Krishna V, Bharath D, Lavanya R, Vairaprakash P, Adline Princy S. Staphylococcus aureus Quorum Regulator SarA Targeted Compound, 2-[(Methylamino)methyl]phenol Inhibits Biofilm and Down-Regulates Virulence Genes. *Frontiers in Microbiology.* 2017;8(1290).
76. Le KY, Otto M. Quorum-sensing regulation in staphylococci-an overview. *Front Microbiol.* 2015;6:1174.
77. Queck SY, Jameson-Lee M, Villaruz AE, Bach TH, Khan BA, Sturdevant DE, et al. RNAIII-independent target gene control by the agr quorum-sensing system: insight into the evolution of virulence regulation in Staphylococcus aureus. *Mol Cell.* 2008;32(1):150-8.
78. Ahmad W, Zhai Z, Gao C. Adaptive anti-bacterial biomaterial surfaces and their applications. *Materials Today Bio.* 2019;2:100017.

79. Bjarnsholt T, Buhlin K, Dufrêne YF, Gomelsky M, Moroni A, Ramstedt M, et al. Biofilm formation – what we can learn from recent developments. *Journal of Internal Medicine*. 2018;284(4):332-45.
80. de Castro Melo P, Ferreira LM, Filho AN, Zafalon LF, Vicente HIG, de Souza V. Comparison of methods for the detection of biofilm formation by *Staphylococcus aureus* isolated from bovine subclinical mastitis. *Braz J Microbiol*. 2013;44(1):119-24.
81. Kırmusaoğlu S. Staphylococcal Biofilms: Pathogenicity, Mechanism and Regulation of Biofilm Formation by Quorum-Sensing System and Antibiotic Resistance Mechanisms of Biofilm-Embedded Microorganisms. In: Dhanasekaran D, Thajuddin N, editors. *Microbial Biofilms - Importance and Applications*. Rijeka: InTech; 2016. p. Ch. 10.
82. O'Toole GA. Microtiter dish biofilm formation assay. *J Vis Exp*. 2011(47):2437.
83. Joo H-S, Otto M. Molecular basis of in vivo biofilm formation by bacterial pathogens. *Chem Biol*. 2012;19(12):1503-13.
84. Bjarnsholt T, Alhede M, Alhede M, Eickhardt S, Moser C, Kühl M, et al. The in vivo biofilm. *Trends in microbiology*. 2013;21.
85. Di Martino P. Extracellular polymeric substances, a key element in understanding biofilm phenotype. *AIMS Microbiol*. 2018;4(2):274-88.
86. Otto M. Staphylococcal biofilms. *Curr Top Microbiol Immunol*. 2008;322:207-28.
87. Archer NK, Mazaitis MJ, Costerton JW, Leid JG, Powers ME, Shirtliff ME. *Staphylococcus aureus* biofilms: properties, regulation, and roles in human disease. *Virulence*. 2011;2(5):445-59.
88. Chung PY, Toh YS. Anti-biofilm agents: recent breakthrough against multi-drug resistant *Staphylococcus aureus*. *Pathog Dis*. 2014;70(3):231-9.
89. Koo H, Allan RN, Howlin RP, Stoodley P, Hall-Stoodley L. Targeting microbial biofilms: current and prospective therapeutic strategies. *Nature reviews Microbiology*. 2017;15(12):740-55.
90. Lister JL, Horswill AR. *Staphylococcus aureus* biofilms: recent developments in biofilm dispersal. *Frontiers in cellular and infection microbiology*. 2014;4:178.
91. Schilcher K, Andreoni F, Dengler Haunreiter V, Seidl K, Hasse B, Zinkernagel AS. Modulation of *Staphylococcus aureus* Biofilm Matrix by Subinhibitory Concentrations of Clindamycin. *Antimicrobial agents and chemotherapy*. 2016;60(10):5957-67.
92. Speziale P, Pietrocola G, Foster TJ, Geoghegan JA. Protein-based biofilm matrices in *Staphylococci*. *Frontiers in cellular and infection microbiology*. 2014;4:171-.
93. Fluckiger U, Ulrich M, Steinhuber A, Döring G, Mack D, Landmann R, et al. Biofilm formation, *icaADBC* transcription, and polysaccharide intercellular adhesin synthesis by *staphylococci* in a device-related infection model. *Infection and immunity*. 2005;73(3):1811-9.
94. Beitelshes M, Hill A, Jones CH, Pfeifer BA. Phenotypic Variation during Biofilm Formation: Implications for Anti-Biofilm Therapeutic Design. *Materials (Basel)*. 2018;11(7):1086.

95. Le KY, Otto M. Quorum-sensing regulation in staphylococci-an overview. *Frontiers in Microbiology*. 2015;6:1174-.
96. Tan L, Li SR, Jiang B, Hu XM, Li S. Therapeutic Targeting of the *Staphylococcus aureus* Accessory Gene Regulator (*agr*) System. *Frontiers in Microbiology*. 2018;9:55-.
97. Boles BR, Horswill AR. *agr*-Mediated Dispersal of *Staphylococcus aureus* Biofilms. *PLOS Pathogens*. 2008;4(4):e1000052.
98. Sharma-Kuinkel BK, Mann EE, Ahn J-S, Kuechenmeister LJ, Dunman PM, Bayles KW. The *Staphylococcus aureus* *LytSR* Two-Component Regulatory System Affects Biofilm Formation. *Journal of Bacteriology*. 2009;191(15):4767-75.
99. Yarwood JM, Schlievert PM. Quorum sensing in *Staphylococcus* infections. *The Journal of clinical investigation*. 2003;112(11):1620-5.
100. Metcalf DG, Bowler PG. Biofilm delays wound healing: A review of the evidence. *Burns Trauma*. 2013;1(1):5-12.
101. Larsen T, Fiehn N-E. Dental biofilm infections – an update. *APMIS*. 2017;125(4):376-84.
102. Fleming D, Rumbaugh K. The Consequences of Biofilm Dispersal on the Host. *Scientific reports*. 2018;8(1):10738-.
103. Spurlock SL, Hanie EA. Antibiotics in the treatment of wounds. *Vet Clin North Am Equine Pract*. 1989;5(3):465-82.
104. Wilkins M, Hall-Stoodley L, Allan RN, Faust SN. New approaches to the treatment of biofilm-related infections. *J Infect*. 2014;69 Suppl 1:S47-52.
105. Bjarnsholt T, Alhede M, Alhede M, Eickhardt-Sorensen SR, Moser C, Kuhl M, et al. The in vivo biofilm. *Trends in microbiology*. 2013;21(9):466-74.
106. Vulin C, Leimer N, Huemer M, Ackermann M, Zinkernagel AS. Prolonged bacterial lag time results in small colony variants that represent a sub-population of persisters. *Nature communications*. 2018;9(1):4074-.
107. Lewis K. Persister cells, dormancy and infectious disease. *Nat Rev Microbiol*. 2007;5(1):48-56.
108. Ayrapetyan M, Williams T, Oliver JD. Relationship between the Viable but Nonculturable State and Antibiotic Persister Cells. *J Bacteriol*. 2018;200(20).
109. McCarthy H, Rudkin JK, Black NS, Gallagher L, O'Neill E, O'Gara JP. Methicillin resistance and the biofilm phenotype in *Staphylococcus aureus*. *Frontiers in cellular and infection microbiology*. 2015;5:1.
110. Wang Y, Tan X, Xi C, Phillips KS. Removal of *Staphylococcus aureus* from skin using a combination antibiofilm approach. *npj Biofilms and Microbiomes*. 2018;4(1):16.
111. Ahmed A, Azim A, Gurjar M, Baronia AK. Current concepts in combination antibiotic therapy for critically ill patients. *Indian J Crit Care Med*. 2014;18(5):310-4.
112. Sharma D, Misba L, Khan AU. Antibiotics versus biofilm: an emerging battleground in microbial communities. *Antimicrobial Resistance & Infection Control*. 2019;8(1):76.

113. Hoiby N, Bjarnsholt T, Givskov M, Molin S, Ciofu O. Antibiotic resistance of bacterial biofilms. *Int J Antimicrob Agents*. 2010;35(4):322-32.
114. van Hoek AHAM, Mevius D, Guerra B, Mullany P, Roberts AP, Aarts HJM. Acquired antibiotic resistance genes: an overview. *Frontiers in Microbiology*. 2011;2:203-.
115. O'Toole DK. The Natural Environment May Be the Most Important Source of Antibiotic Resistance Genes. *mBio*. 2014;5(4):e01285-14.
116. Munita JM, Arias CA. Mechanisms of Antibiotic Resistance. *Microbiol Spectr*. 2016;4(2):10.1128/microbiolspec.VMBF-0016-2015.
117. MacLean RC, San Millan A. The evolution of antibiotic resistance. *Science*. 2019;365(6458):1082-3.
118. Kapoor G, Saigal S, Elongavan A. Action and resistance mechanisms of antibiotics: A guide for clinicians. *J Anaesthesiol Clin Pharmacol*. 2017;33(3):300-5.
119. Gajdács M. The Concept of an Ideal Antibiotic: Implications for Drug Design. *Molecules*. 2019;24(5):892.
120. Pankey GA, Sabath LD. Clinical Relevance of Bacteriostatic versus Bactericidal Mechanisms of Action in the Treatment of Gram-Positive Bacterial Infections. *Clinical Infectious Diseases*. 2004;38(6):864-70.
121. Bollenbach T. Antimicrobial interactions: mechanisms and implications for drug discovery and resistance evolution. *Current opinion in microbiology*. 2015;27:1-9.
122. Wald-Dickler N, Holtom P, Spellberg B. Busting the Myth of "Static vs Cidal": A Systemic Literature Review. *Clinical infectious diseases : an official publication of the Infectious Diseases Society of America*. 2018;66(9):1470-4.
123. Nemeth J, Oesch G, Kuster SP. Bacteriostatic versus bactericidal antibiotics for patients with serious bacterial infections: systematic review and meta-analysis. *Journal of Antimicrobial Chemotherapy*. 2014;70(2):382-95.
124. Ocampo PS, Lázár V, Papp B, Arnoldini M, Abel zur Wiesch P, Busa-Fekete R, et al. Antagonism between Bacteriostatic and Bactericidal Antibiotics Is Prevalent. *Antimicrobial Agents and Chemotherapy*. 2014;58(8):4573-82.
125. JAWETZ E, GUNNISON JB. ANTIBIOTIC SYNERGISM AND ANTAGONISM: AN ASSESSMENT OF THE PROBLEM. *Pharmacological Reviews*. 1953;5(2):175-92.
126. Wang J, Xia L, Wang R, Cai Y. Linezolid and Its Immunomodulatory Effect: In Vitro and In Vivo Evidence. *Frontiers in Pharmacology*. 2019;10(1389).
127. Beer J, Wagner CC, Zeitlinger M. Protein binding of antimicrobials: methods for quantification and for investigation of its impact on bacterial killing. *AAPS J*. 2009;11(1):1-12.
128. Wishart DS, Feunang YD, Guo AC, Lo EJ, Marcu A, Grant JR, et al. DrugBank 5.0: a major update to the DrugBank database for 2018. *Nucleic Acids Res*. 2018;46(D1):D1074-d82.
129. Tipper DJ. Mode of action of β -lactam antibiotics. *Pharmacology & Therapeutics*. 1985;27(1):1-35.

130. Marcellini L, Giammatteo M, Aimola P, Mangoni ML. Fluorescence and electron microscopy methods for exploring antimicrobial peptides mode(s) of action. *Methods Mol Biol.* 2010;618:249-66.
131. Cushnie TP, O'Driscoll NH, Lamb AJ. Morphological and ultrastructural changes in bacterial cells as an indicator of antibacterial mechanism of action. *Cell Mol Life Sci.* 2016;73(23):4471-92.
132. Tacconelli E, Carrara E, Savoldi A, Harbarth S, Mendelson M, Monnet DL, et al. Discovery, research, and development of new antibiotics: the WHO priority list of antibiotic-resistant bacteria and tuberculosis. *The Lancet Infectious Diseases.* 2018;18(3):318-27.
133. Choquet-Kastylevsky G, Vial T, Descotes J. Allergic adverse reactions to sulfonamides. *Curr Allergy Asthma Rep.* 2002;2(1):16-25.
134. Achari A, Somers DO, Champness JN, Bryant PK, Rosemond J, Stammers DK. Crystal structure of the anti-bacterial sulfonamide drug target dihydropteroate synthase. *Nature Structural Biology.* 1997;4(6):490-7.
135. Nakamoto M, Kunimura K, Suzuki J-I, Kodera Y. Antimicrobial properties of hydrophobic compounds in garlic: Allicin, vinylidithiin, ajoene and diallyl polysulfides. *Exp Ther Med.* 2020;19(2):1550-3.
136. Nagy P. Kinetics and mechanisms of thiol-disulfide exchange covering direct substitution and thiol oxidation-mediated pathways. *Antioxid Redox Signal.* 2013;18(13):1623-41.
137. Kollef MH. Broad-Spectrum Antimicrobials and the Treatment of Serious Bacterial Infections: Getting It Right Up Front. *Clinical Infectious Diseases.* 2008;47(Supplement_1):S3-S13.
138. Liu Y, Ding S, Shen J, Zhu K. Nonribosomal antibacterial peptides that target multidrug-resistant bacteria. *Nat Prod Rep.* 2019;36(4):573-92.
139. Zeng X, Lin J. Beta-lactamase induction and cell wall metabolism in Gram-negative bacteria. *Frontiers in Microbiology.* 2013;4(128).
140. Gupta S, Govil D, Kakar PN, Prakash O, Arora D, Das S, et al. Colistin and polymyxin B: a re-emergence. *Indian J Crit Care Med.* 2009;13(2):49-53.
141. Klein NC, Cunha BA. The selection and use of cephalosporins: a review. *Adv Ther.* 1995;12(2):83-101.
142. Foster TJ. Antibiotic resistance in *Staphylococcus aureus*. Current status and future prospects. *FEMS Microbiology Reviews.* 2017;41(3):430-49.
143. Gould SWJ, Cuschieri P, Rollason J, Hilton AC, Easmon S, Fielder MD. The need for continued monitoring of antibiotic resistance patterns in clinical isolates of *Staphylococcus aureus* from London and Malta. *Annals of clinical microbiology and antimicrobials.* 2010;9:20-.
144. Guo Y, Song G, Sun M, Wang J, Wang Y. Prevalence and Therapies of Antibiotic-Resistance in *Staphylococcus aureus*. *Frontiers in cellular and infection microbiology.* 2020;10(107).
145. Wales PH. Antibacterial Resistance In Wales 2008-2017 In: Wales N, editor. wales.nhs.uk: NHS Wales; 2017.

146. Organisation WH. WHO publishes list of bacteria for which new antibiotics are urgently needed 2017 [updated 27/02/2017; cited 2020 05/02]. Available from: <https://www.who.int/news-room/detail/27-02-2017-who-publishes-list-of-bacteria-for-which-new-antibiotics-are-urgently-needed>.
147. Morgenstern M, Erichsen C, Hackl S, Mily J, Militz M, Friederichs J, et al. Antibiotic Resistance of Commensal *Staphylococcus aureus* and Coagulase-Negative Staphylococci in an International Cohort of Surgeons: A Prospective Point-Prevalence Study. *PLoS One*. 2016;11(2):e0148437.
148. England PH. English Surveillance Programme for Antimicrobial Utilisation and Resistance (ESPAUR) 2018-2019. 2019.
149. Huijbers PM, van Hoek AH, Graat EA, Haenen AP, Florijn A, Hengeveld PD, et al. Methicillin-resistant *Staphylococcus aureus* and extended-spectrum and AmpC beta-lactamase-producing *Escherichia coli* in broilers and in people living and/or working on organic broiler farms. *Vet Microbiol*. 2015;176(1-2):120-5.
150. Choo EJ, Chambers HF. Treatment of Methicillin-Resistant *Staphylococcus aureus* Bacteremia. *Infect Chemother*. 2016;48(4):267-73.
151. Khan TM, Kok YL, Bukhsh A, Lee L-H, Chan K-G, Goh B-H. Incidence of methicillin resistant *Staphylococcus aureus* (MRSA) in burn intensive care unit: a systematic review. *Germes*. 2018;8(3):113-25.
152. Peng H, Liu D, Ma Y, Gao W. Comparison of community- and healthcare-associated methicillin-resistant *Staphylococcus aureus* isolates at a Chinese tertiary hospital, 2012–2017. *Scientific Reports*. 2018;8(1):17916.
153. Harkins CP, Pichon B, Doumith M, Parkhill J, Westh H, Tomasz A, et al. Methicillin-resistant *Staphylococcus aureus* emerged long before the introduction of methicillin into clinical practice. *Genome Biol*. 2017;18(1):130-.
154. Saito M, Katayama Y, Hishinuma T, Iwamoto A, Aiba Y, Kuwahara-Arai K, et al. "Slow VISA," a novel phenotype of vancomycin resistance, found in vitro in heterogeneous vancomycin-intermediate *Staphylococcus aureus* strain Mu3. *Antimicrob Agents Chemother*. 2014;58(9):5024-35.
155. McGuinness WA, Malachowa N, DeLeo FR. Vancomycin Resistance in *Staphylococcus aureus*. *Yale J Biol Med*. 2017;90(2):269-81.
156. Périchon B, Courvalin P. VanA-Type Vancomycin-Resistant *Staphylococcus aureus*. *Antimicrobial Agents and Chemotherapy*. 2009;53(11):4580-7.
157. Foucault M-L, Courvalin P, Grillot-Courvalin C. Fitness Cost of VanA-Type Vancomycin Resistance in Methicillin-Resistant *Staphylococcus aureus*. *Antimicrobial Agents and Chemotherapy*. 2009;53(6):2354-9.
158. Lewis K. Platforms for antibiotic discovery. *Nat Rev Drug Discov*. 2013;12(5):371-87.
159. Ribeiro da Cunha B, Fonseca LP, Calado CRC. Antibiotic Discovery: Where Have We Come from, Where Do We Go? *Antibiotics* (Basel, Switzerland). 2019;8(2):45.
160. Fernandes R, Amador P, Prudêncio C. β -Lactams: chemical structure, mode of action and mechanisms of resistance. *Reviews in Medical Microbiology*. 2013;24(1):7-17.

161. Griffith EC, Wallace MJ, Wu Y, Kumar G, Gajewski S, Jackson P, et al. The Structural and Functional Basis for Recurring Sulfa Drug Resistance Mutations in *Staphylococcus aureus* Dihydropteroate Synthase. *Frontiers in Microbiology*. 2018;9:1369-.
162. Henriques-Normark B, Normark S. Bacterial vaccines and antibiotic resistance. *Ups J Med Sci*. 2014;119(2):205-8.
163. Reygaert WC. An overview of the antimicrobial resistance mechanisms of bacteria. *AIMS Microbiol*. 2018;4(3):482-501.
164. Costa SS, Viveiros M, Amaral L, Couto I. Multidrug Efflux Pumps in *Staphylococcus aureus*: an Update. *Open Microbiol J*. 2013;7:59-71.
165. Kaatz GW, DeMarco CE, Seo SM. MepR, a repressor of the *Staphylococcus aureus* MATE family multidrug efflux pump MepA, is a substrate-responsive regulatory protein. *Antimicrobial agents and chemotherapy*. 2006;50(4):1276-81.
166. Karlsson D. Studies on emergence and spread of antibiotic resistant *Streptococcus pneumoniae* [Doctoral]. Stockholm, Sweden: Karolinska Institutet; 2010.
167. Savage VJ, Chopra I, O'Neill AJ. *Staphylococcus aureus* biofilms promote horizontal transfer of antibiotic resistance. *Antimicrob Agents Chemother*. 2013;57(4):1968-70.
168. Bitrus AA, Zunita Z, Bejo SK, Othman S, Nadzir NAA. In vitro transfer of methicillin resistance determinants *mecA* from methicillin resistant *Staphylococcus aureus* (MRSA) to methicillin susceptible *Staphylococcus aureus* (MSSA). *BMC microbiology*. 2017;17(1):83-.
169. Davies J, Davies D. Origins and evolution of antibiotic resistance. *Microbiol Mol Biol Rev*. 2010;74(3):417-33.
170. Mulvey MR, Simor AE. Antimicrobial resistance in hospitals: How concerned should we be? *Canadian Medical Association Journal*. 2009;180(4):408-15.
171. Tello A, Austin B, Telfer TC. Selective pressure of antibiotic pollution on bacteria of importance to public health. *Environmental health perspectives*. 2012;120(8):1100-6.
172. Stokes JM, Yang K, Swanson K, Jin W, Cubillos-Ruiz A, Donghia NM, et al. A Deep Learning Approach to Antibiotic Discovery. *Cell*. 2020;180(4):688-702.e13.
173. Fund AA. AMR Action Fund [Web Page]. <https://www.amractionfund.com/>: AMR Action Fund; 2020 [2020:]
174. Plymouth Uo. ABX: The Antibiotic Discovery Accelerator Network - University of Plymouth <https://www.plymouth.ac.uk/research/biomedical-research-group/abx>: University of Plymouth; 2020 [
175. CARB-X. Accelerators / Other Partners - CARB-X <https://carb-x.org/partners/global-accelerator-network/>: CARB-X; 2020 [
176. Blaskovich MAT, Hansford KA, Butler MS, Jia Z, Mark AE, Cooper MA. Developments in Glycopeptide Antibiotics. *ACS Infect Dis*. 2018;4(5):715-35.
177. Chellat MF, Raguž L, Riedl R. Targeting Antibiotic Resistance. *Angewandte Chemie International Edition*. 2016;55(23):6600-26.

178. Johnson BK, Abramovitch RB. Small Molecules That Sabotage Bacterial Virulence. *Trends Pharmacol Sci.* 2017;38(4):339-62.
179. Vadekeetil A, Saini H, Chhibber S, Harjai K. Exploiting the antivirulence efficacy of an ajoene-ciprofloxacin combination against *Pseudomonas aeruginosa* biofilm associated murine acute pyelonephritis. *Biofouling.* 2016;32(4):371-82.
180. Zainal M, Mohamad Zain N, Mohd Amin I, Ahmad VN. The antimicrobial and antibiofilm properties of allicin against *Candida albicans* and *Staphylococcus aureus* – A therapeutic potential for denture stomatitis. *The Saudi Dental Journal.* 2020;33(2):105-11.
181. Lee NLS, Yuen KY, Kumana CR. β -Lactam Antibiotic and β -Lactamase Inhibitor Combinations. *JAMA.* 2001;285(4):386-8.
182. Vicente D, Perez-Trallero E. [Tetracyclines, sulfonamides, and metronidazole]. *Enferm Infecc Microbiol Clin.* 2010;28(2):122-30.
183. Greber KE, Dawgul M. Antimicrobial Peptides Under Clinical Trials. *Curr Top Med Chem.* 2017;17(5):620-8.
184. Maura D, Ballok AE, Rahme LG. Considerations and caveats in anti-virulence drug development. *Current opinion in microbiology.* 2016;33:41-6.
185. Valiquette L, Laupland KB. Digging for new solutions. *Can J Infect Dis Med Microbiol.* 2015;26(6):289-90.
186. Blunt JW, Copp BR, Keyzers RA, Munro MH, Prinsep MR. Marine natural products. *Nat Prod Rep.* 2015;32(2):116-211.
187. Raynbird MY, Silva F, Smallman H, Khokhar SS, Neef D, Evans GJS, et al. Short Total Synthesis of Ajoene, (E,Z)-4,5,9-Trithiadodeca-1,6,11-triene 9-oxide, in Batch and (E,Z)-4,5,9-Trithiadodeca-1,7,11-triene in Continuous Flow. *Chemistry.* 2020;26(38):8363-7.
188. Rossiter SE, Fletcher MH, Wuest WM. Natural Products as Platforms To Overcome Antibiotic Resistance. *Chemical reviews.* 2017;117(19):12415-74.
189. Silva LN, Zimmer KR, Macedo AJ, Trentin DS. Plant Natural Products Targeting Bacterial Virulence Factors. *Chemical Reviews.* 2016;116(16):9162-236.
190. Taylor PW. Alternative natural sources for a new generation of antibacterial agents. *Int J Antimicrob Agents.* 2013;42(3):195-201.
191. Bernier S, Surette M. Concentration-dependent activity of antibiotics in natural environments. *Frontiers in Microbiology.* 2013;4:20.
192. Cowan MM. Plant products as antimicrobial agents. *Clinical microbiology reviews.* 1999;12(4):564-82.
193. Abet V, Mariani A, Truscott FR, Britton S, Rodriguez R. Biased and unbiased strategies to identify biologically active small molecules. *Bioorganic & Medicinal Chemistry.* 2014;22(16):4474-89.
194. Jakobsen TH, van Gennip M, Phipps RK, Shanmugham MS, Christensen LD, Alhede M, et al. Ajoene, a sulfur-rich molecule from garlic, inhibits genes controlled by quorum sensing. *Antimicrob Agents Chemother.* 2012;56(5):2314-25.

195. Junio HA, Sy-Cordero AA, Ettefagh KA, Burns JT, Micko KT, Graf TN, et al. Synergy-directed fractionation of botanical medicines: a case study with goldenseal (*Hydrastis canadensis*). *J Nat Prod*. 2011;74(7):1621-9.
196. Albaridi NA. Antibacterial Potency of Honey. *Int J Microbiol*. 2019;2019:2464507-.
197. Mandal MD, Mandal S. Honey: its medicinal property and antibacterial activity. *Asian Pac J Trop Biomed*. 2011;1(2):154-60.
198. Jenkins R, Burton N, Cooper R. Manuka honey inhibits cell division in methicillin-resistant *Staphylococcus aureus*. *The Journal of antimicrobial chemotherapy*. 2011;66:2536-42.
199. Jenkins R, Cooper R. Improving antibiotic activity against wound pathogens with manuka honey in vitro. *PloS one*. 2012;7(9):e45600-e.
200. Mao Q-Q, Xu X-Y, Cao S-Y, Gan R-Y, Corke H, Beta T, et al. Bioactive Compounds and Bioactivities of Ginger (*Zingiber officinale* Roscoe). *Foods*. 2019;8(6):185.
201. Rahmani AH, Shabrmi FMA, Aly SM. Active ingredients of ginger as potential candidates in the prevention and treatment of diseases via modulation of biological activities. *Int J Physiol Pathophysiol Pharmacol*. 2014;6(2):125-36.
202. Arreola R, Quintero-Fabián S, López-Roa RI, Flores-Gutiérrez EO, Reyes-Grajeda JP, Carrera-Quintanar L, et al. Immunomodulation and anti-inflammatory effects of garlic compounds. *J Immunol Res*. 2015;2015:401630-.
203. Block E, Ahmad S, Catalfamo JL, Jain MK, Apitz-Castro R. The chemistry of alkyl thiosulfinate esters. 9. Antithrombotic organosulfur compounds from garlic: structural, mechanistic, and synthetic studies. *Journal of the American Chemical Society*. 1986;108(22):7045-55.
204. Charron CS, Milner JA, Novotny JA. Garlic. In: Caballero B, Finglas PM, Toldrá F, editors. *Encyclopedia of Food and Health*. Oxford: Academic Press; 2016. p. 184-90.
205. Fuchs AL, Weaver AJ, Jr., Tripet BP, Ammons MCB, Teintze M, Copié V. Characterization of the antibacterial activity of Bald's eyesalve against drug resistant *Staphylococcus aureus* and *Pseudomonas aeruginosa*. *PloS one*. 2018;13(11):e0208108-e.
206. Girish VM, Liang H, Aguilan JT, Nosanchuk JD, Friedman JM, Nacharaju P. Anti-biofilm activity of garlic extract loaded nanoparticles. *Nanomedicine: Nanotechnology, Biology and Medicine*. 2019;20:102009.
207. Kaschula CH, Hunter R, Parker MI. Garlic-derived anticancer agents: structure and biological activity of ajoene. *Biofactors*. 2010;36(1):78-85.
208. Kaschula CH, Tuveri R, Ngarande E, Dzobo K, Barnett C, Kusza DA, et al. The garlic compound ajoene covalently binds vimentin, disrupts the vimentin network and exerts anti-metastatic activity in cancer cells. *BMC Cancer*. 2019;19(1):248.
209. Lee DY, Li H, Lim HJ, Lee HJ, Jeon R, Ryu J-H. Anti-inflammatory activity of sulfur-containing compounds from garlic. *J Med Food*. 2012;15(11):992-9.
210. Li G, Ma X, Deng L, Zhao X, Wei Y, Gao Z, et al. Fresh Garlic Extract Enhances the Antimicrobial Activities of Antibiotics on Resistant Strains in Vitro. *Jundishapur J Microbiol*. 2015;8(5):e14814-e.

211. Petrovska BB, Cekovska S. Extracts from the history and medical properties of garlic. *Pharmacogn Rev.* 2010;4(7):106-10.
212. Shang A, Cao S-Y, Xu X-Y, Gan R-Y, Tang G-Y, Corke H, et al. Bioactive Compounds and Biological Functions of Garlic (*Allium sativum* L.). *Foods.* 2019;8(7):246.
213. Ferri N, Yokoyama K, Sadilek M, Paoletti R, Apitz-Castro R, Gelb MH, et al. Ajoene, a garlic compound, inhibits protein prenylation and arterial smooth muscle cell proliferation. *Br J Pharmacol.* 2003;138(5):811-8.
214. Reiter J, Levina N, van der Linden M, Gruhlke M, Martin C, Slusarenko AJ. Diallylthiosulfinate (Allicin), a Volatile Antimicrobial from Garlic (*Allium sativum*), Kills Human Lung Pathogenic Bacteria, Including MDR Strains, as a Vapor. *Molecules.* 2017;22(10):1711.
215. Ranjbar-Omid M, Arzanlou M, Amani M, Shokri Al-Hashem SK, Amir Mozafari N, Peeri Doghaheh H. Allicin from garlic inhibits the biofilm formation and urease activity of *Proteus mirabilis* in vitro. *FEMS Microbiology Letters.* 2015;362(9).
216. Nakamoto M, Kunimura K, Suzuki JI, Kodera Y. Antimicrobial properties of hydrophobic compounds in garlic: Allicin, vinylidithiin, ajoene and diallyl polysulfides. *Exp Ther Med.* 2020;19(2):1550-3.
217. Naganawa R, Iwata N, Ishikawa K, Fukuda H, Fujino T, Suzuki A. Inhibition of microbial growth by ajoene, a sulfur-containing compound derived from garlic. *Applied and environmental microbiology.* 1996;62(11):4238-42.
218. Farrag HA, Hosny AE-DMS, Hawas AM, Hagra SAA, Helmy OM. Potential efficacy of garlic lock therapy in combating biofilm and catheter-associated infections; experimental studies on an animal model with focus on toxicological aspects. *Saudi Pharm J.* 2019;27(6):830-40.
219. Bjarnsholt T, Jensen PO, Rasmussen TB, Christophersen L, Calum H, Hentzer M, et al. Garlic blocks quorum sensing and promotes rapid clearing of pulmonary *Pseudomonas aeruginosa* infections. *Microbiology.* 2005;151(Pt 12):3873-80.
220. Yoshida S, Kasuga S, Hayashi N, Ushiroguchi T, Matsuura H, Nakagawa S. Antifungal activity of ajoene derived from garlic. *Applied and environmental microbiology.* 1987;53(3):615-7.
221. Ross ZM, O'Gara EA, Hill DJ, Sleightholme HV, Maslin DJ. Antimicrobial properties of garlic oil against human enteric bacteria: evaluation of methodologies and comparisons with garlic oil sulfides and garlic powder. *Applied and environmental microbiology.* 2001;67(1):475-80.
222. Wallock-Richards D, Doherty CJ, Doherty L, Clarke DJ, Place M, Govan JRW, et al. Garlic Revisited: Antimicrobial Activity of Allicin-Containing Garlic Extracts against *Burkholderia cepacia* Complex. *PLOS ONE.* 2014;9(12):e112726.
223. Furner-Pardoe J, Anonye BO, Cain R, Moat J, Ortori CA, Lee C, et al. Anti-biofilm efficacy of a medieval treatment for bacterial infection requires the combination of multiple ingredients. *Scientific Reports.* 2020;10(1):12687.
224. Nakamoto M, Ohishi K, Kunimura K, Amano H, Wakamatsu J. Identification and determination of antibacterial constituents in residue discharged from garlic-processing plant. *European Food Research and Technology.* 2020;246(5):1041-9.

225. Bologna JL, Jean L. Bologna JLRPR, Jorizzo JL, Rapini RP. *Dermatology: Elsevier Health Sciences*.
226. Wu X, Santos RR, Fink-Gremmels J. Analyzing the antibacterial effects of food ingredients: model experiments with allicin and garlic extracts on biofilm formation and viability of *Staphylococcus epidermidis*. *Food Sci Nutr*. 2015;3(2):158-68.
227. Miron T, Rabinkov A, Mirelman D, Wilchek M, Weiner L. The mode of action of allicin: Its ready permeability through phospholipid membranes may contribute to its biological activity. *Biochimica et biophysica acta*. 2000;1463:20-30.
228. Loi VV, Huyen NTT, Busche T, Tung QN, Gruhlke MCH, Kalinowski J, et al. *Staphylococcus aureus* responds to allicin by global S-thioallylation – Role of the Brx/BSH/YpdA pathway and the disulfide reductase MerA to overcome allicin stress. *Free Radical Biology and Medicine*. 2019;139:55-69.
229. Lihua L, Jianhuit W, Jialini Y, Yayin L, Guanxin L. Effects of allicin on the formation of *Pseudomonas aeruginosa* biofilm and the production of quorum-sensing controlled virulence factors. *Polish journal of microbiology*. 2013;62(3):243-51.
230. Cai Y, Wang R, Pei F, Liang B-B. Antibacterial Activity of Allicin Alone and in Combination with β -Lactams against *Staphylococcus* spp. and *Pseudomonas aeruginosa*. *The Journal of Antibiotics*. 2007;60(5):335-8.
231. Borlinghaus J, Albrecht F, Gruhlke MCH, Nwachukwu ID, Slusarenko AJ. Allicin: chemistry and biological properties. *Molecules*. 2014;19(8):12591-618.
232. Akhtar S, Khali J, Akhtar N. Study of Synergistic Effect of Allicin with Antibacterials Against Micro-organisms. *Annals of King Edward Medical University, Lahore*. 2009;15:138-40.
233. Smirnova G, Oktyabrsky O. Glutathione in Bacteria. *Biochemistry*. 2005;70:1199-211.
234. Leontiev R, Hohaus N, Jacob C, Gruhlke MCH, Slusarenko AJ. A Comparison of the Antibacterial and Antifungal Activities of Thiosulfinate Analogues of Allicin. *Scientific Reports*. 2018;8(1):6763.
235. Wang H, Li X, Liu X, Shen D, Qiu Y, Zhang X, et al. Influence of pH, concentration and light on stability of allicin in garlic (*Allium sativum* L.) aqueous extract as measured by UPLC. *Journal of the Science of Food and Agriculture*. 2015;95(9):1838-44.
236. Yoo M, Lee S, Kim S, Shin D. Optimizing conditions for E-and Z-ajoene formation from garlic juice using response surface methodology. *Food Sci Nutr*. 2014;2(5):605-11.
237. Amagase H. Clarifying the Real Bioactive Constituents of Garlic. *The Journal of Nutrition*. 2006;136(3):716S-25S.
238. Walder R, Kalvatchev Z, Garzaro D, Barrios M, Apitz-Castro R. In vitro suppression of HIV-1 replication by ajoene [(e)-(z)-4,5,9-trithiadodeca-1,6,11-triene-9 oxide]. *Biomed Pharmacother*. 1997;51(9):397-403.
239. Rendu F, Daveloose D, Debouzy JC, Bourdeau N, Levy-Toledano S, Jain MK, et al. Ajoene, the antiplatelet compound derived from garlic, specifically inhibits platelet release reaction by affecting the plasma membrane internal microviscosity. *Biochemical Pharmacology*. 1989;38(8):1321-8.

240. Kaschula CH, Hunter R, Cotton J, Tuveri R, Ngarande E, Dzobo K, et al. The garlic compound ajoene targets protein folding in the endoplasmic reticulum of cancer cells. *Molecular Carcinogenesis*. 2016;55(8):1213-28.
241. Jakobsen TH, Warming AN, Vejborg RM, Moscoso JA, Stegger M, Lorenzen F, et al. A broad range quorum sensing inhibitor working through sRNA inhibition. *Scientific Reports*. 2017;7(1):9857.
242. Cho S-J, Ryu J-H, Surh Y-J. Ajoene, a Major Organosulfide Found in Crushed Garlic, Induces NAD(P)H:quinone Oxidoreductase Expression Through Nuclear Factor E2-related Factor-2 Activation in Human Breast Epithelial Cells. *J Cancer Prev*. 2019;24(2):112-22.
243. Urbina JA, Marchan E, Lazard K, Visbal G, Apitz-Castro R, Gil F, et al. Inhibition of phosphatidylcholine biosynthesis and cell proliferation in *Trypanosoma cruzi* by ajoene, an antiplatelet compound isolated from garlic. *Biochem Pharmacol*. 1993;45(12):2381-7.
244. Christensen LD, van Gennip M, Jakobsen TH, Alhede M, Hougen HP, Høiby N, et al. Synergistic antibacterial efficacy of early combination treatment with tobramycin and quorum-sensing inhibitors against *Pseudomonas aeruginosa* in an intraperitoneal foreign-body infection mouse model. *Journal of Antimicrobial Chemotherapy*. 2012;67(5):1198-206.
245. Geiger O, López-Lara IM, Sohlenkamp C. Phosphatidylcholine biosynthesis and function in bacteria. *Biochimica et Biophysica Acta (BBA) - Molecular and Cell Biology of Lipids*. 2013;1831(3):503-13.
246. (EUCAST) ECoAST. EUCAST Disc Diffusion - Manual V6.0. Version 6 ed. http://www.eucast.org/ast_of_bacteria/disk_diffusion_methodology/; EUCAST; 2017.
247. Testing. TECoAS. Breakpoint tables for interpretation of MICs and zone diameters. <http://www.eucast.org>: The European Committee on Antimicrobial Susceptibility Testing.; 2019 [v 9.0:[Clinical Guidelines for Antibiotic Use]].
248. Microbiology ECfASTotESoC, Diseases I. Determination of minimum inhibitory concentrations (MICs) of antibacterial agents by broth dilution. *Clinical Microbiology and Infection*. 2003;9(8):ix-xv.
249. Miles AA, Misra SS, Irwin JO. The estimation of the bactericidal power of the blood. *J Hyg (Lond)*. 1938;38(6):732-49.
250. Van den Driessche F, Rigole P, Brackman G, Coenye T. Optimization of resazurin-based viability staining for quantification of microbial biofilms. *J Microbiol Methods*. 2014;98:31-4.
251. Saxena S, Banerjee G, Garg R, Singh M. Comparative Study of Biofilm Formation in *Pseudomonas aeruginosa* Isolates from Patients of Lower Respiratory Tract Infection. *J Clin Diagn Res*. 2014;8(5):DC09-DC11.
252. Stepanovic S, Vukovic D, Dakic I, Savic B, Svabic-Vlahovic M. A modified microtiter-plate test for quantification of staphylococcal biofilm formation. *J Microbiol Methods*. 2000;40(2):175-9.
253. Harris LG, Nigam Y, Sawyer J, Mack D, Pritchard DI. *Lucilia sericata* chymotrypsin disrupts protein adhesin-mediated staphylococcal biofilm formation. *Applied and environmental microbiology*. 2013;79(4):1393-5.

254. Wind CM, de Vries HJC, van Dam AP. Determination of in vitro synergy for dual antimicrobial therapy against resistant *Neisseria gonorrhoeae* using Etest and agar dilution. *International Journal of Antimicrobial Agents*. 2015;45(3):305-8.
255. BLISS CI. THE TOXICITY OF POISONS APPLIED JOINTLY¹. *Annals of Applied Biology*. 1939;26(3):585-615.
256. Prichard MN, Shipman C, Jr. A three-dimensional model to analyze drug-drug interactions. *Antiviral Res*. 1990;14(4-5):181-205.
257. RICHARDS RG, GWYNN IA. Backscattered electron imaging of the undersurface of resin-embedded cells by field-emission scanning electron microscopy. *Journal of Microscopy*. 1995;177(1):43-52.
258. Heydorn A, Nielsen AT, Hentzer M, Sternberg C, Givskov M, Ersboll BK, et al. Quantification of biofilm structures by the novel computer program COMSTAT. *Microbiology*. 2000;146 (Pt 10):2395-407.
259. Vorregaard M. Comstat2-a modern 3D image analysis environment for biofilms: Technical University of Denmark; 2008.
260. Seeman T. Snippy: Rapid haploid variant calling and core genome alignment github.com/2020 [Program Download and Tutorial for Snippy]. Available from: <https://github.com/tseemann/snippy>.
261. Price MN, Dehal PS, Arkin AP. FastTree: computing large minimum evolution trees with profiles instead of a distance matrix. *Mol Biol Evol*. 2009;26(7):1641-50.
262. Alcock BP, Raphenya AR, Lau TTY, Tsang KK, Bouchard M, Edalatmand A, et al. CARD 2020: antibiotic resistance surveillance with the comprehensive antibiotic resistance database. *Nucleic Acids Res*. 2020;48(D1):D517-d25.
263. Zankari E, Hasman H, Cosentino S, Vestergaard M, Rasmussen S, Lund O, et al. Identification of acquired antimicrobial resistance genes. *J Antimicrob Chemother*. 2012;67(11):2640-4.
264. Ryder VJ, Chopra I, O'Neill AJ. Increased mutability of *Staphylococci* in biofilms as a consequence of oxidative stress. *PloS one*. 2012;7(10):e47695-e.
265. Altschul SF, Madden TL, Schäffer AA, Zhang J, Zhang Z, Miller W, et al. Gapped BLAST and PSI-BLAST: a new generation of protein database search programs. *Nucleic acids research*. 1997;25(17):3389-402.
266. Livak KJ, Schmittgen TD. Analysis of Relative Gene Expression Data Using Real-Time Quantitative PCR and the 2- $\Delta\Delta$ CT Method. *Methods*. 2001;25(4):402-8.
267. Stephen KE, Homrighausen D, DePalma G, Nakatsu CH, Irudayaraj J. Surface enhanced Raman spectroscopy (SERS) for the discrimination of *Arthrobacter* strains based on variations in cell surface composition. *Analyst*. 2012;137(18):4280-6.
268. Yang Z, Yin S, Li G, Wang J, Huang G, Jiang B, et al. Global Transcriptomic Analysis of the Interactions between Phage ϕ Abp1 and Extensively Drug-Resistant *Acinetobacter baumannii*. *mSystems*. 2019;4(2):e00068-19.

269. Kannappan A, Gowrishankar S, Srinivasan R, Pandian SK, Ravi AV. Antibiofilm activity of *Vetiveria zizanioides* root extract against methicillin-resistant *Staphylococcus aureus*. *Microb Pathog*. 2017;110:313-24.
270. Champion O, Wagley S, W Titball R. *Galleria mellonella* as a model host for microbiological and toxin research. *Virulence*. 2016;7.
271. Technologies B. TruLarv - Research Grade *Galleria mellonella* 2020 [Available from: <https://biosystemstechnology.com/products>].
272. Ignasiak K, Maxwell A. *Galleria mellonella* (greater wax moth) larvae as a model for antibiotic susceptibility testing and acute toxicity trials. *BMC Research Notes*. 2017;10(1):428.
273. Rampersad SN. Multiple applications of Alamar Blue as an indicator of metabolic function and cellular health in cell viability bioassays. *Sensors (Basel)*. 2012;12(9):12347-60.
274. Kintarak S, Whawell SA, Speight PM, Packer S, Nair SP. Internalization of *Staphylococcus aureus* by Human Keratinocytes. *Infection and Immunity*. 2004;72(10):5668-75.
275. Tacconelli E, Carrara E, Savoldi A, Harbarth S, Mendelson M, Monnet DL, et al. Discovery, research, and development of new antibiotics: the WHO priority list of antibiotic-resistant bacteria and tuberculosis. *Lancet Infect Dis*. 2018;18(3):318-27.
276. Årdal C, Baraldi E, Theuretzbacher U, Outtersson K, Plahte J, Ciabuschi F, et al. Insights into early stage of antibiotic development in small- and medium-sized enterprises: a survey of targets, costs, and durations. *Journal of Pharmaceutical Policy and Practice*. 2018;11(1):8.
277. Towse A, Hoyle CK, Goodall J, Hirsch M, Mestre-Ferrandiz J, Rex JH. Time for a change in how new antibiotics are reimbursed: Development of an insurance framework for funding new antibiotics based on a policy of risk mitigation. *Health Policy*. 2017;121(10):1025-30.
278. Savjani KT, Gajjar AK, Savjani JK. Drug solubility: importance and enhancement techniques. *ISRN Pharm*. 2012;2012:195727-.
279. MacGowan AP, Wise R. Establishing MIC breakpoints and the interpretation of in vitro susceptibility tests. *J Antimicrob Chemother*. 2001;48 Suppl 1:17-28.
280. Engel J, Kleemann A, Kutscher B, Reichert D. *Pharmaceutical Substances*, 5th Edition, 2009: Syntheses, Patents and Applications of the most relevant APIs: Thieme; 2014.
281. Peters BM, Ovchinnikova ES, Krom BP, Schlecht LM, Zhou H, Hoyer LL, et al. *Staphylococcus aureus* adherence to *Candida albicans* hyphae is mediated by the hyphal adhesin Als3p. *Microbiology (Reading, England)*. 2012;158(Pt 12):2975-86.
282. French GL. Bactericidal agents in the treatment of MRSA infections—the potential role of daptomycin. *Journal of Antimicrobial Chemotherapy*. 2006;58(6):1107-17.
283. Balouiri M, Sadiki M, Ibensouda SK. Methods for in vitro evaluating antimicrobial activity: A review. *J Pharm Anal*. 2016;6(2):71-9.
284. Lenhard JR, Bulman ZP. Inoculum effect of beta-lactam antibiotics. *J Antimicrob Chemother*. 2019;74(10):2825-43.

285. Lewis CL, Craig CC, Senecal AG. Mass and Density Measurements of Live and Dead Gram-Negative and Gram-Positive Bacterial Populations. *Applied and Environmental Microbiology*. 2014;80(12):3622-31.
286. Haney EF, Trimble MJ, Cheng JT, Vallé Q, Hancock REW. Critical Assessment of Methods to Quantify Biofilm Growth and Evaluate Antibiofilm Activity of Host Defence Peptides. *Biomolecules*. 2018;8(2):29.
287. Corte L, Casagrande Pierantoni D, Tascini C, Roscini L, Cardinali G. Biofilm Specific Activity: A Measure to Quantify Microbial Biofilm. *Microorganisms*. 2019;7(3):73.
288. Bjarnsholt T. The role of bacterial biofilms in chronic infections. *APMIS Suppl*. 2013(136):1-51.
289. Ghallab A. In vitro test systems and their limitations. *EXCLI J*. 2013;12:1024-6.
290. Laureti L, Matic I, Gutierrez A. Bacterial Responses and Genome Instability Induced by Subinhibitory Concentrations of Antibiotics. *Antibiotics (Basel, Switzerland)*. 2013;2(1):100-14.
291. Kubistova L, Dvoracek L, Tkadlec J, Melter O, Licha I. Environmental Stress Affects the Formation of *Staphylococcus aureus* Persists Tolerant to Antibiotics. *Microb Drug Resist*. 2018;24(5):547-55.
292. Klumpp S, Hwa T. Bacterial growth: global effects on gene expression, growth feedback and proteome partition. *Curr Opin Biotechnol*. 2014;28:96-102.
293. Shannon O, Flock JI. Extracellular fibrinogen binding protein, Efb, from *Staphylococcus aureus* binds to platelets and inhibits platelet aggregation. *Thrombosis and haemostasis*. 2004;91(4):779-89.
294. Poole K. Bacterial stress responses as determinants of antimicrobial resistance. *Journal of Antimicrobial Chemotherapy*. 2012;67(9):2069-89.
295. Hassan A. The Antibacterial Activity of Dimethyl Sulfoxide (DMSO) with and without of Some Ligand Complexes of the Transitional Metal Ions of Ethyl Coumarin against Bacteria Isolate from Burn and Wound Infection 2014.
296. Hawkey PM. The origins and molecular basis of antibiotic resistance. *Bmj*. 1998;317(7159):657-60.
297. Meletiadiis J, Pournaras S, Roilides E, Walsh TJ. Defining Fractional Inhibitory Concentration Index Cutoffs for Additive Interactions Based on Self-Drug Additive Combinations, Monte Carlo Simulation Analysis, and In Vitro-In Vivo Correlation Data for Antifungal Drug Combinations against *Aspergillus fumigatus*. *Antimicrobial Agents and Chemotherapy*. 2010;54(2):602.
298. Zhao W, Sachsenmeier K, Zhang L, Sult E, Hollingsworth RE, Yang H. A New Bliss Independence Model to Analyze Drug Combination Data. *J Biomol Screen*. 2014;19(5):817-21.
299. Khalili H, Soltani R, Negahban S, Abdollahi A, Gholami K. Reliability of Disk Diffusion Test Results for the Antimicrobial Susceptibility Testing of Nosocomial Gram-positive Microorganisms: Is E-test Method Better? *Iran J Pharm Res*. 2012;11(2):559-63.
300. Flanagan JN, Steck TR. The Relationship Between Agar Thickness and Antimicrobial Susceptibility Testing. *Indian journal of microbiology*. 2017;57(4):503-6.

301. England PH. Annual epidemiological commentary: Gram-negative, MRSA and MSSA bacteraemia and *C. difficile* infection data, up to and including financial year April 2018 to March 2019. In: Health P, editor. <https://www.gov.uk/government/statistics/mrsa-mssa-and-e-coli-bacteraemia-and-c-difficile-infection-annual-epidemiological-commentary>: Public Health England; 2019.
302. Reeves DS, Holt HA, Phillips I, King A, Miles RS, Paton R, et al. Activity of clindamycin against *Staphylococcus aureus* and *Staphylococcus epidermidis* from four UK centres. *J Antimicrob Chemother.* 1991;27(4):469-74.
303. Swenson JM, Brasso WB, Ferraro MJ, Hardy DJ, Knapp CC, McDougal LK, et al. Detection of inducible clindamycin resistance in staphylococci by broth microdilution using erythromycin-clindamycin combination wells. *Journal of clinical microbiology.* 2007;45(12):3954-7.
304. Levin TP, Suh B, Axelrod P, Truant AL, Fekete T. Potential clindamycin resistance in clindamycin-susceptible, erythromycin-resistant *Staphylococcus aureus*: report of a clinical failure. *Antimicrob Agents Chemother.* 2005;49(3):1222-4.
305. Lee L, Savage VM, Yeh PJ. Intermediate Levels of Antibiotics May Increase Diversity of Colony Size Phenotype in Bacteria. *Computational and Structural Biotechnology Journal.* 2018;16:307-15.
306. Edwards AM. Phenotype switching is a natural consequence of *Staphylococcus aureus* replication. *J Bacteriol.* 2012;194(19):5404-12.
307. Baselga R, Albizu I, De La Cruz M, Del Cacho E, Barberan M, Amorena B. Phase variation of slime production in *Staphylococcus aureus*: implications in colonization and virulence. *Infection and Immunity.* 1993;61(11):4857.
308. Gor V, Takemura AJ, Nishitani M, Higashide M, Medrano Romero V, Ohniwa RL, et al. Finding of Agr Phase Variants in *Staphylococcus aureus*. *mBio.* 2019;10(4):e00796-19.
309. Ziebuhr W, Heilmann C, Götz F, Meyer P, Wilms K, Straube E, et al. Detection of the intercellular adhesion gene cluster (*ica*) and phase variation in *Staphylococcus epidermidis* blood culture strains and mucosal isolates. *Infection and immunity.* 1997;65(3):890-6.
310. Johns BE, Purdy KJ, Tucker NP, Maddocks SE. Phenotypic and Genotypic Characteristics of Small Colony Variants and Their Role in Chronic Infection. *Microbiol Insights.* 2015;8:15-23.
311. Sakamoto C, Yamaguchi N, Nasu M. Rapid and Simple Quantification of Bacterial Cells by Using a Microfluidic Device. *Applied and Environmental Microbiology.* 2005;71(2):1117-21.
312. Kwei J, Halstead FD, Dretzke J, Oppenheim BA, Moiemmen NS. Protocol for a systematic review of quantitative burn wound microbiology in the management of burns patients. *Systematic Reviews.* 2015;4(1):150.
313. Khelissa SO, Jama C, Abdallah M, Boukherroub R, Faille C, Chihib NE. Effect of incubation duration, growth temperature, and abiotic surface type on cell surface properties, adhesion and pathogenicity of biofilm-detached *Staphylococcus aureus* cells. *AMB Express.* 2017;7(1):191.

314. Williamson DA, Carter GP, Howden BP. Current and Emerging Topical Antibacterials and Antiseptics: Agents, Action, and Resistance Patterns. *Clinical microbiology reviews*. 2017;30(3):827-60.
315. Kim S, Chen J, Cheng T, Gindulyte A, He J, He S, et al. PubChem 2019 update: improved access to chemical data. *Nucleic Acids Research*. 2018;47(D1):D1102-D9.
316. Windels EM, Michiels JE, Van den Bergh B, Fauvart M, Michiels J. Antibiotics: Combatting Tolerance To Stop Resistance. *mBio*. 2019;10(5):e02095-19.
317. Pasquaroli S, Zandri G, Vignaroli C, Vuotto C, Donelli G, Biavasco F. Antibiotic pressure can induce the viable but non-culturable state in *Staphylococcus aureus* growing in biofilms. *J Antimicrob Chemother*. 2013;68(8):1812-7.
318. Golus J, Sawicki R, Widelski J, Ginalska G. The agar microdilution method - a new method for antimicrobial susceptibility testing for essential oils and plant extracts. *J Appl Microbiol*. 2016;121(5):1291-9.
319. López E, Blázquez J. Effect of Subinhibitory Concentrations of Antibiotics on Intrachromosomal Homologous Recombination in *Escherichia coli*. *Antimicrobial Agents and Chemotherapy*. 2009;53(8):3411.
320. Abrahamian FM, Goldstein EJC. Microbiology of animal bite wound infections. *Clinical microbiology reviews*. 2011;24(2):231-46.
321. Hillis DM, Bull JJ. An Empirical Test of Bootstrapping as a Method for Assessing Confidence in Phylogenetic Analysis. *Systematic Biology*. 1993;42(2):182-92.
322. Floyd JL, Smith KP, Kumar SH, Floyd JT, Varela MF. LmrS Is a Multidrug Efflux Pump of the Major Facilitator Superfamily from *Staphylococcus aureus*. *Antimicrobial Agents and Chemotherapy*. 2010;54(12):5406-12.
323. Costa SS, Sobkowiak B, Parreira R, Edgeworth JD, Viveiros M, Clark TG, et al. Genetic Diversity of *norA*, Coding for a Main Efflux Pump of *Staphylococcus aureus*. *Frontiers in Genetics*. 2019;9(710).
324. Fournier B, Aras R, Hooper DC. Expression of the multidrug resistance transporter *NorA* from *Staphylococcus aureus* is modified by a two-component regulatory system. *Journal of bacteriology*. 2000;182(3):664-71.
325. Truong-Bolduc QC, Ding Y, Hooper DC. Posttranslational modification influences the effects of *MgrA* on *norA* expression in *Staphylococcus aureus*. *Journal of bacteriology*. 2008;190(22):7375-81.
326. Wistrand-Yuen E, Knopp M, Hjort K, Koskiniemi S, Berg OG, Andersson DI. Evolution of high-level resistance during low-level antibiotic exposure. *Nature communications*. 2018;9(1):1599-.
327. Ghosh D, Veeraraghavan B, Elangovan R, Vivekanandan P. Antibiotic Resistance and Epigenetics: More to It than Meets the Eye. *Antimicrobial Agents and Chemotherapy*. 2020;64(2):e02225-19.
328. Bush SJ, Foster D, Eyre DW, Clark EL, De Maio N, Shaw LP, et al. Genomic diversity affects the accuracy of bacterial single-nucleotide polymorphism-calling pipelines. *GigaScience*. 2020;9(2).

329. Benoit JB, Frank DN, Bessesen MT. Genomic evolution of *Staphylococcus aureus* isolates colonizing the nares and progressing to bacteremia. *PLoS one*. 2018;13(5):e0195860-e.
330. Martínez JL, Rojo F. Metabolic regulation of antibiotic resistance. *FEMS Microbiology Reviews*. 2011;35(5):768-89.
331. Massey RC, Buckling A, Peacock SJ. Phenotypic switching of antibiotic resistance circumvents permanent costs in *Staphylococcus aureus*. *Curr Biol*. 2001;11(22):1810-4.
332. Bhattacharya G, Dey D, Das S, Banerjee A. Exposure to sub-inhibitory concentrations of gentamicin, ciprofloxacin and cefotaxime induces multidrug resistance and reactive oxygen species generation in methicillin-sensitive *Staphylococcus aureus*. *Journal of Medical Microbiology*. 2017;66(6):762-9.
333. Schelli K, Zhong F, Zhu J. Comparative metabolomics revealing *Staphylococcus aureus* metabolic response to different antibiotics. *Microb Biotechnol*. 2017;10(6):1764-74.
334. Une T, Osada Y, Ogawa H. Cefoxitin: synergism with aminoglycosides in vitro. *Arzneimittelforschung*. 1981;31(5):761-4.
335. Blystone R. WWW. Cell biology education. *Cell Biol Educ*. 2004;3(1):11-4.
336. Petrosillo N, Capone A, Di Bella S, Taglietti F. Management of antibiotic resistance in the intensive care unit setting. Expert review of anti-infective therapy. 2010;8:289-302.
337. Bassetti M, Righi E. New antibiotics and antimicrobial combination therapy for the treatment of gram-negative bacterial infections. *Current Opinion in Critical Care*. 2015;21(5):402-11.
338. Tamma PD, Cosgrove SE, Maragakis LL. Combination therapy for treatment of infections with gram-negative bacteria. *Clinical microbiology reviews*. 2012;25(3):450-70.
339. Wormser GP, Keusch GT, Heel RC. Co-trimoxazole (trimethoprim-sulfamethoxazole): an updated review of its antibacterial activity and clinical efficacy. *Drugs*. 1982;24(6):459-518.
340. Sharifi-Rad J, Hoseini Alfatemi S, Sharifi Rad M, Iriti M. Antimicrobial Synergic Effect of Allicin and Silver Nanoparticles on Skin Infection Caused by Methicillin-Resistant *Staphylococcus aureus* spp. *Ann Med Health Sci Res*. 2014;4(6):863-8.
341. Houston P, Rowe SE, Pozzi C, Waters EM, O'Gara JP. Essential role for the major autolysin in the fibronectin-binding protein-mediated *Staphylococcus aureus* biofilm phenotype. *Infect Immun*. 2011;79(3):1153-65.
342. Freire MP, Pierrotti LC, Zerati AE, Benites L, da Motta-Leal Filho JM, Ibrahim KY, et al. Role of Lock Therapy for Long-Term Catheter-Related Infections by Multidrug-Resistant Bacteria. *Antimicrobial Agents and Chemotherapy*. 2018;62(9):e00569-18.
343. Swartjes JJ, Sharma PK, van Kooten TG, van der Mei HC, Mahmoudi M, Busscher HJ, et al. Current Developments in Antimicrobial Surface Coatings for Biomedical Applications. *Curr Med Chem*. 2015;22(18):2116-29.
344. Baidamshina DR, Trizna EY, Holyavka MG, Bogachev MI, Artyukhov VG, Akhatova FS, et al. Targeting microbial biofilms using Ficin, a nonspecific plant protease. *Scientific Reports*. 2017;7(1):46068.

345. Berg CH, Kalfas S, Malmsten M, Arnebrant T. Proteolytic degradation of oral biofilms in vitro and in vivo: potential of proteases originating from *Euphausia superba* for plaque control. *Eur J Oral Sci.* 2001;109(5):316-24.
346. Martin C, Low WL, Gupta A, Amin MC, Radecka I, Britland ST, et al. Strategies for antimicrobial drug delivery to biofilm. *Curr Pharm Des.* 2015;21(1):43-66.
347. Mohsenipour Z, Hassanshahian M. The Effects of *Allium sativum* Extracts on Biofilm Formation and Activities of Six Pathogenic Bacteria. *Jundishapur J Microbiol.* 2015;8(8):e18971-e.
348. King JM, Kulhankova K, Stach CS, Vu BG, Salgado-Pabon W. Phenotypes and Virulence among *Staphylococcus aureus* USA100, USA200, USA300, USA400, and USA600 Clonal Lineages. *mSphere.* 2016;1(3).
349. Limoli DH, Jones CJ, Wozniak DJ. Bacterial Extracellular Polysaccharides in Biofilm Formation and Function. *Microbiol Spectr.* 2015;3(3):10.1128/microbiolspec.MB-0011-2014.
350. Wijesinghe G, Dilhari A, Gayani B, Kottegoda N, Samaranayake L, Weerasekera M. Influence of Laboratory Culture Media on in vitro Growth, Adhesion, and Biofilm Formation of *Pseudomonas aeruginosa* and *Staphylococcus aureus*. *Medical Principles and Practice.* 2019;28(1):28-35.
351. Lutz JB, Zehrer CL, Solfest SE, Walters SA. A new in vivo test method to compare wound dressing fluid handling characteristics and wear time. *Ostomy Wound Manage.* 2011;57(8):28-36.
352. Sugimoto S, Sato F, Miyakawa R, Chiba A, Onodera S, Hori S, et al. Broad impact of extracellular DNA on biofilm formation by clinically isolated Methicillin-resistant and -sensitive strains of *Staphylococcus aureus*. *Scientific Reports.* 2018;8(1):2254.
353. Heal CF, Banks JL, Lepper PD, Kontopantelis E, van Driel ML. Topical antibiotics for preventing surgical site infection in wounds healing by primary intention. *Cochrane Database Syst Rev.* 2016;11(11):CD011426-CD.
354. Jin Y, Guo Y, Zhan Q, Shang Y, Qu D, Yu F. Subinhibitory Concentrations of Mupirocin Stimulate *Staphylococcus aureus* Biofilm Formation by Upregulating. *Antimicrobial Agents and Chemotherapy.* 2020;64(3):e01912-19.
355. Ghosh A, Jayaraman N, Chatterji D. Small-Molecule Inhibition of Bacterial Biofilm. *ACS Omega.* 2020;5(7):3108-15.
356. Abraham NM, Jefferson KK. A low molecular weight component of serum inhibits biofilm formation in *Staphylococcus aureus*. *Microbial pathogenesis.* 2010;49(6):388-91.
357. Farrag HA, Hosny AE-DMS, Hawas AM, Hagra SAA, Helmy OM. Potential efficacy of garlic lock therapy in combating biofilm and catheter-associated infections; experimental studies on an animal model with focus on toxicological aspects. *Saudi Pharmaceutical Journal.* 2019;27(6):830-40.
358. Stiefel P, Schmidt-Emrich S, Maniura-Weber K, Ren Q. Critical aspects of using bacterial cell viability assays with the fluorophores SYTO9 and propidium iodide. *BMC microbiology.* 2015;15:36-.

359. Dengler V, Foulston L, DeFrancesco AS, Losick R. An Electrostatic Net Model for the Role of Extracellular DNA in Biofilm Formation by *Staphylococcus aureus*. *Journal of bacteriology*. 2015;197(24):3779-87.
360. Okshevsky M, Meyer RL. Evaluation of fluorescent stains for visualizing extracellular DNA in biofilms. *J Microbiol Methods*. 2014;105:102-4.
361. Greenwood D, O'Grady F. Scanning electron microscopy of *Staphylococcus aureus* exposed to some common anti-staphylococcal agents. *J Gen Microbiol*. 1972;70(2):263-70.
362. Jefferson KK, Goldmann DA, Pier GB. Use of confocal microscopy to analyze the rate of vancomycin penetration through *Staphylococcus aureus* biofilms. *Antimicrobial agents and chemotherapy*. 2005;49(6):2467-73.
363. Ballal A, Manna AC. Expression of the *sarA* family of genes in different strains of *Staphylococcus aureus*. *Microbiology (Reading, England)*. 2009;155(Pt 7):2342-52.
364. Janda JM, Abbott SL. 16S rRNA gene sequencing for bacterial identification in the diagnostic laboratory: pluses, perils, and pitfalls. *Journal of clinical microbiology*. 2007;45(9):2761-4.
365. Sihto HM, Tasara T, Stephan R, Johler S. Validation of reference genes for normalization of qPCR mRNA expression levels in *Staphylococcus aureus* exposed to osmotic and lactic acid stress conditions encountered during food production and preservation. *FEMS Microbiol Lett*. 2014;356(1):134-40.
366. Xue T, You Y, Shang F, Sun B. Rot and Agr system modulate fibrinogen-binding ability mainly by regulating *clfB* expression in *Staphylococcus aureus* NCTC8325. *Medical Microbiology and Immunology*. 2012;201(1):81-92.
367. Lenz AP, Williamson KS, Pitts B, Stewart PS, Franklin MJ. Localized Gene Expression in *Pseudomonas aeruginosa* Biofilms. *Applied and Environmental Microbiology*. 2008;74(14):4463-71.
368. Kajimura J, Fujiwara T, Yamada S, Suzawa Y, Nishida T, Oyamada Y, et al. Identification and molecular characterization of an N-acetylmuramyl-L-alanine amidase *Sle1* involved in cell separation of *Staphylococcus aureus*. *Mol Microbiol*. 2005;58(4):1087-101.
369. Reed SB, Wesson CA, Liou LE, Trumble WR, Schlievert PM, Bohach GA, et al. Molecular characterization of a novel *Staphylococcus aureus* serine protease operon. *Infection and immunity*. 2001;69(3):1521-7.
370. Luong TT, Dunman PM, Murphy E, Projan SJ, Lee CY. Transcription Profiling of the *mgrA* Regulon in *Staphylococcus aureus*. *Journal of bacteriology*. 2006;188(5):1899-910.
371. Luong T, Sau S, Gomez M, Lee JC, Lee CY. Regulation of *Staphylococcus aureus* Capsular Polysaccharide Expression by *agr* and *sarA*. *Infection and Immunity*. 2002;70(2):444-50.
372. Dunman PM, Murphy E, Haney S, Palacios D, Tucker-Kellogg G, Wu S, et al. Transcription profiling-based identification of *Staphylococcus aureus* genes regulated by the *agr* and/or *sarA* loci. *Journal of bacteriology*. 2001;183(24):7341-53.
373. Cosgriff CJ, White CR, Teoh WP, Grayczyk JP, Alonzo F. Control of *Staphylococcus aureus* Quorum Sensing by a Membrane-Embedded Peptidase. *Infection and Immunity*. 2019;87(5):e00019-19.

374. Ma Z, Lasek-Nesselquist E, Lu J, Schneider R, Shah R, Oliva G, et al. Characterization of genetic changes associated with daptomycin nonsusceptibility in *Staphylococcus aureus*. *PLoS one*. 2018;13(6):e0198366-e.
375. Baldry M, Nielsen A, Bojer MS, Zhao Y, Friberg C, Ifrah D, et al. Norlichexanthone Reduces Virulence Gene Expression and Biofilm Formation in *Staphylococcus aureus*. *PLOS ONE*. 2016;11(12):e0168305.
376. Tuchscher L, Löffler B, Proctor RA. Persistence of *Staphylococcus aureus*: Multiple Metabolic Pathways Impact the Expression of Virulence Factors in Small-Colony Variants (SCVs). *Frontiers in Microbiology*. 2020;11(1028).
377. Kahl BC, Belling G, Becker P, Chatterjee I, Wardecki K, Hilgert K, et al. Thymidine-dependent *Staphylococcus aureus* small-colony variants are associated with extensive alterations in regulator and virulence gene expression profiles. *Infection and immunity*. 2005;73(7):4119-26.
378. Grønnemose RB, Garde C, Wassmann CS, Klitgaard JK, Nielsen R, Mandrup S, et al. Bacteria-host transcriptional response during endothelial invasion by *Staphylococcus aureus*. *Scientific Reports*. 2021;11(1):6037.
379. Lázaro-Díez M, Remuzgo-Martínez S, Rodríguez-Mirones C, Acosta F, Icardo JM, Martínez-Martínez L, et al. Effects of Subinhibitory Concentrations of Ceftaroline on Methicillin-Resistant *Staphylococcus aureus* (MRSA) Biofilms. *PLOS ONE*. 2016;11(1):e0147569.
380. Yang H, Xu S, Huang K, Xu X, Hu F, He C, et al. Anti-staphylococcus Antibiotics Interfere With the Transcription of Leucocidin ED Gene in *Staphylococcus aureus* Strain Newman. *Frontiers in microbiology*. 2020;11:265-.
381. Arciola CR, Campoccia D, Ravaioli S, Montanaro L. Polysaccharide intercellular adhesin in biofilm: structural and regulatory aspects. *Frontiers in cellular and infection microbiology*. 2015;5(7).
382. Khodaparast L, Khodaparast L, Shahrooei M, Stijlemans B, Merckx R, Baatsen P, et al. The Possible Role of *Staphylococcus epidermidis* LPxTG Surface Protein SesC in Biofilm Formation. *PLoS one*. 2016;11(1):e0146704-e.
383. Chapman JR, Balasubramanian D, Tam K, Askenazi M, Copin R, Shopsin B, et al. Using Quantitative Spectrometry to Understand the Influence of Genetics and Nutritional Perturbations On the Virulence Potential of *Staphylococcus aureus*. *Mol Cell Proteomics*. 2017;16(4 suppl 1):S15-S28.
384. Hodille E, Rose W, Diep BA, Goutelle S, Lina G, Dumitrescu O. The Role of Antibiotics in Modulating Virulence in *Staphylococcus aureus*. *Clinical Microbiology Reviews*. 2017;30(4):887.
385. Pstrągowski MT, Bujalska-Zadrożny M. Acyldepsipeptide antibiotics--current state of knowledge. *Polish journal of microbiology*. 2015;64(2):85-92.
386. Schäfer G, Kaschula CH. The immunomodulation and anti-inflammatory effects of garlic organosulfur compounds in cancer chemoprevention. *Anticancer Agents Med Chem*. 2014;14(2):233-40.
387. Nair N, Biswas R, Gotz F, Biswas L. Impact of *Staphylococcus aureus* on pathogenesis in polymicrobial infections. *Infect Immun*. 2014;82(6):2162-9.

388. Liu GY. Molecular pathogenesis of *Staphylococcus aureus* infection. *Pediatr Res*. 2009;65(5 Pt 2):71R-7R.
389. Dinges MM, Orwin PM, Schlievert PM. Exotoxins of *Staphylococcus aureus*. *Clinical Microbiology Reviews*. 2000;13(1):16-34.
390. Balasubramanian D, Harper L, Shopsis B, Torres VJ. *Staphylococcus aureus* pathogenesis in diverse host environments. *Pathog Dis*. 2017;75(1):ftx005.
391. Tong SYC, Davis JS, Eichenberger E, Holland TL, Fowler Jr. VG. *Staphylococcus aureus* Infections: Epidemiology, Pathophysiology, Clinical Manifestations, and Management. *Clinical Microbiology Reviews*. 2015;25(3):603-61.
392. Kane TL, Carothers KE, Lee SW. Virulence Factor Targeting of the Bacterial Pathogen *Staphylococcus aureus* for Vaccine and Therapeutics. *Curr Drug Targets*. 2018;19(2):111-27.
393. Russo TA, Spellberg B, Johnson JR. Important Complexities of the Antivirulence Target Paradigm: A Novel Ostensibly Resistance-Avoiding Approach for Treating Infections. *The Journal of infectious diseases*. 2016;213(6):901-3.
394. Mullish BH, Williams HR. *Clostridium difficile* infection and antibiotic-associated diarrhoea. *Clin Med (Lond)*. 2018;18(3):237-41.
395. Ford CA, Hurford IM, Cassat JE. Antivirulence Strategies for the Treatment of *Staphylococcus aureus* Infections: A Mini Review. *Frontiers in Microbiology*. 2021;11(3568).
396. Vlaeminck J, Raafat D, Surmann K, Timbermont L, Normann N, Sellman B, et al. Exploring Virulence Factors and Alternative Therapies against *Staphylococcus aureus* Pneumonia. *Toxins (Basel)*. 2020;12(11).
397. Igarashi M, Watanabe T, Hashida T, Umekita M, Hatano M, Yanagida Y, et al. Waldiomycin, a novel Walk-histidine kinase inhibitor from *Streptomyces* sp. MK844-mF10. *The Journal of Antibiotics*. 2013;66(8):459-64.
398. Xue L, Chen YY, Yan Z, Lu W, Wan D, Zhu H. Staphyloxanthin: a potential target for antivirulence therapy. *Infect Drug Resist*. 2019;12:2151-60.
399. Fleitas Martínez O, Cardoso MH, Ribeiro SM, Franco OL. Recent Advances in Antivirulence Therapeutic Strategies With a Focus on Dismantling Bacterial Membrane Microdomains, Toxin Neutralization, Quorum-Sensing Interference and Biofilm Inhibition. *Frontiers in cellular and infection microbiology*. 2019;9:74-.
400. Foster TJ, Hook M. Surface protein adhesins of *Staphylococcus aureus*. *Trends in microbiology*. 1998;6(12):484-8.
401. Walsh EJ, Miajlovic H, Gorkun OV, Foster TJ. Identification of the *Staphylococcus aureus* MSCRAMM clumping factor B (ClfB) binding site in the alphaC-domain of human fibrinogen. *Microbiology (Reading, England)*. 2008;154(Pt 2):550-8.
402. Edwards AM, Potts JR, Josefsson E, Massey RC. *Staphylococcus aureus* host cell invasion and virulence in sepsis is facilitated by the multiple repeats within FnBPA. *PLoS pathogens*. 2010;6(6):e1000964-e.

403. Kwiecinski JM, Crosby HA, Valotteau C, Hippensteel JA, Nayak MK, Chauhan AK, et al. Staphylococcus aureus adhesion in endovascular infections is controlled by the ArlRS–MgrA signaling cascade. *PLOS Pathogens*. 2019;15(5):e1007800.
404. Hu C, Xiong N, Zhang Y, Rayner S, Chen S. Functional characterization of lipase in the pathogenesis of Staphylococcus aureus. *Biochemical and Biophysical Research Communications*. 2012;419(4):617-20.
405. Kenny JG, Ward D, Josefsson E, Jonsson I-M, Hinds J, Rees HH, et al. The Staphylococcus aureus response to unsaturated long chain free fatty acids: survival mechanisms and virulence implications. *PLoS one*. 2009;4(2):e4344-e.
406. Cadieux B, Vijayakumaran V, Bernards MA, McGavin MJ, Heinrichs DE. Role of Lipase from Community-Associated Methicillin-Resistant Staphylococcus aureus Strain USA300 in Hydrolyzing Triglycerides into Growth-Inhibitory Free Fatty Acids. *Journal of Bacteriology*. 2014;196(23):4044-56.
407. Matos JE, Harmon RJ, Langlois BE. Lecithinase reaction of Staphylococcus aureus strains of different origin on Baird-Parker medium. *Lett Appl Microbiol*. 1995;21(5):334-5.
408. Bartlett AH, Hulten KG. Staphylococcus aureus pathogenesis: secretion systems, adhesins, and invasins. *Pediatr Infect Dis J*. 2010;29(9):860-1.
409. Clyne M, De Azavedo J, Carlson E, Arbuthnott J. Production of gamma-hemolysin and lack of production of alpha-hemolysin by Staphylococcus aureus strains associated with toxic shock syndrome. *Journal of clinical microbiology*. 1988;26(3):535-9.
410. Berube BJ, Bubeck Wardenburg J. Staphylococcus aureus α -Toxin: Nearly a Century of Intrigue. *Toxins*. 2013;5(6):1140-66.
411. Kwak YK, Vikstrom E, Magnusson KE, Vecsey-Semjen B, Colque-Navarro P, Mollby R. The Staphylococcus aureus alpha-toxin perturbs the barrier function in Caco-2 epithelial cell monolayers by altering junctional integrity. *Infect Immun*. 2012;80(5):1670-80.
412. Tkaczyk C, Hamilton MM, Datta V, Yang XP, Hilliard JJ, Stephens GL, et al. Staphylococcus aureus Alpha Toxin Suppresses Effective Innate and Adaptive Immune Responses in a Murine Dermonecrosis Model. *PLOS ONE*. 2013;8(10):e75103.
413. Bhakdi S, Trantum-Jensen J. Alpha-toxin of Staphylococcus aureus. *Microbiological Reviews*. 1991;55(4):733-51.
414. Walev I, Weller U, Strauch S, Foster T, Bhakdi S. Selective killing of human monocytes and cytokine release provoked by sphingomyelinase (beta-toxin) of Staphylococcus aureus. *Infection and Immunity*. 1996;64(8):2974-9.
415. Huseby M, Shi K, Brown CK, Digre J, Mengistu F, Seo KS, et al. Structure and Biological Activities of Beta Toxin from Staphylococcus aureus. *Journal of Bacteriology*. 2007;189(23):8719-26.
416. Gottfried EL. Lipids of human leukocytes: relation to celltype. *Journal of lipid research*. 1967;8(4):321-7.
417. Schmitz FJ, Veldkamp KE, Van Kessel KP, Verhoef J, Van Strijp JA. Delta-toxin from Staphylococcus aureus as a costimulator of human neutrophil oxidative burst. *J Infect Dis*. 1997;176(6):1531-7.

418. Salgado-Pabon W, Herrera A, Vu BG, Stach CS, Merriman JA, Spaulding AR, et al. Staphylococcus aureus beta-toxin production is common in strains with the beta-toxin gene inactivated by bacteriophage. *J Infect Dis.* 2014;210(5):784-92.
419. Nilsson I-M, Hartford O, Foster T, Tarkowski A. Alpha-Toxin and Gamma-Toxin Jointly Promote Staphylococcus aureus Virulence in Murine Septic Arthritis. *Infection and Immunity.* 1999;67(3):1045-9.
420. Cheung GYC, Yeh AJ, Kretschmer D, Duong AC, Tuffuor K, Fu C-L, et al. Functional characteristics of the Staphylococcus aureus δ -toxin allelic variant G10S. *Scientific Reports.* 2015;5:18023.
421. Otto M. Staphylococcus aureus toxins. *Current opinion in microbiology.* 2014;17:32-7.
422. Spaan AN, Vrieling M, Wallet P, Badiou C, Reyes-Robles T, Ohneck EA, et al. The staphylococcal toxins gamma-haemolysin AB and CB differentially target phagocytes by employing specific chemokine receptors. *Nature communications.* 2014;5:5438.
423. Moraveji Z, Tabatabaei M, Shirzad Aski H, Khoshbakht R. Characterization of hemolysins of Staphylococcus strains isolated from human and bovine, southern Iran. *Iran J Vet Res.* 2014;15(4):326-30.
424. Kateete DP, Kimani CN, Katabazi FA, Okeng A, Okee MS, Nanteza A, et al. Identification of Staphylococcus aureus: DNase and Mannitol salt agar improve the efficiency of the tube coagulase test. *Annals of Clinical Microbiology and Antimicrobials.* 2010;9(1):23.
425. Essers L, Radebold K. Rapid and reliable identification of Staphylococcus aureus by a latex agglutination test. *Journal of Clinical Microbiology.* 1980;12(5):641-3.
426. Olson ME, Nygaard TK, Ackermann L, Watkins RL, Zurek OW, Pallister KB, et al. Staphylococcus aureus nuclease is an SaeRS-dependent virulence factor. *Infect Immun.* 2013;81(4):1316-24.
427. Berends ETM, Horswill AR, Haste NM, Monestier M, Nizet V, von Köckritz-Blickwede M. Nuclease expression by Staphylococcus aureus facilitates escape from neutrophil extracellular traps. *Journal of innate immunity.* 2010;2(6):576-86.
428. Lehman MK, Nuxoll AS, Yamada KJ, Kielian T, Carson SD, Fey PD. Protease-Mediated Growth of Staphylococcus aureus on Host Proteins Is Dependent. *mBio.* 2019;10(2):e02553-18.
429. Zhang Z, Schwartz S, Wagner L, Miller W. A greedy algorithm for aligning DNA sequences. *J Comput Biol.* 2000;7(1-2):203-14.
430. UniProt Consortium T. UniProt: the universal protein knowledgebase. *Nucleic Acids Research.* 2018;46(5):2699-.
431. Salgado-Pabón W, Herrera A, Vu BG, Stach CS, Merriman JA, Spaulding AR, et al. Staphylococcus aureus β -toxin production is common in strains with the β -toxin gene inactivated by bacteriophage. *The Journal of infectious diseases.* 2014;210(5):784-92.
432. Arndt D, Grant JR, Marcu A, Sajed T, Pon A, Liang Y, et al. PHASTER: a better, faster version of the PHAST phage search tool. *Nucleic Acids Res.* 2016;44(W1):W16-21.

433. Zhou Y, Liang Y, Lynch KH, Dennis JJ, Wishart DS. PHAST: a fast phage search tool. *Nucleic Acids Res.* 2011;39(Web Server issue):W347-52.
434. Olson ME, Nygaard TK, Ackermann L, Watkins RL, Zurek OW, Pallister KB, et al. Staphylococcus aureus Nuclease Is an SaeRS-Dependent Virulence Factor. *Infection and Immunity.* 2013;81(4):1316.
435. Ibberson CB, Jones CL, Singh S, Wise MC, Hart ME, Zurawski DV, et al. Staphylococcus aureus Hyaluronidase Is a CodY-Regulated Virulence Factor. *Infection and Immunity.* 2014;82(10):4253-64.
436. Wagner PL, Waldor MK. Bacteriophage control of bacterial virulence. *Infection and immunity.* 2002;70(8):3985-93.
437. Yang H, Xu S, Huang K, Xu X, Hu F, He C, et al. Anti-staphylococcus Antibiotics Interfere With the Transcription of Leucocidin ED Gene in Staphylococcus aureus Strain Newman. *Frontiers in Microbiology.* 2020;11(265).
438. Boerlin P, Kuhnert P, Hüsey D, Schaellibaum M. Methods for identification of Staphylococcus aureus isolates in cases of bovine mastitis. *Journal of clinical microbiology.* 2003;41(2):767-71.
439. Plata-Rueda A, Martínez LC, Santos MHD, Fernandes FL, Wilcken CF, Soares MA, et al. Insecticidal activity of garlic essential oil and their constituents against the mealworm beetle, Tenebrio molitor Linnaeus (Coleoptera: Tenebrionidae). *Scientific Reports.* 2017;7(1):46406.
440. Plata-Rueda A, Martínez LC, Santos MHD, Fernandes FL, Wilcken CF, Soares MA, et al. Insecticidal activity of garlic essential oil and their constituents against the mealworm beetle, Tenebrio molitor Linnaeus (Coleoptera: Tenebrionidae). *Scientific reports.* 2017;7:46406-.
441. Kay S, Edwards J, Brown J, Dixon R. Galleria mellonella Infection Model Identifies Both High and Low Lethality of Clostridium perfringens Toxigenic Strains and Their Response to Antimicrobials. *Frontiers in Microbiology.* 2019;10:1281-.
442. Aleryan M, BJ, CG, SL. Increased Staphylococcus aureus virulence in Galleria mellonella following exposure to sub-lethal concentrations of tedizolid. *ECCMID 28th; 21/04/2018; Madrid: ECCMID; 2018.*
443. Benthall G, Touzel RE, Hind CK, Titball RW, Sutton JM, Thomas RJ, et al. Evaluation of antibiotic efficacy against infections caused by planktonic or biofilm cultures of Pseudomonas aeruginosa and Klebsiella pneumoniae in Galleria mellonella. *International Journal of Antimicrobial Agents.* 2015;46(5):538-45.
444. Buyukguzel E, Kalender Y. Penicillin-induced oxidative stress: effects on antioxidative response of midgut tissues in instars of Galleria mellonella. *J Econ Entomol.* 2007;100(5):1533-41.
445. Mittal M, Siddiqui MR, Tran K, Reddy SP, Malik AB. Reactive oxygen species in inflammation and tissue injury. *Antioxid Redox Signal.* 2014;20(7):1126-67.
446. Mak P, Chmiel D, Gacek GJ. Antibacterial peptides of the moth Galleria mellonella. *Acta Biochim Pol.* 2001;48(4):1191-5.

447. Braff MH, Zaiou M, Fierer J, Nizet V, Gallo RL. Keratinocyte production of cathelicidin provides direct activity against bacterial skin pathogens. *Infection and immunity*. 2005;73(10):6771-81.
448. Sheehan G, Dixon A, Kavanagh K. Utilization of *Galleria mellonella* larvae to characterize the development of *Staphylococcus aureus* infection. *Microbiology*. 2019;165(8):863-75.
449. Pérez-Montarelo D, Viedma E, Murcia M, Muñoz-Gallego I, Larrosa N, Brañas P, et al. Pathogenic Characteristics of *Staphylococcus aureus* Endovascular Infection Isolates from Different Clonal Complexes. *Frontiers in Microbiology*. 2017;8(917).
450. Cools F, Torfs E, Aizawa J, Vanhoutte B, Maes L, Caljon G, et al. Optimization and Characterization of a *Galleria mellonella* Larval Infection Model for Virulence Studies and the Evaluation of Therapeutics Against *Streptococcus pneumoniae*. *Frontiers in Microbiology*. 2019;10(311).
451. Tsai CJ-Y, Loh JMS, Proft T. *Galleria mellonella* infection models for the study of bacterial diseases and for antimicrobial drug testing. *Virulence*. 2016;7(3):214-29.
452. Hoh A, Maier K, editors. Comparative Cytotoxicity Test with Human Keratinocytes, HaCaT Cells, and Skin Fibroblasts to Investigate Skin-Irritating Substances. *Cell and Tissue Culture Models in Dermatological Research; 1993 1993//*; Berlin, Heidelberg: Springer Berlin Heidelberg.
453. Colombo I, Sangiovanni E, Maggio R, Mattozzi C, Zava S, Corbett Y, et al. HaCaT Cells as a Reliable In Vitro Differentiation Model to Dissect the Inflammatory/Repair Response of Human Keratinocytes. *Mediators of Inflammation*. 2017;2017:7435621.
454. Muroya M, Chang K, Uchida K, Bougaki M, Yamada Y. Analysis of cytotoxicity induced by proinflammatory cytokines in the human alveolar epithelial cell line A549. *Biosci Trends*. 2012;6(2):70-80.
455. Allegra E, Titball RW, Carter J, Champion OL. *Galleria mellonella* larvae allow the discrimination of toxic and non-toxic chemicals. *Chemosphere*. 2018;198:469-72.
456. Vandenesch F, Lina G, Henry T. *Staphylococcus aureus* hemolysins, bi-component leukocidins, and cytolytic peptides: a redundant arsenal of membrane-damaging virulence factors? *Frontiers in cellular and infection microbiology*. 2012;2:12-.
457. Kapałczyńska M, Kolenda T, Przybyła W, Zajączkowska M, Teresiak A, Filas V, et al. 2D and 3D cell cultures - a comparison of different types of cancer cell cultures. *Arch Med Sci*. 2018;14(4):910-9.
458. Kim Y, Park N, Rim YA, Nam Y, Jung H, Lee K, et al. Establishment of a complex skin structure via layered co-culture of keratinocytes and fibroblasts derived from induced pluripotent stem cells. *Stem Cell Res Ther*. 2018;9(1):217.
459. Parnell LKS, Volk SW. The Evolution of Animal Models in Wound Healing Research: 1993-2017. *Adv Wound Care (New Rochelle)*. 2019;8(12):692-702.
460. Rasigade JP, Moulay A, Lhoste Y, Tristan A, Bes M, Vandenesch F, et al. Impact of sub-inhibitory antibiotics on fibronectin-mediated host cell adhesion and invasion by *Staphylococcus aureus*. *BMC Microbiology*. 2011;11(1):263.

461. Chaplin DD. Overview of the immune response. *J Allergy Clin Immunol*. 2010;125(2 Suppl 2):S3-S23.
462. Rollin G, Tan X, Tros F, Dupuis M, Nassif X, Charbit A, et al. Intracellular Survival of *Staphylococcus aureus* in Endothelial Cells: A Matter of Growth or Persistence. *Frontiers in Microbiology*. 2017;8:1354-.
463. Esté JA, De Clercq E. Ajoene [(e,z)-4,5,9-trithiadodeca-1,6,11-triene 9 oxide] does not exhibit antiviral activity at subtoxic concentrations. *Biomed Pharmacother*. 1998;52(5):236-8.
464. Lawson LD, Hunsaker SM. Allicin Bioavailability and Bioequivalence from Garlic Supplements and Garlic Foods. *Nutrients*. 2018;10(7):812.
465. Gasser B, Saloheimo M, Rinas U, Dragosits M, Rodríguez-Carmona E, Baumann K, et al. Protein folding and conformational stress in microbial cells producing recombinant proteins: a host comparative overview. *Microb Cell Fact*. 2008;7:11-.
466. Müller A, Eller J, Albrecht F, Prochnow P, Kuhlmann K, Bandow JE, et al. Allicin Induces Thiol Stress in Bacteria through S-Allylmercapto Modification of Protein Cysteines. *The Journal of biological chemistry*. 2016;291(22):11477-90.
467. Schramm FD, Schroeder K, Jonas K. Protein aggregation in bacteria. *FEMS Microbiology Reviews*. 2019;44(1):54-72.
468. Monteiro A, Neto W, Mendes A, Pinto B, Silva LCNd, Freitas G. Effects of Alterations in *Staphylococcus aureus* Cell Membrane and Cell Wall in Antimicrobial Resistance. 2017.
469. Mak TN, Brüggemann H. Vimentin in Bacterial Infections. *Cells*. 2016;5(2):18.
470. Shih Y-L, Rothfield L. The Bacterial Cytoskeleton. *Microbiology and Molecular Biology Reviews*. 2006;70(3):729-54.
471. Lee S-C, Heo J, Woo HC, Lee J-A, Seo YH, Lee C-L, et al. Fluorescent Molecular Rotors for Viscosity Sensors. *Chemistry – A European Journal*. 2018;24(52):13706-18.
472. Marakasova ES, Akhmatova NK, Amaya M, Eisenhaber B, Eisenhaber F, van Hoek ML, et al. Prenylation: From bacteria to eukaryotes. *Molecular Biology*. 2013;47(5):622-33.
473. Chaparro-Aguirre E, Segura-Ramírez PJ, Alves FL, Riske KA, Miranda A, Silva Júnior PI. Antimicrobial activity and mechanism of action of a novel peptide present in the ecdysis process of centipede *Scolopendra subspinipes subspinipes*. *Scientific Reports*. 2019;9(1):13631.
474. Kendrick N, Darie CC, Hoelter M, Powers G, Johansen J. 2D SDS PAGE in Combination with Western Blotting and Mass Spectrometry Is a Robust Method for Protein Analysis with Many Applications. *Adv Exp Med Biol*. 2019;1140:563-74.
475. Wang P, Wilson SR. Mass spectrometry-based protein identification by integrating de novo sequencing with database searching. *BMC Bioinformatics*. 2013;14 Suppl 2(Suppl 2):S24-S.
476. Kim B. Western Blot Techniques. *Methods Mol Biol*. 2017;1606:133-9.
477. Wu S, Duan N, Gu H, Hao L, Ye H, Gong W, et al. A Review of the Methods for Detection of *Staphylococcus aureus* Enterotoxins. *Toxins*. 2016;8(7):176.

478. Gregoire S, Irwin J, Kwon I. Techniques for Monitoring Protein Misfolding and Aggregation in Vitro and in Living Cells. *Korean J Chem Eng.* 2012;29(6):693-702.
479. Chouhan S, Sharma K, Guleria S. Antimicrobial Activity of Some Essential Oils-Present Status and Future Perspectives. *Medicines (Basel).* 2017;4(3):58.
480. Ueck C, Volksdorf T, Houdek P, Vidal-y-Sy S, Sehner S, Ellinger B, et al. Comparison of In-Vitro and Ex-Vivo Wound Healing Assays for the Investigation of Diabetic Wound Healing and Demonstration of a Beneficial Effect of a Triterpene Extract. *PLOS ONE.* 2017;12(1):e0169028.
481. Vockel M, Pollok S, Breitenbach U, Ridderbusch I, Kreienkamp H-J, Brandner JM. Somatostatin Inhibits Cell Migration and Reduces Cell Counts of Human Keratinocytes and Delays Epidermal Wound Healing in an Ex Vivo Wound Model. *PLOS ONE.* 2011;6(5):e19740.
482. Imanishi J. Expression of cytokines in bacterial and viral infections and their biochemical aspects. *J Biochem.* 2000;127(4):525-30.
483. Al Kindi A, Alkahtani AM, Nalubega M, El-Chami C, O'Neill C, Arkwright PD, et al. Staphylococcus aureus Internalized by Skin Keratinocytes Evade Antibiotic Killing. *Frontiers in Microbiology.* 2019;10(2242).
484. Agerer F, Lux S, Michel A, Rohde M, Ohlsen K, Hauck CR. Cellular invasion by Staphylococcus aureus reveals a functional link between focal adhesion kinase and cortactin in integrin-mediated internalisation. *Journal of Cell Science.* 2005;118(10):2189-200.
485. Zavizion B, Zhao Z, Nittayajarn A, Rieder RJ. Rapid Microbiological Testing: Monitoring the Development of Bacterial Stress. *PLOS ONE.* 2010;5(10):e13374.
486. Database resources of the National Center for Biotechnology Information. *Nucleic Acids Res.* 2018;46(D1):D8-d13.

1.0 Appendix

1.1 Antibiotic Sensitivities of Resistance Trained Isolates

Table 1.1 Antibiotic Sensitivities of Resistant trained isolates in comparison to the original isolates. *S. aureus* isolates passaged for 14 days in either antibiotic free media (14Day) sub-MIC gentamicin (14 Day – Gent or sub-MIC NX-AS-401 (14 Day – NX) underwent EUCAST disc diffusion. S = Sensitive, R = Resistant, I = Intermediate. Antibiotic sensitivities were identified using the EUCAST clinical breakpoints V 9.0.

<i>S. aureus</i> Strain	Antibiotic											
	Gentamicin (Sensitive / Resistant)				Clindamycin (Sensitive / Resistant)				Ciprofloxacin (Sensitive / Resistant)			
	Original	14 - Day	14 Day Gent	14 Day - NX	Original	14 - Day	14 Day Gent	14 Day - NX	Original	14 - Day	14 Day Gent	14 Day - NX
NCTC 13142	S	S	S	S	S	S	S	S	S	S	S	S
NCTC 12973	S	S	S	S	S	S	S	S	S	S	S	S
UHW 3	S	S	S	S	R	R	R	R	R	R	R	R
UHW 8	S	S	S	S	S	S	S	S	S	S	S	S
UHW 15	S	S	S	S	S	S	S	S	S	S	S	S
UHW 18	S	S	S	S	S	S	S	S	S	S	S	S
UHW 19	S	S	S	S	S	S	S	S	S	S	S	S
CRI 2	S	S	S	S	R	R	R	R	R	R	R	R

<i>S. aureus</i> Strain	Antibiotic											
	Erythromycin (Sensitive / Resistant)				Tetracycline (Sensitive / Resistant)				Cefoxitin (Sensitive / Resistant)			
	Original	14 - Day	14 Day Gent	14 Day - NX	Original	14 - Day	14 Day Gent	14 Day - NX	Original	14 - Day	14 Day Gent	14 Day - NX
NCTC 13142	S	S	S	S	S	S	S	S	R	R	R	R
NCTC 12973	S	S	S	S	S	S	S	S	S	S	S	S
UHW 3	R	R	R	R	S	S	S	S	R	R	R	R
UHW 8	I	I	I	I	S	S	S	S	S	S	S	S
UHW 15	S	S	S	S	S	S	S	S	S	S	S	S
UHW 18	S	S	S	S	S	S	S	S	S	S	S	S
UHW 19	I	I	I	I	R	R	R	R	S	S	S	S
CRI 2	R	R	R	R	S	S	S	S	R	R	R	R

1.2 Minimum Biofilm Eradication Concentration (MBEC) of antibiotics against *S. aureus* biofilms.

Table 1.3 Average MBEC values for antibiotic against *S. aureus* biofilms measured by Crystal Violet, Resazurin and TVC counts. These values indicate the concentrations required for the named antibiotics to eradicate 50 % (MBEC⁵⁰) of a pre-established *S. aureus* biofilms.

<i>S. aureus</i> Strain	MBEC ⁵⁰ (µg/ml) for:			Average
	Gentamicin	Tetracycline	Cefoxitin	
NCTC 13142	512	512	2048	1024
NCTC 12973	1024	1024	2048	1365.33
UHW 3	512	512	512	512
UHW 8	1024	1024	1024	1024
UHW 15	1024	1024	1024	1024
UHW 18	1024	1024	1024	1024
UHW 19	1024	1024	1024	1024
CRI 2	1024	1024	1024	1024

1.3 Nanodrop reading for cDNA samples

Table 1.3 Nanodrop reading for cDNA sample prior to qPCR.

Samples were quantified via mySPEC (VWR,UK). Once cDNA was quantified, the samples were diluted to 50 µg/ml. Samples were once again measured prior to performance of qPCR.

Strain	Time	NX-AS-401 concentration (µg/ml)	Nanodrop Reading			µl required for 10µl of 50µg/ml.		
			Replicate			Replicate		
			1	2	3	1	2	3
NCTC 13142	2	0	88.41	86.53	98.71	5.66	5.78	5.07
	2	128	22.38	42.50	51.28	22.34	11.76	9.75
	2	256	156.08	126.54	58.82	3.20	3.95	8.50
	4	0	247.70	109.59	481.97	2.02	4.56	1.04
	4	128	55.81	73.56	68.83	8.96	6.80	7.26
	4	256	92.63	78.60	83.74	5.40	6.36	5.97
	24	0	183.09	208.60	196.98	2.73	2.40	2.54
	24	128	187.00	223.85	169.01	2.67	2.23	2.96
	24	256	173.59	184.94	235.09	2.88	2.70	2.13
NCTC 12973	2	0	90.01	207.28	188.51	5.56	2.41	2.65
	2	128	96.06	77.44	80.73	5.21	6.46	6.19
	2	256	114.00	60.33	79.08	4.39	8.29	6.32
	4	0	550.01	350.01	391.98	0.91	1.43	1.28
	4	128	98.33	95.68	71.62	5.08	5.23	6.98
	4	256	95.44	93.85	82.49	5.24	5.33	6.06
	24	0	117.20	213.26	147.10	4.27	2.34	3.40
	24	128	259.18	317.27	163.53	1.93	1.58	3.06
	24	256	83.28	88.60	97.90	6.00	5.64	5.11
UHW 3	2	0	109.67	109.91	84.23	4.56	4.55	5.94
	2	128	92.88	75.64	52.39	5.38	6.61	9.54
	2	256	117.01	89.46	114.72	4.27	5.59	4.36
	4	0	470.92	607.73	172.89	1.06	0.82	2.89
	4	128	87.83	77.10	62.17	5.69	6.49	8.04
	4	256	140.04	111.26	127.19	3.57	4.49	3.93
	24	0	111.94	142.27	122.08	4.47	3.51	4.10
	24	128	150.00	105.59	165.14	3.33	4.74	3.03
	24	256	78.69	67.23	73.20	6.35	7.44	6.83
UHW 8	2	0	257.40	205.59	353.44	1.94	2.43	1.41
	2	128	148.74	96.17	65.50	3.36	5.20	7.63
	2	256	64.18	153.64	183.68	7.79	3.25	2.72
	4	0	298.42	232.13	230.52	1.68	2.15	2.17
	4	128	199.85	83.24	110.10	2.50	6.01	4.54
	4	256	228.98	200.49	132.23	2.18	2.49	3.78
	24	0	94.81	164.80	150.07	5.27	3.03	3.33
	24	128	65.29	66.69	175.43	7.66	7.50	2.85
	24	256	63.87	161.01	151.48	7.83	3.11	3.30

Strain	Time	NX-AS-401 concentration ($\mu\text{g/ml}$)	Nanodrop Reading			μl required for 10 μl of 50 $\mu\text{g/ml}$ STD.		
			Replicate			Replicate		
			1	2	3	1	2	3
UHW 15	2	0	137.15	154.21	140.92	3.65	3.24	3.55
	2	128	165.15	57.57	62.37	3.03	8.68	8.02
	2	256	126.58	126.41	75.42	3.95	3.96	6.63
	4	0	165.72	237.50	233.85	3.02	2.11	2.14
	4	128	109.69	106.64	102.23	4.56	4.69	4.89
	4	256	185.64	150.16	134.49	2.69	3.33	3.72
	24	0	102.48	126.49	203.65	4.88	3.95	2.46
	24	128	112.87	190.44	88.51	4.43	2.63	5.65
	24	256	150.98	130.26	145.52	3.31	3.84	3.44
UHW 18	2	0	236.88	202.08	114.17	2.11	2.47	4.38
	2	128	67.60	52.12	146.32	7.40	9.59	3.42
	2	256	101.44	95.00	114.72	4.93	5.26	4.36
	4	0	265.92	262.02	232.24	1.88	1.91	2.15
	4	128	88.76	86.28	103.17	5.63	5.80	4.85
	4	256	172.01	69.69	73.52	2.91	7.17	6.80
	24	0	154.70	234.21	290.95	3.23	2.13	1.72
	24	128	53.05	55.39	80.63	9.42	9.03	6.20
	24	256	136.18	140.99	94.98	3.67	3.55	5.26
UHW 19	2	0	173.10	89.14	223.40	2.89	5.61	2.24
	2	128	82.90	93.11	69.00	6.03	5.37	7.25
	2	256	205.92	205.02	376.48	2.43	2.44	1.33
	4	0	160.70	201.36	188.53	3.11	2.48	2.65
	4	128	112.66	112.04	88.72	4.44	4.46	5.64
	4	256	143.65	108.60	146.00	3.48	4.60	3.42
	24	0	255.89	182.66	209.27	1.95	2.74	2.39
	24	128	66745.00	68.72	58.40	0.01	7.28	8.56
	24	256	50.71	50.21	62.79	9.86	9.96	7.96
UHW CRI 2	2	0	127.65	190.39	86.76	3.92	2.63	5.76
	2	128	80.49	84.56	71.09	6.21	5.91	7.03
	2	256	267.69	198.09	230.39	1.87	2.52	2.17
	4	0	189.45	203.57	217.43	2.64	2.46	2.30
	4	128	89.27	111.96	90.16	5.60	4.47	5.55
	4	256	128.60	97.96	104.46	3.89	5.10	4.79
	24	0	453.96	384.76	296.63	1.10	1.30	1.69
	24	128	183.22	118.75	70.38	2.73	4.21	7.10
	24	256	69.92	57.50	52.34	7.15	8.70	9.55

1.4 Calculated Primer Efficiencies.

Table 1.4 Primer Efficiencies:

The table shows the calculated efficiency, slope, and the amplification of the gene per each cycle (Amp). For the slope values closer to -3.3 represent optimal efficiency and Amp values closer to 2 indicate replication of a gene during a single PCR cycle. Primers that demonstrated less 90 % efficiency (grey boxes) after optimisation were not utilised against that target strain.

	13142			12973			UHW 3			UHW 8		
	Efficiency (%)	Slope	Amp	Efficiency (%)	Slope	Amp	Efficiency (%)	Slope	R ²	Efficiency (%)	Slope	R ²
<i>16S</i>	99.21	-3.34	1.99	98.96	-3.34	1.99	99.99	-3.33	1.99	99.15	-3.34	1.99
<i>gyrB</i>	99.15	-3.34	1.99	94.68	-3.45	1.95	94.42	-3.46	1.95	98.24	-3.37	1.98
<i>icaA</i>	97.62	-3.38	1.98	100.00	-3.33	1.99	96.56	-3.38	1.97	99.93	-3.33	2.00
<i>sle1</i>	98.00	-3.37	1.98	99.99	-3.41	1.97	96.80	-3.40	1.96	95.73	-3.43	1.95
<i>sarA</i>	92.06	-3.53	1.92	94.66	-3.45	1.95	98.10	-3.37	1.98	<90		
<i>hld</i>	99.88	-3.41	1.97	94.42	-3.46	1.95	97.79	-3.38	1.97	96.65	-3.38	1.97
<i>agr</i>	99.93	-3.33	2.00	94.34	-3.46	1.95	100.00	-3.32	2.00	95.94	-3.42	1.96
<i>alt</i>	94.96	-3.45	1.95	96.57	-3.38	1.97	<90			100.00	-3.32	2.00
<i>clfA</i>	99.76	-3.41	1.96	94.22	-3.47	1.94	<90			105.00	-3.33	2.00
<i>lytR</i>	97.81	-3.38	1.97	101.00	-3.32	2.00	98.20	-3.37	1.98	100.00	-3.32	2.00
<i>sigB</i>	99.78	-3.34	1.99	98.14	-3.37	1.98	99.73	-3.34	1.99	<90		
<i>spIF</i>	98.29	-3.37	1.98	97.37	-3.39	1.97	<90			96.67	-3.38	1.97
<i>fnbA</i>	93.49	-3.49	1.93	95.73	-3.43	1.95	94.24	-3.47	1.94	93.02	-3.50	1.93
<i>rot</i>	92.06	-3.53	1.92	99.93	-3.33	1.99	<90			99.15	-3.34	1.99
<i>hla</i>	92.98	-3.50	1.93	97.54	-3.38	1.98	101.00	-3.32	2.00	96.47	-3.38	1.97

	UHW 15			UHW 18			UHW 19			CRI 2		
	Efficiency (%)	Slope	R ²	Efficiency (%)	Slope	R ²	Efficiency (%)	Slope	R ²	Efficiency (%)	Slope	R ²
<i>16S</i>	100.00	-3.32	2.00	100.00	-3.32	2.00	97.99	-3.37	1.98	99.96	-3.33	1.99
<i>gyrB</i>	95.73	-3.43	1.95	100.00	-3.32	2.00	100.00	-3.32	2.00	99.99	-3.33	2.00
<i>icaA</i>	94.42	-3.46	1.95	94.43	-3.46	1.95	<90			94.22	-3.46	1.95
<i>sle1</i>	<90			<90			100.00	-3.32	2.00	99.23	-3.34	1.99
<i>sarA</i>	100.00	-3.32	2.00	100.00	-3.32	2.00	96.04	-3.39	1.97	103.00	-3.31	2.00
<i>hld</i>	100.00	-3.32	2.00	<90			<90			96.48	-3.39	1.97
<i>agr</i>	99.79	-3.33	1.99	100.00	-3.32	2.00	<90			100.00	-3.32	2.00
<i>alt</i>	<90			99.99	-3.33	1.99	93.39	-3.50	1.93	99.99	-3.33	1.99
<i>clfA</i>	100.00	-3.32	2.00	96.67	-3.38	1.97	97.65	-3.38	1.98	93.42	-3.49	1.93
<i>lytR</i>	100.00	-3.32	2.00	93.59	-3.49	1.93	<90			100.00	-3.32	2.00
<i>sigB</i>	94.96	-3.45	1.95	100.00	-3.32	2.00	94.66	-3.45	1.95	98.47	-3.36	1.98
<i>spIF</i>	<90			100.00	-3.32	2.00	92.16	-3.53	1.92	97.78	-3.38	1.98
<i>fnbA</i>	<90			98.00	-3.37	1.98	100.00	-3.32	2.00	97.73	-3.38	1.98
<i>rot</i>	100.00	-3.32	2.00	100.00	-3.32	2.00	100.00	-3.32	2.00	96.88	-3.38	1.97
<i>hla</i>	<90			93.12	-3.50	1.93	98.14	-3.37	1.98	100.00	-3.32	2.00

1.5 Single Nucleotide Polymorphisms (SNPs) identified from *S. aureus* isolates.

All eight *S. aureus* strains were continually passaged in antibiotic free media and media containing sub-MIC NX-AS-401 or gentamicin to identify. Isolates underwent illumina sequencing to identify genomic changes caused by repeated antibiotic exposure.

Table 1.5 A-C Detected single nucleotide polymorphisms (SNPs) Identified from NCTC 13142 resistance trained isolates.

A = SNPS identified in NX-AS-401 resistant trained isolate, B = SNPS identified in gentamicin resistant trained isolate and C = SNPs identified in isolates passage in antibiotic free media for 14 days.

A – NX-AS-401

CHROM	POS	TYPE	REFERENCE	ALTERNATE	EFFECT	GENE	PRODUCT
1	54847	complex	TAT	GAA			
1	66397	ins	C	CT			
1	97934	snp	G	A			
10	29432	del	TA	T			
11	42562	complex	ATAA	GTAT	synonymous_variant c.114_117delTTATinsATAC p.40		hypothetical protein
17	17377	snp	G	T	missense_variant c.312G>T p.Met104Ile		hypothetical protein
17	17394	snp	G	T			
18	22157	snp	T	C			
50	9677	complex	CTTAAA	TTAAAG	synonymous_variant c.604_609delCTTAAAsTTAAAG p.204		IS1182 family transposase ISSep1
50	9867	complex	CATT	ATTC	missense_variant c.794_797delCATTinsATTC p.ThrLeu265AsnSer		IS1182 family transposase ISSep1
50	10213	snp	A	G	synonymous_variant c.1140A>G p.Lys380Lys		IS1182 family transposase ISSep1
50	10240	snp	C	T	synonymous_variant c.1167C>T p.Ile389Ile		IS1182 family transposase ISSep1
50	10457	complex	ATAGC	GTAGT	missense_variant c.1384_1388delATAGCinsGTAGT p.IleAla462ValVal		IS1182 family transposase ISSep1
51	16710	snp	G	T	missense_variant c.658C>A p.His220Asn	map_2	Protein map
51	16714	snp	C	T	synonymous_variant c.654G>A p.Thr218Thr	map_2	Protein map
51	16718	snp	T	A	missense_variant c.650A>T p.Tyr217Phe	map_2	Protein map
51	16722	snp	C	T	missense_variant c.646G>A p.Glu216Lys	map_2	Protein map

51	16729	snp	C	T	synonymous_variant c.639G>A p.Lys213Lys	map_2	Protein map
51	16747	complex	GAT	TAC	missense_variant c.619_621delATCinsGTA p.Ile207Val	map_2	Protein map
51	16754	complex	CTA	GTT	missense_variant c.612_614delTAGinsAAC p.Ser205Thr	map_2	Protein map
80	12091	snp	A	T			
82	5980	complex	AACTA	TAACT	missense_variant c.533_537delTAGTTinsAGTTA p.IleVal178LysLeu		hypothetical protein
84	50	del	CT	C			
84	10930	complex	AAA	TAT	stop_lost&splice_region_variant c.264_*2delAAAinsTAT p.Ter88Tyrext*?		hypothetical protein
84	10950	snp	G	T			
88	943	snp	T	A	missense_variant c.488T>A p.Ile163Lys	desR	Transcriptional regulatory protein
110	5568	snp	C	T	synonymous_variant c.795G>A p.Gln265Gln		hypothetical protein
129	3078	snp	A	C	missense_variant c.601A>C p.Asn201His		hypothetical protein

B – Gentamicin

CHROM	POS	TYPE	REFERENCE	ALTERNATE	EFFECT	GENE	PRODUCT
1	66397	ins	C	CT			
1	97934	snp	G	A			
10	29432	del	TA	T			
11	42562	complex	ATAA	GTAT	synonymous_variant c.114_117delTTATinsATAC p.40		hypothetical protein
11	42604	snp	T	A	missense_variant c.75A>T p.Leu25Phe		hypothetical protein
17	17377	snp	G	T	missense_variant c.312G>T p.Met104Ile		hypothetical protein
17	17394	snp	G	T			
18	22157	snp	T	C			
33	13457	snp	G	T			
50	9677	complex	CTTAAA	TTAAAG	synonymous_variant c.604_609delCTTAAAsinsTTAAAG p.204		IS1182 family transposase ISSep1
50	9867	complex	CATT	ATTC	missense_variant c.794_797delCATTinsATTC p.ThrLeu265AsnSer		IS1182 family transposase ISSep1
50	10213	snp	A	G	synonymous_variant c.1140A>G p.Lys380Lys		IS1182 family transposase ISSep1
50	10240	snp	C	T	synonymous_variant c.1167C>T p.Ile389Ile		IS1182 family transposase ISSep1
50	10457	complex	ATAGC	GTAGT	missense_variant c.1384_1388delATAGCinsGTAGT p.IleAla462ValVal		IS1182 family transposase ISSep1
51	16690	complex	TTTT	CTTC	synonymous_variant c.675_678delAAAAinsGAAG p.227	map_2	Protein map
51	16710	complex	GAACCGTATATTC	TAACTGTAAATTT	missense_variant c.646_658delGAATATACGGTTCinsAAATTTACAGTTA p.GluTyrThrValHis216LysPheThrValAsn	map_2	Protein map
51	16729	snp	C	T	synonymous_variant c.639G>A p.Lys213Lys	map_2	Protein map
51	16747	complex	GAT	TAC	missense_variant c.619_621delATCinsGTA p.Ile207Val	map_2	Protein map
51	16754	complex	CTA	GTT	missense_variant c.612_614delTAGinsAAC p.Ser205Thr	map_2	Protein map
69	1533	snp	A	T			
69	1558	snp	C	T			
80	12091	snp	A	T			
82	5980	complex	AACTA	TAACT	missense_variant c.533_537delTAGTTinsAGTTA p.IleVal178LysLeu		hypothetical protein
84	50	del	CT	C			

84	10930	complex	AAA	TAT	stop_lost&splice_region_variant c.264_*2delAAAinsTAT p.Ter88Tyrex*?		hypothetical protein
84	10950	snp	G	T			
88	943	snp	T	A	missense_variant c.488T>A p.Ile163Lys	desR	Transcriptional regulatory protein DesR
110	5568	snp	C	T	synonymous_variant c.795G>A p.Gln265Gln		hypothetical protein
125	904	snp	C	T	synonymous_variant c.81G>A p.Gln27Gln		hypothetical protein
134	1601	snp	C	T			
134	1606	snp	G	T			
134	1614	snp	C	A			
134	1619	snp	C	A			
134	1625	complex	CTATC	TTATA			
134	1642	snp	C	A			

C – 14-Day Passage

CHROM	POS	TYPE	REFERENCE	ALTERNATE	EFFECT	GENE	PRODUCT
11	42562	complex	ATAA	GTAT	synonymous_variant c.114_117delTTATinsATAC p.40		hypothetical protein
11	42604	snp	T	A	missense_variant c.75A>T p.Leu25Phe		hypothetical protein
18	22157	snp	T	C			
50	9677	complex	CTTAAA	TTAAAG	synonymous_variant c.604_609delCTTAAAinsTTAAAG p.204		IS1182 family transposase ISSep1
50	9867	complex	CATT	ATTC	missense_variant c.794_797delCATTinsATTC p.ThrLeu265AsnSer		IS1182 family transposase ISSep1
50	10213	snp	A	G	synonymous_variant c.1140A>G p.Lys380Lys		IS1182 family transposase ISSep1
51	16729	snp	C	T	synonymous_variant c.639G>A p.Lys213Lys	map_2	Protein map
51	16747	complex	GAT	TAC	missense_variant c.619_621delATCinsGTA p.Ile207Val	map_2	Protein map
51	16754	complex	CTA	GTT	missense_variant c.612_614delTAGinsAAC p.Ser205Thr	map_2	Protein map
61	14179	complex	ATTT	CTTTA			
82	5980	complex	AACTA	TAACT	missense_variant c.533_537delTAGTTinsAGTTA p.IleVal178LysLeu		hypothetical protein
84	10930	complex	AAA	TAT	stop_lost&splice_region_variant c.264_*2delAAAinsTAT p.Ter88Tyrext*?		hypothetical protein
84	10950	snp	G	T			
88	943	snp	T	A	missense_variant c.488T>A p.Ile163Lys	desR	Transcriptional regulatory protein
99	35	snp	C	T			
110	5568	snp	C	T	synonymous_variant c.795G>A p.Gln265Gln		hypothetical protein
134	1642	snp	C	A			

Table 1.6 A-C Detected single nucleotide polymorphisms (SNPs) Identified from NCTC 12973 resistance trained isolates. A = SNPS identified in NX-AS-401 resistant trained isolate, B = SNPS identified in gentamicin resistant trained isolate and C = SNPs identified in isolates passage in antibiotic free media for 14 days.

A – NX-AS-401

CHROM	POS	TYPE	REF	ALT	EFFECT	GENE	PRODUCT
6	22499	ins	C	CT	frameshift_variant&splice_region_variant c.241_242insA		hypothetical protein
7	32875	del	AT	A			
20	6966	complex	ATG	TTA			
21	22064	complex	CG	TA			
21	22073	snp	A	C			
23	7262	snp	T	G			
23	7268	snp	G	T			
23	7279	snp	A	T			
23	7293	complex	GC	TT			
23	7301	snp	G	A			
23	7306	complex	GTC	ATT			
23	7317	complex	CCA	TCT			
23	7326	complex	CT	AA			
23	7332	snp	A	T			
23	7337	complex	AT	CA			
23	7593	snp	C	A			
28	22339	snp	G	A	synonymous_variant c.126C>T p.Phe42Phe		Antibacterial protein 3
28	22353	snp	A	G	synonymous_variant c.112T>C p.Leu38Leu		Antibacterial protein 3
28	22360	complex	TACGCCATTTT	CACACCGTTAG	missense_variant c.95_105delAAAATGGCGTAinsCTAACGGTGTG p.Glu32Ala		Antibacterial protein 3
28	22379	complex	CTCACAATG	TCTACGATA	missense_variant c.78_86delCATTGTGAGinsTATCGTAGA p.Ser29Asp		Antibacterial protein 3
39	18348	snp	G	A			
45	4632	snp	T	G			
45	4658	complex	GAA	TAT			

52	809	snp	A	G	missense_variant c.340T>C p.Phe114Leu	essG_3	Type VII secretion system protein EsaG
57	9432	complex	GAT	AAC			
57	9443	snp	T	A			
59	5817	snp	A	T			
69	9585	ins	C	CT			
91	6152	snp	C	A			
92	653	ins	C	CTA	frameshift_variant c.544_545insAT p.Trp182fs		hypothetical protein
92	5812	snp	C	A			
92	5828	snp	A	T			
100	1297	snp	T	A	missense_variant c.437T>A p.Val146Glu		hypothetical protein
105	3622	snp	T	C			
134	5768	snp	G	T	missense_variant c.524C>A p.Ala175Asp	gluP	Rhomboid protease GluP
186	241	snp	G	A			
225	338	snp	C	T			
234	547	snp	A	T			
249	1256	snp	C	A			
249	1267	snp	T	A			
249	1289	snp	T	C			

B – Gentamicin

CHROM	POS	TYPE	REF	ALT	EFFECT	GENE	PRODUCT
6	22499	ins	C	CT	frameshift_variant&splice_region_variant c.241_242insA		hypothetical protein
7	32875	del	AT	A			
20	6900	snp	T	A			
20	6913	complex	CAC	TAA			
20	6948	snp	T	A			
20	6966	complex	ATG	TTA			
21	22064	mnp	CG	TA			
21	22073	snp	A	C			
23	7262	snp	T	G			
23	7268	snp	G	T			
23	7279	snp	A	T			
23	7293	mnp	GC	TT			
23	7301	snp	G	A			
23	7306	complex	GTC	ATT			
23	7317	complex	CCA	TCT			
23	7326	complex	CT	AA			
23	7332	snp	A	T			
23	7337	complex	AT	CA			
23	7593	snp	C	A			
23	7619	snp	A	T			
27	15	snp	C	T			
28	22339	snp	G	A	synonymous_variant c.126C>T p.Phe42Phe		Antibacterial protein 3
28	22353	snp	A	G	synonymous_variant c.112T>C p.Leu38Leu		Antibacterial protein 3
28	22360	complex	TACGCCATTTT	CACACCGTTAG	missense_variant c.95_105delAAAATGGCGTAinsCTAACGGTGTG p.Glu32Ala		Antibacterial protein 3
28	22379	complex	CTCACAATG	TCTACGATA	missense_variant c.78_86delCATTGTGAGinsTATCGTAGA p.Ser29Asp		Antibacterial protein 3
39	18348	snp	G	A			
42	8697	snp	A	C	missense_variant c.1729T>G p.Ser577Ala	fusA	Elongation factor G
45	4632	snp	T	G			
45	4658	complex	GAA	TAT			
47	8523	snp	G	A			

49	12148	snp	G	C	synonymous_variant c.150G>C p.Gly50Gly	ctaA	Heme A synthase
52	809	snp	A	G	missense_variant c.340T>C p.Phe114Leu	essG_3	Type VII secretion system protein EsaG
57	9432	complex	GAT	AAC			
57	9443	snp	T	A			
59	5817	snp	A	T			
69	9585	ins	C	CT			
91	6152	snp	C	A			
91	6158	ins	T	TA			
92	653	ins	C	CTA	frameshift_variant c.544_545insAT p.Trp182fs		hypothetical protein
92	5812	snp	C	A			
92	5828	snp	A	T			
95	94	snp	A	G	missense_variant c.464T>C p.Val155Ala	mutL_1	DNA mismatch repair protein MutL
100	1297	snp	T	A	missense_variant c.437T>A p.Val146Glu		hypothetical protein
116	1801	snp	C	T	synonymous_variant c.15C>T p.Ile5Ile	mltF	Membrane-bound lytic murein transglycosylase F
139	103	snp	G	T			
146	555	snp	A	T			
186	241	snp	G	A			
225	338	snp	C	T			
226	6	snp	G	A			
234	547	snp	A	T			

C – 14-Day Passage

CHROM	POS	TYPE	REF	ALT	EFFECT	GENE	PRODUCT
6	22499	ins	C	CT	frameshift_variant&splice_region_variant c.241_242insA		hypothetical protein
7	32875	del	AT	A			
21	22064	complex	CG	TA			
21	22073	snp	A	C			
23	7262	snp	T	G			
23	7268	snp	G	T			
23	7279	snp	A	T			
23	7293	mnp	GC	TT			
23	7301	snp	G	A			
23	7306	complex	GTC	ATT			
23	7317	complex	CCA	TCT			
23	7326	complex	CT	AA			
23	7332	snp	A	T			
23	7337	complex	AT	CA			
23	7593	snp	C	A			
45	4632	snp	T	G			
52	809	snp	A	G	missense_variant c.340T>C p.Phe114Leu	essG_3	Type VII secretion system protein EsaG
57	9432	complex	GAT	AAC			
57	9443	snp	T	A			
59	5817	snp	A	T			
69	9585	ins	C	CT			
92	653	ins	C	CTA	frameshift_variant c.544_545insAT p.Trp182fs		hypothetical protein
92	5812	snp	C	A			
92	5828	snp	A	T			
100	1297	snp	T	A	missense_variant c.437T>A p.Val146Glu		hypothetical protein
116	1801	snp	C	T	synonymous_variant c.15C>T p.Ile5Ile	mltF	Membrane-bound lytic murein transglycosylase F
225	338	snp	C	T			
234	547	snp	A	T			

Table 1.7 A-C Detected single nucleotide polymorphisms (SNPs) Identified from UHW 3 resistance trained isolates. A = SNPS identified in NX-AS-401 resistant trained isolate, B = SNPS identified in gentamicin resistant trained isolate and C = SNPs identified in isolates passage in antibiotic free media for 14 days.

A – NX-AS-401

CHROM	POS	TYPE	REF	ALT	EFFECT	GENE	PRODUCT
1	24609	snp	G	T			
3	84401	snp	A	T			
3	84411	snp	G	A			
3	84417	snp	G	C			
3	84440	del	CTTA	C			
3	84453	snp	A	G			
3	84462	snp	G	A			
3	84484	snp	G	A			
3	84509	complex	GCA	TTT	missense_variant c.14_16delGCAinsTTT p.GlyThr5ValSer		hypothetical protein
3	84532	complex	GCCG	CCCA	missense_variant c.37_40delGCCGinsCCCA p.AlaGly13ProSer		hypothetical protein
3	84545	snp	C	T	missense_variant c.50C>T p.Ala17Val		hypothetical protein
3	84565	complex	GG	AC	missense_variant c.70_71delGGinsAC p.Gly24Thr		hypothetical protein
3	84573	snp	C	T	synonymous_variant c.78C>T p.Asn26Asn		hypothetical protein
3	84581	complex	CGAAG	AGAAA	missense_variant c.86_90delCGAAGinsAGAAA p.Thr29Lys		hypothetical protein
3	84597	complex	CG	GA	missense_variant c.102_103delCGinsGA p.IleVal34MetIle		hypothetical protein
3	84615	complex	CGTA	AGTG	synonymous_variant c.120_123delCGTAinsAGTG p.42		hypothetical protein
3	84628	snp	C	T	missense_variant c.133C>T p.Pro45Ser		hypothetical protein
3	84636	snp	C	T	synonymous_variant c.141C>T p.Ser47Ser		hypothetical protein
3	84643	snp	G	A	missense_variant c.148G>A p.Val50Ile		hypothetical protein
21	15328	ins	C	CT			
21	46865	snp	G	A			
46	357	snp	C	T	synonymous_variant c.19C>T p.Leu7Leu	essG_1	Type VII secretion system protein EsaG
54	10916	snp	T	C	synonymous_variant c.1419A>G p.Ala473Ala	map_4	Protein map

54	10922	complex	AGATG	TGATC	missense_variant c.1409_1413delCATCTinsGATCA p.Ala470Gly	map_4	Protein map
54	11630	snp	G	A	synonymous_variant c.705C>T p.Ile235Ile	map_4	Protein map
54	11638	snp	A	C	missense_variant c.697T>G p.Ser233Ala	map_4	Protein map
54	11648	complex	GAC	TAT	missense_variant c.685_687delGTCinsATA p.Val229Ile	map_4	Protein map
54	11657	complex	TTTT	CTTC	synonymous_variant c.675_678delAAAinsGAAG p.227	map_4	Protein map
54	11677	complex	GAACCGTATATTC	TAACTGTAAATTT	missense_variant c.646_658delGAATATACGGTTCinsAAATTTACAGTTA p.GluTyrThrValHis216LysPheThrValAsn	map_4	Protein map
54	11696	snp	C	T	synonymous_variant c.639G>A p.Lys213Lys	map_4	Protein map
78	102	snp	C	A	missense_variant c.424G>T p.Ala142Ser		hypothetical protein

B – Gentamicin

CHROM	POS	TYPE	REF	ALT	EFFECT	GENE	PRODUCT
1	24609	snp	G	T			
3	84401	snp	A	T			
3	84411	snp	G	A			
3	84417	snp	G	C			
3	84440	del	CTTA	C			
3	84453	snp	A	G			
3	84462	snp	G	A			
3	84484	snp	G	A			
3	84509	complex	GCA	TTT	missense_variant c.14_16delGCAinsTTT p.GlyThr5ValSer		hypothetical protein
3	84532	complex	GCCG	CCCA	missense_variant c.37_40delGCCGinsCCCA p.AlaGly13ProSer		hypothetical protein
3	84545	snp	C	T	missense_variant c.50C>T p.Ala17Val		hypothetical protein
3	84565	complex	GG	AC	missense_variant c.70_71delGGinsAC p.Gly24Thr		hypothetical protein
3	84573	snp	C	T	synonymous_variant c.78C>T p.Asn26Asn		hypothetical protein
3	84581	complex	CGAAG	AGAAA	missense_variant c.86_90delCGAAGinsAGAAA p.Thr29Lys		hypothetical protein
3	84597	mnp	CG	GA	missense_variant c.102_103delCGinsGA p.IleVal34MetIle		hypothetical protein
3	84615	complex	CGTA	AGTG	synonymous_variant c.120_123delCGTAinsAGTG p.42		hypothetical protein
3	84628	snp	C	T	missense_variant c.133C>T p.Pro45Ser		hypothetical protein
3	84636	snp	C	T	synonymous_variant c.141C>T p.Ser47Ser		hypothetical protein
3	84643	snp	G	A	missense_variant c.148G>A p.Val50Ile		hypothetical protein
3	84653	del	AAG	A	frameshift_variant c.159_160delAAG p.Gln53fs		hypothetical protein
3	84664	complex	AA	CG	missense_variant c.169_170delAAinsCG p.Asn57Arg		hypothetical protein
3	84717	complex	GGG	AGA	missense_variant c.222_224delGGGinsAGA p.MetGly74IleGlu		hypothetical protein
3	84728	snp	C	A	missense_variant c.233C>A p.Pro78His		hypothetical protein
3	84751	snp	A	T	missense_variant c.256A>T p.Met86Leu		hypothetical protein
17	48519	snp	G	A			
21	15328	ins	C	CT			
21	46865	snp	G	A			
24	20943	snp	G	A			
24	32340	snp	G	A			
33	26264	snp	A	T			

46	357	snp	C	T	synonymous_variant c.19C>T p.Leu7Leu	essG_1	Type VII secretion system protein EsaG
54	10891	complex	AG	TA	missense_variant c.1443_1444delCTinsTA p.Ser482Thr	map_4	Protein map
54	10904	complex	ACGCTCC	GCTATCT	missense_variant c.1425_1431delGGAGCGTinsAGATAGC p.GluArg476AspSer	map_4	Protein map
54	10916	snp	T	C	synonymous_variant c.1419A>G p.Ala473Ala	map_4	Protein map
54	10922	complex	AGATG	TGATC	missense_variant c.1409_1413delCATCTinsGATCA p.Ala470Gly	map_4	Protein map
54	11630	snp	G	A	synonymous_variant c.705C>T p.Ile235Ile	map_4	Protein map
54	11638	snp	A	C	missense_variant c.697T>G p.Ser233Ala	map_4	Protein map
54	11648	complex	GAC	TAT	missense_variant c.685_687delGTCinsATA p.Val229Ile	map_4	Protein map
54	11657	complex	TTTT	CTTC	synonymous_variant c.675_678delAAAinsGAAG p.227	map_4	Protein map
54	11677	complex	GAACCGTATATTC	TAACTGTAAATTT	missense_variant c.646_658delGAATATACGGTTCinsAAATTTACAGTTA p.GluTyrThrValHis216LysPheThrValAsn	map_4	Protein map
54	11696	snp	C	T	synonymous_variant c.639G>A p.Lys213Lys	map_4	Protein map

C – 14-Day Passage

CHROM	POS	TYPE	REF	ALT	EFFECT	GENE	PRODUCT
1	24609	snp	G	T			
3	84401	snp	A	T			
3	84411	snp	G	A			
3	84417	snp	G	C			
3	84440	del	CTTA	C			
3	84453	snp	A	G			
3	84462	snp	G	A			
3	84484	snp	G	A			
3	84509	complex	GCA	TTT	missense_variant c.14_16delGCAinsTTT p.GlyThr5ValSer		hypothetical protein
3	84532	complex	GCCG	CCCA	missense_variant c.37_40delGCCGinsCCCA p.AlaGly13ProSer		hypothetical protein
3	84545	snp	C	T	missense_variant c.50C>T p.Ala17Val		hypothetical protein
3	84565	complex	GG	AC	missense_variant c.70_71delGGinsAC p.Gly24Thr		hypothetical protein
3	84573	snp	C	T	synonymous_variant c.78C>T p.Asn26Asn		hypothetical protein
3	84581	complex	CGAAG	AGAAA	missense_variant c.86_90delCGAAGinsAGAAA p.Thr29Lys		hypothetical protein
3	84597	complex	CG	GA	missense_variant c.102_103delCGinsGA p.IleVal34MetIle		hypothetical protein
3	84615	complex	CGTA	AGTG	synonymous_variant c.120_123delCGTAinsAGTG p.42		hypothetical protein
3	84628	snp	C	T	missense_variant c.133C>T p.Pro45Ser		hypothetical protein
3	84636	snp	C	T	synonymous_variant c.141C>T p.Ser47Ser		hypothetical protein
3	84643	snp	G	A	missense_variant c.148G>A p.Val50Ile		hypothetical protein
3	84653	del	AAG	A	frameshift_variant c.159_160delAAG p.Gln53fs		hypothetical protein
3	84664	complex	AA	CG	missense_variant c.169_170delAAinsCG p.Asn57Arg		hypothetical protein
3	84680	snp	T	C	missense_variant c.185T>C p.Val62Ala		hypothetical protein
3	84696	snp	G	A	synonymous_variant c.201G>A p.Leu67Leu		hypothetical protein
3	84703	snp	G	T	missense_variant c.208G>T p.Ala70Ser		hypothetical protein
3	84717	complex	GGG	AGA	missense_variant c.222_224delGGGinsAGA p.MetGly74IleGlu		hypothetical protein
3	84728	snp	C	A	missense_variant c.233C>A p.Pro78His		hypothetical protein
3	84751	snp	A	T	missense_variant c.256A>T p.Met86Leu		hypothetical protein
13	72059	complex	GAG	TAT			
17	48519	snp	G	A			
21	15328	ins	C	CT			

21	46865	snp	G	A				
33	26264	snp	A	T				
46	357	snp	C	T	synonymous_variant c.19C>T p.Leu7Leu	essG_1	Type VII secretion system protein EsaG	
54	10891	complex	AG	TA	missense_variant c.1443_1444delCTinsTA p.Ser482Thr	map_4	Protein map	
54	10904	complex	ACGCTCC	GCTATCT	missense_variant c.1425_1431delGGAGCGTinsAGATAGC p.GluArg476AspSer	map_4	Protein map	
54	10916	snp	T	C	synonymous_variant c.1419A>G p.Ala473Ala	map_4	Protein map	
54	10922	complex	AGATG	TGATC	missense_variant c.1409_1413delCATCTinsGATCA p.Ala470Gly	map_4	Protein map	
54	11600	snp	G	A	synonymous_variant c.735C>T p.Asp245Asp	map_4	Protein map	
54	11612	snp	G	T	synonymous_variant c.723C>A p.Ile241Ile	map_4	Protein map	
54	11618	complex	GTCA	ATTC	missense_variant c.714_717delTGACinsGAAT p.Asp239Asn	map_4	Protein map	
54	11630	snp	G	A	synonymous_variant c.705C>T p.Ile235Ile	map_4	Protein map	
54	11638	snp	A	C	missense_variant c.697T>G p.Ser233Ala	map_4	Protein map	
54	11648	complex	GAC	TAT	missense_variant c.685_687delGTCinsATA p.Val229Ile	map_4	Protein map	
54	11657	complex	TTTT	CTTC	synonymous_variant c.675_678delAAAinsGAAG p.227	map_4	Protein map	
54	11677	complex	GAACCGTATATTC	TAACGTAAATTT	missense_variant c.646_658delGAATATACGGTTCinsAAATTTACAGTTA p.GluTyrThrValHis216LysPheThrValAsn	map_4	Protein map	
54	11696	snp	C	T	synonymous_variant c.639G>A p.Lys213Lys	map_4	Protein map	
78	102	snp	C	A	missense_variant c.424G>T p.Ala142Ser		hypothetical protein	

Table 1.8 A-C Detected single nucleotide polymorphisms (SNPs) Identified from UHW 8 resistance trained isolates. A = SNPS identified in NX-AS-401 resistant trained isolate, B = SNPS identified in gentamicin resistant trained isolate and C = SNPs identified in isolates passage in antibiotic free media for 14 days.

A - NX-AS-401

CHROM	POS	TYPE	REF	ALT	NT_POS	AA_POS	EFFECT	GENE	PRODUCT
1	22	snp	A	T					
9	37254	snp	C	T	3460/4101	1154/1366	missense_variant c.3460G>A p.Asp1154Asn	sdrD_1	Serine-aspartate repeat-containing protein D
9	38413	snp	T	A	2301/4101	767/1366	missense_variant c.2301A>T p.Lys767Asn	sdrD_1	Serine-aspartate repeat-containing protein D
9	38419	snp	G	A	2295/4101	765/1366	synonymous_variant c.2295C>T p.Val765Val	sdrD_1	Serine-aspartate repeat-containing protein D
13	27981	snp	C	T					
25	108	ins	T	TA	45/1362	15/453	frameshift_variant c.44dupA p.Asn15fs	speA	Arginine decarboxylase
28	82	snp	T	A					
37	16808	complex	TACGCCA	CACACCG	105/135	33/44	synonymous_variant c.99_105delTGGCGTAinsCGGTGTG p.36		Antibacterial protein 3
37	16827	complex	CTC	TCT	86/135	28/44	missense_variant c.84_86delGAGinsAGA p.Ser29Asp		Antibacterial protein 3
37	16835	snp	G	A	78/135	26/44	synonymous_variant c.78C>T p.Ser26Ser		Antibacterial protein 3
50	15987	snp	T	A					
50	15993	snp	G	T					
50	16000	complex	TGG	AGT					
50	16011	complex	GAC	AAT					
52	16024	complex	TAC	AA					
52	139	snp	T	G					
63	3078	snp	C	T					
69	12851	snp	G	A					
156	174	snp	T	A					

B - Gentamicin

CHROM	POS	TYPE	REF	ALT	NT_POS	AA_POS	EFFECT	GENE	PRODUCT
1	22	snp	A	T					
6	15300	snp	A	C					
6	15320	snp	G	T					
9	37254	snp	C	T	3460/4101	1154/1366	missense_variant c.3460G>A p.Asp1154Asn	sdrD_1	Serine-aspartate repeat-containing protein D
9	38413	snp	T	A	2301/4101	767/1366	missense_variant c.2301A>T p.Lys767Asn	sdrD_1	Serine-aspartate repeat-containing protein D
9	38419	snp	G	A	2295/4101	765/1366	synonymous_variant c.2295C>T p.Val765Val	sdrD_1	Serine-aspartate repeat-containing protein D
13	27981	snp	C	T					
18	1215	snp	T	A					
23	18878	snp	C	T	1889/2988	630/995	missense_variant c.1889G>A p.Ser630Asn		hypothetical protein
28	82	snp	T	A					
37	16808	complex	TACGCCA	CACACCG	105/135	33/44	synonymous_variant c.99_105delTGGCGTAinsCGGTGTG p.36		Antibacterial protein 3
37	16827	mnp	CTC	TCT	86/135	28/44	missense_variant c.84_86delGAGinsAGA p.Ser29Asp		Antibacterial protein 3
37	16835	snp	G	A	78/135	26/44	synonymous_variant c.78C>T p.Ser26Ser		Antibacterial protein 3
50	15987	snp	T	A					
50	15993	snp	G	T					
50	16000	complex	TGG	AGT					
50	16011	complex	GAC	AAT					
50	16024	complex	TAC	AA					
63	3078	snp	C	T					
69	12851	snp	G	A					
126	174	snp	T	A					
159	126	snp	T	G	24/531	8/176	missense_variant c.24T>G p.Ile8Met		Putative phosphoesterase
178	2359	snp	T	A					

C – 14-Day Passage

CHROM	POS	TYPE	REF	ALT	NT_POS	AA_POS	EFFECT	GENE	PRODUCT
6	15300	snp	A	C					
6	15320	snp	G	T					
9	37254	snp	C	T	3460/4101	1154/1366	missense_variant c.3460G>A p.Asp1154Asn	sdrD_1	Serine-aspartate repeat-containing protein D
9	38413	snp	T	A	2301/4101	767/1366	missense_variant c.2301A>T p.Lys767Asn	sdrD_1	Serine-aspartate repeat-containing protein D
9	38419	snp	G	A	2295/4101	765/1366	synonymous_variant c.2295C>T p.Val765Val	sdrD_1	Serine-aspartate repeat-containing protein D
13	27981	snp	C	T					
18	1215	snp	T	A					
28	82	snp	T	A					
37	16808	complex	TACGCCA	CACACCG	105/135	33/44	synonymous_variant c.99_105delTGGCGTAinsCGGTGTG p.36		Antibacterial protein 3
37	16827	complex	CTC	TCT	86/135	28/44	missense_variant c.84_86delGAGinsAGA p.Ser29Asp		Antibacterial protein 3
37	16835	snp	G	A	78/135	26/44	synonymous_variant c.78C>T p.Ser26Ser		Antibacterial protein 3
50	15987	snp	T	A					
50	15993	snp	G	T					
50	16000	complex	TGG	AGT					
50	16011	complex	GAC	AAT					
50	16024	complex	TAC	AA					
52	139	snp	T	G					
63	3078	snp	C	T					
69	12851	snp	G	A					
112	144	snp	T	G	171/171	57/56	stop_lost&splice_region_variant c.171A>C p.Ter57Tyrext*?		hypothetical protein

Table 1.9 A-C Detected single nucleotide polymorphisms (SNPs) Identified from UHW 15 resistance trained isolates. A = SNPS identified in NX-AS-401 resistant trained isolate, B = SNPS identified in gentamicin resistant trained isolate and C = SNPs identified in isolates passage in antibiotic free media for 14 days.

A - NX-AS-401

CHROM	POS	TYPE	REF	ALT	NT_POS	AA_POS	EFFECT	GENE	PRODUCT
1	48396	ins	A	AC	742/747	248/248	frameshift_variant c.742dupG p.Val248fs	hisF	Imidazole glycerol phosphate synthase subunit HisF
4	10777	ins	C	CT	932/957	311/318	frameshift_variant c.932_933insA p.Gln312fs	ribF	Bifunctional riboflavin kinase/FMN adenylyltransferase
6	25365	del	AT	A	25/1368	9/455	frameshift_variant c.25delA p.Ile9fs	nasD_2	Nitrite reductase [NAD(P)H]
15	12784	snp	T	C					
15	23061	snp	C	A	413/519	138/172	missense_variant c.413G>T p.Gly138Val	apt	Adenine phosphoribosyltransferase
23	3975	snp	C	T					
26	21396	snp	T	C	132/132	44/43	stop_lost&splice_region_variant c.132A>G p.Ter44Trpext*?		hypothetical protein
28	509	complex	CTGGG	TTGGT			intergenic_region n.509_513delCTGGGinsTTGGT		tRNA-Lys
28	567	snp	T	C					
69	137	snp	G	A					
72	11901	snp	C	G	820/849	274/282	missense_variant c.820C>G p.Gln274Glu		hypothetical protein
75	11471	snp	T	G					
92	3520	snp	T	A					
101	8400	ins	T	TA					
101	8412	snp	C	A					
113	7755	snp	T	C					
117	6745	ins	A	AT					
133	2778	snp	G	T	2696/3282	899/1093	missense_variant c.2696G>T p.Gly899Val	sdrE	Serine-aspartate repeat-containing protein E
134	1082	snp	A	T	1127/1473	376/490	missense_variant c.1127T>A p.Ile376Lys	gcvPB	putative glycine dehydrogenase subunit 2
205	341	snp	A	T	124/342	42/113	missense_variant c.124A>T p.Ile42Phe		hypothetical protein
205	350	snp	A	C	133/342	45/113	missense_variant c.133A>C p.Thr45Pro		hypothetical protein
205	373	snp	G	T	156/342	52/113	missense_variant c.156G>T p.Leu52Phe		hypothetical protein
246	62	snp	T	C	293/315	98/104	missense_variant c.293A>G p.Asn98Ser		hypothetical protein
246	69	snp	T	C	286/315	96/104	missense_variant c.286A>G p.Lys96Glu		hypothetical protein
253	883	snp	T	G					
253	888	snp	C	T					
253	910	snp	A	T					

B – Gentamicin

CHROM	POS	TYPE	REF	ALT	NT_POS	AA_POS	EFFECT	GENE	PRODUCT
1	48396	ins	A	AC	742/747	248/248	frameshift_variant c.742dupG p.Val248fs	hisF	Imidazole glycerol phosphate synthase subunit HisF
4	10777	ins	C	CT	932/957	311/318	frameshift_variant c.932_933insA p.Gln312fs	ribF	Bifunctional riboflavin kinase/FMN adenylyltransferase
6	25365	del	AT	A	25/1368	9/455	frameshift_variant c.25delA p.Ile9fs	nasD_2	Nitrite reductase [NAD(P)H]
23	3975	snp	C	T					
26	21396	snp	T	C	132/132	44/43	stop_lost&splice_region_variant c.132A>G p.Ter44Trpext*?		hypothetical protein
28	509	complex	CTGGG	TTGGT			intergenic_region n.509_513delCTGGGinsTTGGT		tRNA-Lys
28	567	snp	T	C					
72	11901	snp	C	G	820/849	274/282	missense_variant c.820C>G p.Gln274Glu		hypothetical protein
92	3520	snp	T	A					
101	8400	ins	T	TA					
101	8412	snp	C	A					
117	6745	ins	A	AT					
134	1082	snp	A	T	1127/1473	376/490	missense_variant c.1127T>A p.Ile376Lys	gcvPB	putative glycine dehydrogenase (decarboxylating) subunit 2
205	341	snp	A	T	124/342	42/113	missense_variant c.124A>T p.Ile42Phe		hypothetical protein
205	350	snp	A	C	133/342	45/113	missense_variant c.133A>C p.Thr45Pro		hypothetical protein
205	373	snp	G	T	156/342	52/113	missense_variant c.156G>T p.Leu52Phe		hypothetical protein
253	883	snp	T	G					
253	888	snp	C	T					

C- 14-Day Passage

CHROM	POS	TYPE	REF	ALT	NT_POS	AA_POS	EFFECT	GENE	PRODUCT
1	48396	ins	A	AC	742/747	248/248	frameshift_variant c.742dupG p.Val248fs	hisF	Imidazole glycerol phosphate synthase subunit HisF
4	10777	ins	C	CT	932/957	311/318	frameshift_variant c.932_933insA p.Gln312fs	ribF	Bifunctional riboflavin kinase/FMN adenylyltransferase
6	25365	del	AT	A	25/1368	9/455	frameshift_variant c.25delA p.Ile9fs	nasD_2	Nitrite reductase [NAD(P)H]
23	3975	snp	C	T					
26	21396	snp	T	C	132/132	44/43	stop_lost&splice_region_variant c.132A>G p.Ter44Trpext*?		hypothetical protein
28	509	complex	CTGGG	TTGGT			intergenic_region n.509_513delCTGGGinsTTGGT		tRNA-Lys
28	567	snp	T	C					
72	11901	snp	C	G	820/849	274/282	missense_variant c.820C>G p.Gln274Glu		hypothetical protein
92	3520	snp	T	A					
101	8400	ins	T	TA					
101	8412	snp	C	A					
117	6745	ins	A	AT					
134	1082	snp	A	T	1127/1473	376/490	missense_variant c.1127T>A p.Ile376Lys	gcvPB	putative glycine dehydrogenase (decarboxylating) subunit 2
205	341	snp	A	T	124/342	42/113	missense_variant c.124A>T p.Ile42Phe		hypothetical protein
205	350	snp	A	C	133/342	45/113	missense_variant c.133A>C p.Thr45Pro		hypothetical protein
205	373	snp	G	T	156/342	52/113	missense_variant c.156G>T p.Leu52Phe		hypothetical protein
229	178	snp	G	A					
242	107	snp	A	G					
242	113	snp	T	C					
252	883	snp	T	G					
253	888	snp	C	T					
253	910	snp	A	T					

Table 1.10 A-C Detected single nucleotide polymorphisms (SNPs) Identified from UHW 18 resistance trained isolates. A = SNPS identified in NX-AS-401 resistant trained isolate, B = SNPS identified in gentamicin resistant trained isolate and C = SNPs identified in isolates passage in antibiotic free media for 14 days.

A - NX-AS-401

CHROM	POS	TYPE	REF	ALT	NT_POS	AA_POS	EFFECT	GENE	PRODUCT
1	67765	snp	T	A					
15	7491	snp	G	A	700/840	234/279	missense_variant c.700G>A p.Asp234Asn	lgt	Phosphatidylglycerol--prolipoprotein diacylglyceryl transferase
15	7508	snp	G	A	717/840	239/279	synonymous_variant c.717G>A p.Gln239Gln	lgt	Phosphatidylglycerol--prolipoprotein diacylglyceryl transferase
15	10988	ins	C	CACA					
15	11040	complex	CCC	GCCCA					
16	40464	ins	T	TA	24/480	8/159	frameshift_variant c.23_24insA p.Phe8fs	entA_1	Enterotoxin type A
18	29536	complex	TC	G	44/1767	15/588	frameshift_variant&missense_variant c.43_44delGAinsC p.Asp15fs	sdrD_2	Serine-aspartate repeat-containing protein D
18	29545	complex	TTGGA	CTGCT	35/1767	11/588	missense_variant c.31_35delTCCAAinsAGCAG p.Lys12Arg	sdrD_2	Serine-aspartate repeat-containing protein D
18	29556	snp	T	C	2416/2439	806/812	missense_variant c.2416A>G p.Asn806Asp	sdrD_2	Serine-aspartate repeat-containing protein D
18	29581	complex	GTC	ATT	2391/2439	797/812	missense_variant c.2389_2391delGACinsAAT p.Asp797Asn	sdrD_2	Serine-aspartate repeat-containing protein D
20	28128	snp	T	A					
20	28154	snp	G	T					
20	28428	snp	T	A					
20	28439	complex	GAC	AAT					
20	28453	mnp	GC	AA					
23	3618	ins	A	AT	646/699	216/232	frameshift_variant c.646dupA p.Ile216fs	catE_1	Catechol-2,3-dioxygenase
28	28898	snp	G	T	344/1245	115/414	missense_variant c.344C>A p.Thr115Lys	fabF	3-oxoacyl-[acyl-carrier-protein] synthase 2
32	25595	snp	A	T					
33	25634	ins	A	AACCTTGCCGGC					

59	809	snp	A	G	340/501	114/166	missense_variant c.340T>C p.Phe114Leu	essG_3	Type VII secretion system protein EsaG
65	247	del	CT	C	30/213	25842	frameshift_variant c.30delT p.Thr11fs		IS1182 family transposase ISSau3
69	6817	snp	A	G					
69	6828	snp	T	C					
69	6875	snp	C	A	741/771	247/256	synonymous_variant c.741G>T p.Ser247Ser		hypothetical protein
69	6884	snp	G	A	732/771	244/256	synonymous_variant c.732C>T p.Ile244Ile		hypothetical protein
69	6890	snp	T	C	726/771	242/256	synonymous_variant c.726A>G p.Glu242Glu		hypothetical protein
93	6958	complex	TTAC	ATAT					

B – Gentamicin

CHROM	POS	TYPE	REF	ALT	NT_POS	AA_POS	EFFECT	GENE	PRODUCT
1	67765	snp	T	A					
15	7491	snp	G	A	700/840	234/279	missense_variant c.700G>A p.Asp234Asn	lgt	Phosphatidylglycerol--prolipoprotein diacylglyceryl transferase
15	11040	complex	CCC	GCCCA					
16	40464	ins	T	TA	24/480	8/159	frameshift_variant c.23_24insA p.Phe8fs	entA_1	Enterotoxin type A
18	29536	complex	TC	G	44/1767	15/588	frameshift_variant&missense_variant c.43_44delGAinsC p.Asp15fs	sdrD_2	Serine-aspartate repeat-containing protein D
18	29545	complex	TTGGA	CTGCT	35/1767	11/588	missense_variant c.31_35delTCCAAinsAGCAG p.Lys12Arg	sdrD_2	Serine-aspartate repeat-containing protein D
18	29556	snp	T	C	2416/2439	806/812	missense_variant c.2416A>G p.Asn806Asp	sdrD_2	Serine-aspartate repeat-containing protein D
18	29581	complex	GTC	ATT	2391/2439	797/812	missense_variant c.2389_2391delGACinsAAT p.Asp797Asn	sdrD_2	Serine-aspartate repeat-containing protein D
20	28128	snp	T	A					
20	28154	snp	G	T					
20	28428	snp	T	A					
20	28439	complex	GAC	AAT					
20	28453	complex	GC	AA					
23	3618	ins	A	AT	646/699	216/232	frameshift_variant c.646dupA p.Ile216fs	catE_1	Catechol-2,3-dioxygenase
32	22351	complex	CTC	TCT	86/135	28/44	missense_variant c.84_86delGAGinsAGA p.Ser29Asp		Antibacterial protein 3
33	25634	ins	A	AACCTTGCCGGC					
59	809	snp	A	G	340/501	114/166	missense_variant c.340T>C p.Phe114Leu	essG_3	Type VII secretion system protein EsaG
65	247	del	CT	C	30/213	25842	frameshift_variant c.30delT p.Thr11fs		IS1182 family transposase ISSau3
67	5467	snp	A	T					
67	5555	complex	CGA	TGG					
69	6817	snp	A	G					
69	6828	snp	T	C					
69	6875	snp	C	A	741/771	247/256	synonymous_variant c.741G>T p.Ser247Ser		hypothetical protein
69	6884	snp	G	A	732/771	244/256	synonymous_variant c.732C>T p.Ile244Ile		hypothetical protein
69	6890	snp	T	C	726/771	242/256	synonymous_variant c.726A>G p.Glu242Glu		hypothetical protein
93	6958	complex	TTAC	ATAT					

C- 14-Day Passage

CHROM	POS	TYPE	REF	ALT	NT_POS	AA_POS	EFFECT	GENE	PRODUCT
1	67765	snp	T	A					
15	7491	snp	G	A	700/840	234/279	missense_variant c.700G>A p.Asp234Asn	lgt	Phosphatidylglycerol--prolipoprotein diacylglyceryl transferase
15	7508	snp	G	A	717/840	239/279	synonymous_variant c.717G>A p.Gln239Gln	lgt	Phosphatidylglycerol--prolipoprotein diacylglyceryl transferase
15	10857	ins	A	AT					
15	10988	ins	C	CACA					
15	11040	complex	CCC	GCCCA					
16	40464	ins	T	TA	24/480	8/159	frameshift_variant c.23_24insA p.Phe8fs	entA_1	Enterotoxin type A
18	29536	complex	TC	G	44/1767	15/588	frameshift_variant&missense_variant c.43_44delGinsC	sdrD_2	Serine-aspartate repeat-containing protein D
18	29545	complex	TTGGA	CTGCT	35/1767	11/588	missense_variant c.31_35delTCCAinsAGCAG p.Lys12Arg	sdrD_2	Serine-aspartate repeat-containing protein D
18	29556	snp	T	C	2416/2439	806/812	missense_variant c.2416A>G p.Asn806Asp	sdrD_2	Serine-aspartate repeat-containing protein D
18	29581	complex	GTC	ATT	2391/2439	797/812	missense_variant c.2389_2391delGACinsAAT p.Asp797Asn	sdrD_2	Serine-aspartate repeat-containing protein D
20	28128	snp	T	A					
20	28154	snp	G	T					
20	28428	snp	T	A					
20	28439	complex	GAC	AAT					
20	28453	complex	GC	AA					
23	3618	ins	A	AT	646/699	216/232	frameshift_variant c.646dupA p.Ile216fs	catE_1	Catechol-2,3-dioxygenase
32	22351	complex	CTC	TCT	86/135	28/44	missense_variant c.84_86delGAGinsAGA p.Ser29Asp		Antibacterial protein 3
33	25634	ins	A	AACCTTGCCGGC					
59	809	snp	A	G	340/501	114/166	missense_variant c.340T>C p.Phe114Leu	essG_3	Type VII secretion system protein EsaG
65	124	snp	A	G					
65	247	del	CT	C	30/213	25842	frameshift_variant c.30delT p.Thr11fs		IS1182 family transposase ISSau3
67	5467	snp	A	T					
69	6817	snp	A	G					
69	6828	snp	T	C					
69	6875	snp	C	A	741/771	247/256	synonymous_variant c.741G>T p.Ser247Ser		hypothetical protein
69	6884	snp	G	A	732/771	244/256	synonymous_variant c.732C>T p.Ile244Ile		hypothetical protein
69	6890	snp	T	C	726/771	242/256	synonymous_variant c.726A>G p.Glu242Glu		hypothetical protein
93	6958	complex	TTAC	ATAT					
93	7002	snp	A	C					
93	7024	snp	G	A					

Table 1.11 A-C Detected single nucleotide polymorphisms (SNPs) Identified from UHW 19 resistance trained isolates. A = SNPS identified in NX-AS-401 resistant trained isolate, B = SNPS identified in gentamicin resistant trained isolate and C = SNPs identified in isolates passage in antibiotic free media for 14 days.

A - NX-AS-401

CHROM	POS	TYPE	REF	ALT	NT_POS	AA_POS	EFFECT	GENE	PRODUCT
1	84522	del	CTTA	C					
1	84647	snp	G	A	70/324	24/107	missense_variant c.70G>A p.Ala24Thr		hypothetical protein
1	84735	del	AAG	A	159/324	53/107	frameshift_variant c.159_160delAG p.Gln53fs		hypothetical protein
8	23119	snp	T	A					
38	22040	del	GA	G					
38	22067	snp	T	C					
40	15380	ins	A	AT					
49	583	snp	C	T	291/807	97/268	synonymous_variant c.291C>T p.Phe97Phe		IS1182 family transposase ISSau3
74	12935	snp	C	T					
91	9651	snp	C	T					
101	3307	snp	C	T	127/441	43/146	missense_variant c.127C>T p.Leu43Phe		hypothetical protein
145	1522	snp	T	C					

B – Gentamicin

CHROM	POS	TYPE	REF	ALT	NT_POS	AA_POS	EFFECT	GENE	PRODUCT
1	84522	del	CTTA	C					
1	84647	snp	G	A	70/324	24/107	missense_variant c.70G>A p.Ala24Thr		hypothetical protein
1	84735	del	AAG	A	159/324	53/107	frameshift_variant c.159_160delAG p.Gln53fs		hypothetical protein
4	74326	snp	G	A	404/939	135/312	missense_variant c.404G>A p.Cys135Tyr	menA	1,4-dihydroxy-2-naphthoate octaprenyltransferase
8	33293	snp	T	C	273/840	91/279	synonymous_variant c.273T>C p.Gly91Gly		hypothetical protein
38	22040	del	GA	G					
40	15380	ins	A	AT					
45	7260	snp	A	G	3624/4128	1208/1375	synonymous_variant c.3624A>G p.Ser1208Ser	sdrD	Serine-aspartate repeat-containing protein D
48	15455	snp	G	T	1103/1464	368/487	missense_variant c.1103C>A p.Thr368Asn	glpG	Rhomboid protease GlpG
48	15460	snp	G	T	1098/1464	366/487	missense_variant c.1098C>A p.Asp366Glu	glpG	Rhomboid protease GlpG
49	583	snp	C	T	291/807	97/268	synonymous_variant c.291C>T p.Phe97Phe		IS1182 family transposase ISSau3
73	9800	ins	A	AT					
74	12935	snp	C	T					
91	9651	snp	C	T					
101	3307	snp	C	T	127/441	43/146	missense_variant c.127C>T p.Leu43Phe		hypothetical protein
108	1619	snp	G	A	1023/1359	341/452	synonymous_variant c.1023G>A p.Gln341Gln		hypothetical protein

C- 14-Day Passage

CHROM	POS	TYPE	REF	ALT	NT_POS	AA_POS	EFFECT	GENE	PRODUCT
1	84522	del	CTTA	C					
1	84735	del	AAG	A	159/324	53/107	frameshift_variant c.159_160delAG p.Gln53fs		hypothetical protein
8	23119	snp	T	A					
8	33293	snp	T	C	273/840	91/279	synonymous_variant c.273T>C p.Gly91Gly		hypothetical protein
38	22040	del	GA	G					
40	15380	ins	A	AT					
53	84	ins	T	TA					
73	9800	ins	A	AT					
74	12935	snp	C	T					
91	9651	snp	C	T					
101	3307	snp	C	T	127/441	43/146	missense_variant c.127C>T p.Leu43Phe		hypothetical protein
105	4508	snp	G	T	1271/1284	424/427	missense_variant c.1271G>T p.Ser424Ile		hypothetical protein

Table 1.12 A-B Detected single nucleotide polymorphisms (SNPs) Identified from CRI 2 resistance trained isolates. Since isolate CRI 2 failed to sequence no SNPs could be identified. A = SNPS identified in gentamicin resistant trained isolate and B = SNPs identified in isolates passage in antibiotic free media for 14 days.

A – Gentamicin

CHROM	POS	TYPE	REF	ALT	NT_POS	AA_POS	EFFECT	GENE	PRODUCT
1	181349	snp	T	A					
1	181354	snp	A	T					
1	181385	snp	G	A					
1	181395	snp	A	G					
1	181544	snp	A	G					
1	181555	snp	T	C					
1	508094	snp	A	T					
13	90546	ins	G	GT					
4	88241	complex	ATC	GTT	619/1416	207/471	missense_variant c.619_621delATCinsGTT p.Ile207Val	map_1	Protein map
4	88258	snp	A	G	636/1416	212/471	synonymous_variant c.636A>G p.Ser212Ser	map_1	Protein map
4	88268	snp	G	A	646/1416	216/471	missense_variant c.646G>A p.Glu216Lys	map_1	Protein map
4	88276	complex	GGTTC	AGTTA	654/1416	218/471	missense_variant c.654_658delGGTTCinsAGTTA p.His220Asn	map_1	Protein map
4	88297	complex	AAAAAG	GAAGAA	675/1416	225/471	missense_variant c.675_680delAAAAAGinsGAAGAA p.Arg227Lys	map_1	Protein map
4	88309	snp	C	A	687/1416	229/471	synonymous_variant c.687C>A p.Ile229Ile	map_1	Protein map
4	88327	snp	C	T	705/1416	235/471	synonymous_variant c.705C>T p.Ile235Ile	map_1	Protein map
4	88337	complex	GAC	AAT	715/1416	239/471	missense_variant c.715_717delGACinsAAT p.Asp239Asn	map_1	Protein map
4	88349	snp	A	T	727/1416	243/471	missense_variant c.727A>T p.Thr243Ser	map_1	Protein map
4	88357	snp	C	T	735/1416	245/471	synonymous_variant c.735C>T p.Asp245Asp	map_1	Protein map
6	64487	snp	C	T	365/822	122/273	missense_variant c.365G>A p.Gly122Asp	menB	1,4-dihydroxy-2-naphthoyl-CoA synthase
10	91981	snp	A	G	340/501	114/166	missense_variant c.340T>C p.Phe114Leu	essG_3	Type VII secretion system protein EsaG
17	10740	snp	T	C	555/2937	185/978	synonymous_variant c.555T>C p.Asn185Asn		hypothetical protein
19	38519	ins	G	GCCATTTTAAA			intergenic_region n.38519_38520insCCATTTTAAA		tRNA-Arg
19	38705	del	TA	T					

B- 14-Day Passage

CHROM	POS	TYPE	REF	ALT	NT_POS	AA_POS	EFFECT	GENE	PRODUCT
1	181544	snp	A	G					
1	181555	snp	T	C					
1	181665	snp	A	T	684/777	228/258	synonymous_variant c.684T>A p.Ser228Ser		hypothetical protein
1	181671	snp	T	A	678/777	226/258	synonymous_variant c.678A>T p.Gly226Gly		hypothetical protein
3	90546	ins	G	GT					
4	88241	complex	ATC	GTT	619/1416	207/471	missense_variant c.619_621delATCinsGTT p.Ile207Val	map_1	Protein map
4	88258	snp	A	G	636/1416	212/471	synonymous_variant c.636A>G p.Ser212Ser	map_1	Protein map
4	88268	snp	G	A	646/1416	216/471	missense_variant c.646G>A p.Glu216Lys	map_1	Protein map
4	88276	complex	GGTTC	AGTTA	654/1416	218/471	missense_variant c.654_658delGGTTCinsAGTTA p.His220Asn	map_1	Protein map
4	88297	complex	AAAAAG	GAAGAA	675/1416	225/471	missense_variant c.675_680delAAAAAGinsGAAGAA p.Arg227Lys	map_1	Protein map
4	88309	snp	C	A	687/1416	229/471	synonymous_variant c.687C>A p.Ile229Ile	map_1	Protein map
4	88327	snp	C	T	705/1416	235/471	synonymous_variant c.705C>T p.Ile235Ile	map_1	Protein map
4	88717	complex	GTCA	AACT	1095/1416	365/471	missense_variant c.1095_1098delGTCAinsAACT p.Ser366Thr	map_1	Protein map
4	88732	complex	GGATAGC	AGACAGA	1110/1416	370/471	missense_variant c.1110_1116delGGATAGCinsAGACAGA p.Ser372Arg	map_1	Protein map
4	89021	del	GT	G	1401/1416	467/471	frameshift_variant c.1401delT p.Thr469fs	map_1	Protein map
10	91981	snp	A	G	340/501	114/166	missense_variant c.340T>C p.Phe114Leu	essG_3	Type VII secretion system protein EsaG
13	87446	snp	C	T	173/492	58/163	missense_variant c.173C>T p.Pro58Leu		hypothetical protein
13	87467	complex	TCTT	CCTC	194/492	65/163	missense_variant c.194_197delTCTTinsCCTC p.IleLeu65ThrSer		hypothetical protein
13	87475	snp	G	T	202/492	68/163	missense_variant c.202G>T p.Ala68Ser		hypothetical protein
19	38519	ins	G	GCCATTTTAAA			intergenic_region n.38519_38520insCCATTTTAAA		tRNA-Arg
19	38705	del	TA	T					

1.6 QUAST report of assembled *S. aureus* isolates.

Table 1.13 QUAST Report:

The table shows the number of contig, largest contig size, assembled genome length of the sequence isolates. Isolates are referred to as (C) = Control, (G) = Gentamicin, (N) = NX-AS-401 and (14DP) = 14 Day Passage.

In the report the criteria; N50 refers to the number of contigs starting largest to smaller needed to cover 50% of the genome, with a value given in base pair. L50 refers to the number of contigs required to cover 50% of the genome in sequences. GC% refers to the number of guanine and cytosine bases present in the genome, for *S. aureus* genomes the average is 32.7%⁽⁴⁸⁶⁾.

	NCTC 13142 (C)	NCTC 13142 (G)	NCTC 13142 (N)	NCTC 13142 (14DP)	NCTC 12973 (C)	NCTC 12973 (G)	NCTC 12973 (N)	NCTC 12973 (14DP)	UHW 3 (N)	UHW 3 (C)	UHW 3 (G)	UHW 3 (14DP)	UHW 8 (C)	UHW 8 (G)	UHW 8 (N)	UHW 8 (14DP)
Contig Number	171	108	150	352	267	71	74	306	66	96	47	76	205	38	135	27
Largest Contig	99608	153786	155220	49844	52215	200279	327612	54543	251901	144701	310758	269854	72288	288404	188073	299250
Genome Length	2704707	2746353	2734726	2658766	2658941	2747335	2759878	2689942	2787085	2764492	2818307	2793862	2574843	2643973	2572072	2648182
N50	27702	43136	37240	12072	17816	107806	79969	15453	95677	51058	146096	87118	22802	158922	34499	246929
L50	30	19	22	66	51	10	12	54	10	17	7	10	35	6	23	5
GC %	32.9	32.8	32.84	32.97	32.94	32.75	32.75	32.94	32.81	32.83	32.74	32.81	33.06	32.83	33.01	32.82

	UHW 15 (C)	UHW 15 (G)	UHW 15 (N)	UHW 15 (14DP)	UHW 18 (C)	UHW 18 (G)	UHW 18 (N)	UHW 18 (14DP)	UHW 19 (N)	UHW 19 (C)	UHW 19 (G)	UHW 19 (14DP)	CRI 2 (C)	CRI 2 (G)	CRI 2 (N)	CRI 2 (14DP)
Contig Number	290	131	84	199	143	282	173	135	112	36	79	70	152	32	43	250
Largest Contig	95635	161571	158270	110177	103435	57524	155529	155391	110168	508249	170764	219341	108023	388001	5057	95110
Genome Length	2656772	2690342	2712253	2667248	2651711	2573826	2624342	2630189	2742637	2765117	2747752	2745814	2737327	2754736	64137	2721953
N50	16183	38879	51735	25399	32604	14870	28803	36523	37645	139661	65040	73822	31480	244598	1341	21437
L50	50	21	15	28	26	48	25	23	24	6	13	12	26	5	16	38
GC %	32.91	32.77	32.73	32.82	32.85	32.96	32.88	32.84	32.82	32.69	32.78	32.73	32.89	32.66	39.22	32.89

Isolate CRI 2 (N) is highlighted red due to low largest contig size, genome length and N50. The GC% is also higher than normal average.

Isolate CRI 2 (G) is highlighted yellow as it has not clustered with other CRI 2 isolate and has demonstrated a larger contig size and N50 value than both the CRI 2 (C) and CRI 2 (14DP) isolate.

MATTCHECK

